

**SOURCE ROCK PROSPECTIVITY OF LOWER CARBONIFEROUS  
LACUSTRINE STRATA, ANGUILE GROUP, CONCHE, NEWFOUNDLAND**

**by**

**©Lucia O. Newton**

A thesis submitted to the  
School of Graduate Studies  
in partial fulfillment of the  
requirements for the degree of  
Master of Science

Department of Earth Sciences  
Memorial University of Newfoundland and Labrador

Date: December 9 2019

St. John's

Newfoundland and Labrador

## ABSTRACT

In Eastern Canada, in a regional Carboniferous rift system (Maritimes Basin Tectonostratigraphic Zone), there are lacustrine basins containing petroliferous source rocks. Near the northern limits for this complex, strata of the Cape Rouge Formation at Conche, Newfoundland, are thought to represent a nearby onshore facies analog for rocks laying farther offshore in the St. Anthony Basin.

Four facies assemblages of mixed sandstone, siltstone, dolostone and black mudstone represent distinct stages of an underfilled lake-basin developed within a half-graben depocenter. The finest-grained facies assemblage, with TOC between 0.23-6.54 wt.%, has organic matter dominated by Type 1 kerogen. Maturation analysis places strata within the oil-generation window ( $R_o=0.5-1.01\%$ ); however, Rock-Eval results indicate little remaining potential for generating hydrocarbons. Based on findings from Conche, the St. Anthony Basin may contain similar half-graben lake-basins with Carboniferous source rock potential. However, source quality and timing for oil generation remain key risks for hydrocarbon exploration offshore.

## ACKNOWLEDGEMENTS

To Elliott Burden, I offer sincere thanks for providing me with the opportunity to study in Newfoundland, and complete field-work in beautiful Conche, an experience I will forever cherish. Thank you for the unwavering technical support throughout the years, and for helping and supporting me with activities outside my academic work scope (IBA, internships, etc.). This research opportunity, and other experiences, furthered my technical development and helped me obtain full time employment. I also express acknowledgement to Dr. Joe Macquaker for his technical oversight and mentorship. I also express my appreciation to my husband, Mark Bishop, for his unconditional moral support. Funding for the project was provided by Research and Development Corporation (RDC) Newfoundland and Petroleum Exploration Enhancement Program (PEEP).

## TABLE OF CONTENTS

<b>ABSTRACT</b> .....	<b>i</b>
<b>ACKNOWLEDGEMENTS</b> .....	<b>ii</b>
<b>TABLE OF CONTENTS</b> .....	<b>iii</b>
<b>LIST OF TABLES</b> .....	<b>vi</b>
<b>LIST OF FIGURES</b> .....	<b>vii</b>
<b>LIST OF ABBREVIATIONS</b> .....	<b>x</b>
<b>LIST OF SYMBOLS</b> .....	<b>xi</b>
<b>LIST OF APPENDICES</b> .....	<b>xii</b>
<b>CHAPTER ONE : INTRODUCTION</b> .....	<b>1</b>
1.01 — Overview and Aims.....	1
1.02 — Study Area.....	9
1.03 — Scientific Objectives .....	10
1.04 — Methods.....	11
1.05 — Geological Setting, History & Stratigraphy of the Maritimes Basin of Atlantic Canada.....	13
1.05.01 Stratigraphy of the Anguille Group, Newfoundland .....	16
1.06 — Hydrocarbon Shows of Lower Carboniferous Age.....	18
1.07 — Offshore Data of the Lower Carboniferous, Maritimes Basin .....	21
1.08 — Previous Work in the Conche Area, Newfoundland.....	23
1.08.01 Palynological and Paleobotanical Assemblages and Formation Ages .....	27
1.09 — Source Rock Fundamentals.....	28
1.09.01 Depositional Models for Organic-rich Mudstones .....	30
1.09.02 Depositional Models for Organic-rich Mudstones in Lacustrine Settings .....	32
1.09.03 Controls on Organic Enrichment and Hydrocarbon Type in Lacustrine Settings ....	35
<b>CHAPTER TWO : METHODS</b> .....	<b>40</b>
2.01 — General Methodology.....	40
2.02 — Field Work Methods.....	41
2.02.01 Field Accessibility, Location and Access.....	41
2.02.02 Field Work Techniques .....	42

2.03 — Petrographic Techniques & Nomenclature .....	45
2.04 — Organic-Matter Characterization.....	46
2.04.01 Visual Kerogen.....	49
2.04.02 Leco Total Organic Carbon (TOC) .....	51
2.04.03 Rock-Eval Pyrolysis.....	52
2.05 — Thermal Maturation Analysis.....	56
2.05.01 Measured Vitrinite Reflectance.....	56
2.05.02 Calculated Vitrinite Reflectance (R <sub>o</sub> Calculated).....	57
<b>CHAPTER THREE : STRATIGRAPHIC RESULTS.....</b>	<b>60</b>
3.01 — Introduction .....	60
3.02 — Sedimentary Geology of the Conche Region.....	60
3.02.01 Strata of the Crouse Harbour Formation .....	60
3.02.02 Strata of the Cape Rouge Formation .....	63
3.03 — Facies Assemblages of the Cape Rouge Formation.....	65
3.03.01 Cape Rouge Facies Assemblage 1 (CR-A1).....	65
3.03.02 Cape Rouge Facies Assemblage 2 (CR-A2).....	67
3.03.03 Cape Rouge Facies Assemblage 3 (CR-A3).....	75
3.03.04 Cape Rouge Facies Assemblage 4 (CR-A4).....	79
3.04 — Stratal Stacking Patterns of the Cape Rouge Formation .....	84
3.04.01 Stratigraphic Section 1: Pyramid Point, Cape Rouge Peninsula .....	85
3.04.02 Stratigraphic Section 2: Martinique Point, Conche Peninsula.....	90
3.04.03 Stratigraphic Section 3: Cape Fox, Conche Peninsula .....	91
3.04.04 Stratigraphic Section 4: West Coast, Rouge Island.....	95
<b>CHAPTER FOUR : SOURCE ROCK RESULTS .....</b>	<b>99</b>
4.01 — Introduction .....	99
4.02 — Optical and electron microscopy of mudstone Facies CR-A4.....	99
4.02.01 Fine-Grained Facies Character .....	107
4.03 — Total Organic Carbon (TOC) .....	108
4.04 — Rock-Eval Pyrolysis.....	110
4.05 — Organic Petrography & Thermal Maturity.....	113
4.06 — Visual Kerogen.....	116

<b>CHAPTER FIVE : DISCUSSION.....</b>	<b>124</b>
5.01 — Introduction, Paleogeography & Paleoclimate.....	124
5.03 — Crouse Harbour Formation Depositional Environment .....	128
5.04 — Cape Rouge Formation Depositional Environment .....	131
5.04.01 Lake Style and Facies Assemblages.....	132
5.04.02 Cape Rouge Assemblage 1 (CR-A1): River-Delta Stream Mouth Bars.....	133
5.04.03 Cape Rouge Assemblage 2 (CR-A2): Lake Margin (Plain) Facies.....	133
5.04.04 Cape Rouge Facies Assemblage 3 (CR-A3): Lake Floor Density Underflow Facies .....	135
5.04.05 The Cape Rouge Assemblage 4 (CR-A4): Offshore Facies .....	136
5.05 — Lake Basin Type.....	138
5.06 — Source Rock Potential .....	139
5.06.01 Thermal Maturity.....	140
5.06.02 Visual Kerogen.....	142
5.06.03 Source Quality and Quantity .....	142
5.07 — Controls on Organic-carbon Enrichment .....	145
5.08 — Comparison with the Albert Formation .....	147
5.09 — Implications for Offshore Exploration .....	149
<b>CHAPTER SIX : CONCLUSION.....</b>	<b>152</b>
6.01 — Areas for future research .....	157
<b>REFERENCES.....</b>	<b>158</b>
<b>APPENDIX 1: GEOCHEMICAL RESULTS.....</b>	<b>169</b>
<b>APPENDIX 2: ROCK-EVAL PYROLYSIS PYROGRAMS.....</b>	<b>173</b>

**LIST OF TABLES**

Table 1 Controls on organic-rich rock development in lake basins.....	39
Table 2 Geochemical parameters describing the petroleum potential (quantity) of immature source rocks.....	47
Table 3 Geochemical parameters describing kerogen type (quality) and character of expelled products.....	48
Table 4 Geochemical parameters describing thermal maturation levels .....	48
Table 5 Classification of organic matter in sedimentary rocks.....	50
Table 6 Stratigraphic section locations .....	85
Table 7 Total Organic Carbon (TOC) results by area.....	109
Table 8 Vitrinite Reflectance (% R <sub>o</sub> ) and Thermal Alteration Index (TAI) results of the Cape Rouge Formation Facies Association CR-A4 .....	120
Table 9 Visual kerogen results of the Cape Rouge Formation Facies Association CR-A4 .....	121

## LIST OF FIGURES

Figure 1.1 Paleogeographic reconstruction of the Proto-North Atlantic Rift system.....	4
Figure 1.2 Geologic map of the Maritimes Basin of Atlantic Canada.....	6
Figure 1.3 St. Anthony Basin regional cross-section.....	7
Figure 1.4 Geologic map of the Conche Study Area, Northern Newfoundland.....	12
Figure 1.5 Stratral groups recognized within the Maritimes Basin of Eastern Canada and correlative units of the British Isles.....	20
Figure 1.6 Geologic map of Carboniferous rocks in sub-basins of the St. Anthony Basin and the Deer Lake Basin.....	24
Figure 1.7 2D Seismic and aeromagnetic surveys offshore Northeastern Newfoundland .....	25
Figure 2.1 Geological map of the Conche and Cape Rouge peninsulas with accessible routes and shorelines .....	43
Figure 2.2 Outcrop photo of a fine-grained interval of the Cape Rouge Formation .....	44
Figure 2.3 A graphical depiction of TOC in a sedimentary sample .....	53
Figure 2.4 Schematic pyrograms depicting the evolution of organic compounds from a rock sample during a Rock-Eval pyrolysis heating program .....	55
Figure 2.5 Example of a vitrinite reflectance (%) vs frequency graph histogram for a kerogen isolated from sample.....	58
Figure 3.1 Geology of the Conche area with stratigraphic section localities and mudstone sample locations .....	61
Figure 3.2 Photographs of coastal cliff face exposures in the Cape Rouge Formation on the Cape Rouge Peninsula .....	64
Figure 3.3 Outcrop photographs of Facies CR-A1 of the Cape Rouge Formation.....	66
Figure 3.4 Outcrop photographs of Facies CR-A2 of the Cape Rouge Formation.....	69
Figure 3.5 Common sedimentary stacking patterns and structures of Facies Assemblage CR-A2 of the Cape Rouge Formation .....	70
Figure 3.6 Desiccation cracks and dolomite relationships of Facies CR-A2 .....	71
Figure 3.7 Trace fossils of Facies Assemblage CR-A2 .....	73

Figure 3.8 Trace fossils of Facies Assemblage CR-A2 .....	74
Figure 3.9 Photo of domal stromatolite .....	75
Figure 3.10 Sedimentary stacking patterns of Facies Assemblage CR-A3 .....	77
Figure 3.11 Sedimentary structures of Facies Assemblage CR-A3.....	78
Figure 3.12 Sedimentary stacking patterns of Facies Assemblage CR-A4 .....	80
Figure 3.13 Sedimentary stacking patterns and structures of Facies Assemblage CR-A4 .....	81
Figure 3.14 Hydrocarbon shows and pyrobitumen occurrences of Facies Assemblage CR-A4.....	82
Figure 3.15 Terrestrial plant imprints and trace fossils of Facies Assemblage CR-A4....	84
Figure 3.16 Stratigraphic section locations.....	86
Figure 3.17 Measured stratigraphic section #1 at Pyramid Point, Cape-Rouge Peninsula .....	88
Figure 3.18 Outcrop photos of fine-grained facies (Facies Assemblage CR-A4) of measured stratigraphic section #1 at Pyramid Point, Cape Rouge Peninsula .....	89
Figure 3.19 Measured stratigraphic section #2 at Martinique Point, Conche Peninsula ..	93
Figure 3.20 Outcrop photos of fine-grained facies (Facies Assemblage CR-A4) of measured section #2 at Martinique Point, Conche Peninsula.....	94
Figure 3.21 Measured stratigraphic section #3 at Cape Fox, Conche Peninsula.....	96
Figure 3.22 Outcrop photos of fine-grained facies (Facies Assemblage CR-A4) of measured section #3 at Cape Fox, Conche Peninsula .....	97
Figure 3.23 Measured stratigraphic section #4 at Rouge Island.....	98
Figure 4.1 Optical micrographs of hydrocarbon occurrences in mudstone and dolostone facies, Facies Assemblage CR-A4.....	101
Figure 4.2 Fine-grained mudstone character from the middle & lower intervals of Facies Assemblage CR-A4 .....	102
Figure 4.3 Fine-grained mudstone character from the middle & lower intervals of Facies Assemblage CR-A4 .....	103
Figure 4.4 Fine-grained mudstone characteristics from middle and lower intervals of Facies Assemblage CR-A4.....	104

Figure 4.5 Fine-grained mudstone character from the upper intervals of Facies Assemblage CR-A4 .....	105
Figure 4.6 Fine-grained mudstone character from the upper intervals of Facies Assemblage CR-A4 .....	106
Figure 4.7 Total Organic Carbon (TOC) and Hydrogen Index (HI) distributions.....	111
Figure 4.8 Source potential graphs from Rock-Eval pyrolysis and thermal maturity data analyzed in the Conche study area .....	112
Figure 4.9 Hydrocarbon and thermal maturity indicator graphs from all Rock-Eval pyrolysis and thermal maturity data .....	115
Figure 4.10 Vitrinite reflectance histograms from the Conche Peninsula .....	117
Figure 4.11 Vitrinite reflectance histograms from the Cape Rouge Peninsula.....	118
Figure 4.12 Vitrinite reflectance histograms from Rouge Island .....	119
Figure 4.13 Visual kerogen distribution by area for the Cape Rouge Formation.....	123
Figure 5.1 Paleogeographic reconstruction maps of the Late Devonian to Early Pennsylvanian .....	126
Figure 5.2 Depositional environment for the Cape Rouge and Crouse Harbour Formations .....	129
Figure 5.3 Simplified underfilled lake model.....	141
Figure 5.4 Pyrolysis S <sub>2</sub> versus total organic carbon (TOC) plot.....	146
Figure 5.5 T <sub>max</sub> and HI Plot.....	146

## LIST OF ABBREVIATIONS

### **General Abbreviations:**

BSE: Back-Scattered Imagery  
Rock-Eval: Rock-Eval Pyrolysis  
SEM: Scanning Electron Microscopy  
TOC: Total Organic Carbon  
R<sub>o</sub>: Vitrinite Reflectance  
Wt: Weight  
TAI: Thermal Alteration Index  
P: Porosity  
TD: Total Depth (meters)  
TVT: True Vertical Thickness (meters)  
TST: True Stratigraphic Thickness (meters)  
TVD: True Vertical Depth (meters)  
MD: Measured Depth (meters)  
SI: Siltstone  
VFSS: Very Fine-grained Sandstone  
FSS: Fine-grained Sandstone  
MSS: Medium-grained Sandstone

### **Mineral Abbreviations:**

An: Anorthite [CaAl<sub>2</sub>Si<sub>2</sub>O<sub>8</sub>]  
Anl: Analcime [NaAl(Si<sub>2</sub>O<sub>6</sub>)·H<sub>2</sub>O]  
Ca: Calcite [CaCO<sub>3</sub>]  
Fe-Dol: Ferrous Dolomite [Ca(Fe)(CO<sub>3</sub>)<sub>2</sub>]  
Il: Ilmenite [FeTiO<sub>3</sub>]  
Py: Pyrite [FeS<sub>2</sub>]  
PyB: Pyrobitumen [insoluble CS<sub>2</sub>]  
Po: Pyrrhotite [Fe<sub>1-x</sub>S]  
Ttn: Titanite [CaTiSiO<sub>5</sub>]

### **Facies Abbreviations:**

CR-A1: Cape Rouge Facies Assemblage 1  
CR-A2: Cape Rouge Facies Assemblage 2  
CR-A3: Cape Rouge Facies Assemblage 3  
CR-A4: Cape Rouge Facies Assemblage 4

## LIST OF SYMBOLS

	—	<i>Current Ripples</i>
	—	<i>Wave Ripples</i>
	—	<i>Mudcracks Infilled with Dolomite</i>
	—	<i>Mudcracks</i>
	—	<i>Horizontal Laminations</i>
	—	<i>Chaotic Bedding</i>
	—	<i>Internal Folds</i>
	—	<i>Fault</i>
	—	<i>Plant Imprint</i>
	—	<i>Gastropod Cast</i>
	—	<i>Worm Burrow</i>
	—	<i>Tree Branch cast</i>
	—	<i>Dolomite Bed</i>
	—	<i>Globby Dolomite</i>
	—	<i>Pyrobitumen or 'Dead Oil'</i>
	—	<i>Oil Show</i>
	—	<i>Rock Sample</i>
	—	<i>TOC Sample</i>
	—	<i>Thin Section</i>
	—	<i>Thin Section &amp; TOC Sample</i>
	—	<i>GPS Location Marker</i>
	—	<i>Lithofacies Transition</i>
	—	<i>Rip up clasts</i>
	—	<i>Missing Section</i>
	—	<i>Trough-Cross Strata</i>
	—	<i>Normal Bedding</i>

## **LIST OF APPENDICES**

- Appendix 1: Geochemical Results (including sample locations, Leco TOC, Rock-Eval Pyrolysis,  $R_o$  and TAI)
- Appendix 2: Rock-Eval Pyrolysis Pyrograms

## CHAPTER ONE: INTRODUCTION

### 1.01 — Overview and Aims

In today's world and likewise throughout the ancient rock record, lake systems show extreme diversity expressing variability in morphology, size, tectonic-setting, chemistry and physics (Kelts, 1988; Renaut and Gierlowski-Kordesch, 2010). Broadly viewed, the overall occurrence of modern lakes is controlled by climate and tectonic activity, resulting in a greatly contrasting variety of lake morphologies and depositional environments. Unlike the marine realm, where global phenomena link the atmosphere, hydrosphere and lithosphere, lake systems have relatively smaller volumes of water and local sediment supplies, resulting in a wide range of physical characteristics (Kelts, 1988; Bohacs, 2001). Compositionally, lake systems can include deposits of sedimentary strata that are calcareous, siliciclastic, volcanoclastic, carbonaceous and evaporitic. Moreover, lake waters can be organically barren to eutrophic dominated (Carroll and Bohacs, 1999; Renaut and Gierlowski-Kordesch, 2010). In terms of sequence stratigraphy, lake deposits often closely resemble marine stratigraphy with stratal sequences that range from submarine fans to deltaic (Renaut and Gierlowski-Kordesch, 2010).

Despite significant variability of lake environments within modern settings, lakes preserved in the rock record often contain a simplified sequence of reoccurring lithologic and stratigraphic stacking patterns. Lacustrine strata have been described and categorized by Bohacs and Carroll (2001) and Bohacs et al. (2000) as three end-member families of

lake basin types (Carroll and Bohacs, 2001), namely “overfilled,” “balance-filled”, and “underfilled” lake basins. The occurrence and depositional style of these three end-member basin types are controlled primarily by climate (water and sediment supply) and accommodation space (driven by tectonics) (Carroll and Bohacs, 2001). These two drivers influence the distribution, character and occurrence of lake strata including hydrocarbon play elements (source, seal, and reservoir) (Bohacs et al., 2000). The predictable nature of lake-basin together with the principles of sequence-stratigraphy, is thus used as a tool in hydrocarbon exploration in lacustrine settings (Renaut and Gierlowski-Kordesch, 2010; Bohacs et al., 2000; Carroll and Bohacs, 2001).

Ancient lake deposits are important for many reasons. They contain the essential building blocks for conventional and unconventional hydrocarbon systems (including seal, source, and reservoir facies) and are also important sites for the deposition of uranium, oil shale, coal and other essential strategic materials for chemical and electrical applications (e.g., borates and lithium carbonates) (Bohacs et al., 2000; Prothero and Schwab, 2004). Furthermore, lake strata are commonly used for climate change studies and are also major reservoirs of biodiversity (Bohacs et al., 2000).

Within the context and general direction for this study, petroleum companies and academics alike have long recognized the importance of lacustrine settings for the preservation of oil-prone strata (Powell, 1986; Kelts, 1988, Bohacs et al., 2000). At one point mined for their oil shales (e.g., Strathclyde group, Scotland), more recently, lacustrine deposits attract commercial interest after the discovery of highly prolific conventional and unconventional resource basins worldwide, including, the Eocene

Green River Formation, Uinta Basin, Utah (Bradley, 1964), Lower Cretaceous Lagoa Feia Formation, Campos Basin, Offshore Brazil (Bertani and Carozzi, 1985; Trindade et al., 1995), Barremian to Aptian Bucomazi Formation of West Africa (Powell, 1986; Lomando, 1996), and extensive intramontane basins throughout China (Zhai et al., 1984; Desheng et al., 1995; Katz and Xingcai, 1998).

In widespread locations across the proto-North Atlantic rift system (Figure 1.1), and in particular, the Upper Paleozoic Maritimes Basin of Atlantic Canada and in contiguous parts of Northwest Europe, lacustrine source rocks of early Carboniferous age have been explored and mined as hydrocarbon resources. These organic-rich rocks were apparently deposited in similar, paleogeographic, climatic and tectonic environments. In Eastern Canada, within the Maritimes Basin, proven and developed hydrocarbon systems are preserved in the subsurface of the Cumberland sub-basin at the Stoney Creek and McCully oil and gas fields respectively, with hydrocarbon systems sourced from the Lower Carboniferous Lacustrine Horton Group Albert Formation (Follows and Tyson, 1998). Comparatively, in the Midland Valley of Scotland, Lower Carboniferous oil shales of the Lacustrine Strathclyde group (previously named the Lower and Upper Oil Shale Groups) were mined between 1851-1993 and distilled for crude oil and other oil products (Carruthers et al., 1912; Follows and Tyson, 1998). In recent years, oil shales that had been historically mined for oil distillation and conventional extraction have attracted interest as potential sources for hydrocarbons in contiguous offshore and onshore basins.

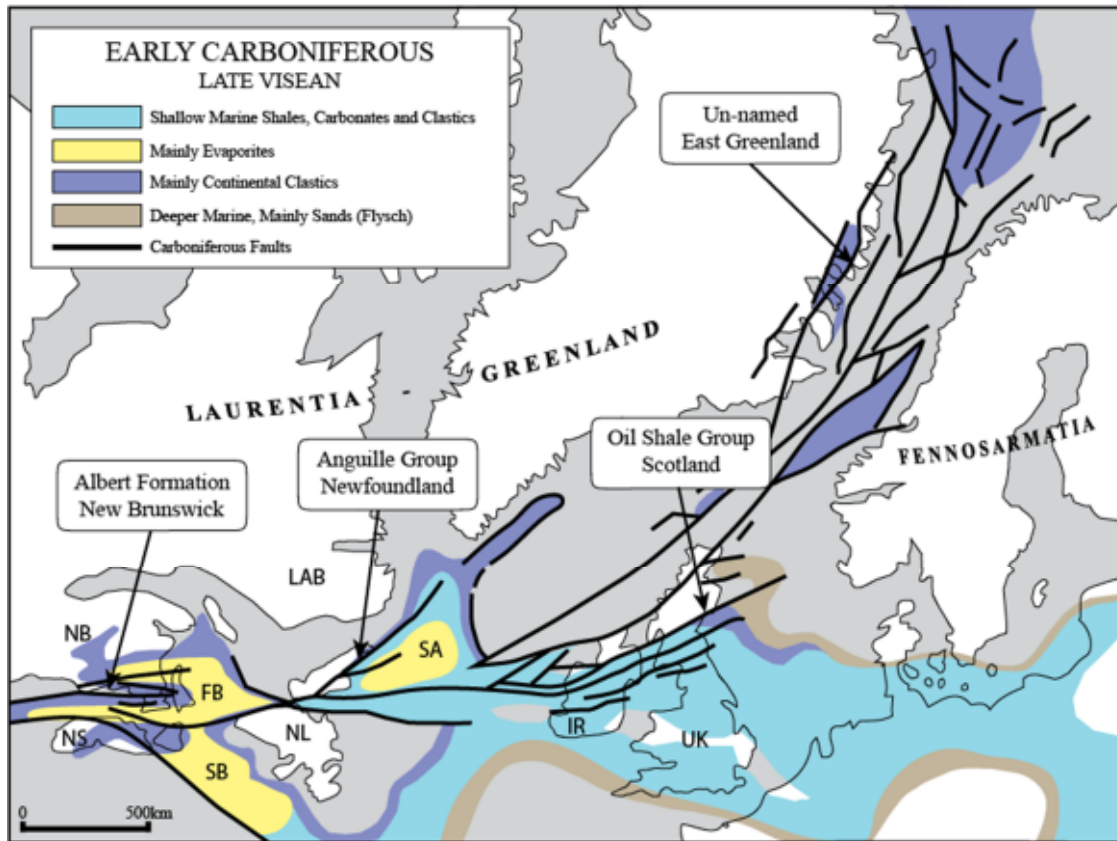


**Figure 1.1 Paleogeographic reconstruction of the Proto-North Atlantic Rift system**

Paleogeographic reconstruction of the proto-North Atlantic rift system during the early Carboniferous showing the major fault trends in black lines along with the principle depositional environments and lithologies in bright colors. Proven source rock deposits are noted, including the Albert Formation of New Brunswick, Oil Shale Group of Scotland, and un-named facies of East Greenland (modified from Ziegler, 1988). Abbreviations: NB, New Brunswick; NS, Nova Scotia; LAB, Labrador; IR, Ireland; UK, United Kingdom; FB, Fundy Basin; SB, Sydney Basin; SA, St. Anthony Basin.

This interest has led geoscientists to search for source rocks of similar age and composition across a proto-North Atlantic rift system (Figure 1.1) that includes the Maritimes Basin in Nova Scotia and New Brunswick (Utting et al., 1989), Newfoundland (Baird, 1950; 1957; 1966; Hyde, 1979; Knight, 1983; Hamblin et al., 1995), and other contiguous basins in Greenland (Christiansen et al., 1990; Piasecki et al., 1990), Ireland, and Scotland (Follows and Tyson, 1998) (Figure 1.1, Figure 1.2).

Onshore Newfoundland within the Maritimes Basin Tectonostratigraphic Zone (Lavoie et al., 2009), Lower Carboniferous fine-grained deposits occur within the Anguille Group (Horton Group equivalent), a terrestrial basin-fill deposit (Figure 1.2). The Anguille Group is found in basins that include the Bay St. George Basin (Snakes Bight Formation), the Deer Lake Basin (Forty-Five Brook and Saltwater Cove formations) (Hyde et al., 1988) and the White Bay Sub-Basin (Cape Rouge and Crouse Harbour formations) (Baird, 1957; 1966; Hamblin et al., 1995) (Figure 1.2).

Extending off the northeastern coast of Newfoundland, Carboniferous strata of the Maritimes Basin are preserved within the St. Anthony Basin. This basin is extensive, comprising an area of  $\sim 67,000 \text{ km}^2$  and reaching depths over 6.5 km beneath the seabed (Grant and McAlpine 1990; Hu and Dietrich, 2010) (Figure 1.3). This large offshore basin preserves a complex tectonic and depositional history; however, it is poorly characterized with limited wellbore and seismic data. Here, upper Carboniferous strata have been verified by two exploration wells, Verrazano L-77 and Hare Bay E-21

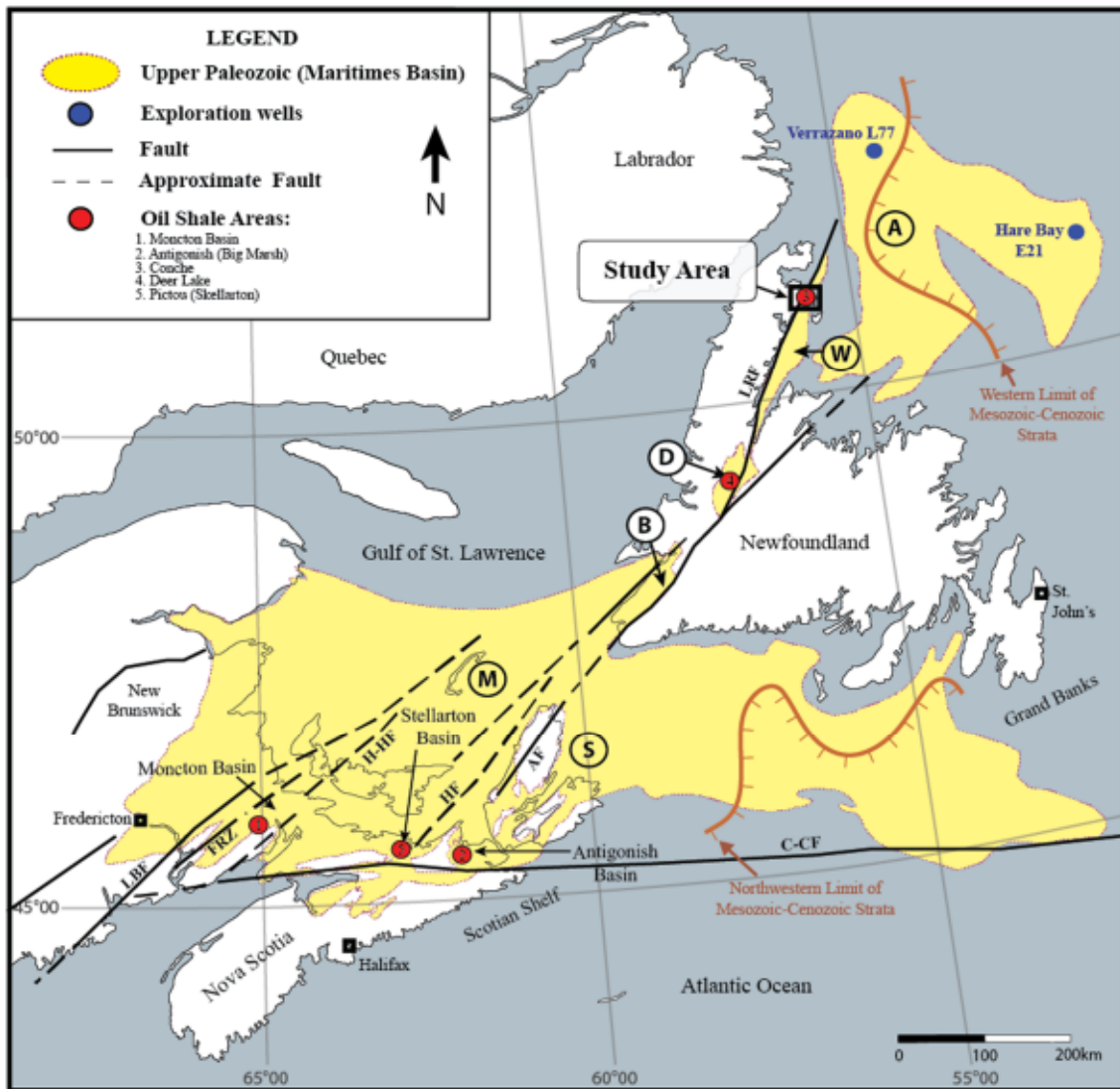


**Figure 1.2 Geologic map of the Maritimes Basin of Atlantic Canada**

A map of the Maritimes Basin of Atlantic Canada with known oil shale deposits (red dots) (Modified from Hu and Dietrich, 2010; Gibling et al., 2008; Rust et al., 1987). The thesis study area is marked by a black rectangle. Basin abbreviations: M, Magdalen Basin; S, Sydney Basin; B, Bay St. George Basin; D, Deer Lake Basin; W, White Bay Sub-basin; A, St. Anthony Basin. Fault abbreviations: LBF, Lubec-Bellisle Fault; FRZ, Fundy Rift Zone; H-HF, Harvey-Hopewell Fault; HF, Hollow Fault; AF, Aspy Fault; C-CF, Cobequid-Chedabucto Fault; LRF, Long Range Fault.



(Figure 1.2, Figure 1.3). These holes were drilled in the late 1980s to test both Upper and Lower Carboniferous plays, respectively. However, Verrazano-L-77, drilled in the northwest of the basin, failed to reach its lower Carboniferous target due to mechanical failure. Seismic surveys (2D) shot between the two exploration wells display large-scale structures related to extensional tectonics and salt movement (Grant and McAlpine 1990; Hu and Dietrich, 2010).

For onshore Newfoundland, some of the most promising Lower Carboniferous successions occur within the Cape Rouge and Crouse Harbour formations of the Anguille Group (Horton Group equivalent). These formations are exposed on two promontories and outlying islands of the White-Bay Sub-basin in the Conche region of northern Newfoundland (Figure 1.2, Figure 1.4). In this region, an estimated 1500 m of lacustrine strata are exposed in coastal outcrops. Here, oil seeps have been documented within mudstone successions (Baird, 1957; 1966; Hamblin et al., 1995). Preliminary analyses, on a limited number of samples (n=24), indicate Total Organic Carbon (TOC) values range up to 4.54% with thermal maturities in the oil window ( $R_o$  1.27%) (Hamblin et al., 1995). Most importantly, sediments of the Cape Rouge and Crouse Harbour formations in the Conche region represent the only onshore analogue to Lower Carboniferous source rocks off the eastern seaboard of the Northern Peninsula, including the offshore extension of the White-Bay Sub-basin and the greater St. Anthony Basin (Figure 1.2, Figure 1.6). Unlike their counterparts in the other Atlantic provinces and eastward in the Midland Valley of Scotland, no commercial reserves have been identified within the St. Anthony Basin or its onshore analogues. In Newfoundland, in part, this could simply be due to the

limited exploration activity; few boreholes have been drilled and with little seismic data acquired. The Conche region, where thick successions of lacustrine mudstone, sandstone, and siltstone are exposed, offers a unique onshore analogue for the offshore St. Anthony Basin. Currently, these successions are characterized by a limited number of analyses (Hamblin et al., 1995) in strata that display significant vertical and lateral facies variability.

The primary aim of this thesis is to characterize the depositional setting (lake basin type) of Lower Carboniferous strata at Conche and to understand their source rock prospectivity (occurrence, distribution, quality and quantity). In measuring strata, a lake-basin model will be created using the principles of sequence stratigraphy and the mechanics of lake sediment deposition. To decipher lake-style and fill-evolution, it is necessary to map varied suites of strata, and identify sedimentary structures and bedding patterns together with trace-fossil assemblages.

With an understanding of lake-basin type and source rock prospectivity, sedimentary stacking patterns and source rock potential will be better understood for analog basins offshore in the White Bay Sub-basin and the adjacent St. Anthony Basin.

## **1.02 — Study Area**

The study area encompasses the Conche and Cape Rouge peninsulas, rocky headlands located within the White Bay Sub-basin of the greater Maritimes Basin and on the eastern seaboard of the Great Northern Peninsula (Figure 1.4). Also included are

adjacent islands to the east, namely Rouge Island, Red Island, Pigeon Island, and Groais Island (commonly known as Northern Grey Island) (Figure 1.4).

### **1.03 — Scientific Objectives**

Research objectives include:

- Review literature on stratigraphy and source rock models for lacustrine settings with attention to the variety of lake-basin models and the distribution and character of hydrocarbon play elements (refer to Chapter 1, p.32).
- Review analogue lacustrine basins with proven source rocks (e.g., Albert Formation of New Brunswick, Canada) and compare prospective source rocks with those identified at Conche (refer to Chapter 1, p.18 & Chapter 5, p.147).
- Conduct a geological survey of Cape Rouge Formation in the Conche region, including the Conche-Cape Rouge peninsulas and adjacent islands to the east (Rouge, Red, Pigeon, & Groais Island) (refer to Chapter 3, p.60).
- Map stratigraphic sections of the Cape Rouge Formation around the study area to gain an understanding of the variety and distribution of strata, including both organic-rich and non-organic rich sections (refer to Chapter 3, p.84).
- Identify areas where fine-grained strata and oil seeps are common and therein generate a large suite of mudstone samples for Total Organic Carbon (TOC), Rock-Eval Pyrolysis and petrographic analysis (refer to Chapter 4, p.99 & Figure 3.1).
- Define source rock quality and quantity of fine-grained facies at Conche using TOC, Rock-Eval Pyrolysis and petrographic analysis (refer to Chapter 5, p.139).
- Determine a lake-basin type (underfilled, balanced filled or overfilled lake-basins)

- from facies associations and stratal stacking patterns (refer to Chapter 5, p.138).
- Use the Conche region study as a contribution towards better understanding the hydrocarbon potential and key risks for offshore Paleozoic successions in the St. Anthony Basin (refer to Chapter 5, p. 149).

#### **1.04 — Methods**

Fluvial-lacustrine successions of the Cape Rouge Formation were mapped in the Conche area (Figure 1.4) in June and July 2012 (encompassing 25 days). Here, stratigraphic sections were measured and illustrated following a sequence-stratigraphic approach for lake-basin models (see Carroll and Bohacs, 1999; 2001; Bohacs et al. 2000). Stratigraphic sections (on accessible shorelines) showing vertical and lateral facies variability have photo illustrations and measurements for sedimentary structures and trace fossil assemblages. Where mudstone successions were found, fine-grained samples were collected. Later, in the lab, mudstones were analyzed for TOC (LECO), Rock-Eval Pyrolysis (Rock-Eval), and thermal maturity (Vitrinite Reflectance, Visual Kerogen and Thermal Alteration Index). Larger mudstone samples were also collected for thin section preparation and later analysis with conventional petrography and electron-optical (backscattered electron imagery) techniques. See Chapter 2 for more a detailed methodology of laboratory techniques.

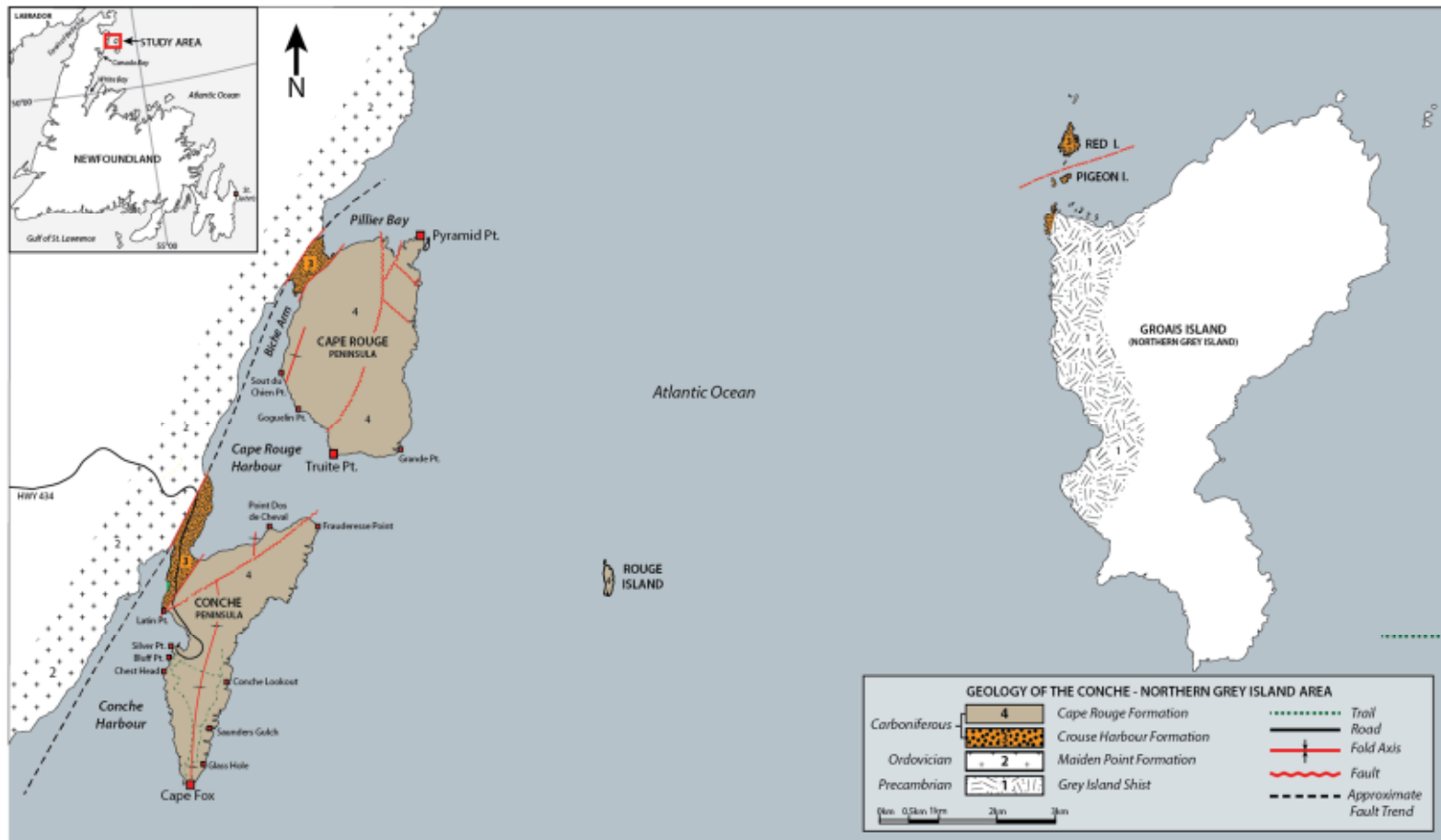


**Figure 1.4 Geologic map of the Conche Study Area, Northern Newfoundland**

Map includes the Conche and Cape Rouge peninsulas, Rouge, Red, Pigeon, and Groais islands (modified from Baird, 1966 and Hamblin et al., 1995).

## **1.05 — Geological Setting, History & Stratigraphy of the Maritimes Basin of Atlantic Canada**

The Carboniferous Period marks a period of significant change in Earth's geological record during which dramatic environmental and tectonic changes occurred globally. Throughout the Carboniferous Period plant species evolved, widespread forests flourished, amphibians diversified, and reptiles appeared first on land (Encyclopedia Britannica, 2009).

During the Lower Paleozoic, from New England through Atlantic Canada and Eastern and Western Europe, a series of lacustrine, marginal marine and marine sediments were deposited in linear fault-bound basins. This rift system has been referred to as the Proto North Atlantic Rift-System by Ziegler (1988) (Figure 1.1) (Williams, 1973; Ziegler, 1988; Smith et al., 1991; Gibling et al., 2008).

Lacustrine strata deposited during the early Carboniferous Period are preserved as remnants of this extensive rift system and extend eastward from the Horton Group of the Maritime Provinces to the Anguille Group of Northern Newfoundland through to the Strathclyde Group of the Midland Valley of Scotland and north into the enigmatic deposits of Eastern Greenland (Ziegler, 1988; Follows and Tyson, 1998; "Sedimentary Basins and Hydrocarbon Potential of Newfoundland and Labrador", 2000; Dean et al., 2011).

In the Atlantic region of Canada, from the Late Devonian to Late Triassic, a series of thick Lower Paleozoic basins, collectively identified as the Maritimes Basin, was

deposited during a period of active extensional tectonism (Williams, 1973; Smith et al., 1991; Gibling et al., 2008). Encompassing an area of roughly 330,000 km<sup>2</sup>, the basin underlies the offshore areas of the Gulf of St. Lawrence, Cabot Strait, southwestern Grand Banks, and Northeastern Newfoundland, and onshore areas in Quebec, Nova Scotia, New Brunswick, Prince Edward Island, and Newfoundland (Figure 1.2) (Knight, 1983; Gibling et al., 2008; Dietrich et al., 2011). The Maritimes Basin is a composite basin that contains a number of basins and sub-basins (Gibling et al., 2008). These include the Magdalen, Sydney, Deer Lake and St. Anthony basins and numerous local sub-basins, including the Moncton, Cumberland, Antigonish, Bay St. George and White Bay (Figure 1.2) (Dietrich et al., 2011).

Largely filled with fluvial and lacustrine sediments with minor marine incursions, the Maritimes Basin has complex basin-fill relationships (Knight, 1983). Given its complexity, various stratigraphic nomenclatures exist for the basin (see Dietrich et al., 2011 for a complete list of publications, page 73). For the purpose of this thesis, a stratigraphic column for the Maritimes Basin of Eastern Canada and equivalents in the British Isles (Northern Ireland and Scotland) is presented below (Figure 1.5). The Eastern Canada stratigraphy includes the southern Maritimes Basin (Quebec, Nova Scotia, and Prince Edward Island) and the northern Maritimes Basin (Newfoundland, including the Deer Lake Basin and the Bay St. George sub-basins) (compiled from Dietrich et al., 2011; Hamblin et al., 1995). Carboniferous strata within the Maritimes Basin unconformably over eroded Acadian terrain, and disconformably, conformably and rarely unconformably are overlain by the Windsor Group, or in the easternmost regions by younger Mesozoic-

Cenozoic sediments of Atlantic Canada's continental margin (Figure 1.2, Figure 1.3, Figure 1.5) (Mossman, 1992; Dietrich et al., 2011).

Basins and sub-basins of the Maritimes basin record the final stages of the convergence of the supercontinent Pangea. Positioned in a near equatorial latitude and in the collisional zone between Laurasia and Gondwana, the basin preserves a record for the closure of the Rheic Ocean (Morel and Irving, 1978; Ziegler, 1988; Hamblin et al., 1995; Gibling et al., 2008). Regionally, the basins and sub-basins carry a complex history of subsidence and inversion, reactivation of major lineaments, emplacement of salt bodies, and erosion of overlying strata (Gibling et al., 2008).

The early history of the Maritimes basin, from Mid- to Late Devonian, is preserved in a highly fragmented record marking the end of the Acadian Orogeny and the development of local extensional basins (Gibling et al., 2008). Regional extension prevailed from the Late Devonian to Early Carboniferous (Mississippian Period) during which a series of linear fault-bound basins developed along a common E-W to NE-SW orientation. The basins are generally thick and developed across terrane boundaries (e.g., Avalon/Meguma boundary) as a consequence of reactivation of Acadian thrusts during extension (Murphy and Rice, 1998; Gibling et al., 2008). Regionally, dark mudstones of the Horton Group and equivalents (Tournaisian age) were deposited in a number of half-graben rifts during extensional phases (Hamblin et al., 1995).

In New Brunswick, the Horton Group consists of the Albert Formation (Lacustrine organic-carbon rich mudstones, siltstones and sandstones), unconformably

overlain by the non-marine Sussex Group (Dietrich et al., 2011). Together, these rocks are equivalent to the Anguille Group of Newfoundland. These Early Mississippian rocks record the initiation of sedimentation in the Maritimes Basin and collectively have a similar stratigraphic framework of:

- (1) basal fluvial/alluvial clastics,
- (2) fine-grained lacustrine sediments and minor restricted marine deposits and,
- (3) upper coarse-grained fluvial/alluvial/deltaic sediments (Hamblin and Rust, 1989; Hamblin et al., 1995; Gibling et al., 2008; Dietrich et al., 2011).

In a conventional hydrocarbon play analysis, fine-grained lacustrine deposits have potential for generating hydrocarbons while the upper coarse-grained members are potential reservoir facies (Hamblin et al., 1995). Regionally, the Horton Group and equivalents are thought to be the main source rock interval for the entire Maritimes Basin (Gibling et al., 2008).

#### **1.05.01 Stratigraphy of the Anguille Group, Newfoundland**

A thick succession of Anguille Group strata (Figure 1.5), found along a narrow (~26 km) elongate zone in Western/Northern Newfoundland, trends northeast along the Cabot Fault Zone from Cape Anguille to White Bay (Figure 1.2) (Belt, 1969). Onshore deposits are localized in the Bay St. George and Deer Lake basins, and on the smaller headland promontories and islands in the White Bay Sub-basin and offshore in the St. Anthony Basin.

In southwest Newfoundland in the Bay St. George Basin, the Anguille Group contains four formations. These include (from oldest to youngest); the fluvial Kennels Brook Formation; the lacustrine Snakes Bight Formation, the fluvial-deltaic Friars Cove Formation, and the fluvial-lacustrine-deltaic Spot Falls Formation (Figure 1.5) (Knight, 1983). Further northeast along the Cabot Fault zone, the Deer Lake Basin is composed of non-marine sediments ranging from Tournaisian to Westphalian in age (Hyde et al., 1988). The initial fill is divided by fault blocks on deeper structures in the basin. These prominent features include the Birchy Ridge Block and the Fisher Hills Block (Miller and Wright, 1984; Hyde et al., 1988). The Anguille Group in the Birchy Ridge Block is composed of three formations, from oldest to youngest, the Gold Cove Formation, the Saltwater Cove Formation, and the Cape Rouge Formation. The Fisher Hills Block contains four formations that include from oldest to youngest, the Blue Gulch Block Formation and the Forty-five Block Formations (together equivalent to the Gold Cove Formation), the Saltwater Cove Formation, and the Thirty-fifth Block Formation (equivalent to the Cape Rouge Formation) (Hyde et al., 1988) (composite stratigraphy illustrated in Figure 1.5). In the Conche area of the White Bay Sub-basin, Baird (1957; 1966) divided the upper Anguille Group into two non-marine intervals, including the potentially age-equivalent Crouse Harbour Formation and the Cape Rouge Formation (Figure 1.5).

## 1.06 — Hydrocarbon Shows of Lower Carboniferous Age

Hydrocarbon shows occur in regionally age equivalent (Lower Carboniferous) lacustrine and marginal marine deposits within the Maritimes Basin of Eastern Canada, the Midland Valley of Scotland, and eastern Greenland.

In the Midland Valley of Scotland, the Calders Member of the Oil Shale Group is a historically rich oil shale deposit that developed along the Proto North Atlantic Rift system in predominantly lacustrine and locally marine settings (e.g., Dean et al. 2011). The oil shales, most notably the Pumperston and Dalmahoy oil shales (Asbian), were distilled for oil between 1851 and 1962 (Parnell, 1988; Follows and Tyson, 1998). Oil shale TOC values range from 10-12% and have Type II to Type I oil-prone kerogens (mean HI 400-800). There was an estimated total production of 75 million barrels of oil with a peak annual production of over two million barrels of oil. An estimated 65 million tonnes of recoverable oil are thought to remain in place (Follows and Tyson, 1998; Kerr, 1994).

Active petroleum systems with Tournaisian source rocks (Horton Group and equivalents) occur in several areas across the Maritimes Basin (Christiansen et al., 1990; Piasecki et al., 1990; Follows and Tyson, 1998; Hyde et al., 1988; Desilva, 1999). Hydrocarbon shows include, most notably, the Stoney Creek and McCully oil and gas fields in New Brunswick, oil seeps in Nova Scotia, and oil and gas shows in diamond drill holes and wells in the Magdalen Basin, Bay St. George Basin, Deer Lake Sub-basin

and White Bay Sub-basin (Baird, 1957; 1966; Hamblin et al., 1995; Desilva, 1999) (Figure 1.2).

The Stoney Creek and McCully Fields, in the Moncton Sub-basin of New Brunswick (Figure 1.2), are the only commercially produced oil and gas fields onshore in the Maritimes Basin. Both fields are sourced from lacustrine organic-rich strata of the middle Frederick Brook Member (Greiner, 1962), Horton Group, and are interpreted to have been deposited in the deepest parts of stratified lakes ( $\leq 60\text{m?}$ ) formed in tropical or sub-tropical environments (Greiner, 1962; 1974; Follows and Tyson, 1998). TOC values in the Frederick Brook Member range from 0.2-29.3% but mainly range from 3-14% (Smith et al., 1991; Follows and Tyson, 1998). HI values range from 350-850 indicating oil prone Type 1 kerogen (Follows and Tyson, 1998). Macerals are typically dominated by liptinite and lamalginite with minor amounts of telalginite contents (Follows and Tyson, 1998).

The Stoney Creek Field, discovered in 1909, commercially produced 29 Bcf of gas and 0.85 million barrels of 37°API oil between 1909-1991 (Hamblin et al., 1995; Desilva, 1999; Keighley, 2008). Production has been difficult, and today an estimated 90% of the reserves remain in place (Keighley, 2008). The McCully Field has an estimated 1 Tcf of gas in place and is currently producing gas that is exported to the Northeastern USA (Keighley, 2008). The richest sections of the Albert Formation yield as much as 93 litres/tonne (Macauley et al. 1984).

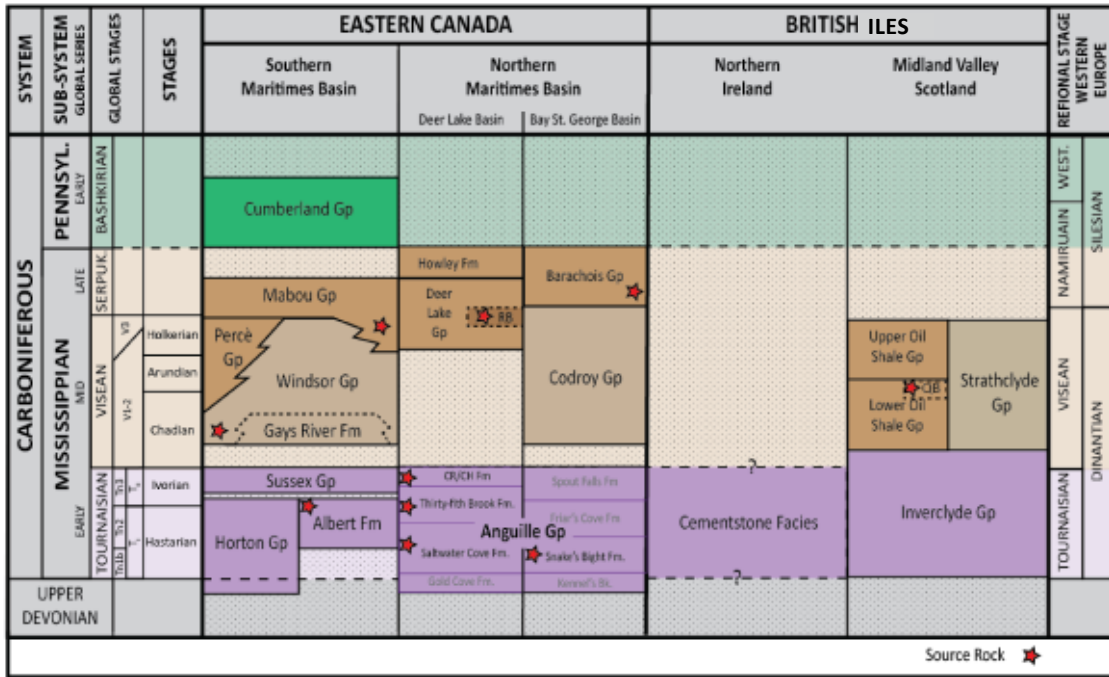


**Figure 1.5 Stratigraphic groups recognized within the Maritimes Basin of Eastern Canada and correlative units of the British Isles**

A simplified Early Paleozoic stratigraphic column for the Maritimes Basin of Eastern Canada and equivalent stratal groups of the British Isles (Northern Ireland and Scotland). Eastern Canada stratigraphy includes the southern Maritimes Basin (Quebec, Nova Scotia, and Prince Edward Island) and the northern Maritimes Basin (Newfoundland, including the Deer Lake Basin and the Bay St. George sub-basins) (compiled from Detrich et al., 2011; Hamblin et al., 1995). British Isles stratigraphy includes the Midland Valley of Scotland (compiled from Tyson and Follows, 1998 and Belt et al., 1967). Group, formation and facies names referred to in text, and source rock intervals indicated with red stars. Abbreviations: RB, Rocky Brook Formation; QB, Queensferry Beds; CR/CH Formation, Cape Rouge and Crouse Harbour formations; West., Westphalian.

In Newfoundland, oil shows, associated with organic-rich facies of the Anguille Group (Horton Group equivalents), are exposed in regionally distinct formations in the Bay St. George, Deer Lake, and White Bay sub-basins (Figure 1.2). In the Bay St. George Basin, the Snakes Bight Formation contains dark shales with TOC values of 1.29-1.85%. However, given high thermal maturation values ( $HI < 4$ ), they have limited hydrocarbon generating potential (Hyde, 1983; Sinclair, 1990). In the Conche area of the White Bay Sub-basin (Figure 1.4), prospective source rock deposits have been reported in the Cape Rouge and Crouse Harbour formations where several thousand meters of strata are exposed. Here, oil seeps have been documented with bituminous material (Baird, 1957; 1966; Hamblin et al., 1995). In many instances bituminous material is now pyrobitumen (dead oil); however some live oil is seeping out of Crouse Harbour Formation dolostones at Pilier Bay (Hamblin et al., 1995) (Figure 1.4). Preliminary analysis of potential source rocks indicates a dominance of Type 1 kerogen in the oil window (1.0 to 1.2% vitrinite  $R_o$ ) with TOC values between 1-4% (Hamblin et al., 1995).

### **1.07 — Offshore Data of the Lower Carboniferous, Maritimes Basin**

Only two exploration wells, Bradelle L-49 and Irishtown No.1, drilled in the Magdalen Basin in the Gulf of St. Lawrence (Figure 1.2), have successfully tested Lower Carboniferous offshore strata within any part of the Maritimes Basin of Atlantic Canada. To the east within the St. Anthony Basin, two old exploration wells (drilled in the 1980s) simply confirm the presence of any Carboniferous strata on the Newfoundland shelf. Neither of these wells tested hydrocarbons.

St. Anthony Basin wells Verrazano L-77 and Hare Bay E-21 (Figure 1.2, Figure 1.3) (Barss et al., 1979; McWhae et al., 1980; Hu and Dietrich, 2010; 2013) penetrated the northern and eastern limits of the St Anthony Basin. Verrazano L-77 was intended to test a Lower Carboniferous structural play that lacked Mesozoic-Cenozoic cover. However, due to drilling complications the well was abandoned early (Total Depth 460mMD/446mSS) (Hu and Dietrich, 2010; Eastcan et al. 2013) (Figure 1.3). Biostratigraphy shows Verrazano L-77 hit late Viséan to early Namurian strata (Utting et al., 1976) that were once deeply buried; vitrinite reflectance values ( $R_o$ ) are 1.4-1.7% (Hamblin et al., 1995). Farther east, the Hare Bay E-21 exploration well targeted an Upper Carboniferous play laying beneath thick Mesozoic-Cenozoic cover, and overlying salt diapirs (equivalent to Windsor/Codroy Group strata elsewhere) (Figure 1.3). Hare Bay successfully reached a TD of 4874mMD/4828mSS, recovering two cores from Upper Carboniferous strata (“Schedule of Wells Newfoundland and Labrador Offshore Area: BP et al. Hare Bay E-21,” 2007). For the deepest cored section, between 4516.50 and 4525.50mMD (4487.4-4496.1mSS), sandstones yielded relatively high porosity values (up to 15%), likely related to secondary porosity development (Hu and Dietrich, 2010). Given that neither well penetrated Lower Carboniferous strata, and with poor log quality in the Upper Carboniferous sections, little can be concluded regarding the source rock prospectivity of Paleozoic plays offshore Newfoundland.

In 1968 Tenneco Oil & Minerals Ltd. acquired a series of 2D seismic lines (completion date 04-Oct-1968) from the White Bay Sub-basin, the St. Anthony Basin and along the Labrador shelf (Domino, Harrison, Saglek areas). In the White Bay Sub-basin,

five seismic lines in the “Notre Dame block” (2D lines: ND-1A; ND-1C; ND-2A, ND-3A, ND-3B) run roughly perpendicular to the coastline (Figure 1.6). Moreover, Tenneco Oil & Minerals Ltd. conducted an aeromagnetic survey in 1967 (Figure 1.7) (Plasse and Graves, 1985); however, the company has since sold their Canadian assets and their original East Coast data cannot be located. Microfiche copies of their 2D seismic lines are on file at the Canada-Newfoundland and Labrador Offshore Petroleum Board (C-NLOPB), but the quality is extremely poor and there are no nearby wells to use to correlate the seismic data with the strata.

### **1.08 — Previous Work in the Conche Area, Newfoundland**

Alexander Murray, during his first year in Newfoundland, described the geology of the eastern seaboard of the Northern Peninsula, including descriptions of the Carboniferous strata in the Conche area (Murray and Howley, 1881; Murray and Howley, 1918). In 1938, Johnson visited the area; his geological observations remain as unpublished files at the Mines Branch in St. John’s (Baird, 1957). Baird also visited Conche and released an unpublished report for the Geological Survey of Newfoundland (Baird, 1957). This was later followed by a published study in 1966. The published paper (Baird, 1966) describes the Lower Paleozoic bedrock geology of the Maiden Point Formation (previously referred to as the Canada Head Formation) (Ordovician), Groais Island Schists (Precambrian, potentially Cambro-Ordovician), and the Lower Carboniferous cover rocks. A geological map illustration includes major faults, folds, and the distribution of geological units on the Conche and Cape Rouge peninsulas and on several outlying islands. Baird formally defined two formations of Lower Carboniferous

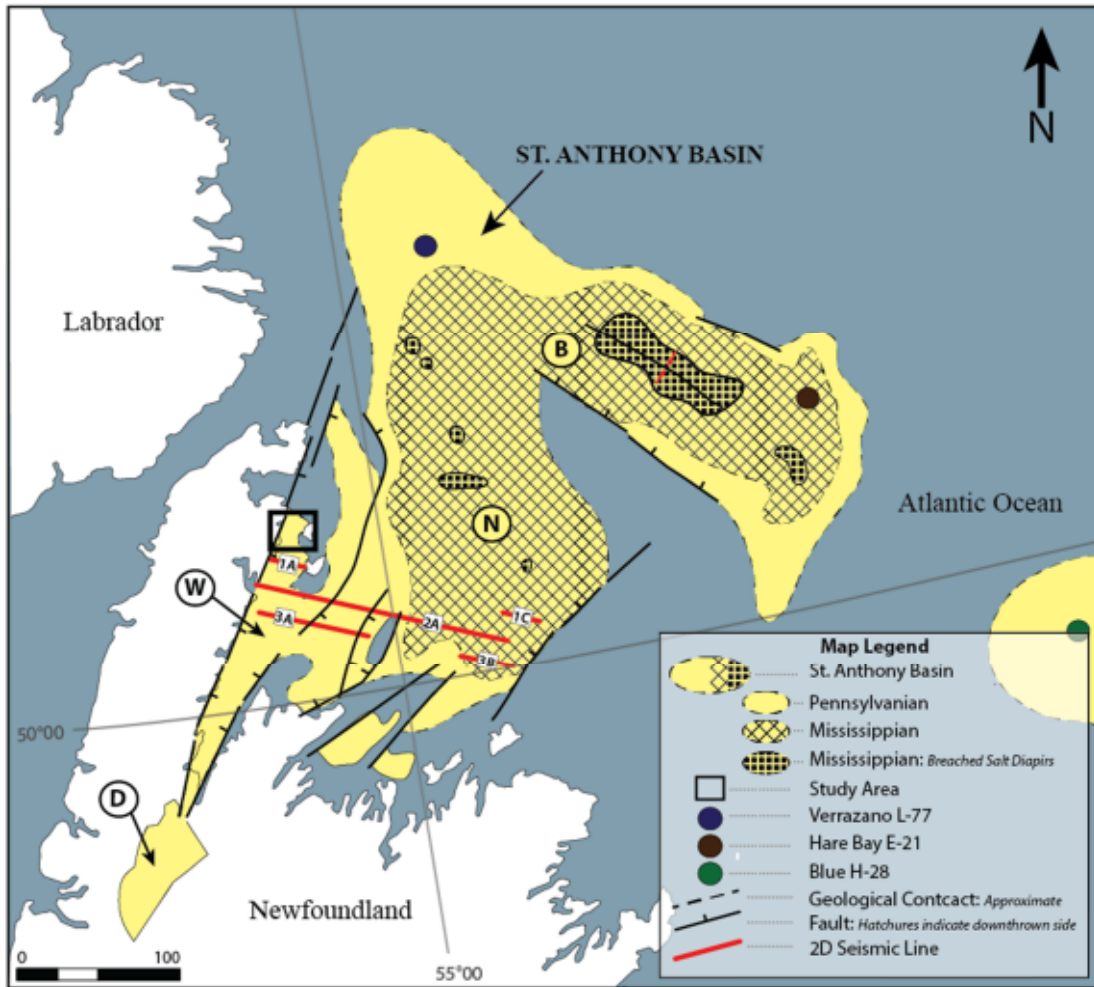


**Figure 1.6 Geologic map of Carboniferous rocks in sub-basins of the St. Anthony Basin and the Deer Lake Basin**

Distribution of Carboniferous rocks in sub-basins of the St. Anthony Basin and the Deer Lake Basin (modified from Keen and Williams, 1990). Offshore 2D seismic lines presented in dark blue. Abbreviations: W, White Bay Sub-basin; N, Notre Dame Sub-basin; B, Belle Island Sub-basin, Deer Lake Sub-basin.

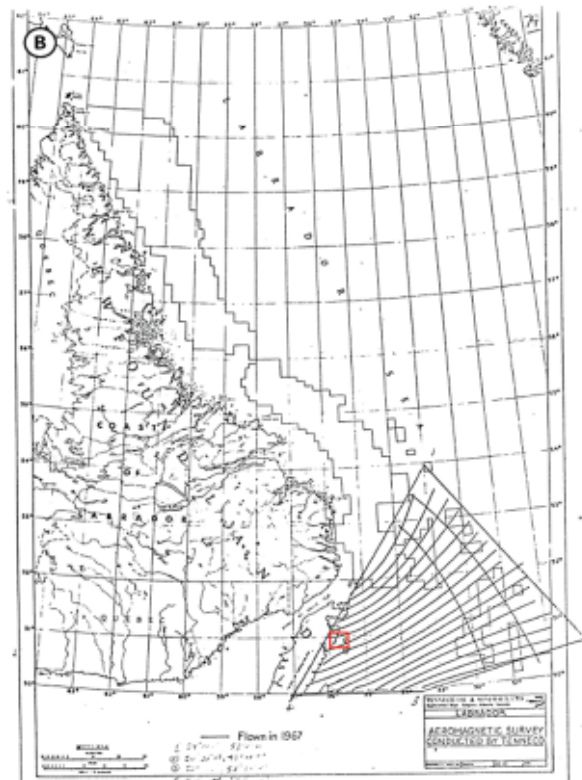
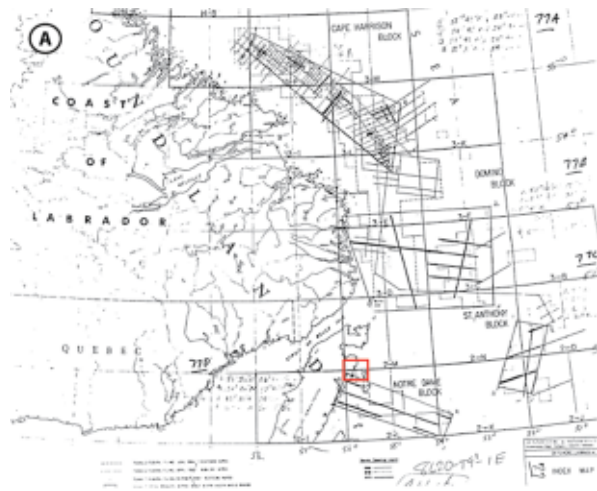


**Figure 1.7 2D Seismic and aeromagnetic surveys offshore Northeastern Newfoundland (Tenneco Oil)**

A) 2D seismic line coverage (1968) of the White Bay Sub-basin, the St. Anthony Basin and along the Labrador shelf. Red Square highlights the Conche study area. B) Aeromagnetic reconnaissance survey map (1967) of the St. Anthony Basin (after Plasse and Graves, 1985). Red Square highlights the Conche study area.

age that underlie portions of the Conche and Cape Rouge peninsulas, Rouge Island, the northwestern tip of Groais Island, and several smaller islands. These formations are the Crouse Harbour Formation (~275m thick), composed of poorly sorted conglomerate, sandstone and minor siltstone; and the Cape Rouge Formation (~1250m thick), composed of fine-grained sandstones, siltstones and mudstones (Baird, 1966).

Decades later, Hamblin et al. (1995) published a comprehensive paper describing the sedimentology, palynology, and source rock potential of the Conche area. Four sections were measured, three from the Crouse Harbour Formation (Latin Point, Pilier West and East) and one from the Cape Rouge Formation (Truite Point) (Figure 1.4). Twenty-four fine-grained samples were collected from these localities and analyzed for palynology and geochemistry. Results indicate deposition of potential source rock facies in an intermittently anoxic lacustrine environment (Hamblin et al., 1995). Spore studies, fluorescence and reflectance analyses indicate thermal maturity, specifically in the later stages of the oil window. Organic matter characteristics, biomarker features, and lithofacies characteristics show considerable similarities with Horton Group strata in the Maritime Provinces (Hamblin et al., 1995).

Recently, Dr. Elliott Burden and Dr. Joe MacQuacker of Memorial University revisited the area in 2010 and again in 2011 as a joint research project with Dr. Geoffrey Clayton of Trinity College Dublin. Samples collected during these field seasons were incorporated into two undergraduate theses from Memorial University. These included palynology and lithofacies variability studies by Froude (2012) and Hussey (2011), respectively.

### 1.08.01 Palynological and Paleobotanical Assemblages and Formation Ages

With several paleobotanical and palynological studies on record (Baird, 1966; Hamblin et al., 1995), and an unpublished undergraduate Honours Thesis by Froude (2012), the Cape Rouge and Crouse Harbour formations are considered Tournaisian in age.

Baird (1957; 1966) collected fossil plants from the Cape Rouge Formation west of Pyramid Point (Figure 1.4). Here, seed-fern remains were identified as *Sphenopteris (Aneimites) strigosa* Bell and *Sphenopteridium macconochiei?* Kidston from the Lower Carboniferous (Late Tournaisian or early Viséan). Similar species have been documented in the Albert and Kennebecasis formations, New Brunswick and in the Cheverie Formation, Nova Scotia along with upper beds of the Anguille Formation, Newfoundland (Baird, 1966). Abundant spores were also collected from the Cape Rouge Formation (locality between Truite Point and Grande Point (Figure 1.4)), however, the majority of the spores were highly corroded. Among the identifiable spores, Barss (in Baird, 1966) classified them as equivalents to those discovered and reported in the Horton Group of Nova Scotia (that is Cheverie Formation type section and Ainslie – Strathlorne Formation of Cape Breton). Baird (1966) concluded that Carboniferous strata from the Conche area are age equivalent to the Upper Horton (Tournaisian) strata in Nova Scotia.

Hamblin et al. (1995) conducted a more extensive palynological study of both the Cape Rouge and Crouse Harbour formations. Miospore assemblages verify earlier reports

in Baird (1966) with a late Tournaisian age for both the Cape Rouge and Crouse Harbour formations. Reported taxa belong to the *Spelaeotriletes cabotii* Assemblage Subzone of the *Vallatisporites vallatus* Assemblage Zone (Hamblin et al., 1995). Based on the revised bio- and lithostratigraphic subdivisions of Belgium, this subzone is T<sub>11</sub> age (or Tn3 age) (Hamblin et al., 1995). Hamblin et al. (1995) report miospore taxa assemblages containing *Vallatisporites vallatus* and *Spelaeotriletes pretiosus* var. *pretiosus* are indicative of deposition in a moderately humid climate.

Froude (2012) analyzed palynology samples from organic-rich sediments collected during the 2011 field season by Dr. Elliott Burden and Dr. Joe MacQuaker. Froude documented the fossil genera present, preservation, and thermal maturation indexes. However, given poor preservation, Froude's conclusions regarding age and maturation were generally inconclusive as the majority of the spores were highly corroded. Despite generally poor spore preservation, Froude identified similar species to those documented by Hamblin et al. (1995).

### **1.09 — Source Rock Fundamentals**

For an active petroleum system to exist, a variety of fundamental elements and processes must come together for the accumulation of petroleum products. Elements and processes include source, reservoir, seal and overburden rock, together with the formation of traps and the generation-migration-accumulation of hydrocarbons (Magoon and Dow, 1994). The most critical element rests with the presence of source rock and without it, all other elements and processes needed to generate a play become irrelevant (Rojas et al.,

2013). A source rock can be broadly defined as any rock that is capable of generating petroleum upon burial and heating, given that it contains an appropriate amount and type of organic matter (Tissot and Welte, 1984; Gluyas and Swarbrick, 2004). Typically, an average mudstone contains TOC values of around 0.8% while typical source rocks range between 1.5-15%.

An effective source rock must (1) contain an appropriate quantity of organic matter (measured through TOC analysis), (2) organic matter must be of desired quality (measured through Visual Kerogen Analysis and/or Rock-Eval pyrolysis), and (3) organic matter must reach an appropriate level of thermal maturation through burial (measured through  $R_o$ , TAI, and Rock-Eval Pyrolysis) (Peters and Cassa 1984, 1994; Tissot and Welte, 1994).

Organic-rich mudstones are often dark-colored rocks that are composed of silt- and clay-sized particles and enriched in organic material (Tourtelot, 1979; Laracy, 2012). Generally, they are argillaceous, however, carbonates can also be prospective source rock targets (Rojas et al., 2013). Their makeup is variable, and can include a wide variety of components including quartz, clays, calcium carbonate, organic matter, chemical precipitants (e.g., carbonates/sulphides) and skeletal remains, all of which are commonly modified by diagenetic overprinting (MacQuaker and Bohacs, 2007; Laracy, 2012). The type of organic matter bound in these rocks is dependent on depositional environment (e.g., terrestrial, marine, lacustrine); however, the degree of organic matter enrichment is dependent on three factors. These include relative rates of production, destruction, and dilution of organic matter during deposition (Bohacs et al., 2005). For a rock to be

sufficiently enriched in organic matter, the production rates must surpass those of organic matter destruction (both in the oxic and sulfidic zones) and dilution (Bohacs et al., 2005), and is highly dependent upon rates of sediment accumulation (e.g., Aplin and Macquaker, 2011). Bohacs et al., 2005 express organic-matter enrichment in a simple relation:

$$\text{Organic-matter enrichment} = \text{Production} - (\text{Destruction} + \text{Dilution})$$

Moreover, in order for these organically enriched rocks to produce hydrocarbons, the bound organic matter must be buried to a point where sufficient heat and pressure generate mature kerogen (Rojas et al., 2013). Kerogen is divided into four main end member “types” according to maceral composition (their original organic source material) and on the atomic ratios of hydrogen, carbon, and oxygen (Tyson, 1995; Gluyas and Swarbrick, 2009; Rojas et al., 2013). Macerals include liptinite (Type I), exinite (Type II), vitrinite (Type III), and inertinite (Type IV) (Gluyas and Swarbrick, 2009). In order to properly characterize source rocks, it is important to differentiate the various types of kerogen as the abundance of each will influence the type of petroleum product produced (oil, gas, or mixed), its hydrocarbon yield, and the timing of hydrocarbon generation and expulsion from a source rock (Tissot and Welte, 1984; Gluyas and Swarbrick, 2009; Rojas et al., 2013).

### **1.09.01 Depositional Models for Organic-rich Mudstones**

Conventional models for the deposition of organic-rich mudstones are dependent upon the establishment of oxygen-depleted (anoxic) sediments for the preservation of organic matter. In anoxic environments, conditions are established to deter benthic

scavengers and protect organic matter from oxidation (Rojas et al., 2013). Favorable conditions for organic-carbon enrichment occur in low energy environments where fine-grained mineral particles are deposited slowly and light, low density organic matter accumulates faster than it is destroyed (Tourtelot, 1979; Rojas et al., 2013). Conventional models also share several other key commonalities. They state that fine-grained particles are delivered to the water bottom by suspension settling processes and mudstone variability is driven by the productivity of the overlying oxic environment versus detrital particle input. Generally, the point where conventional models differ is related to the mechanisms in which bottom water anoxia and water column stratification are generated (Tourtelot, 1979; Laracy, 2012).

In recent years, conventional depositional models for the production and preservation of organic matter have been closely re-examined. Studies (e.g., MacQuaker and Howell, 1999; Macquaker and Jones, 2002; MacQuaker and Adams, 2003; MacQuaker and Bohacs, 2007; Schieber et al., 2007; Schieber and Southard, 2009) demonstrate that persistent anoxia is not always required for the preservation or accumulation of organic-rich mudstones and that mudstones are in all likelihood deposited in higher energy environments than once perceived. Moreover, recent studies also indicate suspension settling processes are not the only dominant mud transport mechanism and mudstone variability reflects not only changes in productivity but also changes in detrital input (e.g., MacQuaker and Howell, 1999; Macquaker and Jones, 2002; MacQuaker and Adams, 2003; MacQuaker and Bohacs, 2007; Schieber et al., 2007; Schieber and Southard, 2009, Laracy, 2012).

### **1.09.02 Depositional Models for Organic-rich Mudstones in Lacustrine Settings**

In recent years, the breadth of research on both ancient and modern lake systems and their relation to source rock potential has increased significantly. Recent publications (e.g., Katz, 1990; Anadón et al. 1991; Carroll and Bohacs, 1999; 2001, Bohacs et al., 2000; 2003) on basin-scale lacustrine environments integrate sedimentology, stratigraphy, biofacies, and inorganic and organic geochemistry. While research on modern and Quaternary deposits often focuses on sediment delivery and dispersal patterns together with organic production and preservation rates (Bohacs et al., 2000). Together, modern and ancient sediment studies have increased our understanding of controlling factors on the occurrence, distribution, and hydrocarbon generative potential of ancient lake deposits (Bohacs et al., 2000).

Bohacs et al. (2000; 2003), along with works by Carroll and Bohacs (1999; 2001), have developed a model for predicting sedimentation patterns, hydrocarbon play elements (source, seal, reservoir), and hydrocarbon characteristics of lacustrine basins from the analysis of geological and geochemical indicators. Their predictive model is based on two factors that govern lake sediment deposition: (1) climate (precipitation/evaporation ratio), and (2) tectonics (Bohacs et al., 2000). The authors have noted a linked relationship of water+sediment supply with climate, and accommodation space with tectonism. They have used these relationships to derive a predictive model that groups together three end-member types of lake-basins. The end-member lake-basin types include: “overfilled” lake basins, “balance-filled” lake basins, and “underfilled” lake basins. These end-member lake-basin types are defined based on parasequence

models for stacking patterns, facies associations, sedimentary structures, geochemical indicators, biomarker assemblages, and organic maceral compositions (Bohacs et al., 2000; 2003, Carroll and Bohacs, 1999; 2001). The three end-member lake basin types include:

**(1) Overfilled Lake Basins:** Overfilled lake basins form when the rate of water+sediment is greater than the available accommodation. This typically occurs in systems where precipitation/evaporation (P/E) rates are high or where subsidence is low. Deposits in overfilled lake basins are commonly interbedded with fluvial deposits and coals. Water-level fluctuations in overfilled basins are minimal as water outflows are in equilibrium with inflows. This relatively constant water level records stratal sections that lack strong vertical lithological variation. Parasequences development is influenced mainly by fluvial channel avulsion and shoreline progradation. Overfilled lake basins are characterized by Type I-III kerogen (strongly influenced by terrestrial organic matter), and typically have low to moderate TOC values. Source rocks generate both oil and gas (Bohacs et al., 2000).

**(2) Balance-Filled Lake Basins:** Balance-filled lake basins form when accommodation space is roughly in balance with sediment+water supply. In these lake-basins, water inflows do not match outflow rates and therefore, the water inflows can periodically fill accommodation space. Lake fluctuations are commonly influenced by climatic cycles that periodically expose lake margins to desiccation and fluvial erosion. Basin fill thus records both progradation of clastics and vertical-aggradation related to desiccation. Balance-filled lakes typically have high rates of organic-carbon enrichment given favorable combinations of chemical stratification, water depth, primary

productivity, and burial rates (Bohacs et al., 2000). This results in the highest TOC enrichments of all three end-member types of lake basins, with predominantly Type I but also mixed Type I-III kerogen on sequence boundaries (Bohacs et al., 2000).

**(3) Underfilled Lake Basins:** Underfilled lake basins are created when accommodation space is high compared to low supplies of water+sediment (Bohacs et al., 2000). Given the large accommodation space and limited water+sediment, these lakes have closed drainage hydrology resulting in short lived lakes with shorelines that fluctuate greatly. Desiccation is common in underfilled lake basins, as are thin parasequences. Common depositional environments in underfilled basins include mudflats, perennial saline lakes, saline playas, and deep perennial saline lakes. During periods of highstand, facies can include carbonates, evaporites, laminates, organic-rich mudrocks, stromatolites, and littoral bioherms. During periods of lowstand, facies can include evaporites, mudflat deposits, eolianites, paleosols, and strata dominated with desiccation features. Productivity rates in underfilled lake basins is often high with source rocks dominated by Type I kerogen. However, source rocks are typically lean, given high rates of organic matter destruction due to frequent desiccation, erosion, and oxidation common to these lake environments (Bohacs et al., 2000; Renaut and Gierlowski-Kordesch, 2010).

As observed in the three-end member types of basins, tectonics and climate greatly influence sequence stratigraphic patterns (Carroll and Bohacs, 1999; Bohacs et al., 2000; Renaut and Gierlowski-Kordesch, 2010). Given the dynamic nature of climatic and tectonic variables over time, lake-basins often record a transition from one lake basin

type to another (underfilled, balance-filled, overfilled) through time (Bohacs et al., 2000). Changes in climate often influence lake deposits as cyclical patterns (e.g., represented in balance-filled lake basins as deepening and shallowing cycles). As precipitation/evaporation ratio increases over time, lake basins can evolve from underfilled to balance-filled lake basins. In contrast, as the precipitation/evaporation ratio decreases with time, lake basins dry up and evolve back to underfilled lake basins. Tectonic changes (e.g., activation of new basin-bounding faults) affect lake basins over longer time lines, resulting in varying subsidence rates often expressed as large scale changes in lake-basin type (Bohacs et al., 2000; Renaut and Gierlowski-Kordesch, 2010; Bohacs et al., 2000).

### **1.09.03 Controls on Organic Enrichment and Hydrocarbon Type in Lacustrine Settings**

The deposition and enrichment of organic-matter in lacustrine sediments can occur in both deep and shallow lakes. In shallow or swampy lake margins, thin coal seams and lignite deposits can be preserved in low oxygen settings generated from the accumulation of organic rich-peat, deposited from in situ macrophytes or vegetation. In contrast, in deeper water settings, carbonaceous shales or oil shales can be deposited from the accumulation of organic-rich oozes (Renaut and Gierlowski-Kordesch, 2010).

Organic matter bound in lacustrine sediments originates from both autogenic (microbial, bacterial or algal) and allogenic (stems, spores, pollen, leaves) organic material (Gierlowski-Kordesch, 2010) producing Type I to Type III kerogen types

(Powell, 1986). Organic matter from land plants can include herbaceous and woody plant material, whereas organic matter supplied from the water column may include cyanobacteria mats, phytoplankton, fish, microbial plates, rhizopod algae, submerged macrophytes and microphytes, charophytes, zooplankton, benthic organisms, and feces from larger grazing organisms (Kelts, 1988). The organic content concentration in lacustrine settings generally ranges from <1% to >20% (Powell, 1986). Cell membranes of autochthonous organic material are lipid rich and generally form oil-prone kerogens whereas allochthonous organic matter is more likely to generate gas-prone kerogens (Bohacs et al., 2000).

As in marine environments, the preservation and enhancement of organic matter in lacustrine environments is dependent on three factors. Organic matter enrichment requires an environment that has sufficient primary productivity, limited organic matter destruction (e.g., by microbial decay or post depositional factors), and organic matter must not be overly diluted by clastic or carbonaceous sedimentary input (Gierlowski-Kordesch, 2010).

Moreover, the accumulation of organic-rich rocks can occur in lake environments that have well mixed oxygenated or stratified and anoxic water columns. In well-oxygenated lakes, organic carbon enrichment can occur if primary productivity rates are greater than those of microbial decay and mineral dilution (Renaut and Gierlowski-Kordesch, 2010); however, it is common for organic matter to be destroyed by microbial respiration (Cole, 1979; Bohacs et al., 2000). Moreover, the preservation potential for organic matter in lakes with a stratified water column can be high if anoxic waters are

generated, thereby deterring benthonic scavengers and bacterial respiration from destroying organic matter (Kelts, 1988; Bohacs et al., 2000; Renaut and Gierlowski-Kordesch, 2010).

The degree of organic carbon enrichment and the type of organic matter produced are strongly influenced by lake basin type. Overfilled lake basins have high concentrations of terrestrial plant material input and aquatic production (Bohacs et al., 2000). Terrestrial organic matter typically exceeds aquatic production, thus, source rocks from these lake basins commonly generate more gas than other lake basin types (Bohacs et al., 2000). Moreover, organic enrichment in overfilled lake basins is commonly negatively affected by often constant clastic dilution by fluvial inputs. For preservation to be promoted, thermal stratification must occur in these lake basins (Bohacs et al., 2000).

Balance filled lakes have the most source rock potential with lake conditions that favor organic carbon enrichment. Here, seasonal/intermittent fluvial inputs supply the lake environments with organic matter that is then concentrated in the lake by evaporation (Bohacs et al., 2000). Organic matter preservation is favored when chemical stratification is developed and dilution is minimized. Commonly in these lake environments fluvial input is restricted to transgressions and often traps sediments in the near-shore environment thereby reducing dilution and favoring organic enrichment in the lake-centers (Bohacs et al., 2000).

In underfilled lake basins, primary productivity rates are often high and dilution by clastic input can be limited as sediments are often restricted to nearshore or lower lake

plain environments during highstands (Bohacs et al., 2000). Where underfilled lake basins struggle is with respect to the long-term preservation of organic matter, as underfilled lake basins experience frequent aerial exposures that can degrade organic matter (Bohacs et al., 2000). Both underfilled and balance filled lakes commonly have oil-prone source rocks from algal-bacterial material (Bohacs et al., 2000). A helpful table by Bohacs et al. 2000 summarizes the controls of organic matter development in all three lake basin types (Table 1).

**Table 1 Controls on organic-rich rock development in lake basins**

Table from Bohacs et al., 2000.

Lake Type	Production	Destruction	Dilution	Source Potential
<b>Overfilled</b>	+ Nutrient input increased – Fresh water input dilutes nutrients – Overall production decreases with increasing lake volume	– Increased oxygen supply to bottom – Homogeneous water mass makes wind mixing more effective – Cold underflow – Increased turbulence	– Abundant clastic detritus ± Abundant advected terrigenous clastics	• Moderate to poor oil/gas • Mixed gas/oil • Marked lateral variability TOC: <1–7% (muds) < 80% (coals) OMT: mixed algal/terrigenous (I/II) HI: 50–600 mg HC/g Relatively thick (< tens of meters)
<b>Balanced fill</b>	+ Appreciable nutrient input + Nutrients concentrated by episodic drying + Larger percent of lake volume in photic zone	+ Closed basin and episodic drying promotes density stratification + Large amount of production consumes oxygen at bottom	+ Varying, but relatively minor clastic detritus + Minor component of advected terrigenous organic matter – Episodic floods or flashy discharge may deliver significant clastic debris	• Moderate to excellent oil • Mostly oil, some gas? • Little lateral variation TOC: 1–30% OMT: mostly algal (I), some terrigenous (II) HI: 500–700 mg HC/g Relatively thin (1–10m)
<b>Underfilled</b>	± Variable nutrient input + Nutrients concentrated by episodic drying – Extreme concentration of solutes kills organisms – Water available for production only part of time	– Episodic drying oxidizes organic matter – Episodic freshening introduces oxygen, consumers	– Semi-arid climates yield highest clastic input + Minimal input of terrigenous organic matter + Significant amount of fill due to precipitated minerals	• Poor to excellent oil • Mostly oil • Minimal lateral variation TOC: <0.5–20% OMT: Algal (Type I), HI: 650–1150 mg HC/g Relatively thin (meters)

\* + Positive for organic enrichment, – Negative for organic enrichment, ± Variable influence on organic enrichment, TOC = total organic carbon, OMT = organic matter type, HI = hydrogen index.

## CHAPTER TWO: METHODS

### 2.01 — General Methodology

The data presented in this thesis are derived from outcrop samples collected from localities in the Conche study area, and include measured stratigraphic sections where geological and sequence-stratigraphic relationships are observed. In all of these localities, the Cape Rouge Formation is targeted for study and samples are collected, documented and photographed as stratigraphic sections are logged.

Stratal sections of the Cape Rouge Formation are examined and measured to resolve stratigraphic stacking patterns, distribution of hydrocarbon play element (location of source prone intervals), lake-basin style and fill evolution. Four sections are logged from localities that include the Conche Peninsula (Fox Head and the western coast), Cape Rouge Peninsula (Pyramid Point) and Rouge Island (Figure 2.1). Moreover, general geologic observations and facies trends collected from cliff-face exposure, are used to underpin the regional distribution, variation, and occurrence of facies and oil seeps. These widespread observations, in congruence with data collected from rock samples, aid in the determination of lake-style, evolution, and source prospectivity.

Mudstone samples collected from fine-grained facies assemblages throughout the study area (Figure 3.1, p.61) are analyzed by optical and electron microscopy together with a suite of geochemical source rock analyses. Geochemical analyses include a suite

of thermal maturation analyses (vitrinite reflectance (% R<sub>o</sub>), visual kerogen, and Thermal Alteration Index (TAI)), Rock-Eval Pyrolysis and Total Organic Carbon (TOC).

## **2.02 — Field Work Methods**

### **2.02.01 Field Accessibility, Location and Access**

The Conche Peninsula is located at the end of Highway NL-434 on the eastern seaboard of the Northern Peninsula, Newfoundland. A series of walking and ATV trails transect the Conche Peninsula and greatly aid access to the coastline and cliff faces (Figure 2.1). On this peninsula, up to one third of the coastline is not easily accessible. Steep cliff faces are studied from nearby lookouts (Glass Hole, Saunders Gulch, and Conche lookouts) or by boat (Figure 2.1). The eastern coastline (from Frauderesse Point to the Glass Hole Lookout) consists of near vertical ocean facing cliffs where stratigraphic sections cannot be studied in detail. Both the northern and western coastlines of the Conche Peninsula can be traversed entirely by foot, excluding several small sections where inland routes must be taken.

To the north of the Conche Peninsula, the Cape Rouge Peninsula has no road access; it can be reached only by boat. Over half of that coastline is made up of steep cliffs with limited access. The southern shoreline (Truite Point area) has some narrow cobble beaches where some cliff face exposures can be accessed and measured. Other short sections are accessible on the western coast of the peninsula and where abandoned pastures expand to the edge of the bay. Pyramid Point, located at the northwestern tip of the Cape Rouge Peninsula, provides some of the best exposures of the Cape Rouge

Formation on the peninsula. However, there are no cobble beaches for landing.

Disembarking at the base of jagged cliffs is challenging and can only be done when the ocean is calm. Moreover, the entire Pilier Bay area has few accessible landing areas as cobble beaches are scarce and cliff faces steep (Figure 2.1).

Islands to the east, including Rouge Island, Red Island and Groais Island, must be accessed with caution. Outcrops can be best accessed on the western coast of Rouge Island, the southern tip of Red Island, and the northwestern tip of Groais Island. Pigeon Island was not visited as sea conditions made landing unsafe (Figure 2.1).

### **2.02.02 Field Work Techniques**

Strata of the Cape Rouge Formation are logged and described in a manner similar to procedures outlined in Stow (2006). Given the abundance of faults throughout the peninsulas and steep cliff faces rising from the sea, assembling long, continuous stratigraphic sections in the area is not possible. As an alternative strategy, shorter continuous sections (20-160 meters TVT) at accessible locations are measured, collected and photographed to provide a context for basin-fill type, and to understand the distribution of fine-grained facies and other hydrocarbon play elements in the area. Four stratigraphic successions presented in this thesis represent the varieties and assemblages of strata for the Cape Rouge Formation. Where fine-grained sections are exposed and accessible (Figure 2.1), suites of mudstone samples are collected in evenly distributed younging upwards successions (Figure 2.2). Later, in the lab, these rocks are subsampled

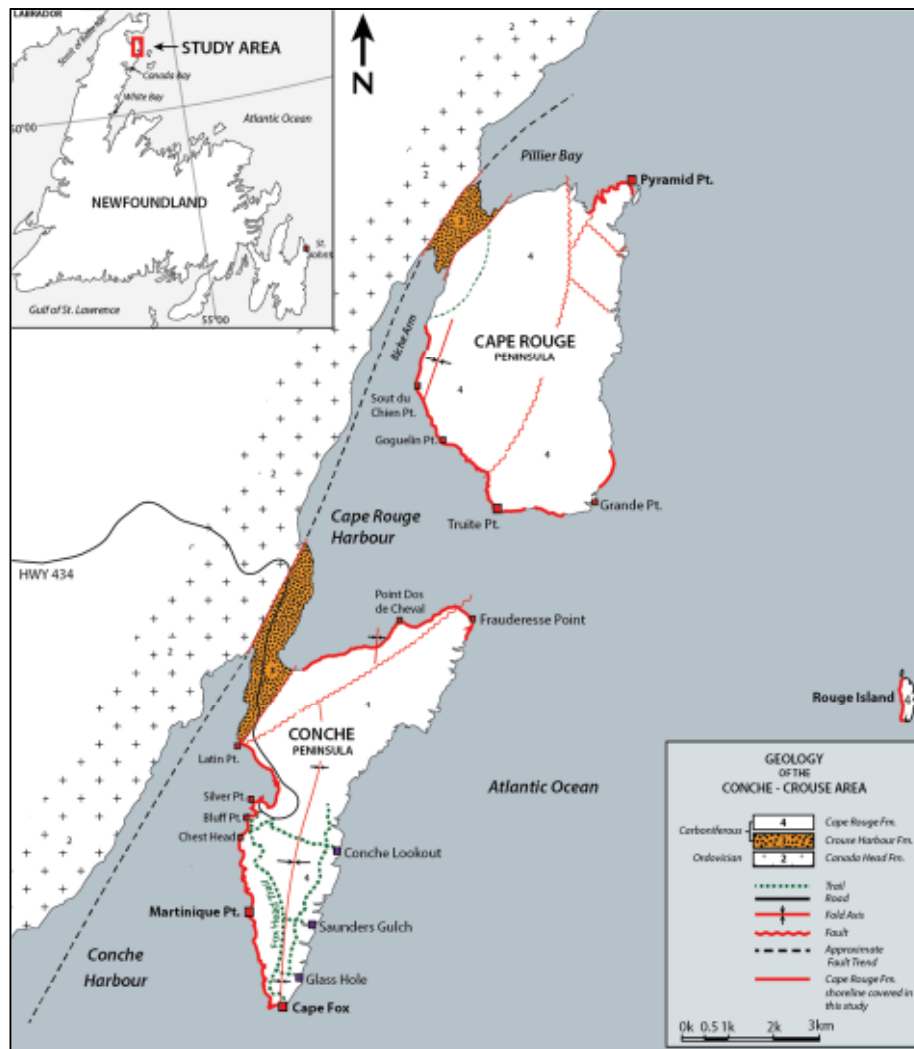


**Figure 2.1 Geological map of the Conche and Cape Rouge peninsulas with accessible routes and shorelines**

Map modified from Baird (1966). Map features highway, roads, trails (dashed green), cliff face lookouts (dark purple squares), geological formations, and large-scale structures. Coastline exposures of the Cape Rouge Formation studied in this thesis are highlighted with red solid lines. The shoreline of the Cape Rouge Peninsula from Cape Fox to Latin Point is nearly completely accessible by foot with a few exceptions where inland routes must be taken. On the Cape Rouge Peninsula, the shoreline from Truite Point to the mouth of Birch Arm has limited accessibility from land and sea. A short area of coastline north of Grande Point is accessible as is a 400m shore west from Pyramid Point. There is easy access to the Crouse Harbour rocks in the isthmuses of the Cape Rouge and Conche peninsulas. Islands to the east including Red Island, Pigeon Island, and Groais Island are excluded from this map.

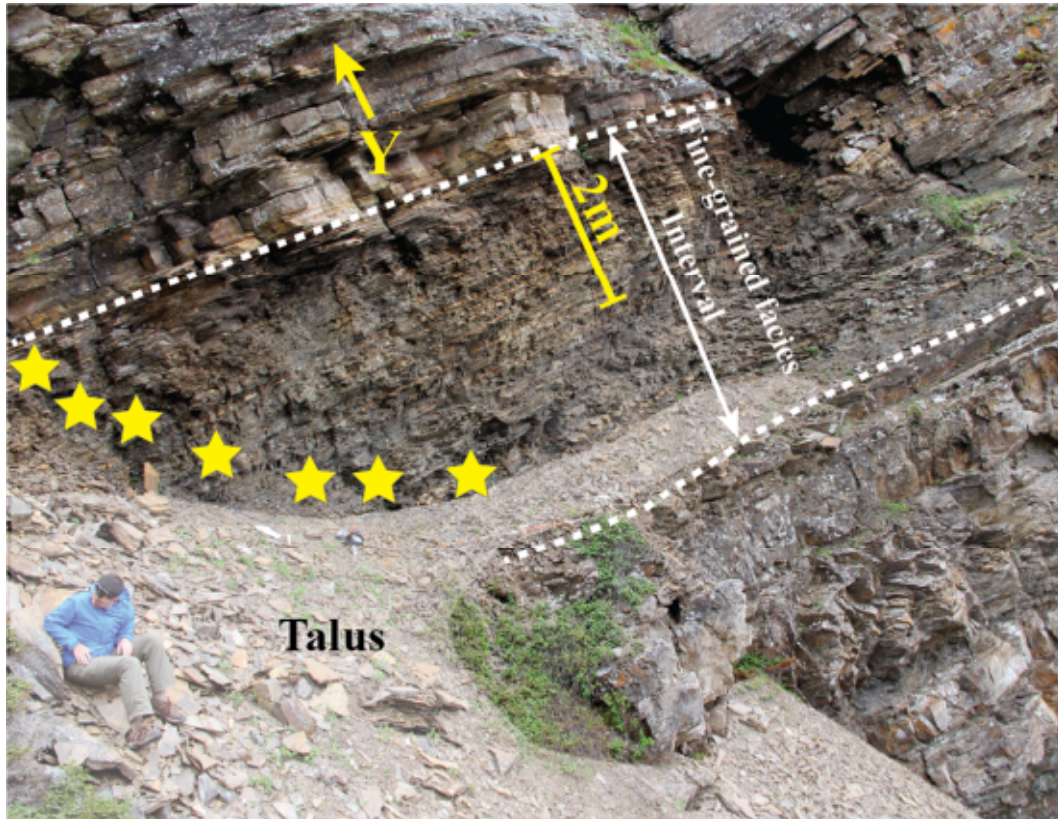


**Figure 2.2 Outcrop photo of a fine-grained interval of the Cape Rouge Formation**  
Yellow stars denoting sample locations. Exposure younging upwards (yellow arrow).

for Rock-EVAL, TOC, and thermal maturation analysis. In addition, many of the samples collected for geochemistry are also prepared for thin sections analysis.

### 2.03 — Petrographic Techniques & Nomenclature

Lithofacies classification for fine-grained sedimentary rocks follows the nomenclature system of MacQuaker and Adams (2003). In this classification, mudstones are fine-grained sedimentary rocks with >50% of the material being 63 $\mu$ m or less in size (MacQuaker and Adams, 2003). Moreover, the authors provide a means of descriptive classification based on the presence of major rock constituents (that include grain origin, size and mineralogy) together with the fine-grained textural characteristics. In order to follow this descriptive classification scheme, optical and electron (backscattered electron imagery) microscopy analysis is completed to study textural characteristics and rock constituents (MacQuaker and Adams, 2003). For this study, thirty (30) fine-grained samples of varying grain-size and composition are analyzed by optical and scanning electron microscopy. Polished thin-sections cut to  $\sim$ 20 $\mu$ m x 24mm x 46mm and larger 20 $\mu$ m x 51mm x 76mm dimensions by Wagner Petrographic in Utah, are scanned with an Epson 1250 flat-bed scanner, to record and document textural details at a  $10^{-2}$  to  $10^{-3}$ m scale. Optical petrography is completed at Memorial University on a Nikon Eclipse E600 polarized light microscope with a Nikon digital DXM1200F camera. Optical microscopy provides a platform for generating petrographic descriptions of mineral composition (both framework and matrix grains) and distribution, grain-size, fabric, textural information and sedimentary structures at a  $10^{-3}$  to  $10^{-4}$  m-scale.

In addition to optical petrography descriptions, electron microscopy is completed on fine-grained samples using a Scanning Electron Microscope (SEM) offering Backscattered Electron (BSE) imagery. Electron microscopy is used to characterize

mineralogy and textural relationships at a  $10^{-4}$  to a  $10^{-5}$  m-scale. Before analysis, all thin sections are coated in carbon. For mineralogy and the study of textural relationships and grain boundaries, samples are analyzed using a FEI Mineral Liberation Analyzer (MLA) 650 Field Emission Gun (FEG) and Scanning Electron Microscope (SEM) instrument. The MLA instrument is fitted with XFlash drift and Backscattered Electron (BSE) detectors and Energy Dispersive x-ray (EDS) Spectrometers. The MLA operates at an accelerating voltage of 25.00 kV with a  $10\mu\text{A}$  beam current (spot size  $5.31\mu\text{m}$ ) at an approximate working distance of 15mm.

## **2.04 — Organic-Matter Characterization**

There are a variety of standard geochemical and petrographic methods used in hydrocarbon exploration to characterize sedimentary organic matter and determine the hydrocarbon-generating capacity of a sedimentary rock sample (Philip and Galvez-Sinibladí, 1991; Peters and Cassa, 1994; Peters et al., 2005; Rojas et al., 2013). Common source rock analyses include: (1) organic geochemistry (e.g., TOC, Rock-Eval<sup>®</sup>, Gas Chromatography (GC), GC/mass spectrometry); (2) organic petrography (e.g., maceral identification, visual kerogen, vitrinite reflectance, thermal alteration index); and (3) palynology (spore, algae and phytoclast identification). Results from these analyses provide information on the quality, quantity, type and thermal maturity of sedimentary organic matter (Philip and Galvez-Sinibladí, 1991; Peters and Cassa, 1994; Peters et al., 2005).

Source potential is evaluated based on the quality and quantity of kerogen macerals trapped in sedimentary rocks. The quantity of organic matter is determined from measurements that establish the total organic carbon (TOC) expressed as a percentage of whole-rock weight (wt.%) (Table 2). Moreover, the quality of organic matter in sedimentary rocks can be determined from Rock-Eval<sup>®</sup> Pyrolysis parameters (estimates the amount of organic hydrogen and oxygen present and its thermal maturity), vitrinite reflectance and visual kerogen analysis (determines thermal maturity and organic matter types, respectively) (Table 3, Table 4, Table 5). Together these routine geochemical and petrographic techniques help resolve the type, amount, and thermal maturity of organic matter. From these analyses, the type of petroleum generated (if any) and the remaining generating potential may be determined (Peters et al., 2005b; Rojas et al., 2013).

**Table 2 Geochemical parameters describing the petroleum potential (quantity) of immature source rocks (from Peters and Cassa, 1994)**

Petroleum Potential	Organic Matter		
	TOC	Rock-Eval Pyrolysis	
	Weight %	S <sub>1</sub>	S <sub>2</sub>
Poor	0-0.5	0-0.5	0-2.5
Fair	0.5-1	0.5-1	2.5-5
Good	1-4	1.-2	5-10
Very Good	2-4	2-4	10-20
Excellent	>4	>4	>20

**Table 3 Geochemical parameters describing kerogen type (quality) and character of expelled products (from Peters and Cassa, 1994)**

Source Rock Quality	TOC (Wt.%)	Pyrolysis S <sub>2</sub>
None	<0.5	<2
Poor	0.5-1	2-3
Fair	1-2	3-5
Good	2-5	5-10
Very Good	>5	>10

Product Type	Kerogen Type	Hydrogen Index
Gas	III	50-200
Mixed Gas + Oil	II/III	200-300
Oil	II	300-600
Oil	I	>600

**Table 4 Geochemical parameters describing thermal maturation levels (from Peters and Cassa, 1994)**

Stage of Thermal Maturity	Maturation		
	R <sub>o</sub> (%)	T <sub>max</sub> (°C)	TAI
Immature	0.2-0.6	<435	1.5-2.6
Early Mature	0.6-0.65	435-445	2.6-2.7
Peak Mature	0.65-0.9	445-450	2.7-2.9
Late Mature	0.9-1.35	450-470	2.9-3.3
Postmature	>1.35	>470	>3.3

For this study several industry standard methods and techniques are employed to refine the source potential (organic matter quality and quantity and thermal maturity) for fine-grained rocks of the Cape Rouge Formation. These include:

- (1) LECO Total Organic Carbon (TOC),
- (2) Rock-Eval<sup>®</sup> Pyrolysis,
- (3) Vitrinite Reflectance (% R<sub>o</sub>),
- (4) Visual Kerogen, and
- (5) Thermal Alteration Index (TAI).

Eighty-nine (89) samples (28 samples from the Cape Rouge Peninsula, 52 samples from the Conche Peninsula, and 9 samples from Rouge Island) are analyzed by LECO TOC and Rock-Eval Pyrolysis geochemical techniques. Moreover, 14 samples (5 from the Cape Rouge Peninsula, 7 from the Conche Peninsula, and 2 from Rouge Island) are analyzed by optical petrography for %R<sub>o</sub>, visual kerogen, and TAI. Geochemical and optical petrography analysis is completed at Geomark Research, Ltd. source rock laboratory in Humble Texas. R<sub>o</sub>, visual kerogen, and TAI analysis is completed by Dr. Bob Landis of Geomark Research laboratory. All analyses follow laboratory methodology and procedures published by Peters et al. (2005).

#### **2.04.01 Visual Kerogen**

Visual kerogen analysis is completed on maceral populations from 14 samples from the study area (Figure 3.1). Macerals are defined as organic matter components in coal or sedimentary rocks that have distinct chemical and physical characteristics (Spackman, 1958; Peters and Cassa, 1994; Stasiuk et al., 2002; Hackley 2016). They are

**Table 5 Classification of organic matter in sedimentary rocks (From Stasiuk et al., 2002)**

Group	Maceral	Comment (added herein)
Vitrinite	Telinite	In practice, the individual macerals of the vitrinite group are indistinguishable in fine-grained shales and therefore collectively identified as 'vitrinite'.
	Collotelinite	
	Vitrodetrinite	
	Collodetrinite	
	Gelinite	
Liptinite	Corpogelinite	Occurs as discrete bodies (telalginite) and lamellar masses (lamalginite)
	Alginite	
Inertinite	Bituminite (amorphinite)	Amorphous organic matter. Occurs as a continuum grading from organic-rich (lamalginite) to mineral-rich (mineral bituminous groundmass).
	Liptodetrinite	
	Sporinite	
	Cutinite	
	Suberinite	
	Resinite	
	Chlorophyllinite	
	Fusinite	
	Semifusinite	
	Funginite	
Secretinite		
Inertinite	Macrinite	Similar to the Vitrinite Group, the individual macerals of the inertinite group generally are not distinguished in practice.
	Micrinite	
	Inertodetrinite	

grouped into four main groups based upon their source and composition. These include:

1) liptinite, derived from algal material; 2) vitrinite, derived from woody tissue from vascular plants; 3) Inertinite, which includes macerals exposed to oxidation or combustion (Table 5); and 4) amorphous organic matter (bituminite), derived from bacterial or algal precursors (Peters and Cassa 1994, Hackley 2016). Maceral identification helps define environments of deposition and, potentially, hydrocarbon types.

#### **2.04.02 Leco Total Organic Carbon (TOC)**

TOC measurements, corresponding to total organic carbon per gram of rock (measured in wt.%), are a standard means for determining organic richness (organic matter quantity) of a rock. TOC consists of three components: (1) carbon in extractable organic matter (EOM carbon), (2) convertible carbon, and (3) a residual carbon fraction (Jarvie, 1991) (Figure 2.3). EOM generally forms a small part of a sample and is composed of carbon enclosed in hydrocarbons that have already formed from the thermal cracking of kerogen but are not yet expelled (Jarvie, 1991). Convertible carbon is material remaining in kerogen and continuing to hold some hydrocarbon generating potential for a sediment sample (Jarvie, 1991). In contrast, residual carbon is a part of the kerogen that carries no remaining potential to generate hydrocarbons. This is mainly due to the chemical structure and composition (low hydrogen per unit of organic carbon) of this organic matter (Jarvie, 1991) (Figure 2.3).

In this study, TOC is measured with the Leco combustion method and analyzed on a LECO C230 instrument. Larger samples are crushed and divided into 1g test samples. In order to remove inorganic carbon (e.g., carbonates), pulverized samples are dissolved in hydrochloric acid (HCL) for a minimum of 2 hours. When the dissolution of carbonates is complete (samples do not effervesce when agitated), samples are rinsed and washed through a filtration apparatus to remove the acid. The samples are then placed in the LECO crucible and dried in a low temperature oven (110°C) for a minimum of 2 hours. After drying, samples are weighed to obtain % carbonate based on weight loss.

To determine TOC, the LECO C230 instrument is first calibrated to a standard that has a known carbon concentration. This is completed by combustion of known standards by heating to 1200°C in the presence of oxygen. Combustion products include carbon monoxide and carbon dioxide. The combustion of unknown samples is then completed and the response is compared to that of the calibrated standard, thereby generating a known TOC value (Jarvie, 1991).

For quality checks, standards are routinely analyzed with the unknowns. Moreover, random and selected reruns are completed to verify data. The acceptable standard deviation for a TOC measure is 3% variation from an established value.

#### **2.04.03 Rock-Eval Pyrolysis**

Rock-Eval pyrolysis is a method that provides data on the quality, type, and thermal maturity of organic matter and the petroleum potential of a rock sample (Philip and Galvez-Sinibaldi, 1991). It is used to determine source quality by estimating ratios for organic hydrogen and oxygen released during heating and volatilization of a rock in a laboratory environment (for a complete guideline for evaluating rock samples using Rock-Eval pyrolysis refer to Peters (1986) and Rojas et al. (2013)).

Pyrolysis refers to a controlled heating program of organic matter bound in whole rock samples, that, in the absence of oxygen, yields hydrocarbons and CO<sub>2</sub> (Peters, 1986). Upon completion of a pyrolysis analysis, the recorded output, known as a Rock-Eval pyrogram, consists of three peaks (referred to as S<sub>1</sub>, S<sub>2</sub>, S<sub>3</sub>) and a temperature maximum (T<sub>max</sub>) measurement (Figure 2.4). The first peak (S<sub>1</sub>) represents the

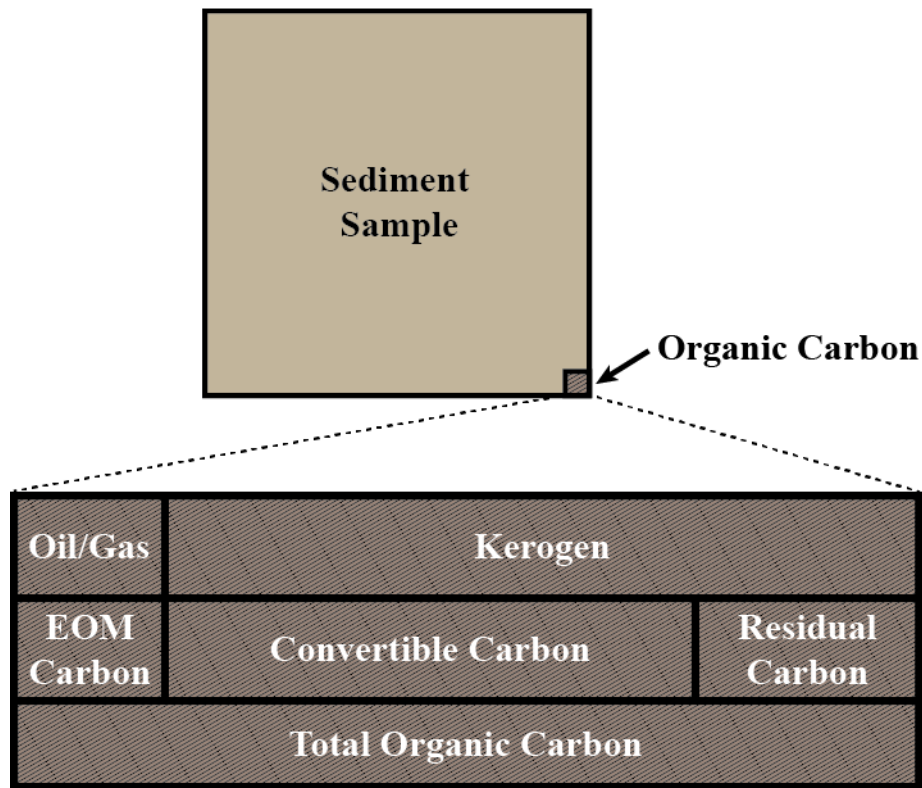


**Figure 2.3 A graphical depiction of TOC in a sedimentary sample**

TOC is made up of three constituents including extractable organic matter (EOM), convertible carbon (remaining potential to generate hydrocarbons), and the residual carbon (no remaining potential to generate hydrocarbons) (after Jarvie, 1995).

amount of hydrocarbons thermally distilled from a rock at a pyrolysis temperature of approximately 300°C (Philip and Galvez-Sinibaldi, 1991; Peters et al., 2005). The S<sub>1</sub> peak is commonly known as the “free oil content” and reported as mg Hydrocarbon (HC)/g rock (Rojas et al., 2013). This peak represents the quantity of hydrocarbon volatilized out of the rock without cracking the kerogen (Espitalie et al. 1977, 1987). The second peak (S<sub>2</sub>) shows the remaining hydrocarbon generating potential of a sample (as mg HC/g rock), and represents the quantity of hydrocarbon released following the

cracking of kerogen (Espitalie et al. 1977, 1987, Philip and Galvez-Sinibaldi, 1991; Rojas et al., 2013). A  $T_{\max}$  measurement is generated at the temperature for peak kerogen conversion. The final peak ( $S_3$ ) represents the quantity of organic  $\text{CO}_2$  released at temperatures up to  $390^\circ\text{C}$ , and is measured in  $\text{mg CO}_2/\text{g rock}$  (Figure 2.4). The  $S_1$ ,  $S_2$ ,  $S_3$  and  $T_{\max}$  measurements are used to characterize source rocks and decipher the basic chemistry and maturity of organic matter in sedimentary rocks (Philip and Galvez-Sinibaldi, 1991; Rojas et al., 2013).

In this study, Rock-Eval pyrolysis is completed with a Rock-Eval II instrument at Geomark Research Ltd. source rock laboratory. Before analysis, whole rock samples are weighed to approximately 100 milligrams, washed, and ground (60 mesh) to a powder. The Rock-Eval II instrument is calibrated with a known rock standard. The standard values are determined from a calibration curve for pure hydrocarbons of varying concentrations. The rock standard is analyzed as an unknown every 10 samples, therein providing a quality control and check upon instrument calibration. If standard results do not meet specifications, the preceding data are rejected, the instrument is recalibrated, and samples are re-analyzed. Acceptable standard deviations for an analysis are:  $T_{\max}$ :  $\pm 2^\circ\text{C}$ ;  $S_1$ : 10% variation from established value;  $S_2$ : 10% variation from established value; and  $S_3$ : 20% variation from established value. The data are checked selectively and randomly on 10% of the samples.

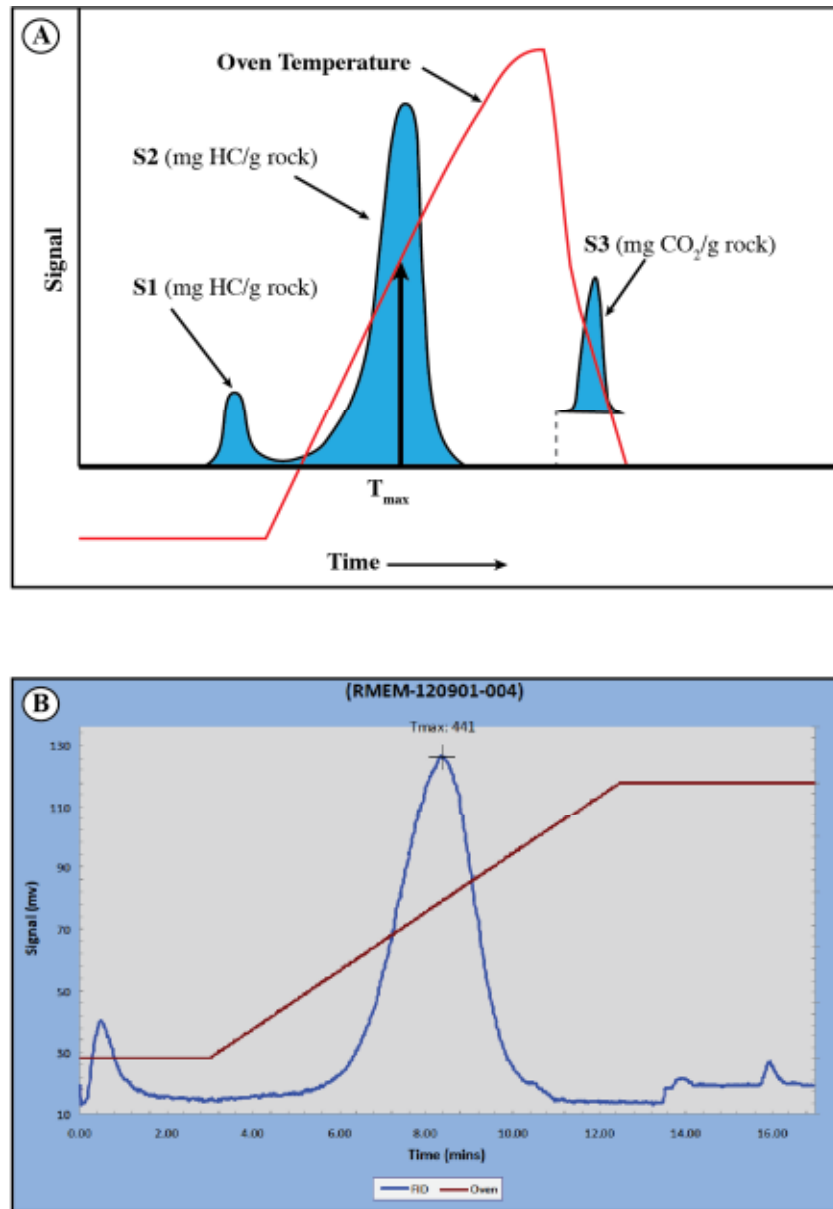


**Figure 2.4 Schematic pyrograms depicting the evolution of organic compounds from a rock sample during a Rock-Eval pyrolysis heating program**

A) Notable pyrogram measurements (after Peters, 1986) show the S<sub>1</sub>, S<sub>2</sub> and S<sub>3</sub> peaks and T<sub>max</sub> generated during Rock-Eval pyrolysis. T<sub>max</sub> intersects the oven temperature where S<sub>2</sub> peak is at a maximum. B) An example pyrogram from this thesis analyzed with a Rock-Eval II instrument with a flame ionization detector (FID). The blue line represents signal from the FID detector and the red line represents the oven temperature. Time (mins) increases from left to right.

## **2.05 — Thermal Maturation Analysis**

Fourteen (14) samples are analyzed for vitrinite reflectance (% R<sub>o</sub>), visual kerogen, and TAI, following the standard analytical procedures described by Peters et al. (2005). Results are used to assess the thermal maturity of rock samples and to verify Rock-Eval maturity estimates.

### **2.05.01 Measured Vitrinite Reflectance**

Vitrinite Reflectance (% R<sub>o</sub>) is an industry standard optical tool for characterizing organic matter and is used as a reliable indicator of organic maturation of sedimentary rocks (Senftle and Landis, 1991; Peters et al., 2005). This analysis is widely considered the most robust tool for determining thermal maturation (Hackley et al., 2015) and is critical to understanding source rock potential.

Vitrinite, a common maceral in kerogen, is derived from terrestrial plants (post Silurian in age) and can be divided into telinite (retains plant structure) and collinite (unstructured). As a rock sample containing vitrinite becomes thermally mature (exposed to increasing heat), the vitrinite macerals become aromatized and reflective, with increasing reflectivity corresponding with an increase of heat. This reflective nature is caused by changes in the composition of the kerogen which typically consists of abundant carbon-ring structures. When the carbon rings in vitrinite are aromatized they develop a more planar character than carbon rings that have not been heated, and therein reflective in nature. The end point for aromatization is the development of graphite, wherein all carbon is aligned (Peters et al., 2005). Vitrinite R<sub>o</sub> (%) values correspond to

various stages of petroleum generation maturation; these include: immature:  $R_o$  (%) = 0.20-0.60; early mature:  $R_o$  (%) = 0.60-0.65%; peak maturity: 0.68-0.90%; late mature: 0.90-1.35%; postmature:  $R_o$  (%) = >1.35%.

Fourteen samples are analyzed for  $R_o$  following laboratory guidelines outlined by Peters et al. (2005). From a rock sample, kerogen macerals are isolated from matrix material, embedded in epoxy, and polished with fine alumina grit. A petrographic microscope equipped with a photometer measures the incident white light reflected from the vitrinite phytoclasts in the kerogen samples.  $R_o$  (%) represents a mean value from a varying number of indigenous (autochthonous or first cycle) phytoclasts for each sample. Allochthonous (recycled) and contaminated (suppressed) vitrinite are also measured but not included in the mean  $R_o$  (%) value. The number of measured particles range from 5-51 phytoclasts per sample.  $R_o$  results for all phytoclasts are displayed as histograms of  $R_o$  versus frequency (Figure 2.5) (Peters et al., 2005). For each histogram, as shown in Figure 2.5, phytoclasts are subdivided according to the number of autochthonous (first cycle), allochthonous (recycled) and suppressed vitrinite (lower  $R_o$ ) grains.

#### **2.05.02 Calculated Vitrinite Reflectance ( $R_o$ Calculated)**

Rock-Eval pyrolysis can be used to estimate thermal maturity of a rock sample using  $T_{max}$  measurements and the Production Index (PI) (Peters et al., 2005). The Production Index (PI) is calculated from the ratio of  $S_2$  to the sum of  $S_1 + S_2$  ( $PI = S_2 / (S_1 + S_2)$ ) and is used to determine the evolution of organic matter (extent of petroleum generation) (Philip and Galvez-Sinibaldi, 1991; Rojas et al., 2013).  $T_{max}$  and PI are often

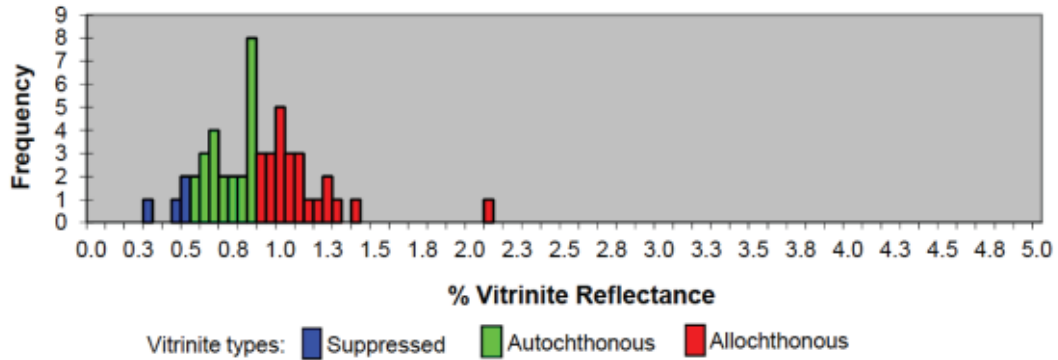


**Figure 2.5 Example of a vitrinite reflectance (%) vs frequency graph histogram for a kerogen isolated from sample (Ln12021-H).**

Kerogen is divided into suppressed (blue), autochthonous (green) and allochthonous (red).

used as thermal maturity indicators, but also depend on the organic matter present, along with other factors. Thermal maturity estimated by Rock-Eval pyrolysis should therefore also be accompanied by other geochemical measurements, including vitrinite reflectance, biomarker parameters, and/or TAI (Peters et al., 2005). Rock-Eval  $T_{max}$  can be converted to vitrinite reflectance ( $R_o$ ) using a simple linear equation:

$$R_o \text{ (Calculated)} = [(0.0180 \times T_{max}) - 7.16]$$

This formula, derived by Jarvie et al. (2001), generates good results for Type II and Type III kerogens with less consistent results for Type I kerogens (Peters et al., 2005). It is not recommended to use this formula on very low ( $T_{max} < 420^\circ\text{C}$ ) or high ( $T_{max} > 500^\circ\text{C}$ ) maturity samples or when  $S_2$  is less than 0.50 mg HC/g rock (Peters et al. 2005). This method for calculating  $R_o$  from  $T_{max}$  should not be used for predicting maturities on individual samples, but rather should be used as estimates on large sample

populations (Peters et al. 2005). Given the inconsistencies with using this method for samples with Type I kerogen, calculated vitrinite reflectance is accompanied by other quantitative geochemical techniques (measured vitrinite reflectance and thermal alteration index) and is used only as a rough estimate for thermal maturities on the total sample population.

### **2.7.2 Thermal Alteration Index (TAI)**

Thermal Alteration Index (TAI) is a numerical scale based on the colour changes that palynomorphs experience with increasing burial (Peters et al., 2005). This method is functional, given that with increasing maturity, palynomorphs change colour from yellow to brown to black (Peters et al., 2005). For hydrocarbon exploration, the most important colour changes are those that occur between a TAI of 2.4-3.1 during the peak of oil generation. Furthermore, the visual examination of the TAI aids in the discrimination of reworked organic matter, enabling the proper estimation of the thermal maturity of a given sample (Peters et al., 2005).

Fourteen (14) samples were measured for TAI following procedures outlined by Peters et al., (2005). TAI analysis is performed using a split-stage comparison microscope where samples are viewed simultaneously with standards (Peters et al., 2005). The TAI scale for this study ranges from 0 (very pale yellow) to 4 (black) and is correlated with vitrinite reflectance. TAI measurements are accurate up to 0.1 units (Peters et al., 2005).

## CHAPTER THREE: STRATIGRAPHIC RESULTS

### 3.01 — Introduction

Chapter three presents geological results from fieldwork observations and laboratory studies of the Cape Rouge and Crouse Harbour formations. Below, four stratigraphic sections representative of the formation are introduced as measured reference strata.

Following the development of a stratigraphic framework, sections from localities on the Conche and Cape Rouge peninsulas and offshore at Rouge Island ( Figure 3.1) are used to define lithofacies assemblages for the Cape Rouge Formation.

### 3.02 — Sedimentary Geology of the Conche Region

An estimated 1500 m of Lower Carboniferous strata is exposed in the Conche area and includes approximately 1200 m of the Cape Rouge Formation and approximately 300 m of the Crouse Harbour Formation (Baird 1957; 1966, Hamblin et al., 1995).

#### 3.02.01 Strata of the Crouse Harbour Formation

The Crouse Harbour Formation is a coarse-grained facies association dominated by conglomerate and coarse-grained sandstone with lesser amounts of siltstone and carbonaceous mudstone, dolostone and fresh-water limestone. This formation is exposed on the isthmuses of the Cape Rouge and Conche peninsulas together with island

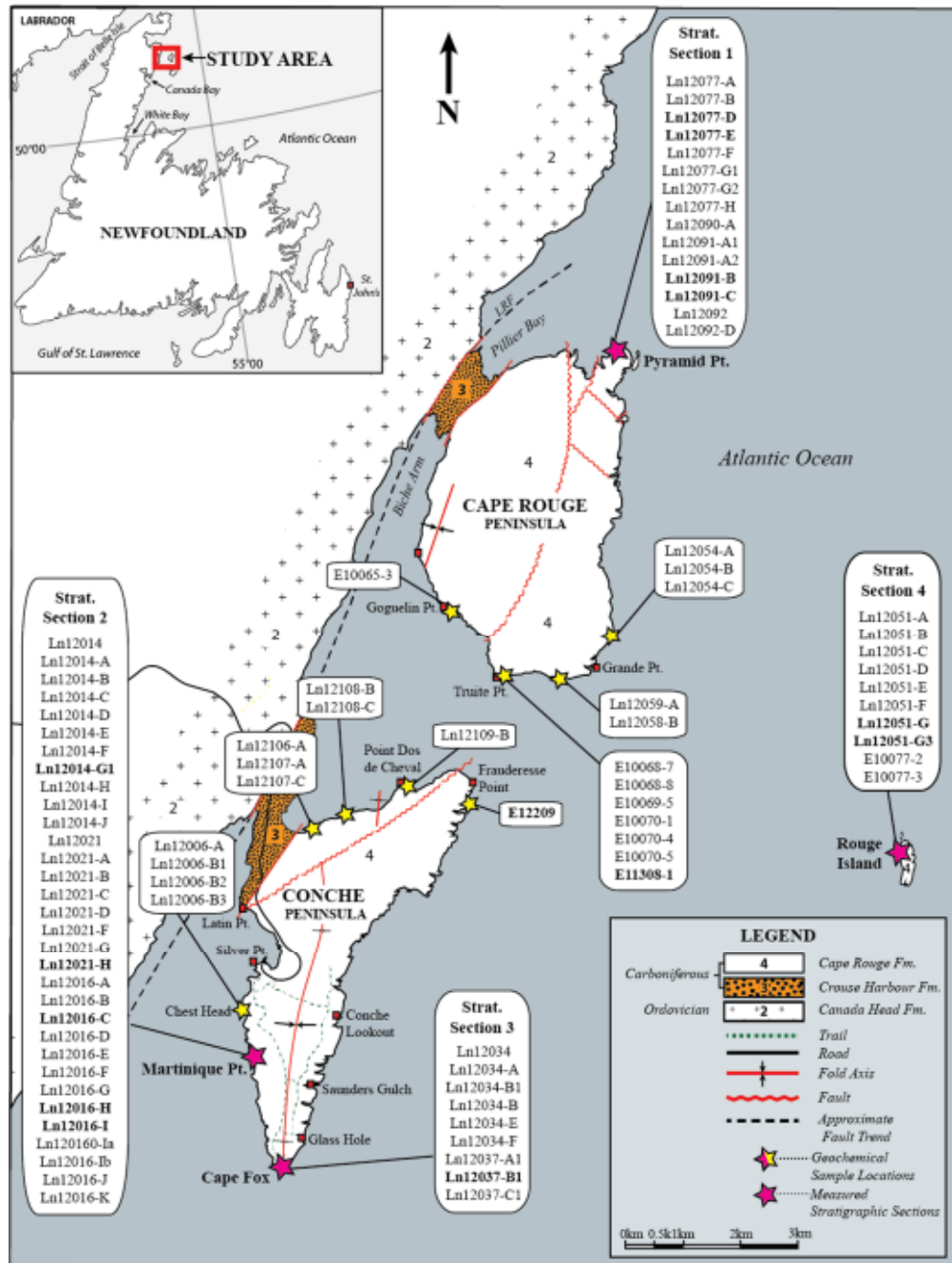


**Figure 3.1 Geology of the Conche area with stratigraphic section localities and mudstone sample locations**

Measured stratigraphic sections are annotated with pink stars. Mudstone sample locations (annotated in pink and yellow stars) are places where analyses include TOC, and Rock-Eval pyrolysis. Samples also analyzed for vitrinite reflectance, TAI, and visual kerogen represented by bolded text (map modified from Baird, 1966).

exposures on Red Island, Pigeon Island, and on the northwestern point of Groais Island. On Groais Island, exposures of the Crouse Harbour Formation are faulted against older schists of Precambrian age (Figure 1.4). On the Conche and Cape Rouge peninsulas, sedimentary rocks of the Crouse Harbour Formation are faulted against Ordovician schists of the Maiden Point Formation. Age relationships between the Crouse Harbour and Cape Rouge formations are ambiguous as there are no visible contacts onshore.

On the isthmuses of the Cape Rouge and Conche peninsulas, the Crouse Harbour Formation is dominated by boulder conglomerates and very-coarse grained sandstones, with inter-fingered mudstone deposits. Boulder conglomerates are poorly sorted to moderately sorted sub-angular to sub-rounded matrix and cobble supported, with sandstone and volcanic clasts. Conglomeratic clasts match local bedrock exposures of the Ordovician Maiden Point Formation. Very-coarse grained sandstones are normally graded with conglomerate lag deposits.

Offshore on Groais Island, the Crouse Harbour Formation is likewise dominated by boulder conglomerates, coarse to medium grained sandstone and with minor freshwater limestone horizons. Conglomerates here are poorly to moderately sorted, matrix supported and with sub-angular to sub-rounded chlorite-schist, quartz, and gneiss clasts that match bedrock exposures of the Grey-Island Schist Formation. Sandstones are feldspathic and coarse-grained and dominated by trough-cross stratification. Fresh water limestones lie on the western point of Groais Island. On Red Island, conglomerates share the same character as those found on Groais Island, and carry clast imbrication that is

unique to this locality. Sandstones here are coarse to very coarse grained, normally graded, and with cross-bedding, ripple stratification and erosive bed bases.

### **3.02.02 Strata of the Cape Rouge Formation**

The Cape Rouge Formation is exposed as coastal outcrops on the Conche and Cape Rouge peninsulas and on Rouge Island. Coastal outcrops often provide extensive continuous sections and occasional three-dimensional exposures ( Figure 3.1)

The Cape Rouge Formation has approximately 1200m of section exposed along the coastlines of the Conche and Cape Rouge peninsulas, together with similar rocks found on Rouge Island (located 6 km offshore). Here, the Cape Rouge Formation strata range from steep (Figure 3.2) to shallow dipping strata that also offer occasional three dimensional exposures (e.g., Pyramid Pt.). This formation is composed of very-fine to medium grained sandstone, siltstone, carbonaceous and zeolite rich mudstone and dolostone stacked as thin-to thick bedded units.

Strata of the Cape Rouge Formation on the Conche Peninsula are gently deformed into a 4.3km long, N-S trending open syncline with a north-trending plunge. This fold is crosscut by a major 3.5km NE-SW trending fault running from Latin Point to Frauderesse Point, and tipping-out offshore at an unknown distance. Numerous smaller faults with axes loosely aligned in a NE-SW direction also transect the Conche Peninsula. On the Cape Rouge Peninsula, another 4km long arching fault transects this peninsula trending from northeast Crouse to Pilier Bay. A series of smaller faults trending NE-SW and NW-

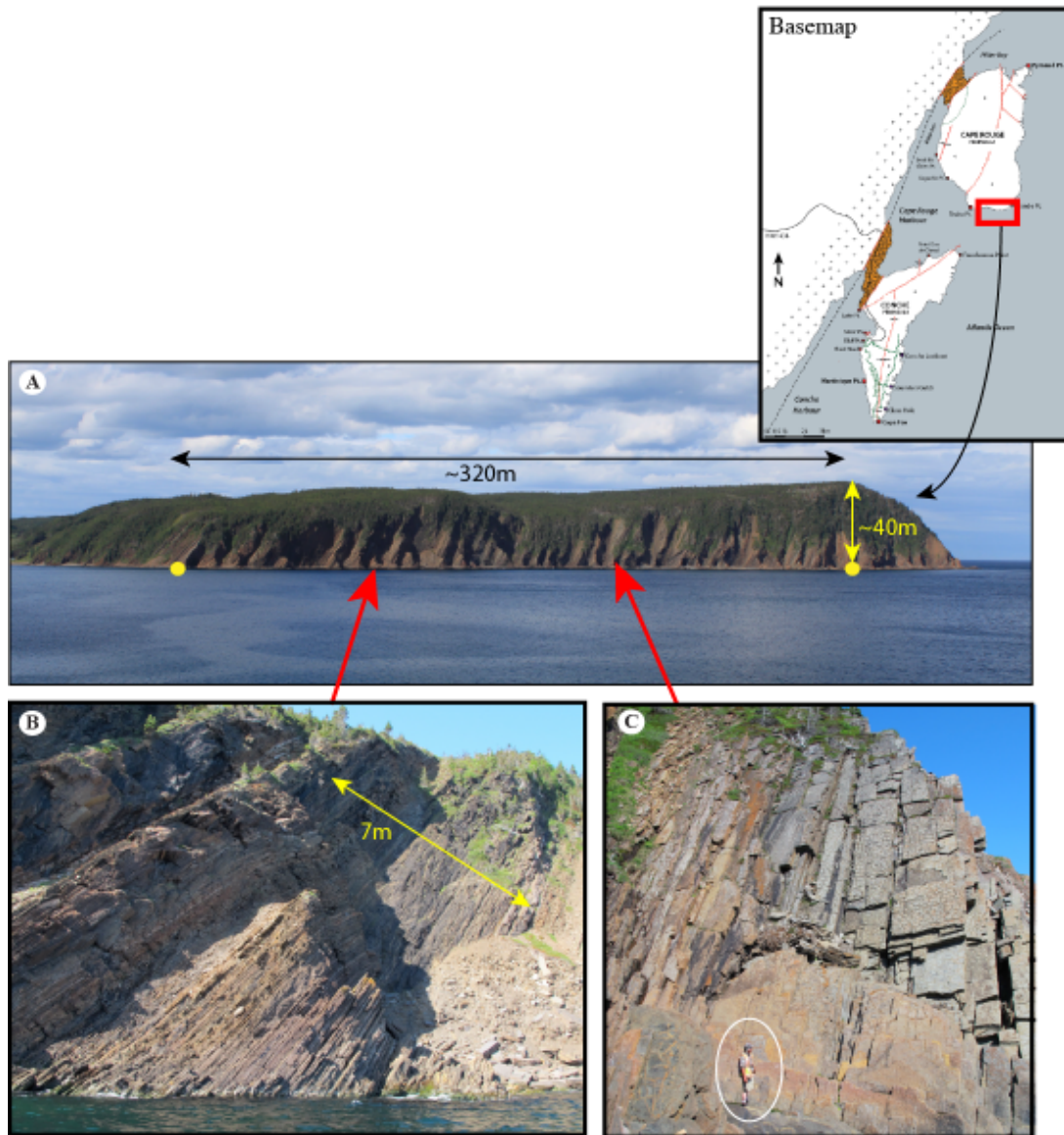


**Figure 3.2 Photographs of coastal cliff face exposures in the Cape Rouge Formation on the Cape Rouge Peninsula**

Steeply dipping coastal exposures of the Cape Rouge Formation. A) A typical section of cliff face exposure from the southern coast of the Cape Rouge Peninsula, ~260m TST (thickness measured from annotated yellow points). B) & C) Zoomed in images of the cliff face exposures along the southern coastline of the Cape Rouge Peninsula. B) 7m thick, fine grained, thinly bedded mudstone interval recessed into the cliff face. C) Steeply dipping slabs of desiccated fine-grained sediments, circled person for scale.

SE crosscut strata on the north-east tip of the peninsula. Moreover, a small scale SSW trending syncline is present on the southwest coast of the peninsula near the “Point Dos de Cheval” ( Figure 3.1).

### **3.03 — Facies Assemblages of the Cape Rouge Formation**

Facies assemblages of the Cape Rouge Formation are characterized by similarities in stacking pattern, lithology, grain-size and sedimentary structures. Four facies assemblages are identified and described:

- Cape Rouge Facies Assemblage 1 (CR-A1): Fine to medium grained well-sorted grey trough cross-bedded, current rippled and planar laminated normally graded sandstone assemblage.
- Cape Rouge Facies Assemblage 2 (CR-A2): Highly desiccated, interbedded grayish-red very-fine to fine-grained sandstone, siltstone and dolostone assemblage.
- Cape Rouge Facies Assemblage 3 (CR-A3): Interbedded very fine-grained olive-grey sandstone, siltstone and dolostone assemblage.
- Cape Rouge Facies Assemblage 4 (CR-A4): Dark-grey to black laminated mudstone, and dolostone assemblage.

#### **3.03.01 Cape Rouge Facies Assemblage 1 (CR-A1)**

CR-A1 facies assemblage contains thick and thin normally graded beds dominated by successions of grey, fine to medium grained well-sorted, trough cross-bedded, current-rippled and planar laminated sandstone. This facies assemblage reaches a maximum

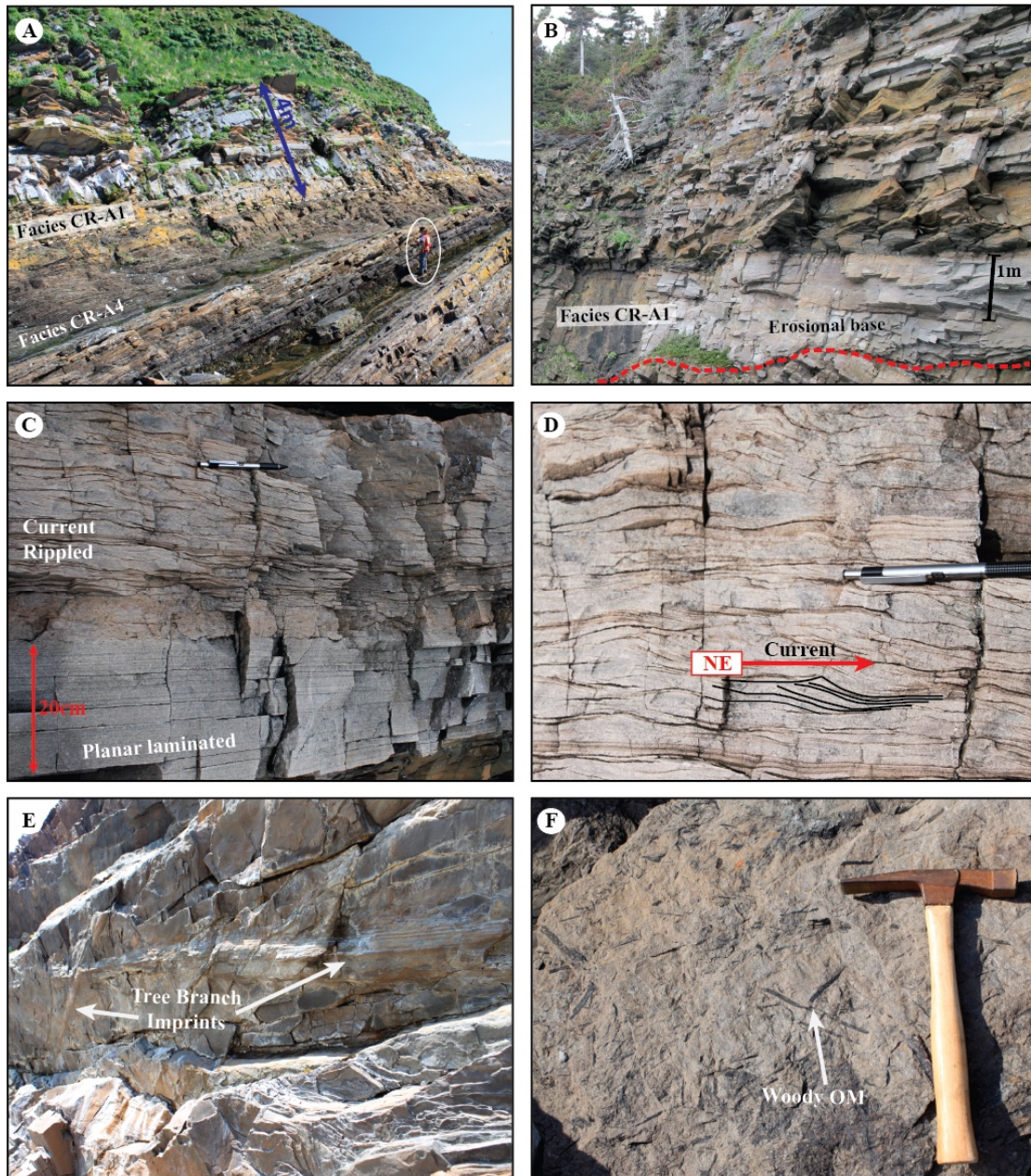


**Figure 3.3 Outcrop photographs of Facies CR-A1 of the Cape Rouge Formation**

A) Cliff face exposure of facies CR-A1 conformably overlying facies CR-A4. B) Cliff face exposure of facies CR-A1 with erosional base. C) Thick bedded medium grained planar laminated sandstone bed overlying current rippled sst. bed. D) Current rippled med.-grained sandstone (arrow indicates direction of sediment dispersal to the NE). E) Sandstone bed base with large scale branch imprints (20 cm diameter branches). F) Sandstone bedding plane with abundant terrestrial plant debris.

thickness of 7m (True Stratigraphic Thickness - TST), with an average thickness of 4m TST. Sandstones are medium to light grey in colour on fresh surfaces (N6-N7 colour on the Munsell colour chart) (Figure 3.3).

Sedimentary structures include planar lamination, trough cross-lamination, and cross-lamination. Sandstones occasionally have concave-up erosional bases (2.5m) but also have sharp bed boundaries (Figure 3.3, b).

Bioturbation was not identified within this facies association. Several large accumulations of woody debris occur along some bedding planes. This debris is typically small and contains large broken woody branches (Figure 3.3, e & f).

### **3.03.02 Cape Rouge Facies Assemblage 2 (CR-A2)**

Facies assemblage CR-A2 is a highly desiccated facies composed of a chaotic mixed succession of very-fine to fine-grained grayish-red sandstone, siltstone, and dark-brown/grey carbonaceous mudstone and dolostone. Rocks of this facies assemblage represent a prominent feature on the Conche and Cape Rouge peninsulas and have an average thickness of 10m TST (with a range from 4m to 17m TST).

Within this facies complex, interleaved sandstone and mudstone bedding is common with mosaic patterns of muddy and silty sediment fracturing (herein thought to be desiccation cracks). Moreover, these sequences are commonly interbedded with oncoidal to massive dolostone beds. Collectively, these deposits suggest a dominantly aggradational fill pattern (Figure 3.4, Figure 3.5, Figure 3.6).

Above and below desiccated strata, there are commonly massive thinly bedded brownish-gray siltstone beds (5-15cm thick) interleaved with medium to thickly bedded (15-40cm) very-fine grained to fine-grained current rippled to massive/homogenous grayish red sandstone beds (Figure 3.4 b, Figure 3.5 a), wavy-parallel fissile very-fine grained sandstone beds, and thinly-bedded (1-10cm) continuous to discontinuous (massive to rippled) dolostone beds (Figure 3.5 a, Figure 3.5 b) composed of silt to sand size particles of dolomite. Some exposures of this facies assemblage lack siltstone with current ripples and massive sandstone beds and are instead dominated by wavy-parallel, fissile, very-fine grained sandstone beds interlayered with discontinuous dolostone beds (Figure 3.5 b). Siltstone and sandstone beds weather to a grayish red (10R 4/2) and have a brownish grey (5yr 4/1) fresh surface colour.

Fine to very-fine grained sandstone beds contain abundant wave and current ripple-lamination (Figure 3.4 a & b). Across this area, 58 paleo-current trends from current lineation and ripple crests show sediment dispersal towards the NE to ENE. Several standing wave-form deposits are also observed within this facies association (Figure 3.4 e) and together indicate multiple channel incisions with concentric fill geometries (Figure 3.5 c & d). Channel-fill thicknesses in this facies range from 0.5m-0.75m and apparently indicate small, shallow high energy channels with widths of 8-10m (W/T 13-16).

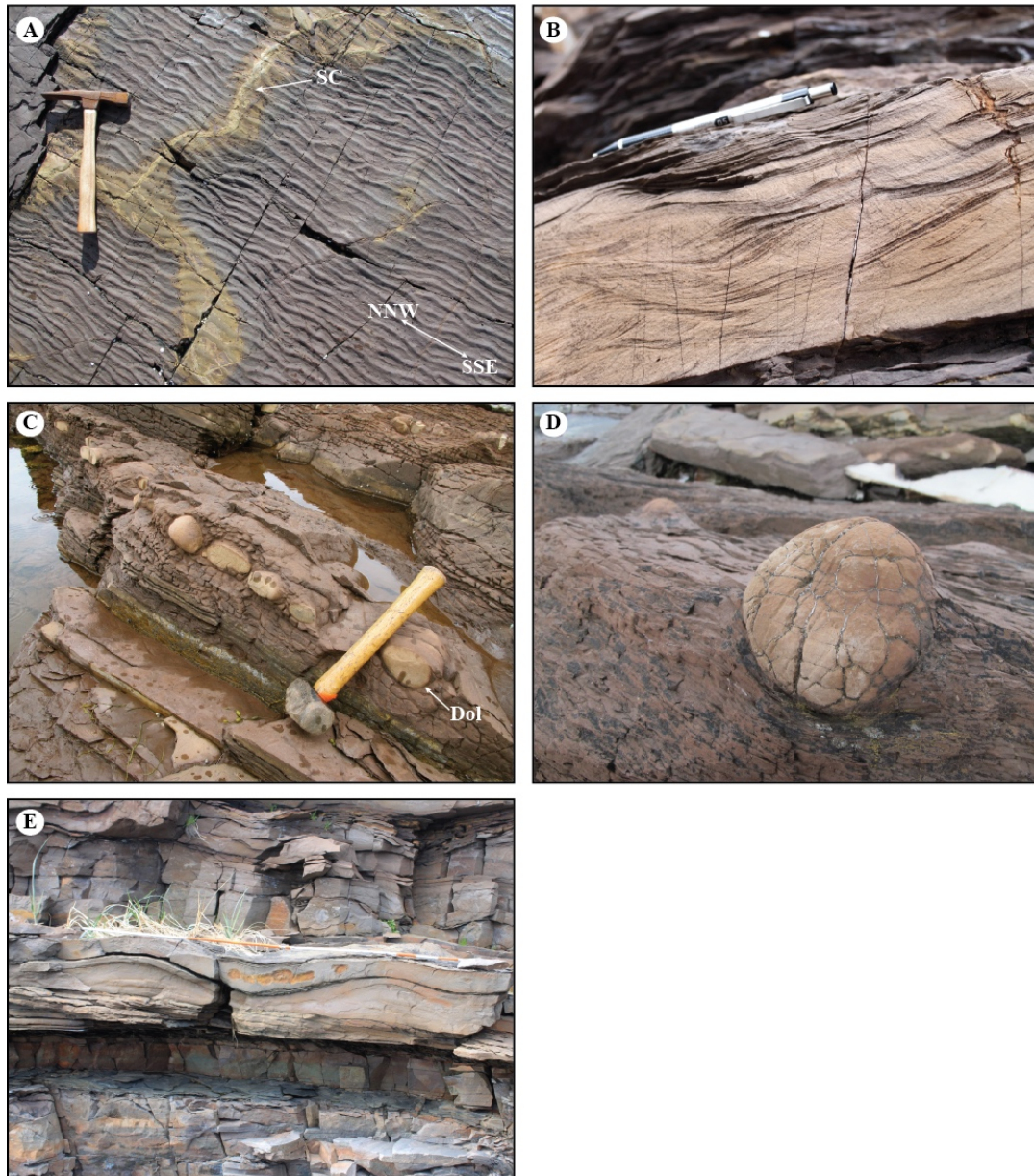


**Figure 3.4 Outcrop photographs of Facies CR-A2 of the Cape Rouge Formation**

A) Symmetrical ripples in very-fine grained sandstone bed with cross-cutting oxidized syneresis cracks (SC). Wave-ripple axis trending NW-SE, representing a bi-directional ENE-WSW flow. Hammer for scale. B) Climbing current rippled very-fine grained sandstone bed (15cm thick). Pencil for scale. C) & D) Platform of spherical dolomite masses in very fine-grained reddish-brown sandstone beds. D) spherical dolomite mass with septarian cracks. E) Standing wave in sandstone bed. 2m Jacobs staff for scale.

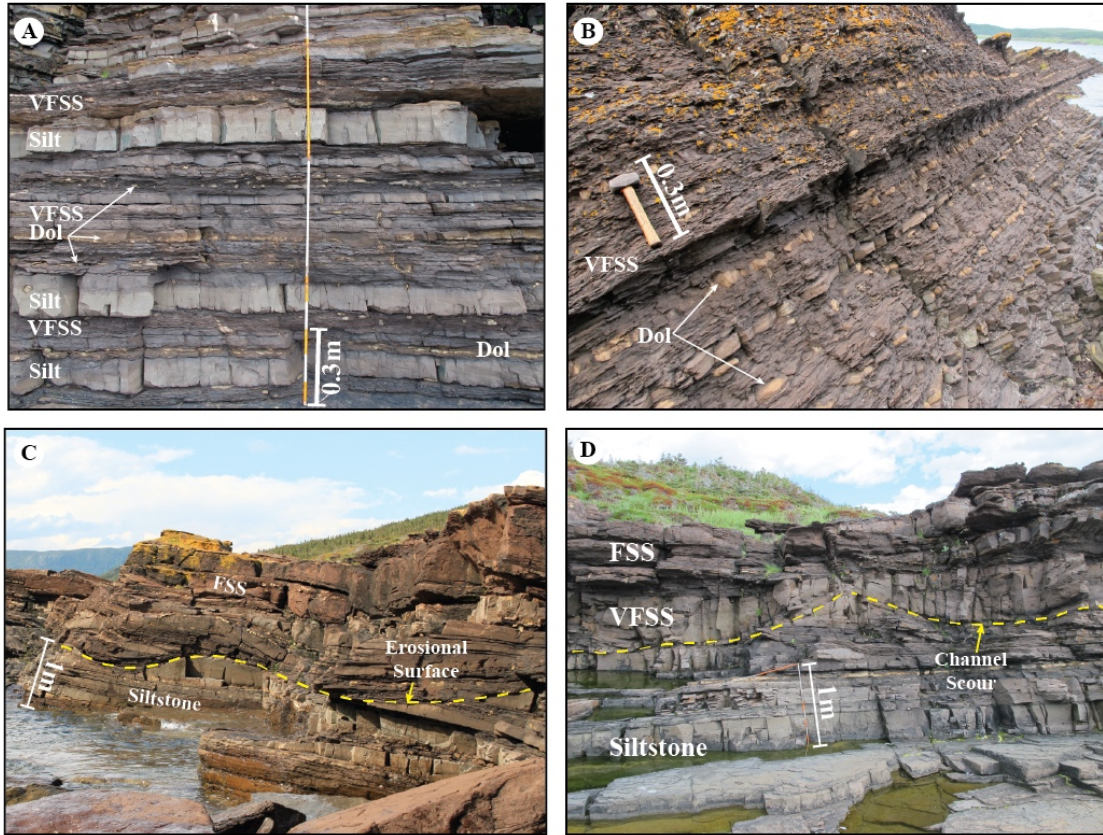


**Figure 3.5 Common sedimentary stacking patterns and structures of Facies Assemblage CR-A2 of the Cape Rouge Formation**

A) & B) Cliff face exposures showing the dominant stacking patterns of this facies assemblage, including siltstone (Silt), very-fine grained sandstone (VFSS) and dolomite (Dol) beds. A) Interlayered wavy to very-fine grained sandstone beds (VFSS) with massive siltstone beds (10-15cm thick) and thin, discontinuous to continuous dolomite beds (light beige colored beds). 2m Jacobs staff for scale. B) Wavy-fissile silty-sandy beds with interlayered thin (2-3cm) discontinuous dolomite beds. C) & D) Scour surfaces of channel incisions in brownish-red fine-grained sandstones.

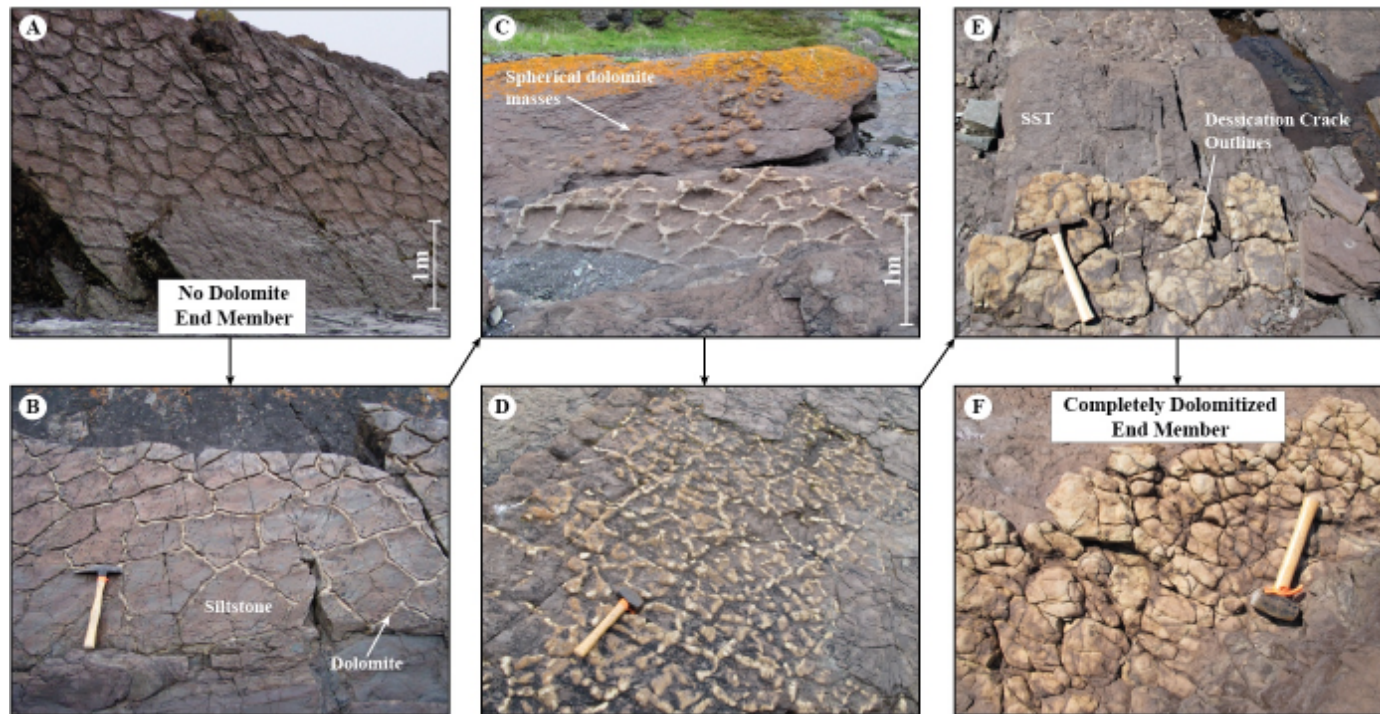


**Figure 3.6 Desiccation cracks and dolomite relationships of Facies CR-A2**

Desiccation cracks are very common within Facies Assemblage CR-A2 and vary from cracks which lack dolomite (A) through to mud-cracked horizons completely obliterated by dolomite (F). A) Polygonal desiccation cracks lacking dolomite. B) Pentagonal to square shaped desiccation cracks. Crack vacancies (~3cm) filled with dolomite. C) Incomplete and radiating desiccation cracks infilled with dolomite; spherical dolomite masses appear to be forming at desiccation crack boundaries. Spherical dolomite masses dominate in underlying bed (see white arrow). D) Chaotic dolomitized bed (likely a former desiccation cracked horizon), hexagon shapes barely visible. E) Completely dolomitized bed with apparent desiccation crack boundaries (see white arrow). F) Completed dolomitized bed. Hammers for scale (0.28m).

A dominant feature of this facies association is large-scale, regular to irregular, polygonal, desiccation cracks (25-40cm wide) that are somewhat variable in general characteristics (Figure 3.6). Individually, the cracks (each 1-5cm wide) are dominantly infilled with light coloured, very pale orange (10YR 8/2) to a grayish orange (10YR 7/4), ferroan dolostone (Figure 3.6 b & c). Desiccation cracks can be perfectly pentagonal or hexagonal in shape to nearly incomplete, radiating and chaotic (Figure 3.6). Moreover, some desiccated horizons can be found to be nearly completely enclosed within chaotic, mounded dolostone beds (Figure 3.6 d-f). Large spherical-shaped dolostone masses (8-15cm diameter) can be found in association with these desiccated horizons (Figure 3.6 c) but are not necessarily restricted to these intervals. Dolomite spherical masses are also found in wavy-fissile very-fine grained sandstone beds (Figure 3.4 c & d).

Bioturbation within these intervals includes horizontal burrows of *Planolites* (Figure 3.7 a) and sinuous traces of *Cochlichnus anguineus* (Figure 3.7 b). Resting traces of *Lockeia* sp. are found along some bedding planes together with molds of potential crustacean nests (Figure 3.7 c & d). Moreover, microbial patches occur throughout this facies association on sandstone and dolostone bed surfaces as irregular wrinkled patches (Figure 3.8 d & f). Carbonized plant fragments and large branches are also identified within this facies association, together with several well preserved fossil stems of *Lepidodendropsis*. Potential domal stromatolites are also observed along several bedding planes, and often associated with desiccation intervals (Figure 3.9). In one basal surface of a single wave ripple, the bed is littered with star-shaped imprints, thought to represent the casting of a *Calamites* leaf whorl (Figure 3.8 e).

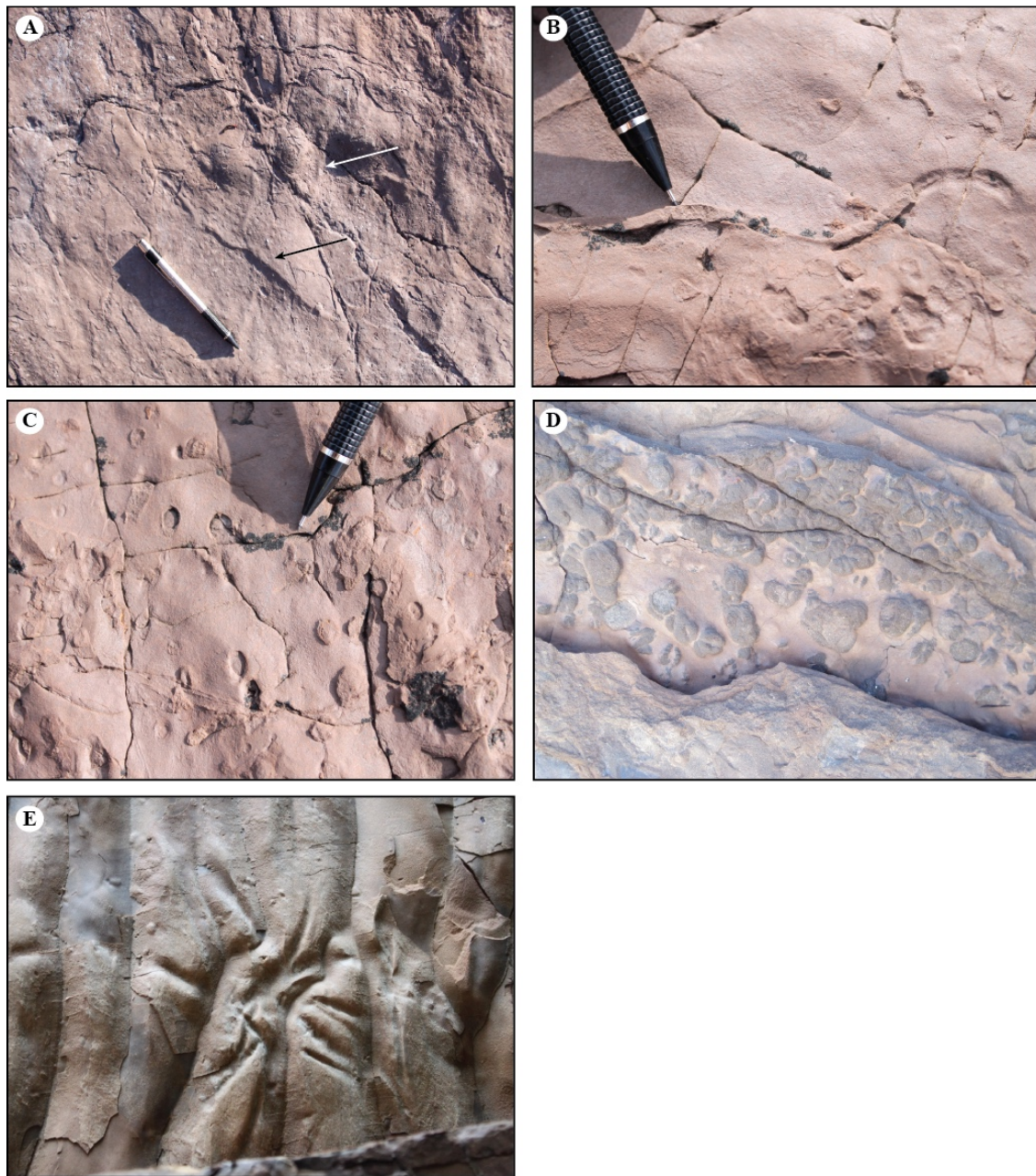


**Figure 3.7 Trace fossils of Facies Assemblage CR-A2**

A) Burrows traces of *Planolites* along bedding planes of very-fine grained sst. B) Sinuous burrows of *Cochlichnus anguineus*. C) *Lockeia* (resting traces of pelecypods) or potential molds of crustacean nests. D) Molds of potential crustacean nests on-top of very-fine grained reddish sst. bed. Rounded “holes” could be mud-rip up casts from a gutter cast. E) Potential leaf imprint of *Calamites* plant on basal surface of a fine-grained wave-ripple sandstone bed.

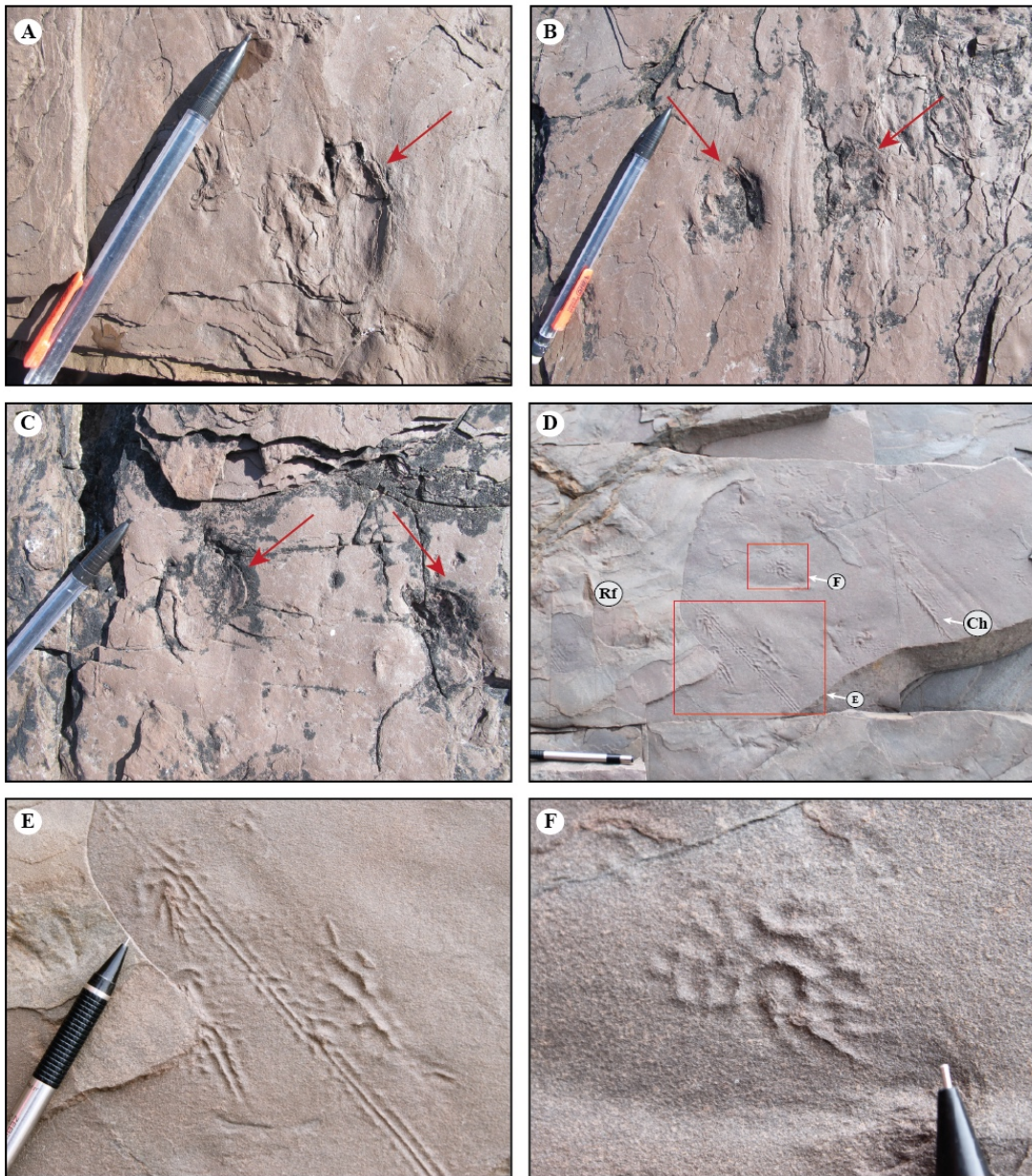


**Figure 3.8 Trace fossils of Facies Assemblage CR-A2**

A), B), & C) Sandstone bedding plane with potential amphibian footprints. Sharply pointed digits possibly suggesting that the producer was clawed (see other examples presented by Kneighley and Pickerill, 1998). All tracks found on same sandstone bed, interlayered between rippled surfaces and desiccation cracked intervals. D) & E) Very-fine grained sandstone basal bed surface with ridge and furrow. Potential arthropod track on fine-grained sandstone bed. Surface littered with impressions. F) An irregularly wrinkled microbial patch.



**Figure 3.9 Photo of domal stromatolite (mechanical pencil for scale).**

Potential tetrapod, amphibian footprints are observed along the southwestern coastline of the Conche Peninsula (UTM Coordinates: 21 U 577615 5635677). Two sets of irregular impressions ~6cm long lay on the top of wave-rippled sandstone beds (Figure 3.8 a, b, & c). These potential “digits” are pointed. However, the number of digits is unclear, and possibly more than four. Inasmuch as careful observations are collected, at this time, no convincing trackways are present.

### **3.03.03 Cape Rouge Facies Assemblage 3 (CR-A3)**

Facies assemblage CR-A3 is composed of gray to olive gray siltstone, very fine-grained sandstone and minor amounts of silty mudstone and silty dolostone (Figure 3.10,

Figure 3.11). Average unit thickness ranges between 10-15m TST. Siltstone and very-fine grained sandstone beds ranging in thickness between 15-50 cm, are normally graded to massive, and, occasionally interbedded with thin, finer grained silty-mudstones (Figure 3.10 b). Siltstones weather to a light olive gray (5YR 6/1) to olive gray (5Y 4/1) colour with medium dark gray (N4) to a medium gray (N5) fresh surface colour. Sandstones weather to an olive gray (5Y 4/1) or pale brown (5YR 5/2) to moderate brown (5YR 3/4) colour and have a medium gray (N5) fresh surface colour (Figure 3.10).

This facies is typified by massive, contorted and convoluted stratification (Figure 3.11 a-c) together with cross and parallel lamination (Figure 3.11 e & f). Convoluted beds are common in siltstone and sandstone beds and generally grade from massive strata to contorted strata at bed tops (Figure 3.11 c).

Ferroan dolomite beds, although rare, occur as thin (3-7 cm thick) silty beds dispersed throughout the facies, weathering to a dark yellowish orange (10YR 6/6) to moderate yellowish brown (10YR 5/4) colour with a dark gray (N3) to medium gray (N5) fresh surface colour. Ferroan dolomite beds are typically silty in nature with planar or cross-lamination and plant debris on some bedding planes. No other evidence for organisms or bioturbation is otherwise seen in this facies. In context, facies CR-A3 is nearly always found above facies CR-A4 and below facies CR-A2 (Figure 3.10 a & c).



**Figure 3.10 Sedimentary stacking patterns of Facies Assemblage CR-A3**

Sedimentary stacking patterns of facies assemblage CR-A3. A) Gently dipping (~11 degrees) siltstone cliff face exposure of facies CR-A3 with a sharp overlying contact with facies CR-A2. B) Cliff face exposure of facies CR-A3 with a sharp underlying contact with facies CR-A4. Succession is composed of massive siltstone beds, ranging in thickness from 5-30cm, interbedded with thin mudstone horizons (recessed into cliff face). 2m Jacobs staff for scale (circled). C)&D) Interbedded siltstone and very-fine grain sandstone beds (average 15cm thick). C) Gradational contact between facies CR-A3 and underlying facies CR-A4.



**Figure 3.11 Sedimentary structures of Facies Assemblage CR-A3**

A) & B) Convolute lamination in very-fine grained sst. C) Convolute lamination in siltstone overlying massive siltstone bed, copper staining on surface exposure. D) Massive siltstone beds with fractures perpendicular to bedding planes infilled with pyrobitumen (dead oil). Surface stained with iron. E) Cross lamination in very-fine grained sandstone and siltstone beds. F) Planar laminated very-fine grained sandstone overlain by trough cross lamination.

### 3.03.04 Cape Rouge Facies Assemblage 4 (CR-A4)

Facies assemblage CR-A4 is composed of dark-grey to black laminated carbonaceous and zeolite-rich mudstones, interbedded with ferroan dolostone. Together, this unit typically ranges in thickness from 4 to 8 m TST. This facies assemblage is characterized by alternating fining-upwards to coarsening-upwards stacking patterns and is commonly found overlying coarser-grained strata of facies assemblages CR-A2 and CR-A3 (Figure 3.12 a).

Mudstones are black (N1) to dark grey (N2) in colour and weather to a medium gray (N5) to a dark gray (N3) colour. In general, fresh surfaces are one to two tones darker (on Munsell colour chart) than their weathered surfaces. Mudstones are even, parallel to wavy laminated and have a fissile character. Some beds have higher concentrations of carbonate (fe-dolomite) and zeolite (analcime) cements resulting in a less fissile character together with greater bed thickness (1-4cm) (Figure 3.12) (refer to Chapter 4 or detailed mineralogy of these mudstones).

Dolostone beds are silt-rich to clay-rich and occur interbedded with mudstones as continuous laminated thin to very-thin beds (Figure 3.12 c) or as lenses (Figure 3.12 d). Dolostone beds are typically 0.5-7cm thick (with an average bed thickness of 2cm) and are either found interbedded within thick mudstones (up to 40cm apart) or closely interbedded with thin (0.5-2cm) mudstones (Figure 3.12 c & d; Figure 3.13).

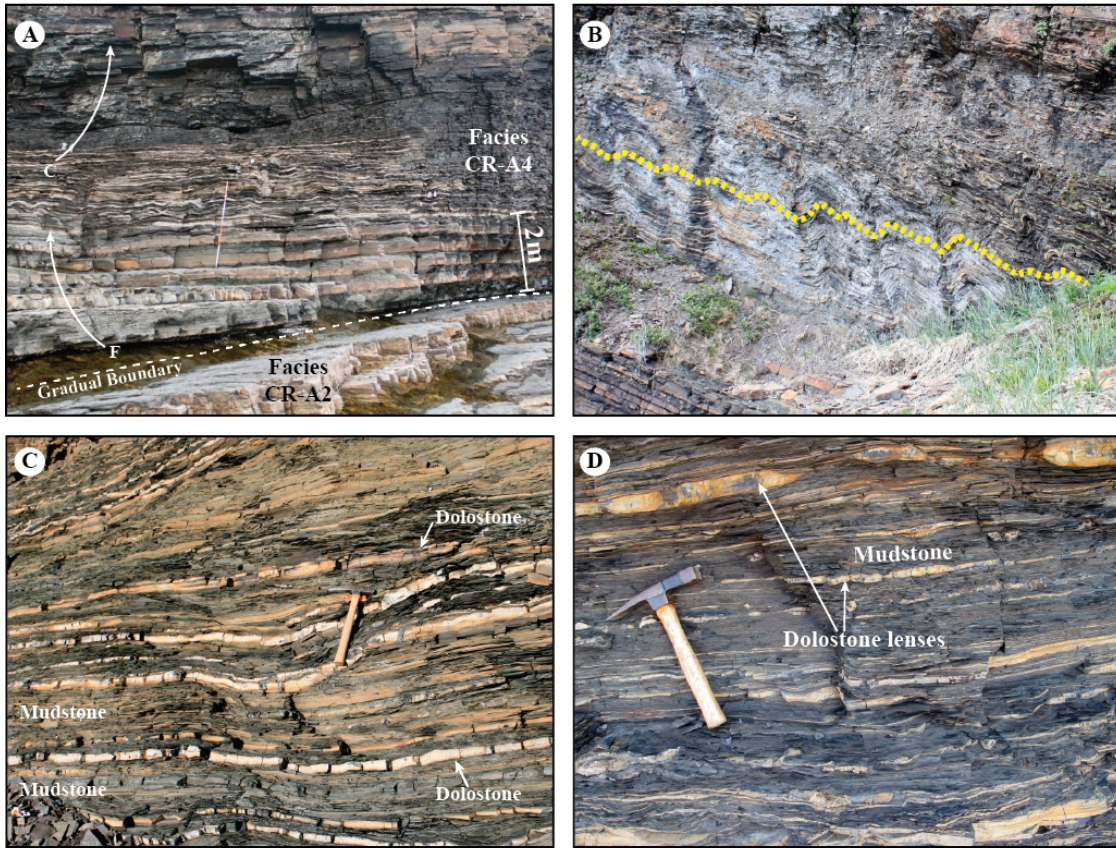


**Figure 3.12 Sedimentary stacking patterns of Facies Assemblage CR-A4**

A) Cliff face exposure of facies CR-A4 with an underlying gradational contact with CR-A2. Mudstones at base are interbedded with 15-20cm very-fine grained sandstone beds grading into pure mudstone-dolomite facies CR-A4. B) Folded mudstone and dolostone strata (see dashed yellow line for folded bedding plane). Section is ~6.5 m thick. C) Interbedded thin (1-3cm) dolostone (light colored) with dark coloured calcareous mudstones. D) Dark (N1) organic-rich (2% TOC) mudstone interbedded with planar laminated to lensoid dolostone beds (0.5-5cm thick).

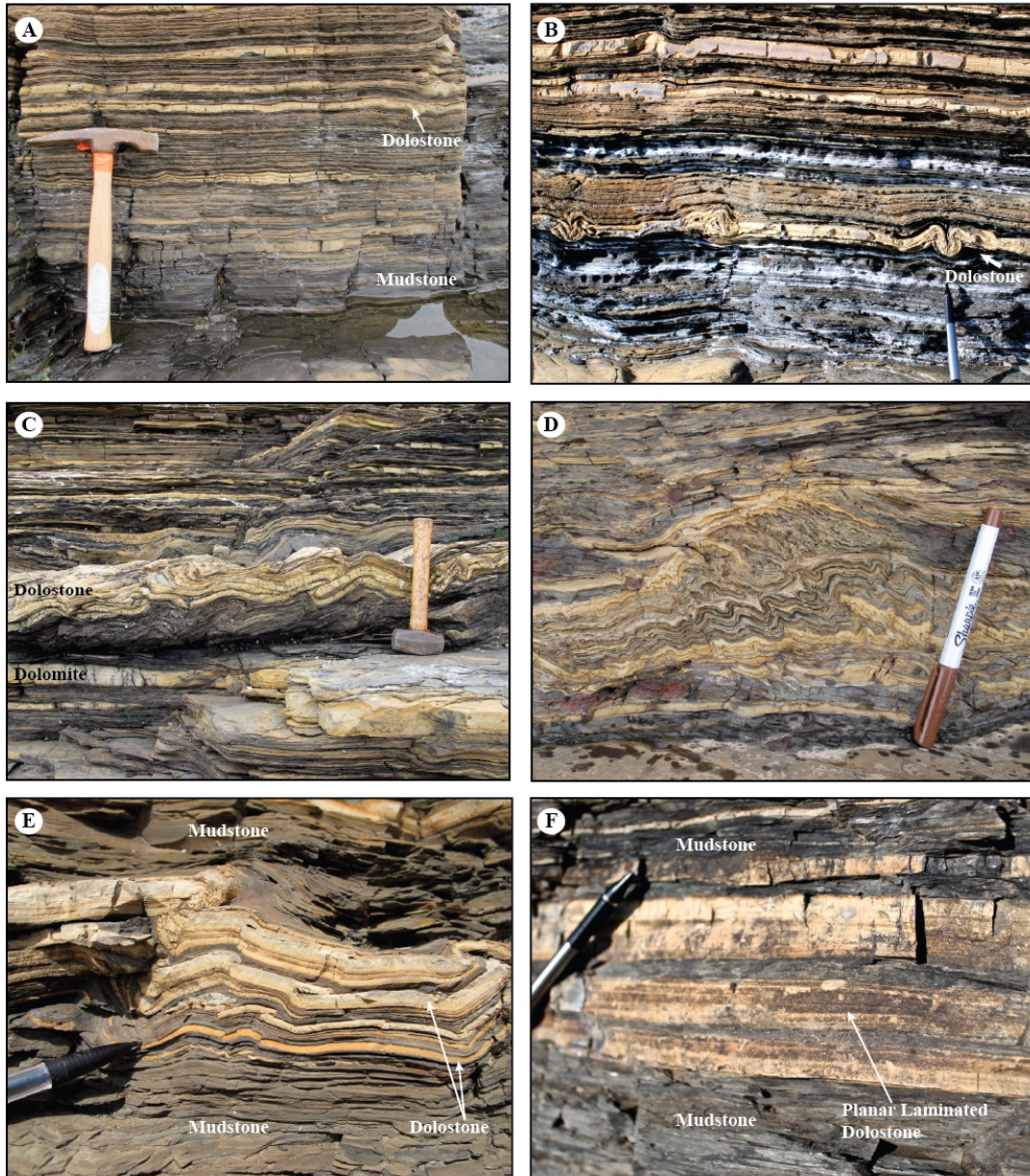


**Figure 3.13 Sedimentary stacking patterns and structures of Facies Assemblage CR-A4**

A) & B) Thinly interbedded succession of planar laminated mudstone and dolostone (0.5cm beds). B) Thinly bedded kinked dolostone beds (0.5cm). C) Contorted succession of interbedded planar laminated dolostone and mudstone. D) Highly contorted laminated mudstone and dolostone beds. E) Stacking succession of dolostone and mudstone beds displaying small thrusts on dolostone beds. F) Planar laminated 1-2.5cm thick dolostone beds in low TOC mudstone (N4).

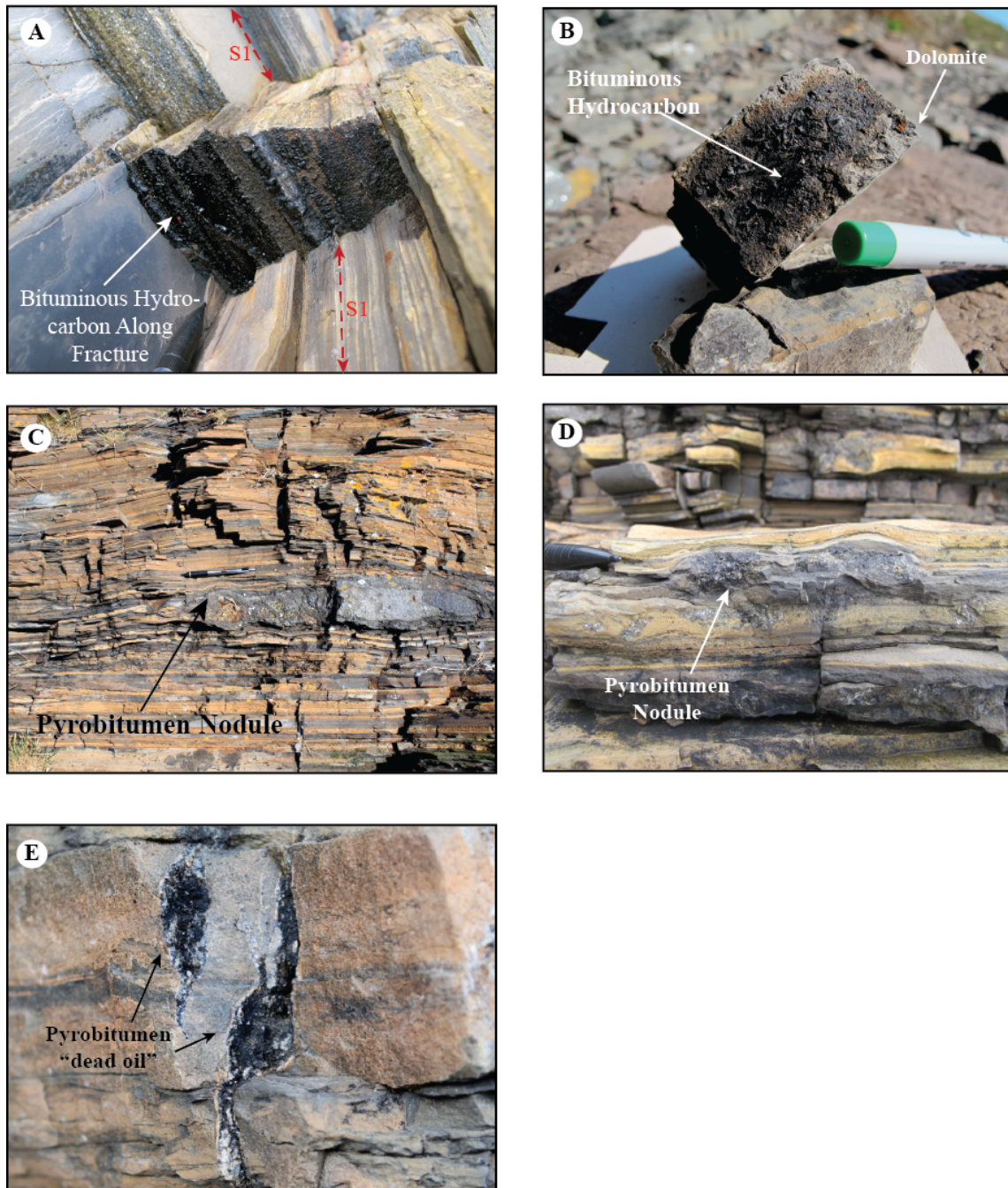


**Figure 3.14 Hydrocarbon shows and pyrobitumen occurrences of Facies Assemblage CR-A4**

A) & B) Fractured dolomite bed with bituminous hydrocarbon along fractured surface.  
 C), D) & E) Pyrobitumen (dead oil) lenses.

Dolostone beds are dominantly planar laminated (sub parallel to parallel) (Figure 3.13 f) and commonly show signs of soft-sediment deformation with folding and shearing along and across bedding planes (Figure 3.13 b, c, & d). Silty dolostones, near the top of this facies assemblage, can retain some evidence for cross-lamination. Dolostones are pale orange (10YR 8/2) to a grayish orange (10YR 7/4) colour on weathered surfaces and dark grey (N2) to black (N1) on fresh surfaces.

Bituminous hydrocarbon seeps are common along dolostone cleavage planes (Figure 3.14 a & b) on the Cape Rouge and Conche peninsulas. Seeps are particularly obvious when outside air temperatures are high ( $> \sim 18^{\circ}\text{C}$ ). Furthermore, pyrobitumen (dead oil) or biodegraded oil residue is found as lenticular nodules along bedding planes (Figure 3.14 c & d) and along cleavage planes (Figure 3.14 e).

Small plant fragments occur along some bedding planes (Figure 3.15 a, b & c). Very minor bioturbation (*Planolites*) is found in mudstone beds near the top of this unit. Several gastropod molds (Figure 3.15 d) are located at Pyramid Point on the Cape Rouge Peninsula. Moreover, spores are a common feature in these beds, though taxonomic identification is challenging (Froude, 2012). High levels of degradation and corrosion obscure or remove important taxonomic features (see Froude, 2012).

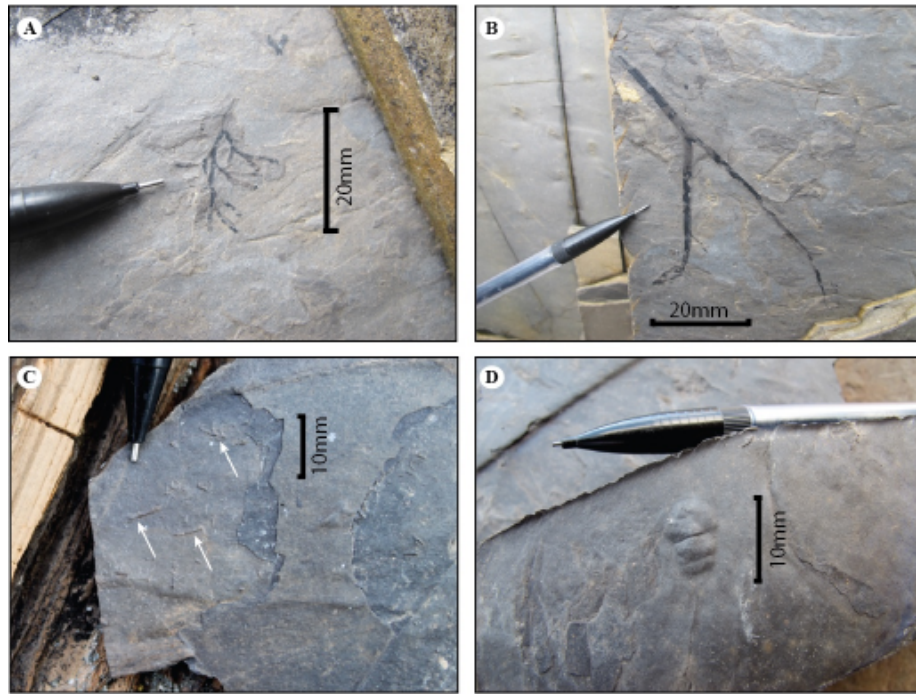


**Figure 3.15 Terrestrial plant imprints and trace fossils of Facies Assemblage CR-A4**

A) & B) Plant fragments along mudstone bedding planes. C) Small-scale (1-6mm) plant imprints on bedding plane. D) Potential gastropod cast.

### 3.04 — Stratal Stacking Patterns of the Cape Rouge Formation

Facies assemblages exhibit both coarsening upwards and aggradational stratal sequences, and on average, have a repetitive and predictive nature. Four reference sections of the Cape Rouge Formation (Figure 3.16) are presented below (Table 6).

**Table 6 Stratigraphic section locations** (refer to Figure 3.16 for section locations)

<b>Stratigraphic Section</b>	<b>Locality</b>	<b>Figure</b>
<b>1: Pyramid Point</b>	Cape Rouge Peninsula	Figure 3.17
<b>2: Martinique Point</b>	Conche Peninsula	Figure 3.19
<b>3: Cape Fox</b>	Conche Peninsula	Figure 3.21
<b>4: Western Coastline</b>	Rouge Island	Figure 3.23

#### **3.04.01 Stratigraphic Section 1: Pyramid Point, Cape Rouge Peninsula**

Stratigraphic section 1 from Pyramid Point on the Cape Rouge Peninsula (Figure 3.16) contains 160 m (TST) of accessible strata that include 82 m of continuous section (Figure 3.17). This section is characterized by thick intervals of fine-grained sediment of which a significant portion are sand-starved. This part of the succession is organized into coarsening-upwards and aggradational stratal stacking patterns. Bituminous hydrocarbon and pyrobitumen shows are common at this locality.

Strata at Pyramid Point are dominated by the fine-grained facies of CR-A4 and CR-A3. Within the context of this study, this section carries the thickest succession of mudstones/dolostone facies assemblage CR-A4 (Figure 3.17, Figure 3.18).

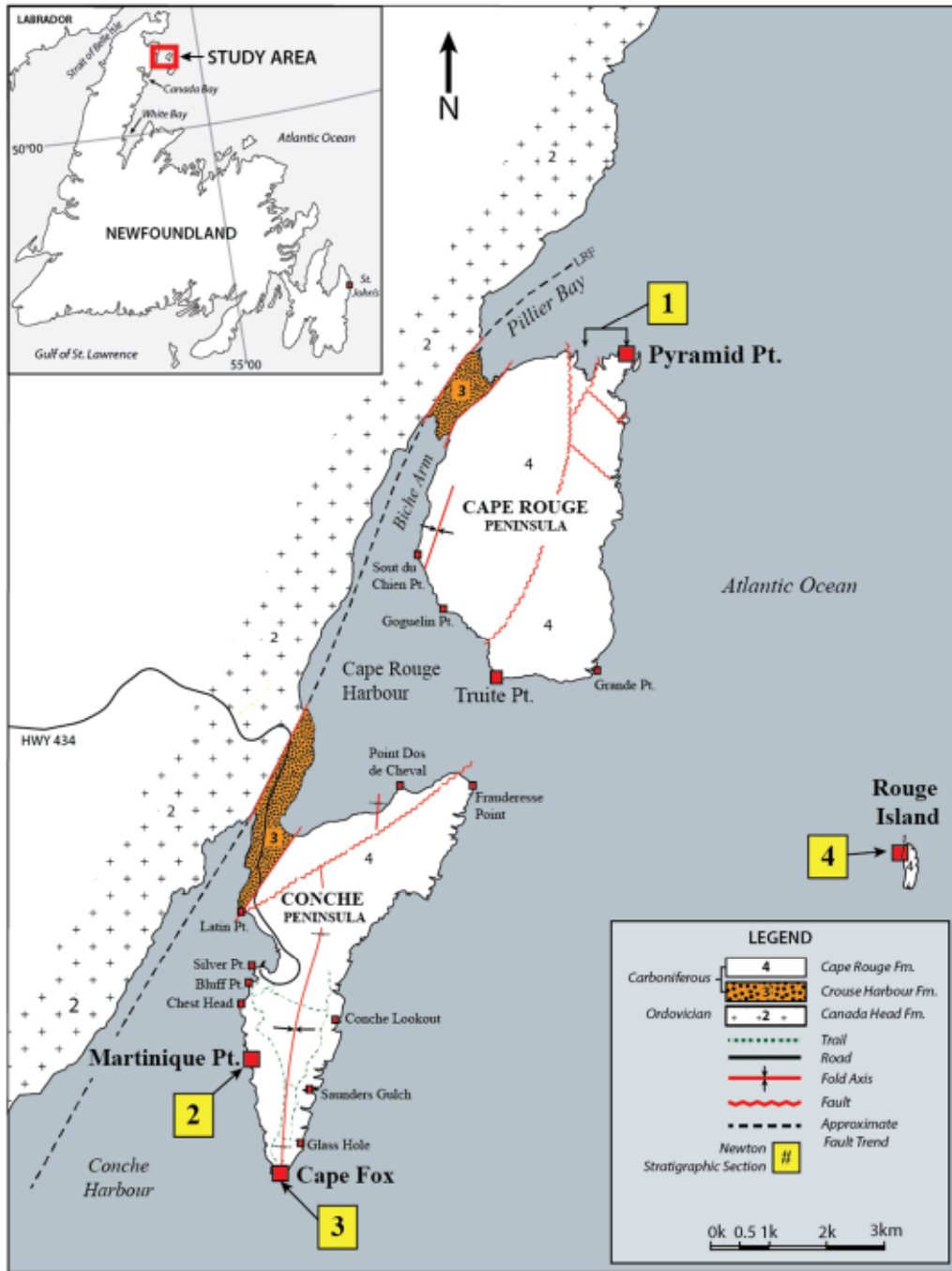
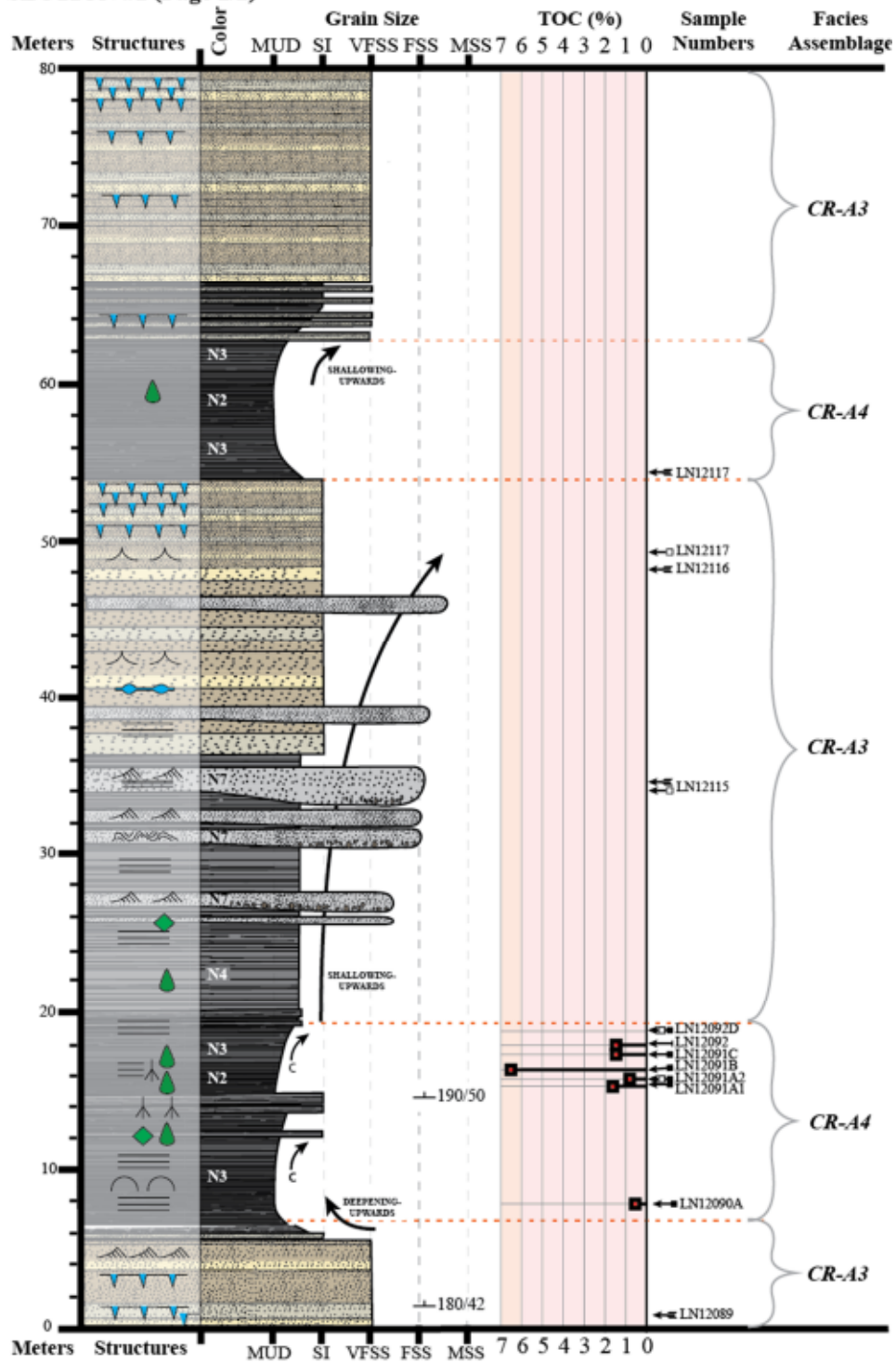
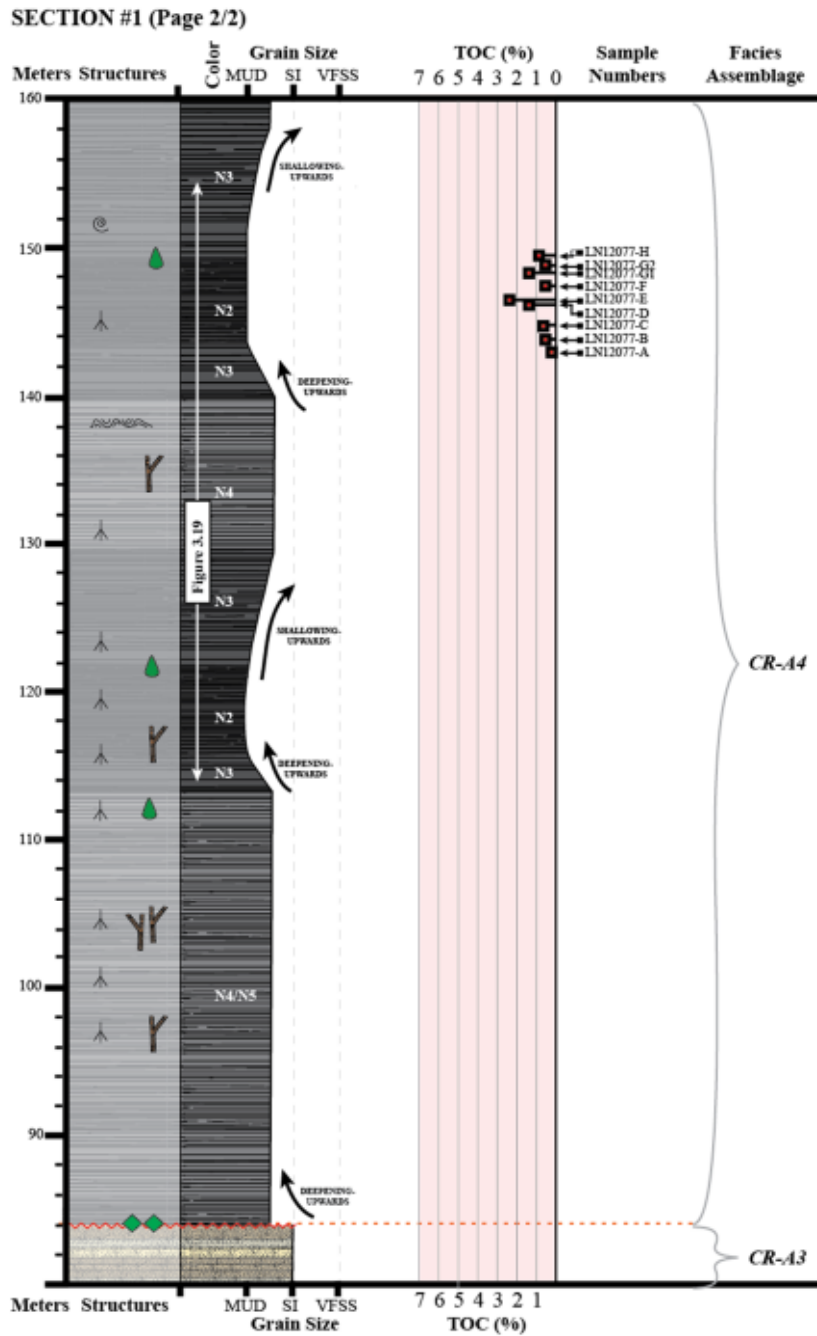


Figure 3.16 Stratigraphic section locations (modified from Baird, 1966)

**CAPE ROUGE FORMATION  
PYRAMID POINT STRATIGRAPHIC SECTION  
SECTION #1 (Page 1/2)**





**Figure 3.17 Measured stratigraphic section #1 at Pyramid Point, Cape-Rouge Peninsula**

Refer to Figure 3.16 for map location. Samples are marked by arrows. TOC values in red. Numbers (e.g., N2, N3) represent rock colours of fresh surfaces (colours based on the genuine Munsell colour chips).

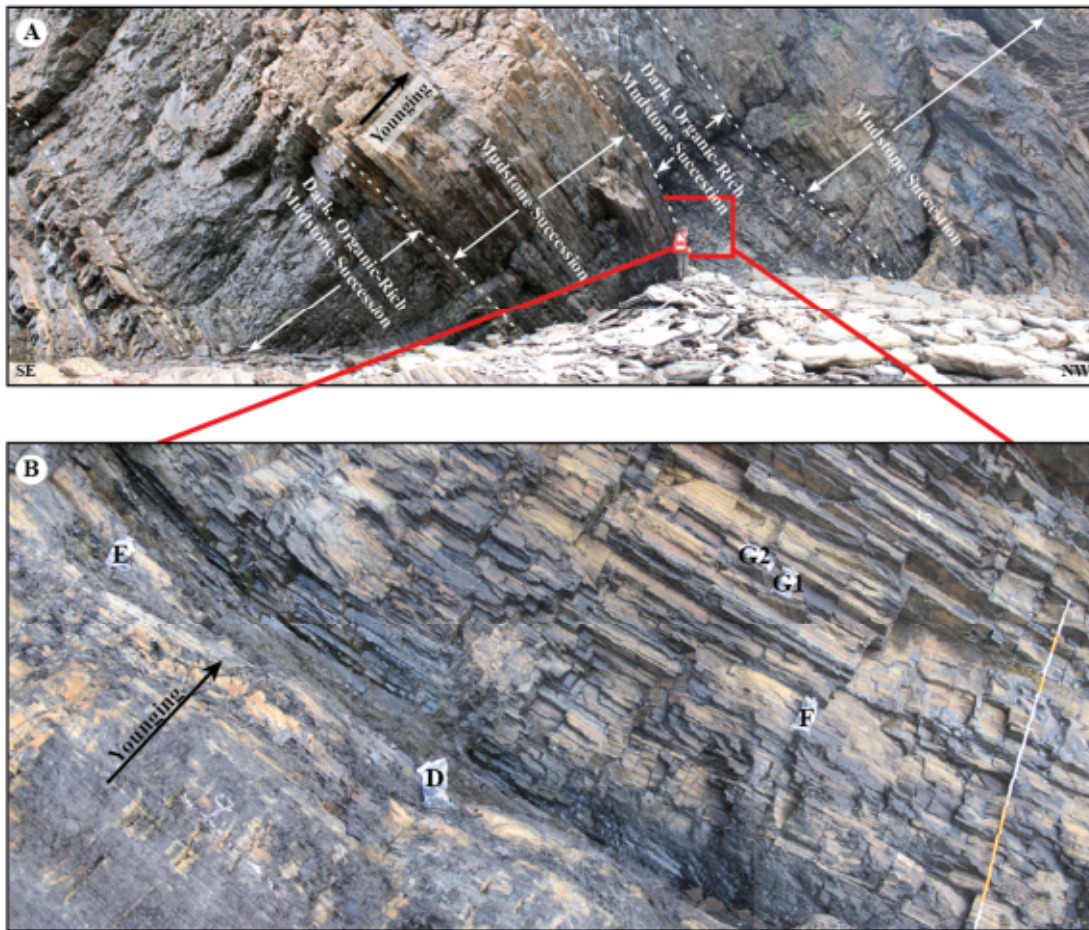


**Figure 3.18 Outcrop photos of fine-grained facies (Facies Assemblage CR-A4) of measured stratigraphic section #1 at Pyramid Point, Cape Rouge Peninsula**

Photographs taken between the 114-154m interval of measured stratigraphic section #1 (Figure 3.17). A) Cliff face exposure of facies CR-A4 from measured section 1 (refer to Figure 3.17 for picture location). B) Cliff face exposure of mudstone interval, facies CR-2, with TOC sample locations marked with letters. Beds increasing in thickness in a younging upwards direction. Meter stick for scale.

An offsetting fault cuts the section (at the 82 m marker; Figure 3.17) into upper and lower parts, and with abundant pyrobitumen along the fault gouge. The lower part (that is between 0-80m) has two complete coarsening upwards successions of stacked very-fine to fine-grained graded sandstone of facies assemblage CR-A3. Occasionally, desiccation cracks occur near the tops of these intervals and where a sharp boundary defines the base of the next fine-grained cycle. Pyrobitumen and bituminous hydrocarbon are common along mudstone and dolostone bedding and cleavage planes (Figure 3.14).

The upper part of this section (between 80-160m) is completely sand starved, and composed primarily of silty carbonaceous mudstone and dolostone with darker units of fissile mudstone (up to ~10m thick). Two complete mudstone and dolostone successions, separated with gradational boundaries, are present here. No desiccation cracks are found in the upper section. Bituminous hydrocarbons, minor plant fragments and gastropod casts occur in the upper and lower mudstone succession (Figure 3.15).

#### **3.04.02 Stratigraphic Section 2: Martinique Point, Conche Peninsula**

Stratigraphic section 2 from Martinique Point holds 82 m (TST) of strata that includes 53 m of continuous section from the Cape Rouge Formation (Figure 3.19). Seven meters of section at the 53m marker are obscured by beach talus. All four facies assemblages are present at this locality (including CR-A1, CR-A2, CR-A3 and CR-A4) occurring in repeating coarsening upwards successions. Three complete coarsening upwards sequences are present within this measured section where bounding surfaces are marked by sharp and gradational changes to muddier strata.

This sequence is exemplified by silt/sand-prone and dolomitic beds, coarsening upwards into facies containing abundant desiccation cracks, spherical ferroan dolomite masses, and bituminous hydrocarbon shows (Figure 3.19).

The most distinctive features of this measured section are the abundant desiccation cracks, with cracks infilled with dolomite, together with spherical dolomite masses.

Fine-grained facies assemblages (CR-A4) occur as thin (2.5m) to thick (~9m) successions interbedded with thin ferroan dolomite beds that tend to commonly occur near the base and top of the unit (Figure 3.20). Oil seeps were observed within both of the fine-grained successions (~16m and 45m markers).

### **3.04.03 Stratigraphic Section 3: Cape Fox, Conche Peninsula**

Stratigraphic section 3 from Cape Fox contains 35 m TST of strata from the Cape Rouge Formation (Figure 3.21). Three facies assemblages at this locality (CR-A2, CR-A3, CR-A4) represent a complete coarsening upwards succession from 2m to 31m above the base.

This succession is characterized by a basal 3 m interval of very-fine grained gray sandstone (facies CR-A2) marked by a gradational contact (at the 3m marker) with an overlying 6.5m thick finer-grained laminated mudstone/dolostone (facies CR-A4).



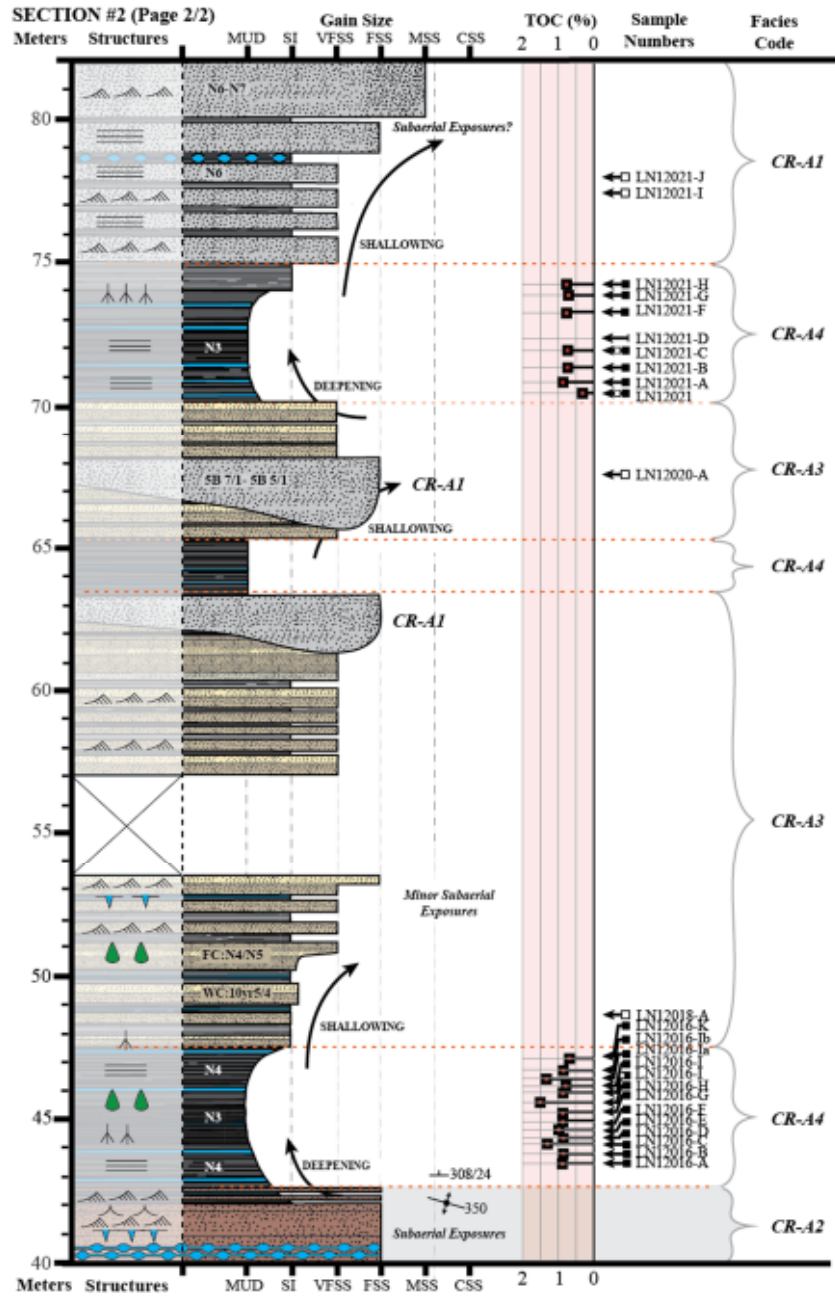


**Figure 3.19 Measured stratigraphic section #2 at Martinique Point, Conche Peninsula**

Refer to Figure 3.16 for map location. LECO TOC values in red. Numbers (e.g., N2, N3) in white present rock colours of fresh surfaces.

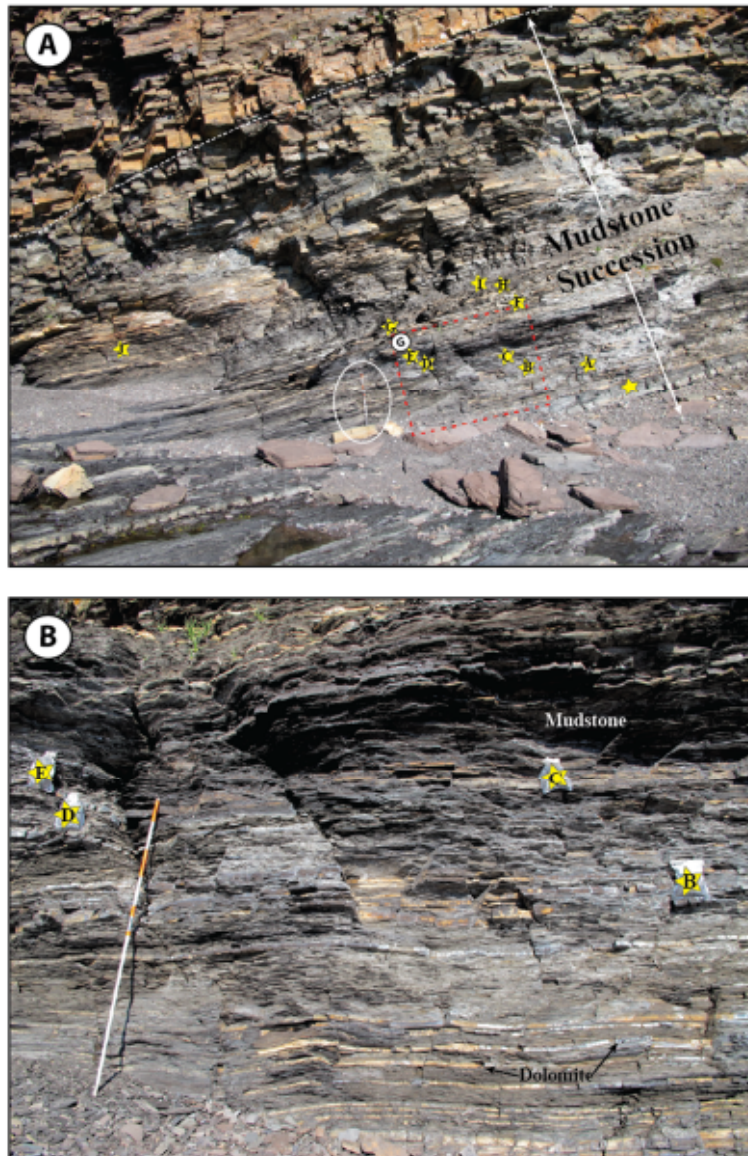


**Figure 3.20 Outcrop photos of fine-grained facies (CR-A4) of measured section #2 at Martinique Point, Conche Peninsula**

Photographs taken between the 14-24m interval of measured stratigraphic section #2 (Figure 3.19). A) Outcrop photograph of facies CR-A2, between 14-24m. Stars represent sample locations for TOC and thin sections. Yellow star represents sample LN12014, with samples LN12014-A through LN12014-J above. A 2m Jacobs staff is circled for scale. Enlargement photograph of region is highlighted in the red dashed square. B) Enlarged photo of the Facies CR-2 succession (G in plot A) with TOC samples B-E, 2m Jacobs staff for scale.

Here, fine-grained strata of CR-A4 are dominated by thin, convoluted beds of dolostone and fissile dark mudstone (Figure 3.22). Minor bituminous hydrocarbon and pyrobitumen shows are present. The laminated mudstone/dolostone interval (facies assemblage CR-A4) is overlain by facies assemblage CR-A3, consisting of interbedded olive-grey siltstones and dolostones (~7m TST). Overlying facies assemblage CR-A3 is a particularly thick (17m TST) succession of facies assemblage CR-A2, containing desiccated, grayish red sandstone. Several sandstone beds are medium-grained with current ripple stratification while finer-grained members have abundant desiccation cracked horizons containing spherical ferroan dolomite masses (Figure 3.22). A sharp boundary, at the 31m interval, represents a transition back to a finer-grained mudstone facies assemblage (CR-A4).

#### **3.04.04 Stratigraphic Section 4: West Coast, Rouge Island**

Stratigraphic section 4 from the western coastline of Rouge Island is 28 m TST of section that includes 21 m of continuous section from the Cape Rouge Formation. Three meters of section is partially obscured with soil cover. Facies assemblages include CR-A1, CR-A3 and CR-A4 (Figure 3.23). This section closely resembles the stacking patterns, facies assemblages and unit thickness of stratigraphic section 2 at Martinique Point (Figure 3.19) between the 68-82m interval. At Rouge Island there is a distinct flooding surface, at the 11m marker, where fine-grained facies CR-A4 sharply overlies coarser grained strata of facies CR-A3. Fine-grained assemblages of facies CR-A4 form a 7m thick succession with interbedded thin ferroan dolomite beds commonly seen near the base and top of the unit. Minor amounts of pyrobitumen occur along bedding planes.

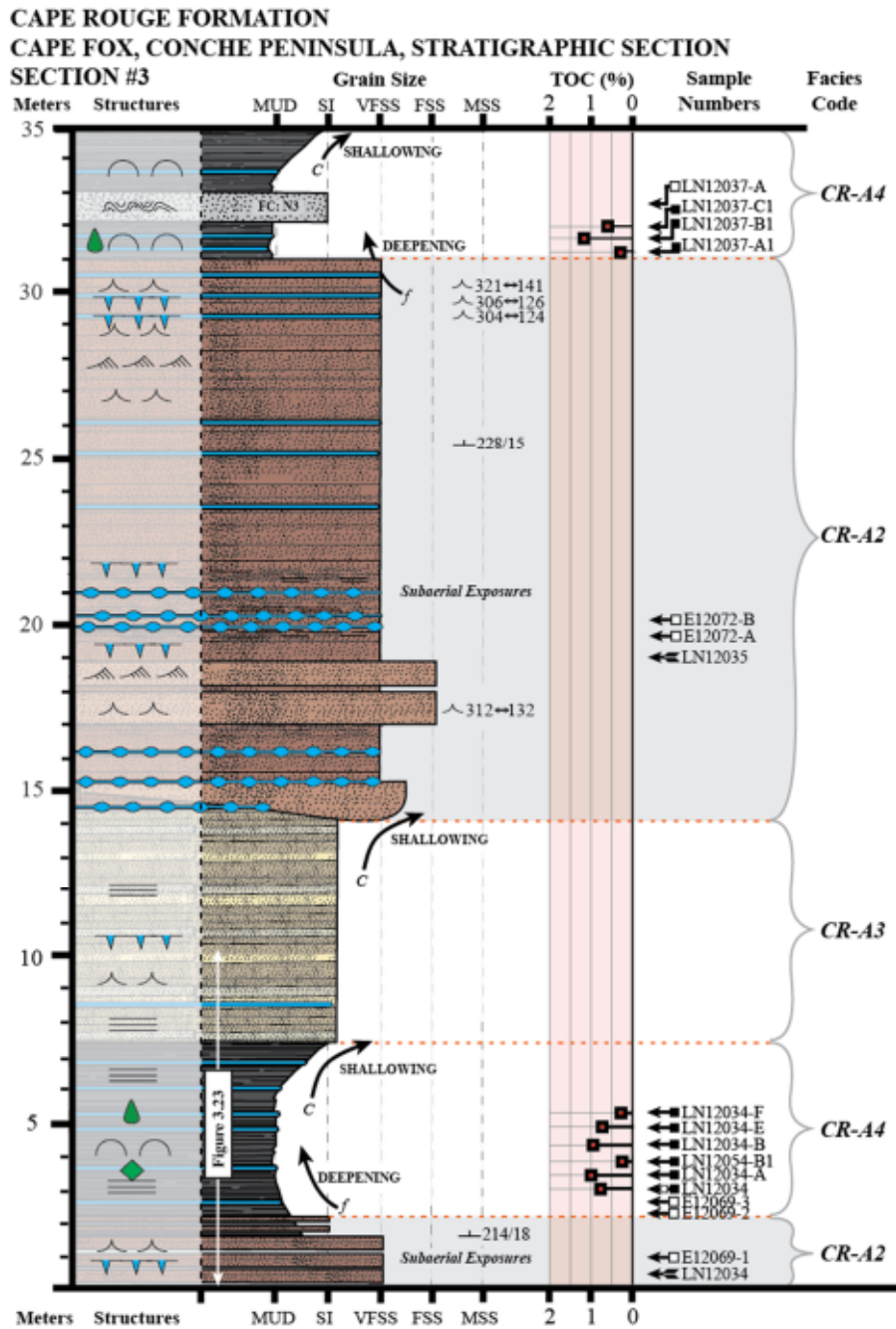


**Figure 3.21 Measured stratigraphic section #3 at Cape Fox, Conche Peninsula**  
Refer to Figure 3.16 for map location. Sample locations for TOC and thin section samples are marked by arrows, TOC values are in red. Numbers (e.g., N2, N3) in white present rock colours of fresh surfaces.

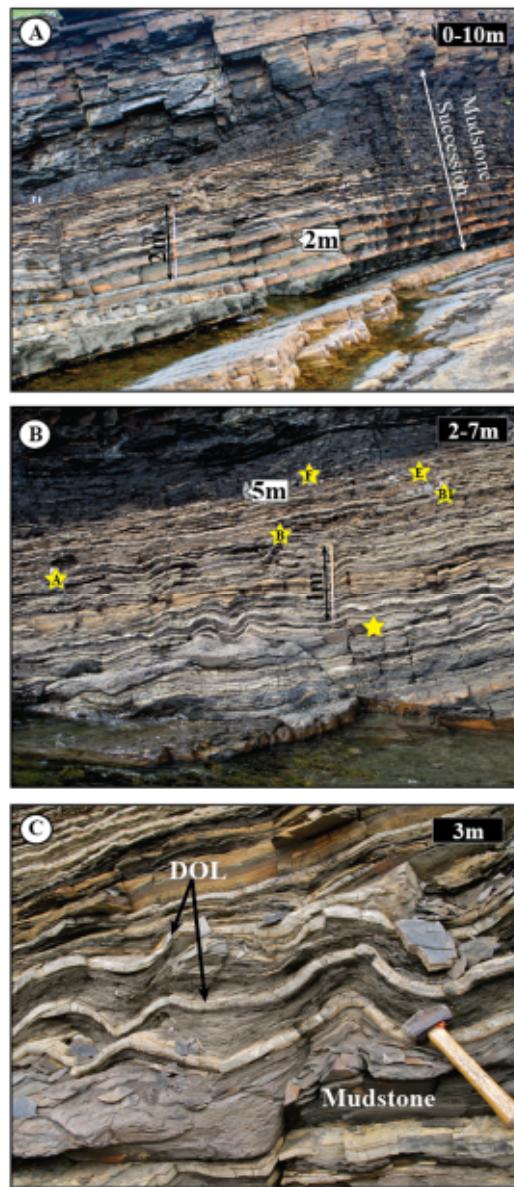


**Figure 3.22 Outcrop photos of fine-grained facies (CR-A4) of measured section #3 at Cape Fox, Conche Peninsula**

Photographs taken between the 0-10m interval of measured stratigraphic section #3 (Figure 3.21). (A) Base of Cape Fox Stratigraphic section representing Facies CR-A4, with ~30cm very fine-grained sandstone beds interbedded with mudstone horizons at the 2m marker, the succession grades into a sand-starved interval with mudstone-dolomite interbeds. 2m Jacobs staff for scale. (B) TOC sample locations within the 2-7m interval of Facies CR-A4. Mudstone and dolomite beds folded at base (C) Contorted dolomite with dark mudstone, hammer for scale.

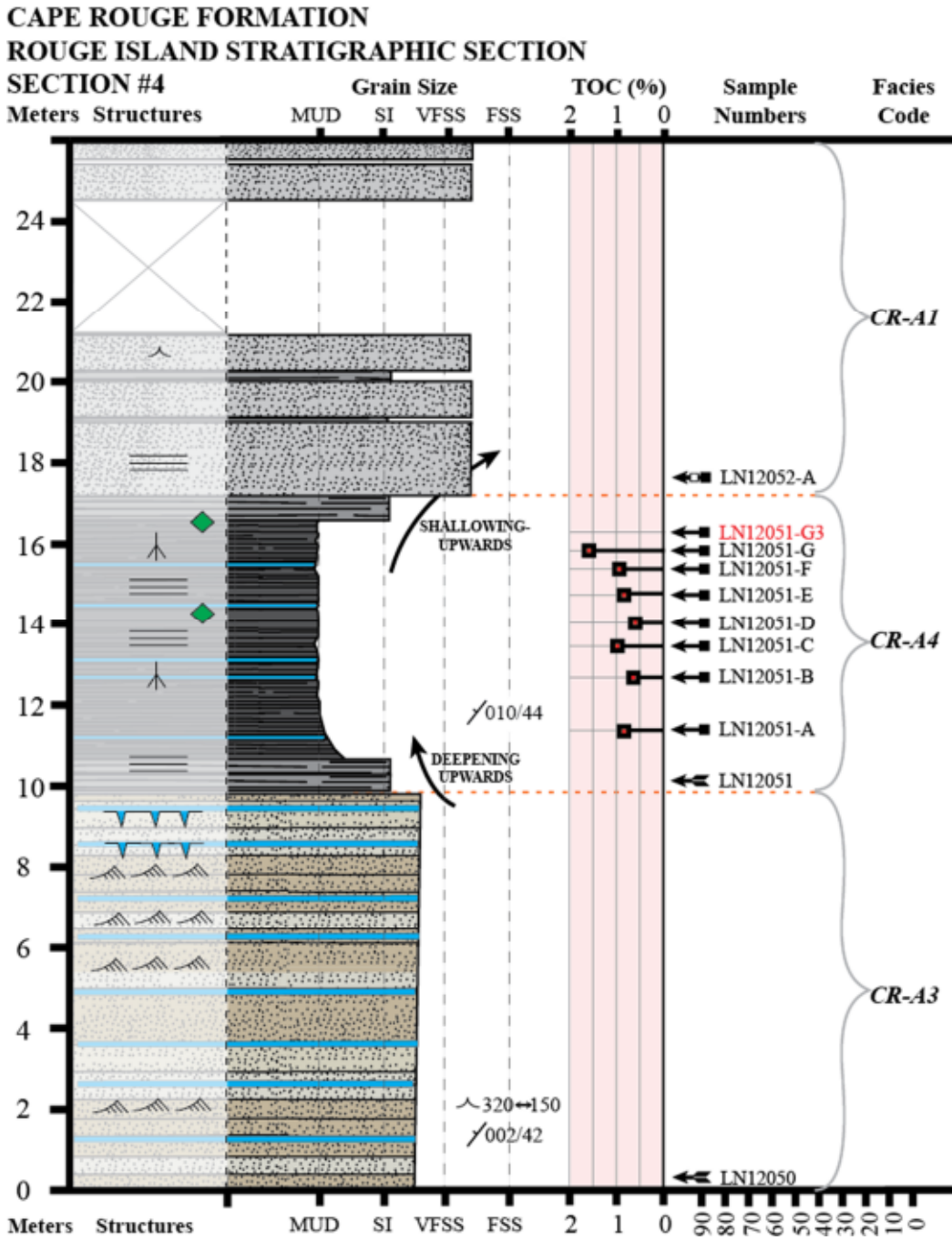


**Figure 3.23 Measured stratigraphic section #4 at Rouge Island**

Refer to Figure 3.16 for map location. Sample locations for TOC and thin sections are marked by arrows with TOC values (%) in red. Numbers (e.g., N2, N3) in white present rock colours of fresh surfaces.

## CHAPTER FOUR: SOURCE ROCK RESULTS

### 4.01 — Introduction

This chapter focuses on the organic-prone intervals of Facies Assemblage CR-A4 which are the key determinants of source rock prospectivity in this area. A varied suite of analysis is used to define source quality, quantity, and distribution. Analyses include optical and electron microscopy, geochemical (LECO Total Organic Carbon (TOC) and Rock-Eval pyrolysis) and thermal maturity analysis (%  $R_o$ , visual kerogen, and TAI). Both optical and electron microscopy analysis are used to compile mineral, textural and organic characteristics at a millimeter to micrometer scale. Moreover, geochemical and thermal maturation analysis are used to provide context for source quality and quantity.

### 4.02 — Optical and electron microscopy of mudstone Facies CR-A4

Fine-grained facies of facies assemblage CR-A4, considered the key part of this source rock study, are dominated by carbonaceous and zeolite rich mudstones and dolostones and display heterogeneity at the millimeter to micrometer scale with characteristics that are otherwise undetectable at the hand-sample scale. These fine-grained facies can be variable with respect to mineral composition, cement, sedimentary structures, and bioturbation content.

The following figures, comprised of optical and backscattered electron optical images, highlight distinguishing mineralogical and textural features common to this facies assemblage (Figure 4.1 through Figure 4.6). Although samples are heterogeneous

at a millimeter to micrometer scale, these mudstones share a number of broad overarching textural and compositional similarities. Mudstones are pervasively cemented by ferroan dolomite and analcime, with minor concentrations of late-stage calcite cement (occurring as dog-tooth calcite in fractures). Moreover, albite, illite, anorthite, pyrite (dominated by framboids), and pyrrhotite are also present in minor and varying concentrations, in addition to accessory minerals. Accessory minerals include quartz, apatite, titanite and monazite. Mudstones are commonly thinly laminated, often alternating between pellet mottled rich and dolomite rich or pyrrhotite bearing beds. Elsewhere, depending upon locality, other mudstones can also contain thin laminae of phosphatized algae mats.

At the millimeter scale, samples of mudstones and dolostones from the Conche and Cape Rouge peninsulas have abundant traces of pyrobitumen, and live oil observed to have migrated along vertical fracture planes, pooled in small microstructural traps (Figure 4.1) and locked between bedding planes (Figure 4.2).

Trace fossils are extremely rare within this facies assemblage. Vertical burrows, 0.5-1mm wide/3-3.5mm long, lined or filled with framboidal pyrite, are infrequently seen at Pyramid Point on the Cape Rouge Peninsula (Figure 4.3 A, E & F).

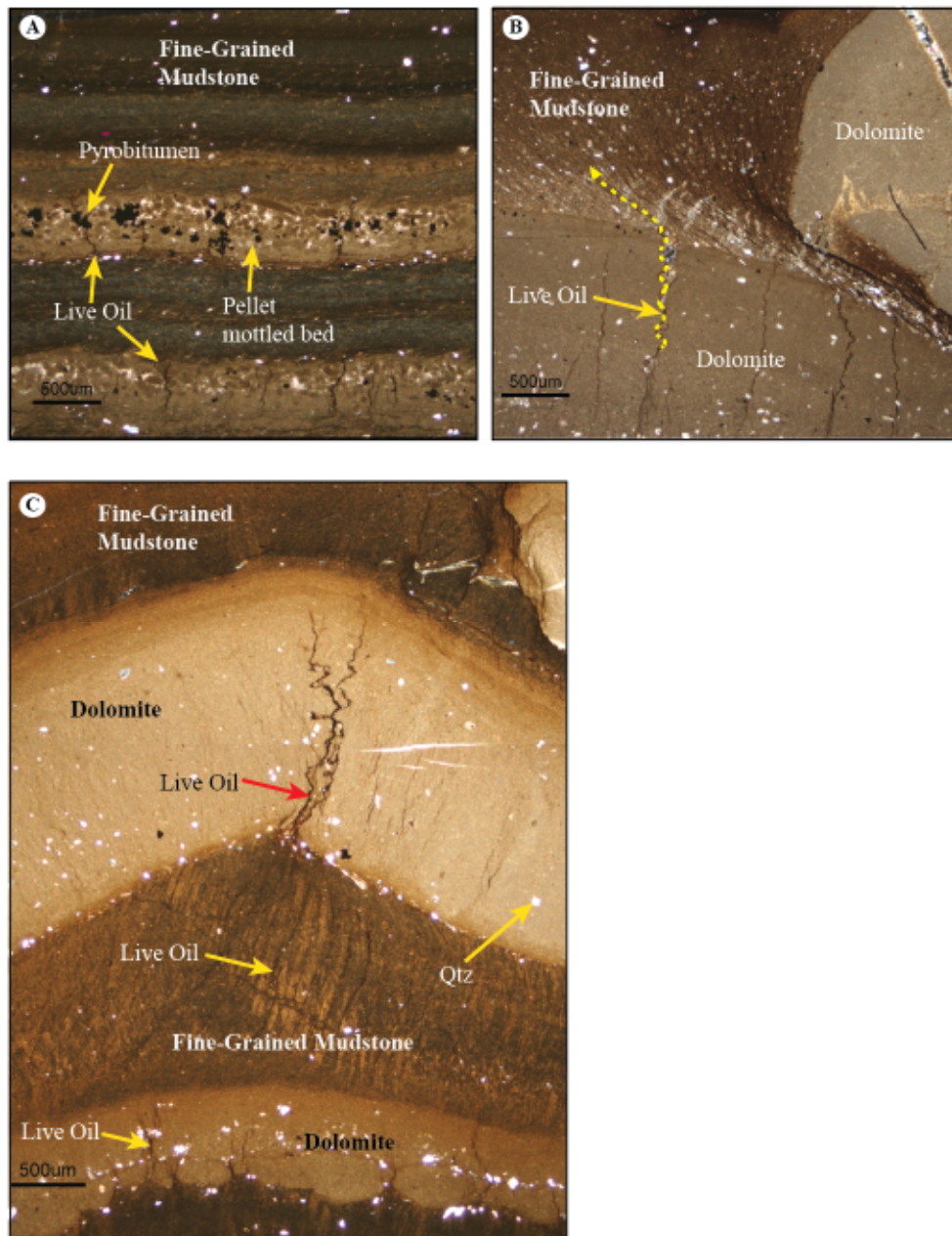


**Figure 4.1 Optical micrographs of hydrocarbon occurrences in mudstone and dolostone facies, Facies Assemblage CR-A4**

A) Pellet mottled mudstone with abundant live oil occupying fractures together with pooled accumulations of pyrobitumen. B) & C) Fractured dolostone interbedded with fine-grained mudstone. Live oil is found to have migrated along fractures, leaking into fine-grained mudstone layers.

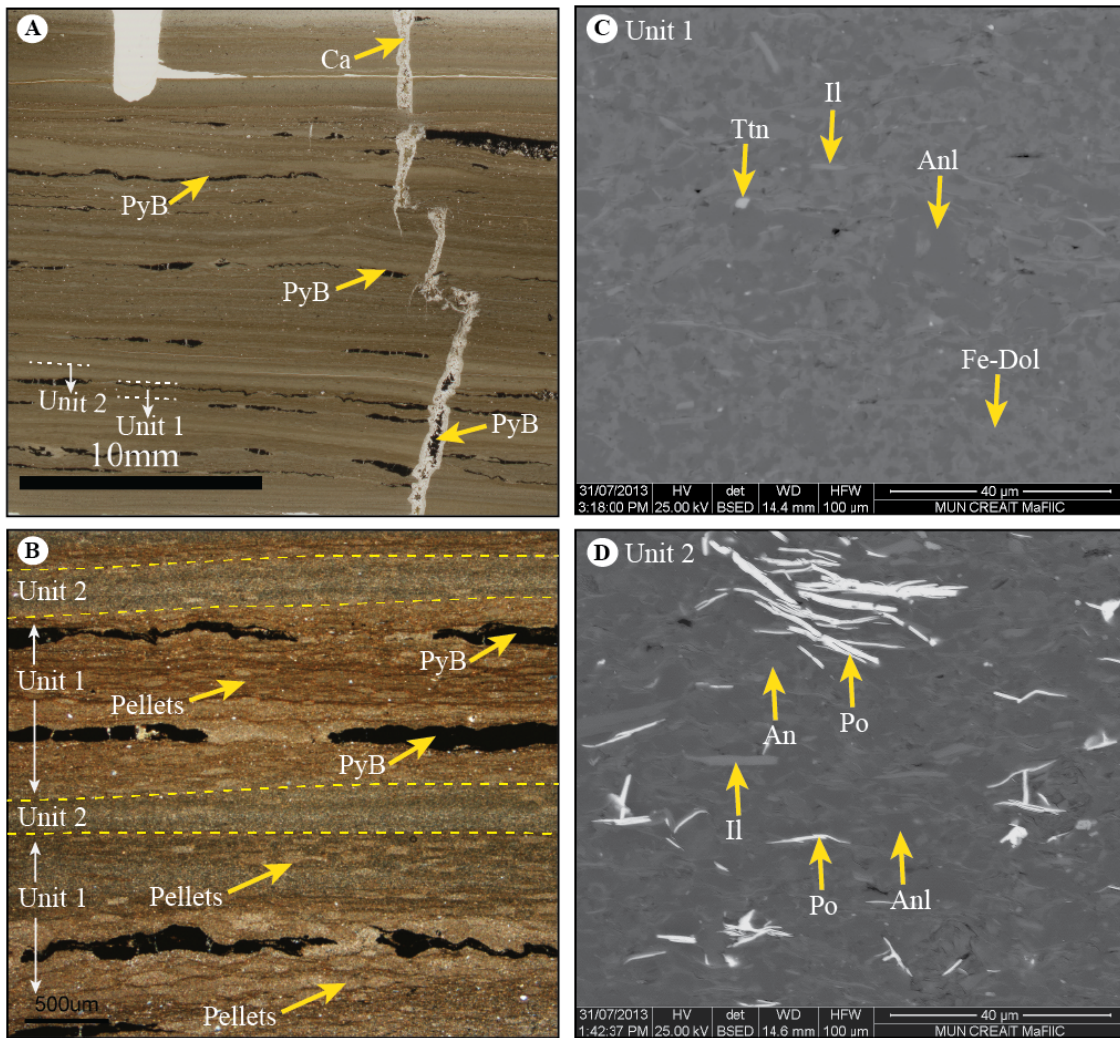


**Figure 4.2 Fine-grained mudstone character from the middle & lower intervals of Facies Assemblage CR-A4**

Thin section scan (A), optical image (B), and backscattered electron optical (C, D) micrographs of fine-grained mudstone from the Cape Rouge Peninsula. A) & B) Thinly interbedded mudstone (even-non parallel to even parallel beds) of pellet mottled, analcime-dolomite-cemented beds (Unit 1), pyrrhotite bearing zeolite-cemented beds (Unit 2) and irregular pyrobitumen lenses (PyB). A) Mudstone crosscut by fracture infilled with calcite and with pyrobitumen. C) Unit 1, composed of fibrous illite (Il), analcime (Anl) and ferrous dolomite (Fe-Dol) cements, and angular titanite grains. D) Unit 2, composed of analcime cement, anorthite, fibrous pyrrhotite (Po), and illite grains.

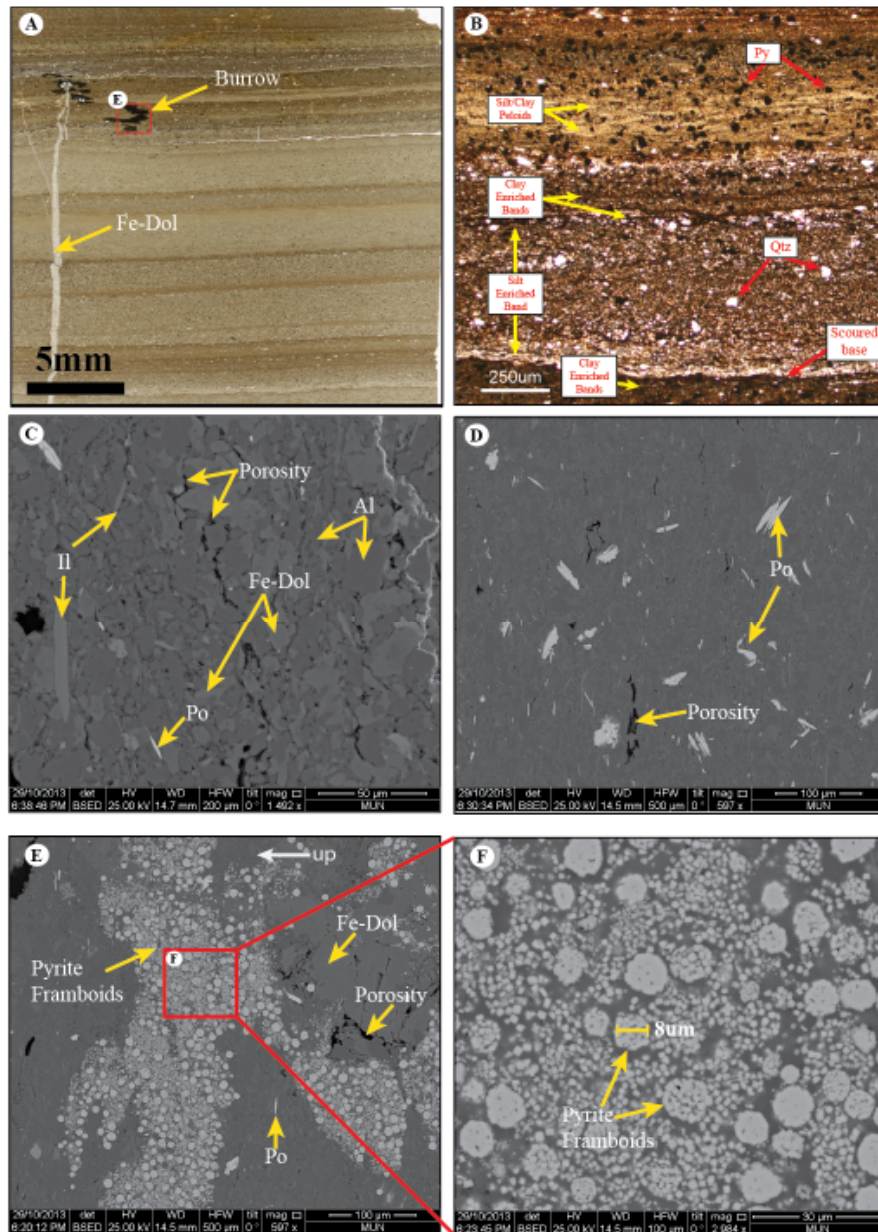


**Figure 4.3 Fine-grained mudstone character from the middle & lower intervals of Facies Assemblage CR-A4**

Thin section scan (A), optical image (B) and backscattered electron optical (C, D, E, F) micrographs of fine-grained mudstone from the Cape Rouge Peninsula. A) & B) Even-non parallel to even parallel mudstone laminae. B) Silt/clay rich peloid lamina inter-laminated with clay rich lamina and silt enriched lamina with scoured bases. C) Ferroan dolomite and albite rich interval with illite and minor pyrrhotite (Po), together with fracture porosity. D) Pyrrhotite (Po) enriched interval. E) & F) *Planolites* burrow completely infilled with pyrite framboids (8µm avg. diameter).

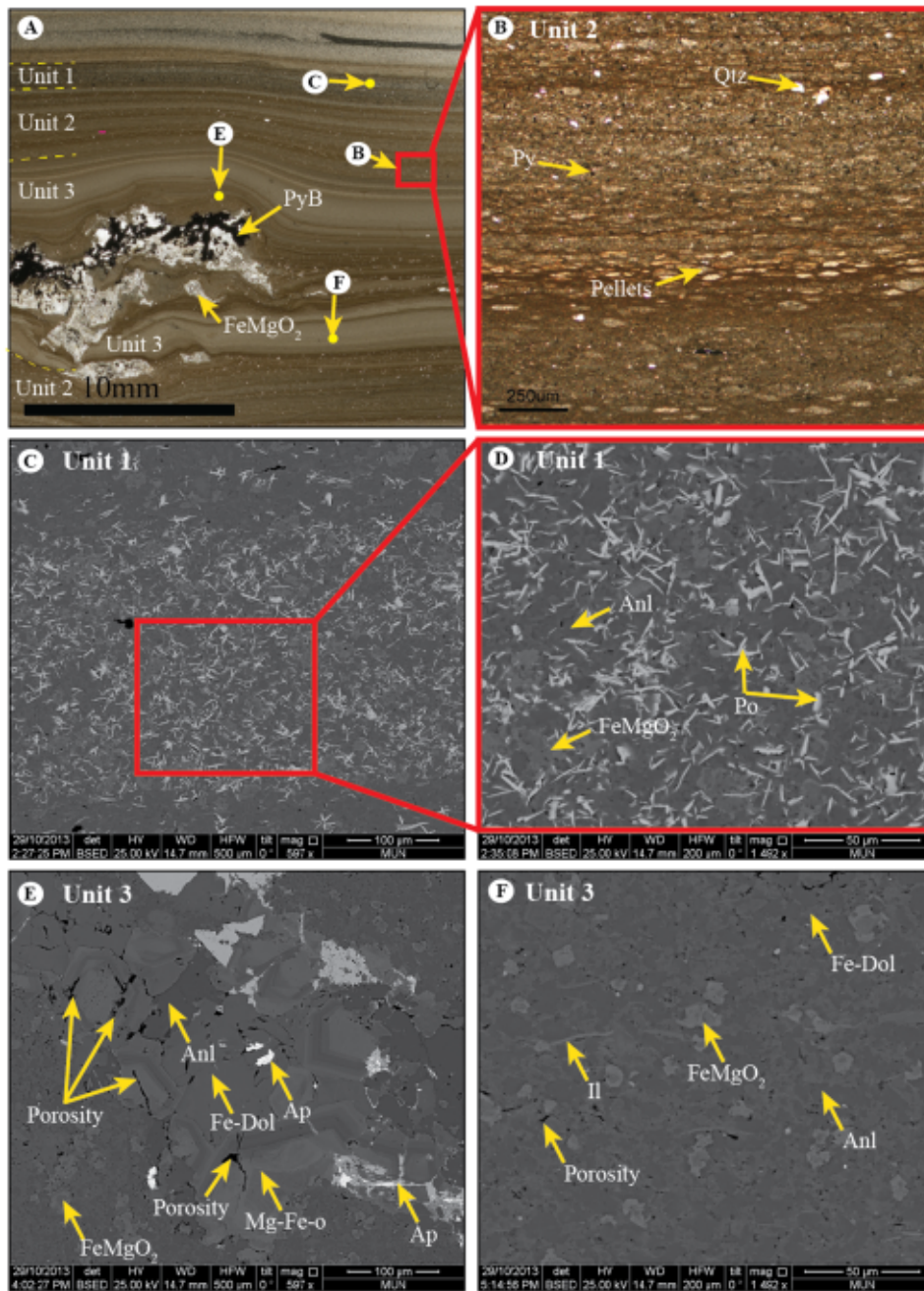


**Figure 4.4 Fine-grained mudstone characteristics from middle and lower intervals of Facies Assemblage CR-A4.**

Thin section scan (A), optical image (B) and backscattered electron optical (C, D, E, F) micrographs of fine-grained mudstone from the Cape Rouge Peninsula. An intensively dolomitized and analcime cemented interbedded mudstone composed of pellet mottled (B) and fibrous-pyrrhotite rich beds (C-D).

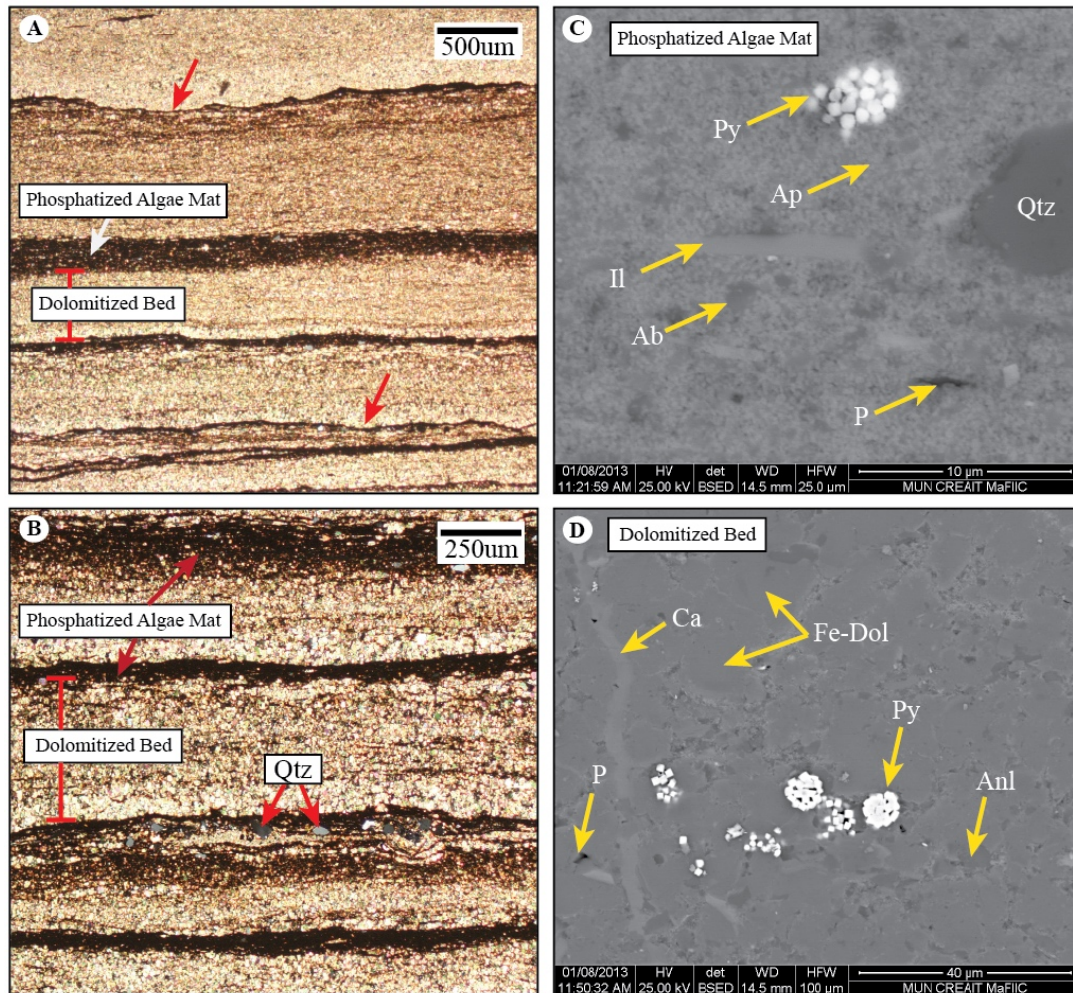


**Figure 4.5 Fine-grained mudstone character from the upper intervals of Facies Assemblage CR-A4.**

Thin section scan (A), optical (B) and backscattered electron optical (C & D) micrographs of fine-grained mudstone from the Conche Peninsula. An intensively dolomitized medium-grained mudstone interbedded with fine-grained laminated phosphatized algae mats. A) Interbedded fine-grained laminated phosphate-rich (dominantly apatite) beds (dark brown-black in color) with eroded beds (red arrow) with thicker, medium-grained dolomitized beds. B) mm-scale wavy-parallel bedding relationships. Phosphatized beds typically have detrital quartz clasts throughout (Qtz). Dolomitized beds are fine to medium-grained. C) Fine-grained phosphatized algae mat composed dominantly of apatite (Ap) with minor amounts of albite (Ab), illite (Il), pyrite (Py) framboids, and detrital quartz grains. Minor microporosity (P) is present. D) Intensively dolomitized med.-grained mudstone bed composed of Fe-rich dolomite (Fe-Dol) with minor concentrations of analcime (Anl), pyrite framboids, and calcite veins (Ca).

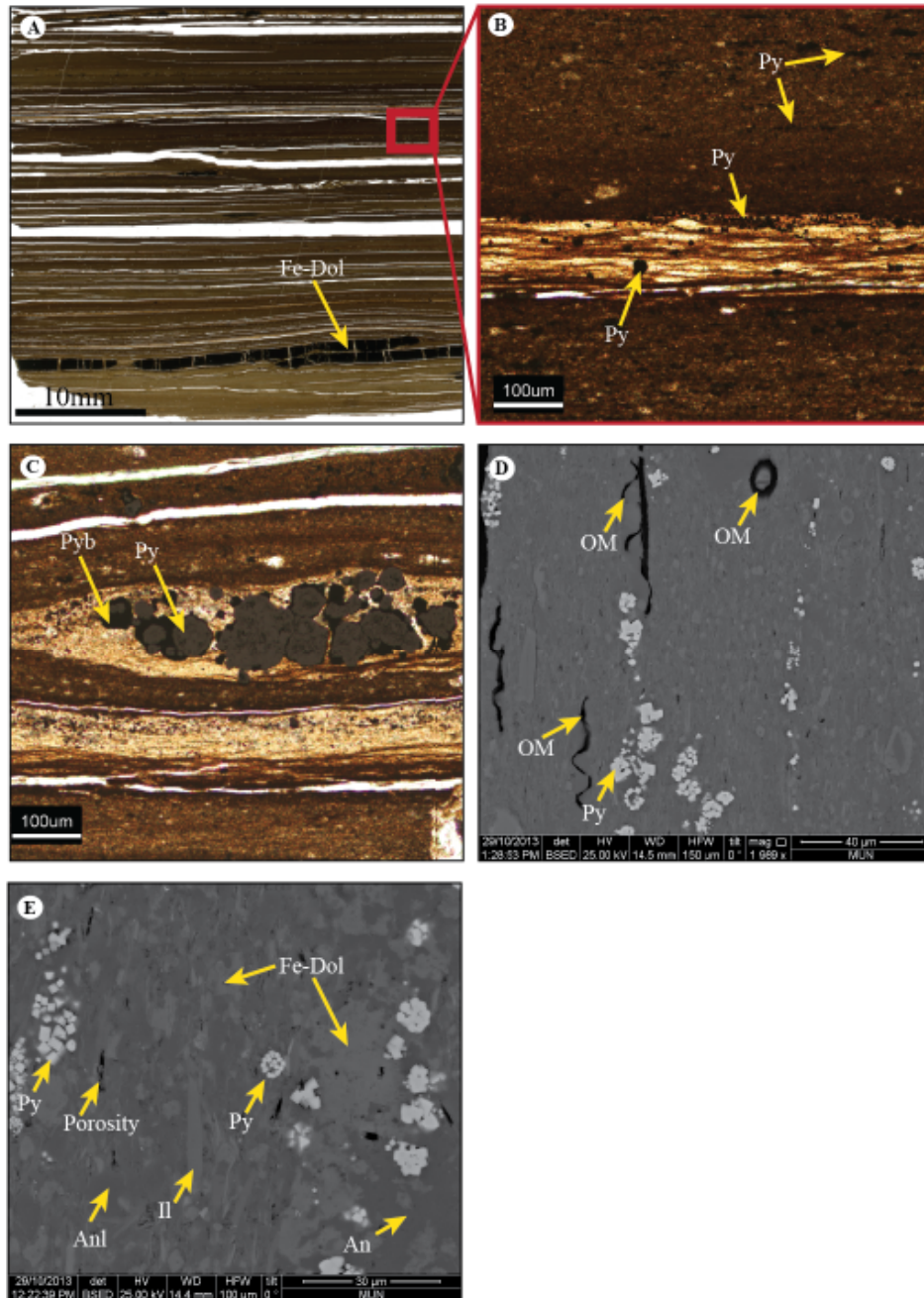


**Figure 4.6 Fine-grained mudstone character from the upper intervals of Facies Assemblage CR-A4.**

Thin section scan (A), optical image (B)/(C), and backscattered electron optical (D)/(E) micrographs of fine-grained mudstone from the Conche Peninsula. This sample represents a thinly interbedded carbonaceous and xolite cemented mudstone with pellet mottled, pyrite-pyrobitumen bearing horizons.

#### 4.02.01 Fine-Grained Facies Character

Mudstone samples from Facies Association CR-A4 are thinly laminated, and often consisting of pellet mottled and pyrrhotite bearing zeolite-cemented laminae (Figure 4.2, Figure 4.3, Figure 4.4). Laminae rich in pellets are commonly dominated by analcime (~50-60%) and ferroan dolomite (~40%) (Figure 4.2 B & C) cements with minor concentrations of framboidal pyrite, illite, anorthite, and quartz. Pyrrhotite bearing zeolite-cemented laminae are dominated by analcime cement (~50-60%) and they contain much less ferroan dolomite (<10%), carry concentrations of fibrous pyrrhotite (~15%) (Figure 4.2 D, Figure 4.4 C & D), and host an unknown iron-bearing mineral ( $\text{FeMgO}_2$  – 10%) (Figure 4.4 E & F), among other minor accessory minerals. Laminae are commonly even-parallel/even-non parallel to wavy parallel.

Thin (0.15-.250mm), discontinuous, wavy lenses of pyrobitumen lay in some bedding planes (Figure 4.2 A & B). Infrequent vertical fractures (.500-.750mm wide) are lined with dog-tooth calcite and migrated pyrobitumen (Figure 4.2 A).

Mudstone characteristics change slightly at the top of these stratal successions. As in those found deeper in a sequence, the mudstones at the top are dominated by analcime and ferroan dolomite cements (Figure 4.5, Figure 4.6) and frequently contain pellet mottled laminae (~100 $\mu\text{m}$  thick) with silt and clay peloids (Figure 4.6 B). However, these mudstones differ in that they frequently host thin (~0.05-0.250mm) fine-grained phosphatized algal mats.

Phosphatized algae mats in these laminae are dominantly clay sized ( $<0.5\mu\text{m}$ ) apatite cement ( $\sim 80\%$ ) (Figure 4.5 C) with minor amounts of framboidal pyrite ( $4\text{-}8\mu\text{m}$ ) ( $\sim 5\%$ ) (Figure 4.5 C) and silt sized ( $10\text{-}30\mu\text{m}$ ) sub-angular to sub-rounded detrital quartz (Figure 4.5 C) and other accessory minerals.

Organic matter includes woody material (Figure 4.6 D) together with plant spores and pyrobitumen. Similar to mudstones deeper in the sequences, these have late stage calcite cementation (Figure 4.5 D) and are thinly laminated. Laminations are often wavy-parallel with sharp and gradation bases (Figure 4.5 A, B; Figure 4.6 A). Often, there are pure ferroan dolostone laminae ( $1\text{-}1.25\text{mm}$  thick) showing signs of soft-sediment deformation (Figure 4.6 A).

#### **4.03 — Total Organic Carbon (TOC)**

Eighty-nine (89) samples from the Cape Rouge Peninsula, the Conche Peninsula, and Rouge Island are analyzed for TOC (for raw data, refer to Appendix 1). Sample localities on the Conche Peninsula include Chest Head, Martinique Point, Cape Fox, Point Dos Cheval, and two locations WSW of Point Dos Cheval. For the Cape Rouge Peninsula, localities include Goguelin Point, Truite Point, two localities NE and SW of Grande Point, and Pyramid Point. Moreover, and farther away, a suite of samples is from the north-western coast of Rouge Island.

TOC results for all samples show a unimodal, positive-skew distribution, with a single high outlier at 6.54% and a range between 0.23-6.54% (Table 7). Excluding this high outlier, the data have a range of 2.09% (Min of 0.23% and Max of 2.32%), a mode

of 1.30%, a median of 0.82%, and a mean of 0.94% (Figure 4.7 [row 1, column 1], Figure 4.8 A).

**Table 7 Total Organic Carbon (TOC) results by area**

<b>TOC (wt%)</b>				
	<b>Min-Max</b>	<b>Mode</b>	<b>Median</b>	<b>Mean</b>
<b>ALL DATA (n=89)</b>	0.23-6.54	1.30	0.82	1
<b>Cape Rouge Peninsula (n=28)</b>	0.23-6.54	1.30	1.30	1.31
<b>Conche Peninsula (n=52)</b>	0.29-1.86	0.93	0.81	0.88
<b>Rouge Island (n=9)</b>	0.60-1.56		0.82	0.86

On the Cape Rouge Peninsula, the 28 mudstone samples analyzed for TOC include Pyramid Point (n=16), Truite Point area (n=7), east Truite Point area (n=2), Goguelin Point (n=1), and the North Grande Point area (n=3) (Appendix 1 [column 8]). All the samples from Pyramid Point are from Stratigraphic Section 1 (8-20m and 140-150m). Here, TOC results are unimodal, with a positive skew distribution and a single point outlier at 6.54% (Figure 4.7 [row 2, column 1]). Excluding the high outlier, the data have a range of 2.09% (Min of 0.23% and Max of 2.32%), mode of 1.30%, median of 1.16%, and a mean of 1.27% (Figure 4.7 [row 2, column 1], Figure 4.8 A).

On the Conche Peninsula, 52 mudstone analyses are from Chest Head (n=4), Martinique Point (n=33), Cape Fox (n=9), Northern Coast (WSW of Point Dos Cheval) (n=5), and Point Dos Cheval (n=1) (for raw data, refer to Appendix 1). Samples from Martinique Point come from the 18-22m interval of Stratigraphic Section 2 and samples from Cape Fox are in the 3-6m interval of Stratigraphic Section 3. TOC results have a near symmetric (slight positive skewness) unimodal distribution with a range of 1.57%

(Min of 0.29% and Max of 1.86%), a mode of 0.93%, a median of 0.81%, and a mean of 0.88% (Figure 4.7 [row 3, column 1], Figure 4.8 A).

For Rouge Island, where 9 mudstone samples are analyzed from the 11-16m interval of Stratigraphic Section 4, the TOC values have a unimodal distribution with a range of 0.96% (Min of 0.60% and Max of 1.56%), a median of 0.82%, and a mean of 0.86% (Figure 4.7 [row 4, column 1], Figure 4.8 A).

#### **4.04 — Rock-Eval Pyrolysis**

Samples are also analyzed by Rock-Eval Pyrolysis (n=89) (for raw data, refer to Appendix 1 [columns highlighted in green] and appendix 2 [pyrograms]). Rock-Eval pyrolysis results include S<sub>1</sub> (mg HC/g), S<sub>2</sub> (mg HC/g), S<sub>3</sub> (mg CO<sub>2</sub>/g), T<sub>max</sub> (temperature at S<sub>2</sub> peak maximum), and derived results that include calculated R<sub>o</sub> (%), Hydrogen Index (HI), Oxygen Index (OI), Production Index (PI), normalized oil content (S<sub>1</sub>/TOC), and S<sub>2</sub>/S<sub>3</sub> ratios.

S<sub>1</sub> results are low, with a range between 0.04-1.05 mg HC/g whole rock, but with two higher outliers of 2.91 and 4.88 mg HC/g in rock from Conche Peninsula.

For all samples, the S<sub>1</sub> median is 0.21 with a mean of 0.31mg HC/g rock. Samples from the Cape Rouge Peninsula tend to have a slightly lower median value of 0.15 and a mean of 0.16 mg HC/g rock. From Conche Peninsula, samples have a slightly higher median of 0.23 and a mean of 0.39 mg HC/g rock. Moreover, the small sample set of Rouge Island material has a median of 0.26 and a mean of 0.34 mg HC/g rock.

S<sub>2</sub> values range between 0.02-13.77 mg HC/g of rock with a high outlier of 34.74 mg HC/g in one sample from the Cape Rouge Peninsula (Figure 4.8 B). Samples

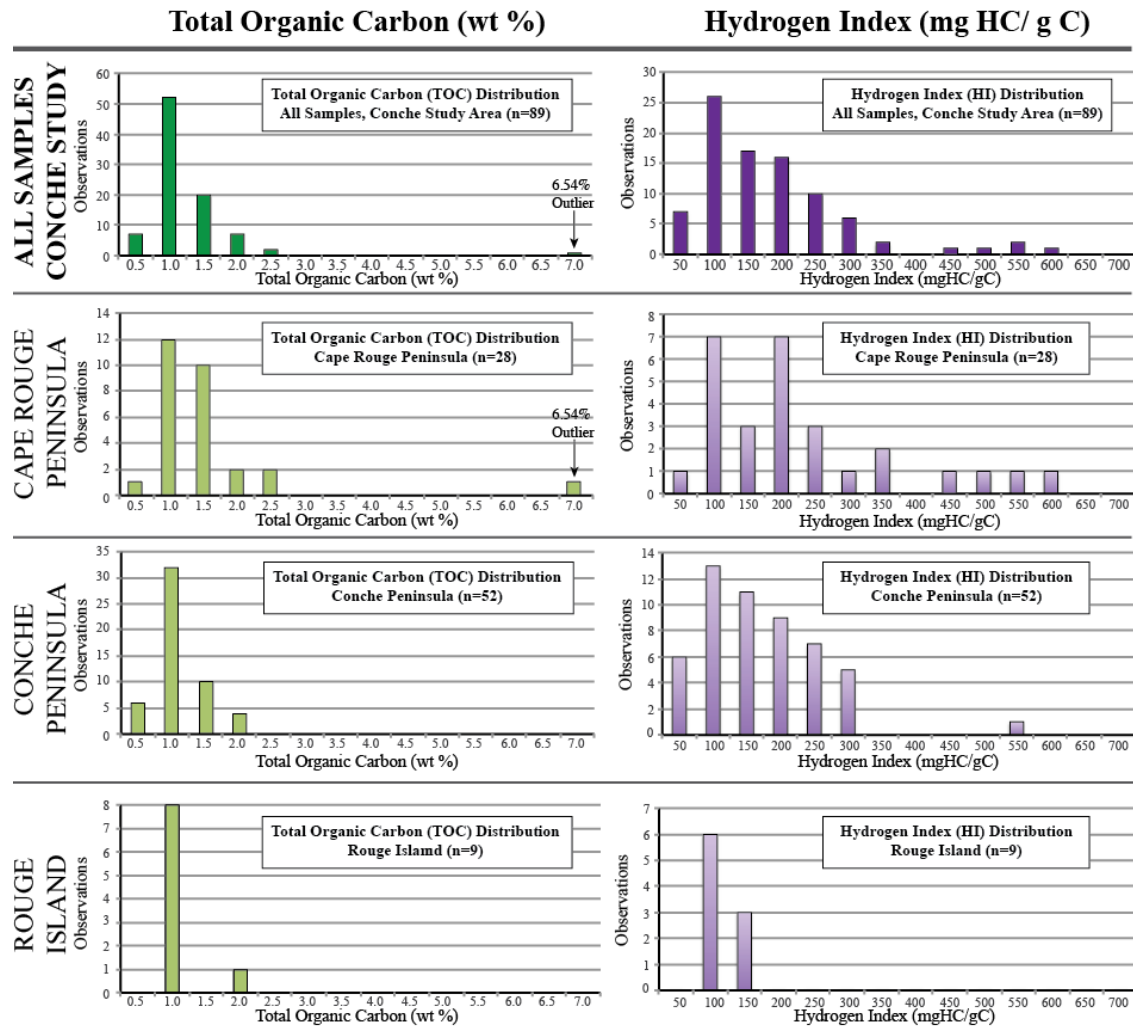


**Figure 4.7 Total Organic Carbon (TOC) and Hydrogen Index (HI) distributions**

Total Organic Carbon (TOC) (wt. %, represented by green histograms) and Hydrogen Index (mg HC/ g C, represented by purple histograms) data distributions for fine-grained samples of the Conche study area (n=89). Data distributions are divided into sample localities that include the Cape Rouge Peninsula (n=28), the Conche Peninsula (n=52), and Rouge Island (n=9).

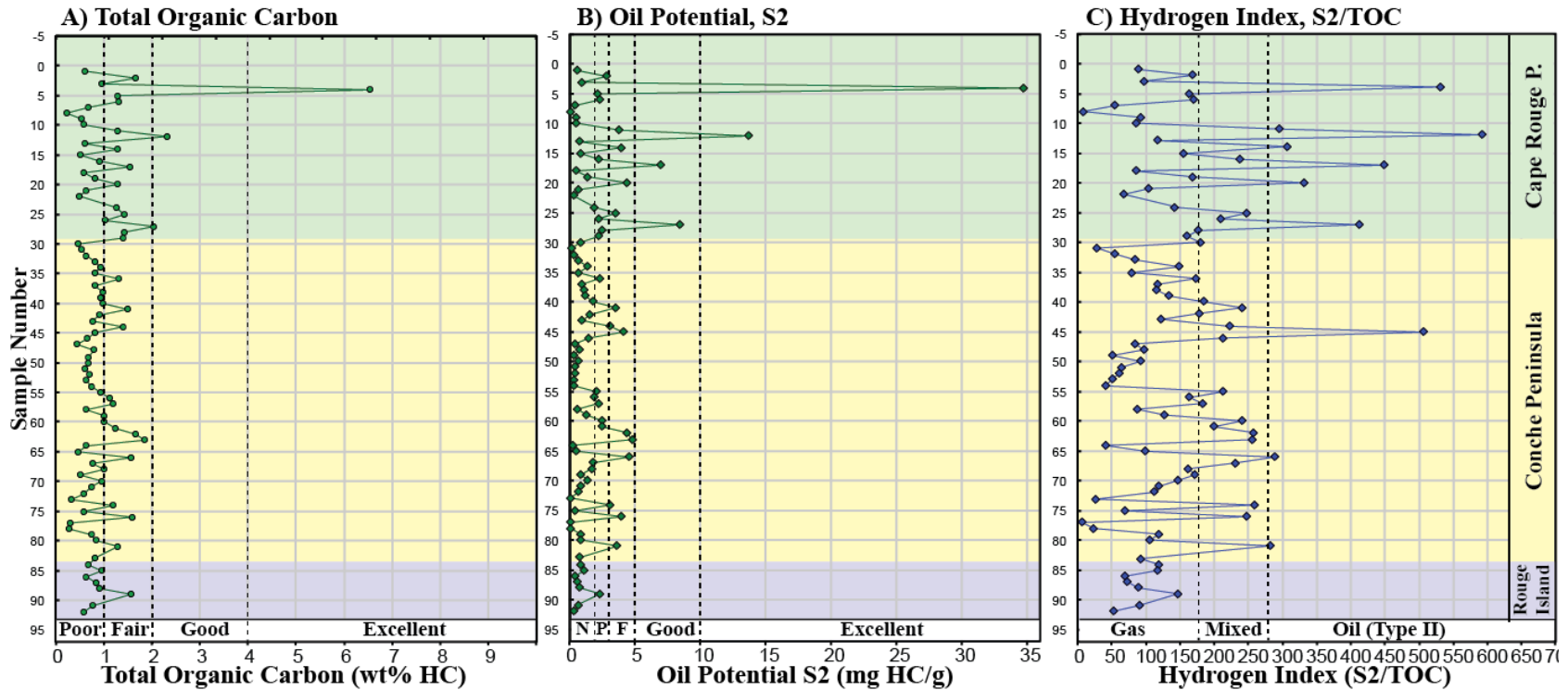


**Figure 4.8 Source potential graphs from Rock-Eval pyrolysis and thermal maturity data analyzed in the Conche study area**

Data encompass samples from the Cape Rouge Peninsula (no. 1-27, highlighted green), the Conche Peninsula (no. 28-79, highlighted yellow), and Rouge Island (no. 80-88), highlighted green). Refer to Appendix 1, column “No.,” for raw data. Graph A) Total Organic Carbon (wt.%) vs. sample numbers. Based on TOC values, the graph divides samples into poor (0-1% TOC), fair (1-2% TOC), good (2-4% TOC), and excellent (>4% TOC) source rock quality. Graph B) Oil Potential (S<sub>2</sub>) vs. sample numbers. Based on S<sub>2</sub> (mg HC/g), the graph divides samples into None (<2), Poor (2-3), Fair (3-5), Good (5-10), and Excellent (>10) oil potential. Graph C) Hydrogen Index (HI) vs. sample numbers. Graph divides samples into hydrocarbon types based on HI values: Gas (<200), Mixed (200-300), and Oil Type II (>300).

with high  $S_2$  values correspond to samples collected from the Cape Rouge Peninsula. Here,  $S_2$  values are between 0.02-13.77, and include a very high outlier with 34.74 mg HC/g whole rock. Samples from the Conche Peninsula have a lower data range for  $S_2$ , between 0.02-4.78 mg HC/g rock.  $S_2$  values from offshore Rouge Island are lower again, between 0.32-2.29 mg HC/g rock (Figure 4.8 B). Hydrogen Index (HI) ( $(S_2 \times 100)/\text{TOC}$ ) results range from 6.64 to 594 mg HC/g TOC (raw data located in appendix 1 [column 16], Figure 4.7 [column 2, row 1], Figure 4.8 C), with a mean of 158.39 and a median of 128.4 mg HC/g TOC. Results have a positive skew with a bimodal distribution (with a minor peak at  $>400$  mg HC/g TOC) (Figure 4.7 [column 2, row 1]). The primary mode has a local mean of 139, and a median of 119, while the second (higher) mode has a mean of 499 and a median of 506 mg HC/g TOC. The higher mode is attributed to data from the Cape Rouge Peninsula and one sample from the Conche Peninsula. HI indices from the Cape Rouge Peninsula have a mean of 204 and a median of 166 mg HC/g TOC while HI indices from the Conche Peninsula have a mean of 145 and a median of 125 mg HC/g TOC. Moreover, HI indices from Rouge Island have lower averages with a mean of 95 and a median of 90 mg HC/g TOC (Figure 4.7 [column 2]). The Production Index (PI) ( $S_1/(S_1+S_2)$ ) ranges from 0.01 to 0.71 (Figure 4.9 B).

#### **4.05 — Organic Petrography & Thermal Maturity**

Thermal maturity distribution is inferred from  $R_o$  and TAI data from 14 samples (Table 8). Moreover, Thermal maturity is also estimated by  $T_{\max}$  and Calculated  $R_o$  parameters from Rock-Eval pyrolysis for 89 samples (Figure 4.9 C, raw data included in appendix 1).

Vitrinite results are presented in histogram format by locality (including allochthonous, autochthonous, and suppressed grains) in Figure 4.10, Figure 4.11 and Figure 4.12. Mean  $R_o$  (%) data, together with the number of vitrinite grains (including divisions based on sample populations of autochthonous, allochthonous, and suppressed vitrinite), laboratory notes, and kerogen type are presented in Table 8. For all samples ( $n=14$ ), the mean  $R_o$  (for autochthonous vitrinite phytoclasts) ranges between 0.5-1.01% (or 0.55-1.12% when including allochthonous macerals). A subset of samples from the Conche and Cape Rouge peninsulas have mean  $R_o$  from 0.5-0.8% and 0.6-1.01%, respectively (Figure 4.10, Figure 4.11), and 2 samples from Rouge Island are  $R_o$  0.73 and 0.75% (Figure 4.12).

In addition to measured  $R_o$ , Rock-Eval Pyrolysis data also provide an estimate for thermal maturity for a broader distribution of samples. Pyrolysis  $T_{max}$  values range between 430-457°C (Figure 4.9 C). With  $T_{max}$  pyrolysis measurements, a calculated  $R_o$  is derived  $[(0.0180 \times T_{max}) - 7.16]$  and used as an estimate of thermal maturity for all samples ( $n=68$ ) (excluding samples with low  $S_2$  shoulders). All calculated  $R_o$  data range from 0.58–1.07%. Regional calculated  $R_o$  values from the Cape Rouge Peninsula and Conche Peninsula range from 0.58-1.05% and 0.69-1.07%, respectively. Offshore, the calculated  $R_o$  values from Rouge Island range from 0.83-1.07% (Figure 4.9 C, refer to red diamonds).

Fourteen samples were also analyzed for TAI with results ranging between 2 to 3- on the Cape Rouge and Conche peninsulas and between 2+ to 3- on Rouge Island

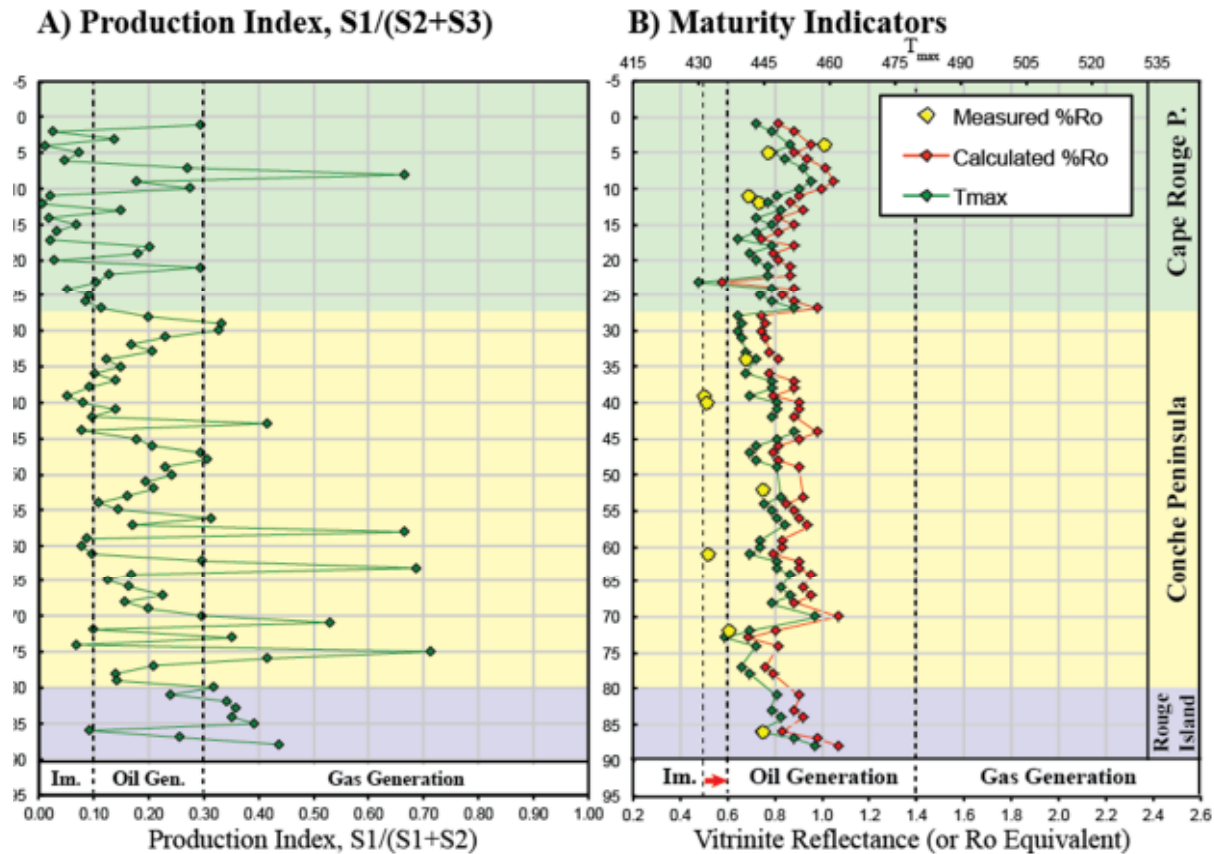


**Figure 4.9 Hydrocarbon and thermal maturity indicator graphs from all Rock-Eval pyrolysis and thermal maturity data**

Data encompass samples collected in the Cape Rouge Peninsula (highlighted green), the Conche Peninsula (highlighted yellow), and Rouge Island (highlighted green). Graph A) Production Index ( $PI = S_1 / (S_1 + S_2)$ ) vs. sample number. Samples subdivided, based on PI into immature, oil generation, and gas generation windows. Graph B) Maturity Indicators, including measured Ro (yellow diamonds), calculated Ro (red diamonds) and  $T_{max}$  (green diamonds) vs. sample number. Samples subdivided, based on % Ro, into immature, oil generation, and gas generation windows.

(Table 8). Fluorescence analyses show yellow to orange colour for algae, liptinite, and AOM2 particles with one red fluorescing algae maceral (Table 8).

#### **4.06 — Visual Kerogen**

Visual kerogen is analyzed optically (% volume by sample) for 14 samples (Table 9). Two samples contained uncertain kerogen macerals and are therefore excluded from further discussion (samples Ln12051-G & E12209). Visual kerogen analysis includes differentiation of terrestrial, lacustrine, and marine organic matter.

Terrestrial visual kerogen includes autochthonous vitrinite (Vit1), allochthonous vitrinite [exotic, (Vit2)], inertinite (oxidized or forest fire derived lingo-cellulose components), exinite (plant spore, cuticles and resins) together with amorphous lipid and humic components derived from terrestrial organic matter (AOM3). Moreover, lacustrine/marine organic matter includes alginate (both lamellar algae and algal clustered cells), algodetrinite (detrital algal remnants), and bacterial degradation of algal remnants (including AOM1: Telalginite degradation and AOM2: lamalginite degradation).

The 12 samples analyzed for visual kerogen are dominated by lamalginite degraded kerogen [(AOM2)  $\leq 75\%$ ] and alginate/algodetrinite kerogen ( $\leq 35\%$ ) (Figure 4.13). All samples contain lesser amounts of amorphous lipid and humid components [(Aom3)  $\leq 23\%$ ], with the exception of the Rouge Island sample Ln12051-G3 that contains no AOM3 kerogen macerals.

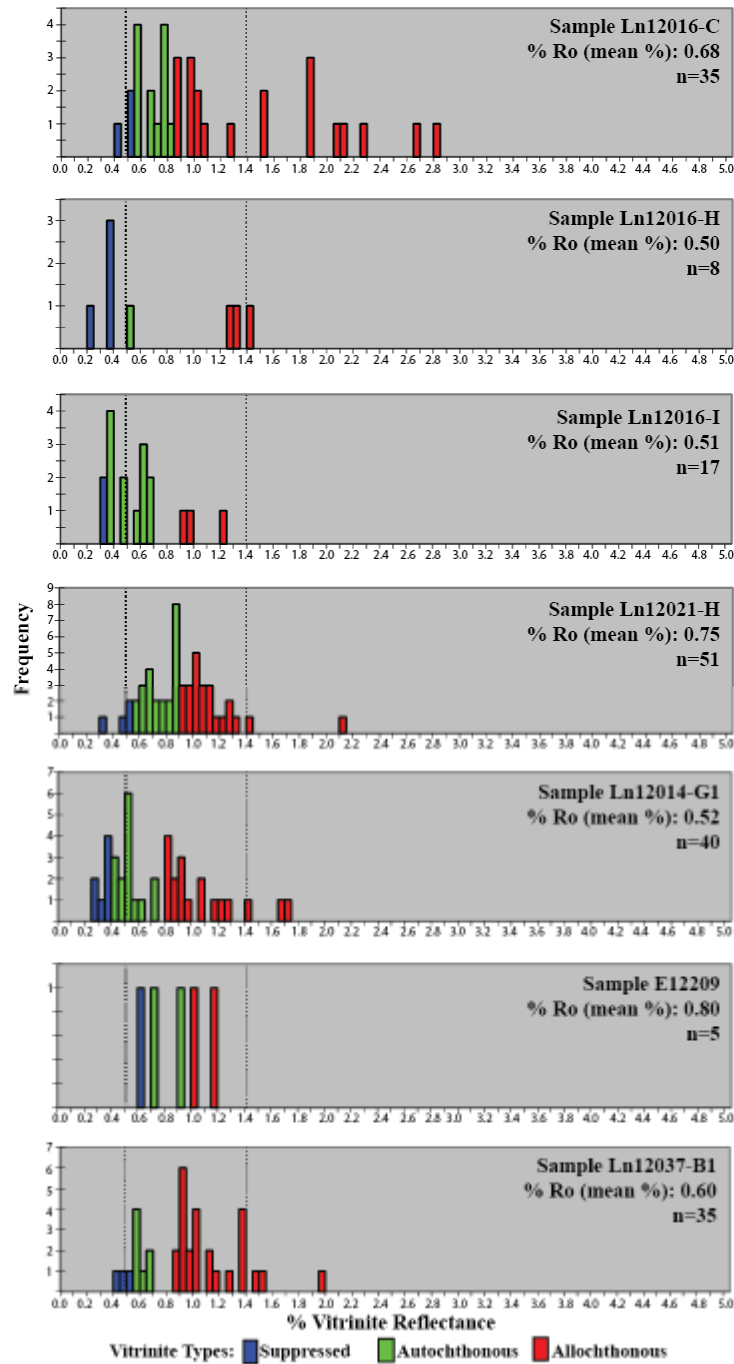


**Figure 4.10 Vitrinite reflectance histograms from the Conche Peninsula**

Autochthonous (green), suppressed (blue) and allochthonous grains (red). The dashed line at 0.5% Ro represents the beginning of the oil generation window and the dashed line at 1.4% Ro represents the ending of the oil generation window.

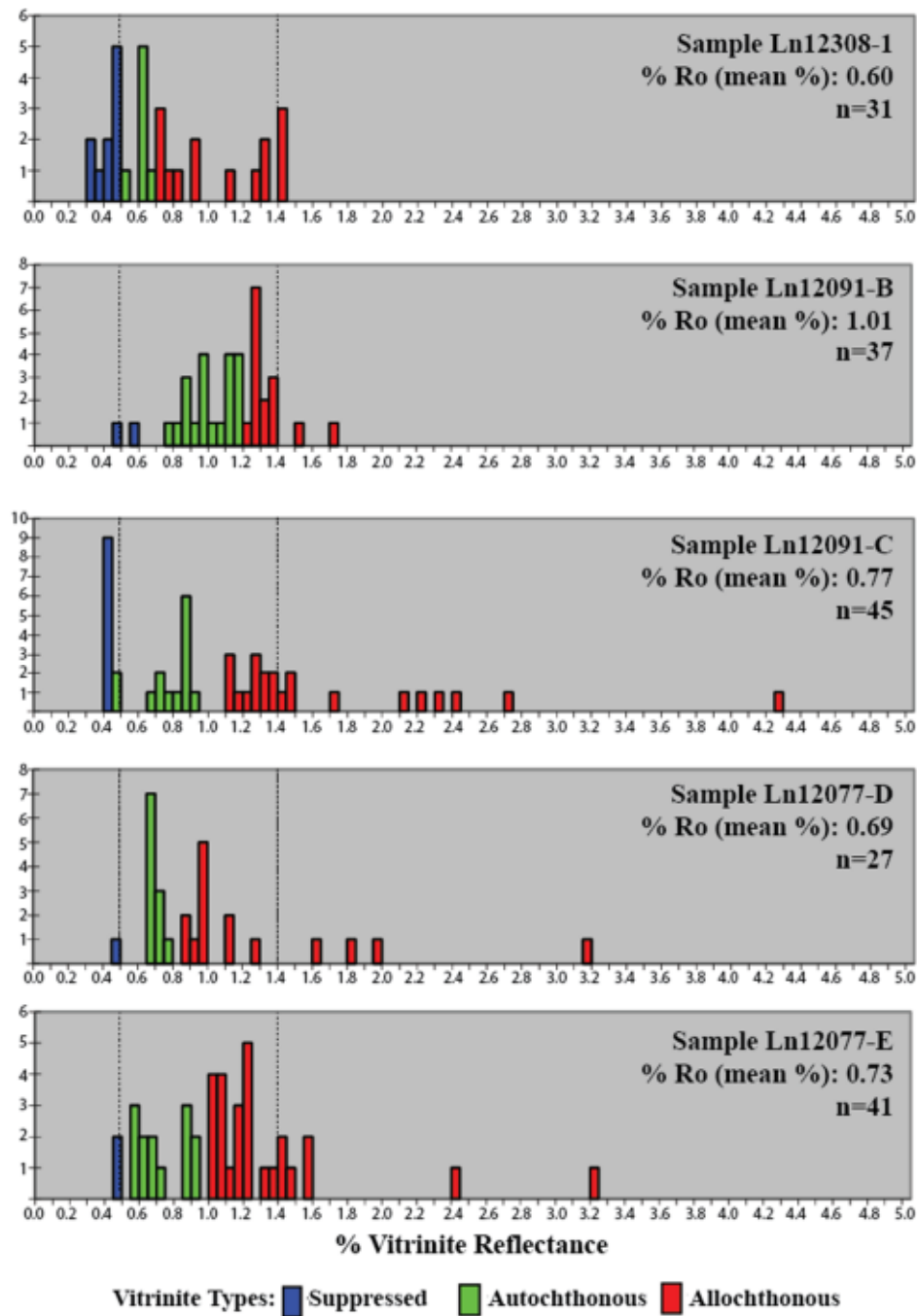


**Figure 4.11 Vitrinite reflectance histograms from the Cape Rouge Peninsula**

Autochthonous (green), suppressed (blue) and allochthonous grains (red). The dashed line at 0.5% Ro represents the beginning of the oil generation window and the dashed line at 1.4% Ro represents the ending of the oil generation window.

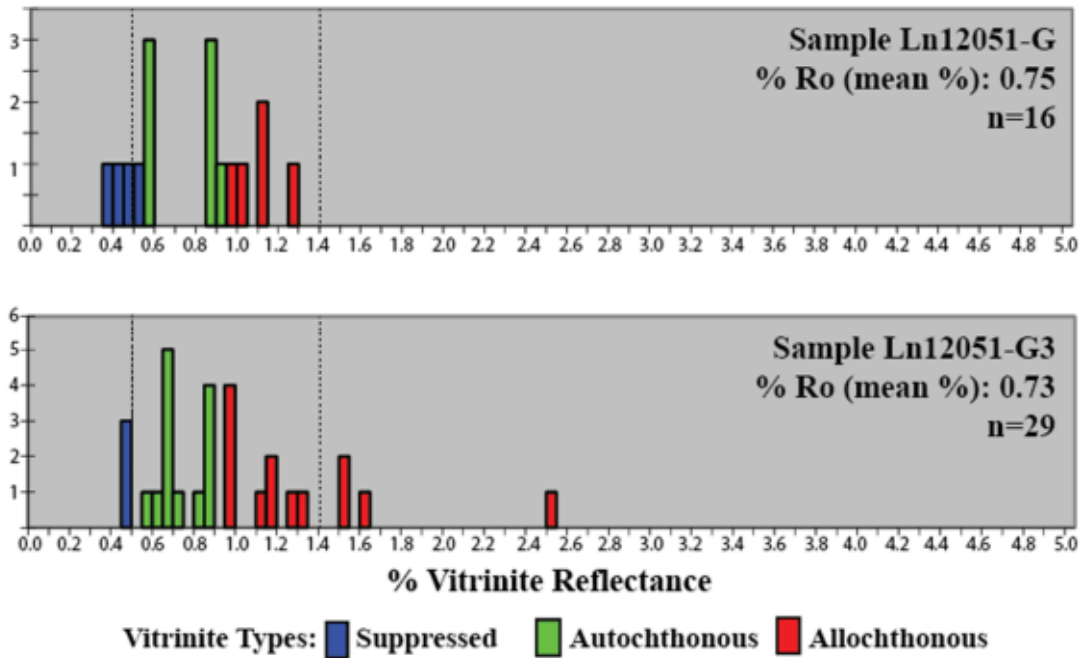


**Figure 4.12 Vitrinite reflectance histograms from Rouge Island**

Autochthonous (green), suppressed (blue) and allochthonous grains (red). The dashed line at 0.5% Ro represents the beginning of the oil generation window and the dashed line at 1.4% Ro represents the ending of the oil generation window.

**Table 8 Vitrinite Reflectance (% R<sub>o</sub>) and Thermal Alteration Index (TAI) results of the Cape Rouge Formation Facies Association CR-A4**

Sample Name	Sample Location	Sample Region	GPS UTM NAD27	TAI	% R <sub>o</sub> (Mean %)	Std. Dev.	No. of Vit. Grains (%)	No. Autoch. Vitrinite (%)	No. Alloch. Vitrinite (%)	No. Supp. Vitrinite (%)	All VRo (mean %)	Comment	Kerogen Type (*)
Ln12014-G1	Martinique Point	CP	21 U 577485 5636278	2	0.52	0.1	40	15	18	7	0.72	Yellow fl. Algae	II
Ln12016-C	Martinique Point	CP	21 U 577462 5636353	2 to 2+	0.68	0.1	35	12	20	3	1.12	Orange fl Algae	II
Ln12016-H	Martinique Point	CP	21 U 577462 5636353	2 to 2+	0.5	0	8	1	3	4	0.65	Yellow fl. Algae	II
Ln12016-I	Martinique Point	CP	21 U 577462 5636353	2 to 2+	0.51	0.12	17	12	3	2	0.55	Yellow fl. Algae	II
Ln12021-H	Martinique Point	CP	21 U 577462 5636353	2 to 3-	0.75	0.11	51	23	24	4	0.89	Orange fl AOM 2	II-III
Ln12037-B1	Cape Fox	CP	21 U 577834 5634761	2 to 2+	0.6	0.08	35	7	25	3	0.94	Yellow/Orange Algae	II-III
E12209	Frauderesse Point	CP	21 U 580579 5639969	3-	0.8	0.14	5	2	2	1	0.73	Uncertain Data	II-III?
Ln12091-B	Pyramid Point	CRP	21 U 582514 5646049	3- to 3	1.01	0.13	37	20	15	2	1.09	Red fl. Algae	II or II-III
Ln12091-C	Pyramid Point	CRP	21 U 582514 5646049	2+ to 3-	0.77	0.14	45	14	22	9	1.12	Orange fl. Bitum.	II
Ln12077-D	Pyramid Point	CRP	21 U 582388 5645949	2 to 2+	0.69	0.04	27	11	15	1	0.99	Yellow fl. Liptinite	II
Ln12077-E	Pyramid Point	CRP	21 U 582388 5645949	2+ to 3-	0.73	0.14	41	13	26	2	1.08	Orange fl. Liptinite	II
E11308-1	Truite Point	CRP	21 U 580808 5641594	2 to 2+	0.6	0.5	31	7	14	10	0.73	Orange fl Bitumen	II
Ln12051-G	West Coast	RI	21 U 586519 5639223	2+ to 3-	0.75	0.17	16	7	5	4	0.74	Uncertain Data	II-III?
Ln12051-G3	West Coast	RI	21 U 586519 5639223	2+ to 3-	0.73	0.11	29	13	13	3	0.93	Yellow Brown fl	II

**Table Abbreviations and Notes:**

CP, Conche Peninsula; CRP, Cape Rouge Peninsula; RI, Rouge Island; TAI, Thermal Alteration Index; % R<sub>o</sub>, mean random Vitrinite Reflectance; Std. Dev., Standard Deviation of R<sub>o</sub> measurements; No. of Vit. Grains, Number of Vitrinite Grains measured; No. Autoch. Vitrinite, Number of Autochthonous Vitrinite (First cycle) grains measured; No. Alloch. Vitrinite, Number of Allochthonous Vitrinite (recycled) grains measured; No. Supp. Vitrinite, Number of Suppressed Vitrinite (Lower VRo) grains measured; All VRo, mean Vitrinite Reflectance of all measured grains; fl, fluorescence.

**Table 9 Visual kerogen results of the Cape Rouge Formation Facies Association CR-A4**

Sample Name	Sample Location	Sample Region	GPS UTM NAD27	Vit1 Vol%	Vit2 Vol%	Inertinite Vol %	Exinite Vol %	Alg/Algodet Vol%	AOM 1 Vol %	AOM 2 Vol %	AOM 3 Vol %	Solid Bit Vol %	Anoxic/Dysoxic/	Kerogen Type	Comments
Ln12014-G1	Martinique Point	CP	21 U 577485 5636278	2	2	1	10	25	0	35	23	2	Dysoxic	II-III	Partially oxid.
Ln12016-C	Martinique Point	CP	21 U 577462 5636353	1	2	1	5	24	0	50	13	4	Dysoxic/anoxic	II or II-III	Partially oxid.
Ln12016-H	Martinique Point	CP	21 U 577462 5636353	0.5	0.5	1	10	20	0	50	15	3	dysoxic	II-III	Partially oxid.
Ln12016-I	Martinique Point	CP	21 U 577462 5636353	0.5	0.5	2	3	15	0	67	10	2	Dysoxic/anoxic	II or II-III	
Ln12021-H	Martinique Point	CP	21 U 577462 5636353	5	10	2	5	30	0	35	8	5	dysoxic	II-III	
Ln12037-B1	Cape Fox	CP	21 U 577834 5634761	10	15	15	10	20	0	20	5	5	dysoxic	II-III	Uncertain
E12209	Frauderesse Point	CP	21 U 580579 5639969	Uncertain Data											
Ln12091-B	Pyramid Point	CRP	21 U 582514 5646049	5	5	10	5	10	0	60	0	5	anoxic	mature II	HC Depleted
Ln12091-C	Pyramid Point	CRP	21 U 582514 5646049	5	5	5	5	25	0	45	0	10	anoxic	II	HC Depleted
Ln12077-D	Pyramid Point	CRP	21 U 582388 5645949	2	2	1	1	20	0	66	2	6	anoxic	II	HC Depleted
Ln12077-E	Pyramid Point	CRP	21 U 582388 5645949	2	1	1	3	6	0	75	6	6	Dysoxic/anoxic	II or II-III	HC Depleted
E11308-1	Truite Point	CRP	21 U 580808 5641594	2	2	2	0	35	0	50	5	4	anoxic	II	
Ln12051-G	West Coast	RI	21 U 586519 5639223	Uncertain Data											
Ln12051-G3	West Coast	RI	21 U 586519 5639223	5	5	3	0	25	0	60	0	2	Dysoxic/anoxic	II or II-III	HC Depleted

**Table Abbreviations and Notes:**

CP, Conche Peninsula; CRP, Cape Rouge Peninsula; RI, Rouge Island

**Terrestrial Organic Matter:**

Vit1, autochthonous vitrinite (Vitrinite 1); Vit2, allochthonous (recycled) vitrinite (Vitrinite 2); Inertinite, oxidized or forest fire derived ligno-cellulose components; Exinite, plant spore, cuticles, resins, and suberins; AOM3, amorphous lipid and humic components derived from terrestrial organic matter.

**Lacustrine/Marine Organic Matter:**

Alginite, algae (both lamellar and algal clustered cells); Algodet, algodetrinite (detrital algal remnants); AOM1 and AOM2, bacterial degradation of algal remnants (AOM1: talalginite degradation, AOM2: lamalginite degradation); M/D-HCs, overmature source rock, amorphous organic matter 2 is mostly non-fluorescent and depleted in hydrocarbons.

There is a higher concentration of AOM3 kerogen macerals in Conche Peninsula samples ( $\leq 23\%$ ) than in Cape Rouge Peninsula samples ( $\leq 6\%$ ). Moreover, all samples contain inertinite ( $\leq 15\%$ ), allochthonous vitrinite [(Vit2)  $\leq 15\%$ ], autochthonous vitrinite [(vit1)  $\leq 10\%$ ] and solid bitumen ( $\leq 10\%$ ) kerogen macerals. Exinite ( $\leq 10\%$ ) is identified in both Cape Rouge and Conche Peninsula samples, but not in the Rouge Island sample (Ln12051-G3) (Figure 4.13).

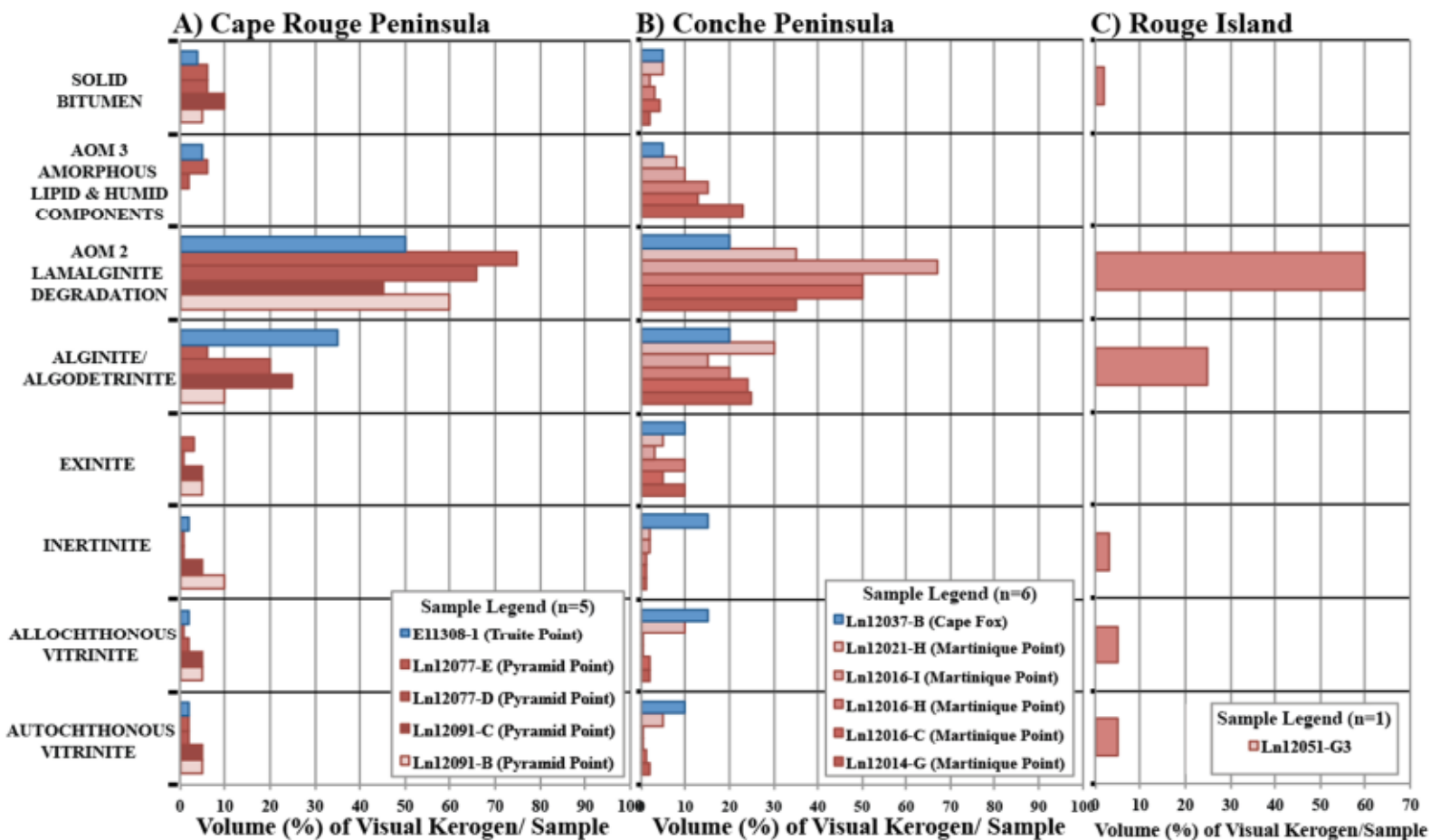


**Figure 4.13 Visual kerogen distribution by area for the Cape Rouge Formation**

Visual kerogen distribution by sample and locality, graph A) Cape Rouge Peninsula (n=5); B) Conche Peninsula (n=6); and C) Rouge Island (n=1). Refer to graph legend for sample lists and locations. Refer to Figure 3.1 for sample locations.

## CHAPTER FIVE: DISCUSSION

### 5.01 — Introduction, Paleogeography & Paleoclimate

Lower Carboniferous rocks of the Cape Rouge and Crouse Harbour formations are interpreted to have been deposited in a non-marine fluvio-lacustrine depositional environment. These formations are thought to have been deposited as early fill in a half-graben depocenter formed along a long, narrow lineament (Hamblin et al., 1995; Hamblin and Rust, 1989). Other similar basin fill assemblages in roughly age-equivalent successions (e.g., Horton Group) are common across the Maritimes Basin (e.g., Bell, 1960; Hamblin and Rust, 1989; Hamblin and Gibling 1996; Calder 1998), where strata generally range in thickness from 600-1600m (Bell, 1960, Martel and Gibling, 1996), and up to a maximum of 3000m in western Cape Breton, Nova Scotia (Hamblin and Rust, 1989, Calder, 1998). Regionally, these basin fill assemblages are remarkably similar to one another, with sequences that include marginal conglomerates (e.g., Murphy et al., 1994, Calder 1998) overlain by alluvial strata that are intertongued with finer-grained lacustrine sequences (Hamblin and Rust, 1989; Martel and Gibling 1996; Calder, 1998).

Farther east, similar basins are found in Britain and apparently along this same intracontinental rift system (Tyson and Follows; 1998, Leeder, 1987 & 1988; Calder, 1998). Together, this widespread deposition is indicative of trans-tensional faulting and deposition of terrestrial dominated facies across central and eastern Euramerica (Hamblin & Rust, 1989, Calder 1998). From lithology and setting, these deposits are thought to be hosts for active petroleum systems and are of interest for hydrocarbon exploration.

The Cape Rouge and Crouse Harbour formations at Conche are deposits of the Tournaisian Stage, verified by palynomorph analyses in Baird (1957, 1966), Hamblin et al. (1995) and Froude (2012). Hamblin (1995) and Froude (2012) assigned spore assemblages from the Crouse Harbour and Cape Rouge formations to the *Spelaeotriletes cabotii* Assemblage Subzone (T<sub>II</sub>) of the *Vallatisporites vallatus* Assemblage Zone of the late Tournaisian (Froude 2012, Hamblin 1995). During this time, paleogeographic reconstructions by Blakey (2016) place the Conche area ~5-10° south of the Carboniferous paleo-equator, while nearby, the St. Anthony Basin offshore sits slightly farther north (Figure 5.1). Blakey's reconstructions show a slow steady northward displacement of the Maritimes Basin from the Late Devonian (Figure 5.1) and with active tectonism and rifting during deposition of the Cape Rouge and Crouse Harbour formations in the Tournaisian. The Conche area was completely land locked during the Devonian with significant tectonic activity occurring during the late-Devonian to early Mississippian as rifting attempted to open up a restricted Carboniferous sea east of the study area (Figure 5.1 A & B). This active rifting initiated the development of the Cape Rouge and Crouse Harbour formations during the Lower Carboniferous along with other lacustrine deposits across this proto-Atlantic rift system (e.g., Albert Formation, Strathlorne/Ainslie formations, Lower Oil shale group). The widespread distribution and proven source rock occurrences highlight the importance of syndepositional tectonism for development and preservation of Carboniferous terrestrial source rocks in rift basins (Follows and Tyson, 1998).

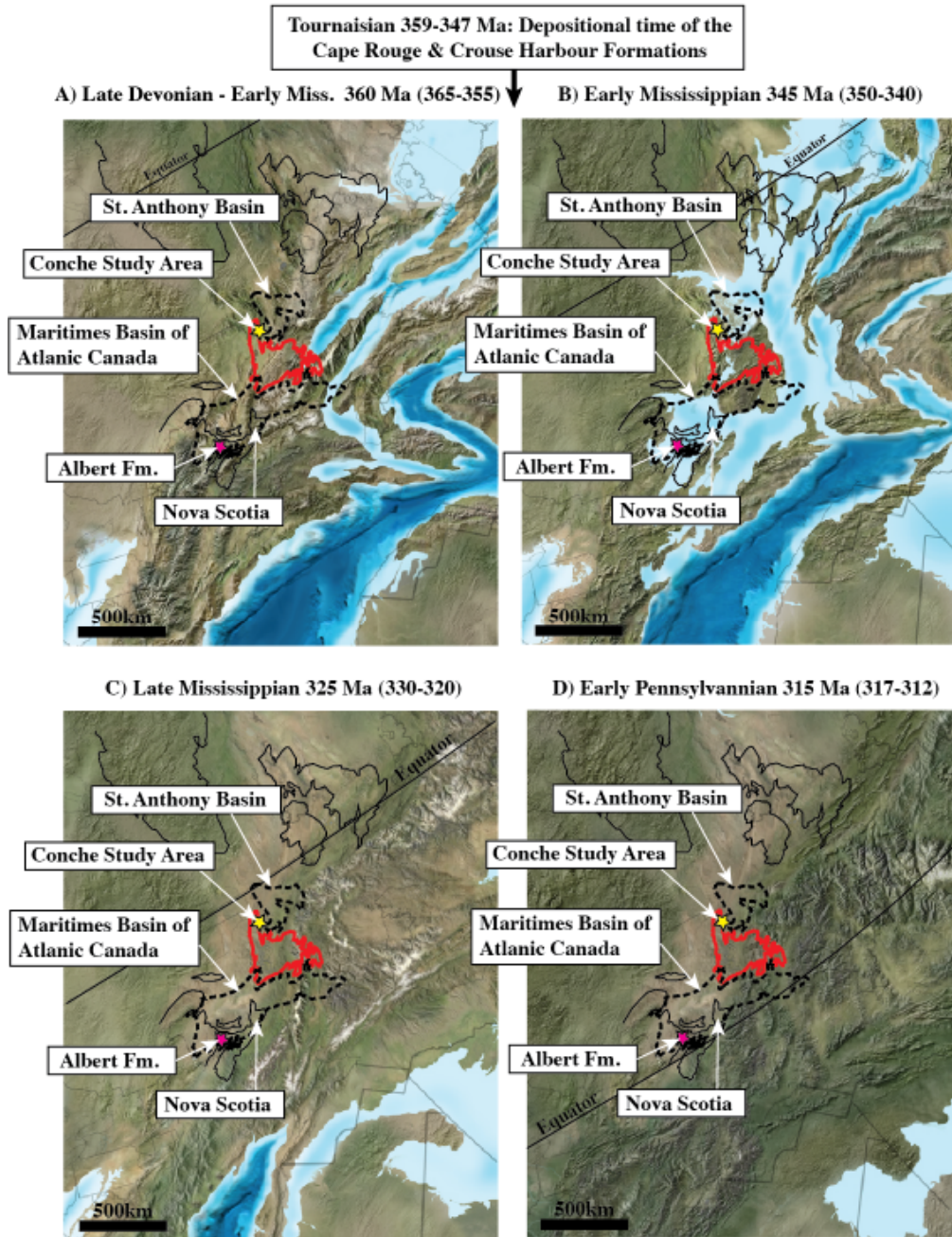


**Figure 5.1 Paleogeographic reconstruction maps of the Late Devonian to Early Pennsylvanian**

The province of Newfoundland is highlighted in red with the Conche study area annotated by a yellow star and the Maritimes Basin by a dashed black line. Other provinces (NS, NB & PEI), Greenland, and the UK are outlined in black. The Paleo equator is represented by the black line. Maps modified after Blakey (2016).

Rapid transtensional subsidence provided accommodation space and preservation potential for sediments entering these basins, while warm, arid to humid, paleoclimates promoted primary productivity. Although sediments of the Cape Rouge and Crouse Harbour formations indicate terrestrial deposition with no marine influence, proximity to a restricted ocean may have affected climate trends in the region (Figure 5.1 A & B). Following deposition of the Cape Rouge and Crouse Harbour formations, rifting continued through the Early Mississippian and began to open up marine pathways close to, if not also within, the study area (Figure 5.1 B). Although no marine strata are preserved at Conche, marine sediments exist further offshore in the St. Anthony Basin and likely within the White Bay Sub-basin. During the later stages of the Carboniferous Period (Figure 5.1 C & D), the Conche study area was again completely landlocked.

It is likely that given low latitudes, the Cape Rouge and Crouse Harbour formations were deposited in a region of relatively high temperatures. Hamblin et al. (1995) interpreted the Cape Rouge Formation to be from a humid environment containing the “climatically sensitive” *Vallatisporites vallatus* spore zone. However, others (e.g., van der Zwan, 1991; Calder 1990) indicate the *Vallatisporites vallatus* spore zone is commonly developed in arid environments. Similarly, the slightly older, but roughly age equivalent Albert Formation, located slightly to the south during the Tournaisian (Figure 5.1) is interpreted by Utting (1987) to have been deposited in a warm sub-tropical dry belt (Calder, 1990). The palynology of terrestrial and lacustrine organisms may be a bit ambiguous. Albert Formation has *Botryococcus* sp. (a taxon also observed in the Cape Rouge Formation at Conche, Hamblin et al., 1995; Froude, 2012), a lacustrine algal

cluster interpreted to be associated with warm, nutrient rich environments that favour algal blooms (Utting, 1987).

At Conche, the abundance of mudcracks and the cyclical nature of stratal stacking patterns indicate extensive intervals of sub-aerial exposure and weather patterns that indicate evaporation. In addition to desiccation features, drainage features (presented below) are thought to represent some cyclical wet (humid) intervals – perhaps seasons. Based on these findings, in addition to regional trends of analog basins, together with palynological and paleogeographic reports by others (e.g., Van der Zwan, 1981; Utting, 1987; Tyson and Follows, 1998; Calder, 1998; Hamblin et al., 1995; Froude 2012; Blakey, 2016), the Cape Rouge and Crouse Harbour formations are considered deposits formed in a semi-arid paleo-climate with seasonal humidity fluctuations.

### **5.03 — Crouse Harbour Formation Depositional Environment**

The Crouse Harbour Formation is a non-marine facies assemblage dominated by coarse-grained clastics. Sediments are interpreted to be sourced from a footwall alluvial fan and a hanging wall braid plain, laying interfingered with the finer-grained axial and distal Cape Rouge Formation rocks (Figure 5.2) (Hamblin et al., 1995).

Footwall sourced alluvial fan deposits are exposed on the isthmuses of the Cape Rouge and Conche peninsulas. They differ in some bedding features and provenance from other equivalent beds preserved on islands laying farther offshore.

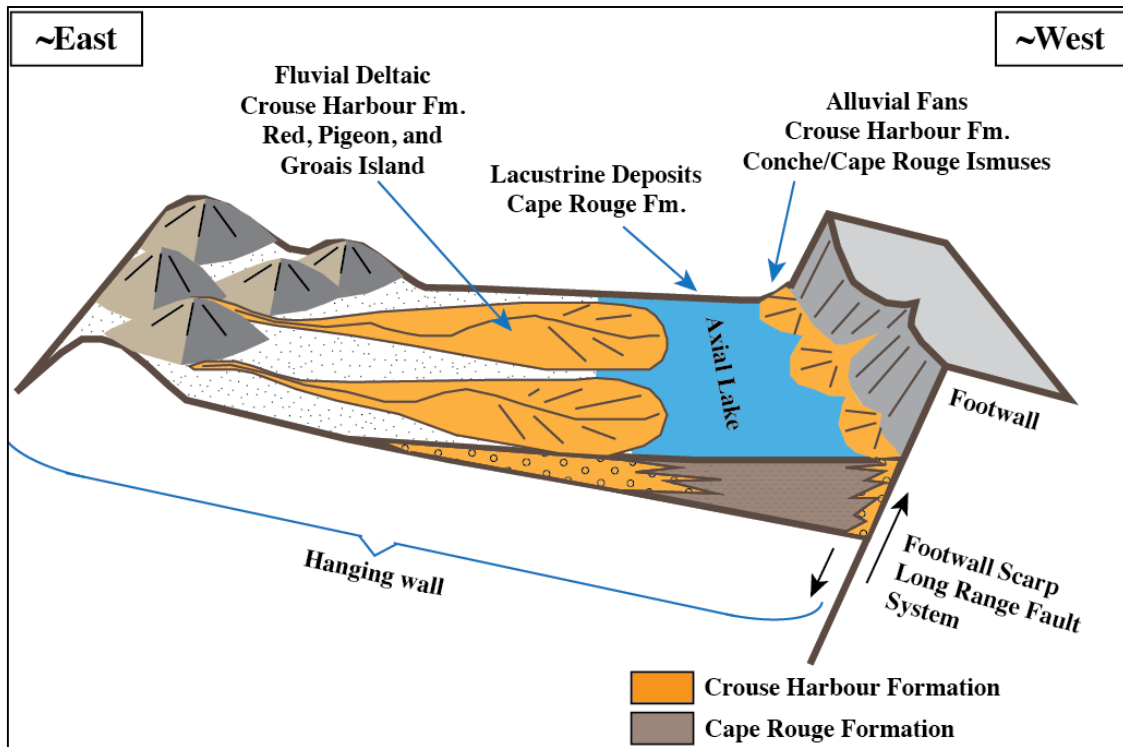


**Figure 5.2 Depositional environment for the Cape Rouge and Crouse Harbour Formations**

Environment of deposition schematic for the Crouse Harbour and Cape Rouge Formation deposited in the Conche Study area, from eastern margin to western margin ~20km (modified after a similar example in Leeder and Gawthorpe, 1987)

Crouse Harbour rocks on Red, and Pigeon islands, and on the NW margin of Groais Island (Figure 1.4) are interpreted to have been deposited on the hanging wall of a half-graben depocenter while those to the west, located on the isthmuses of the Cape Rouge and Conche peninsulas, are interpreted as footwall scarp deposits (Figure 5.2). On the isthmuses of the Cape Rouge and Conche peninsulas, the Crouse Harbour Formation is dominated by poorly to moderately sorted sub-angular to sub-rounded matrix to cobble supported boulder conglomerates together with coarse to very coarse-grained sandstones, infrequently interbedded with thin mudstone deposits. This predominantly coarse-grained

facies and sedimentary architecture suggest deposition as braided stream gravel or perhaps an alluvial fan. Conglomeratic clasts are locally derived from nearby mildly metamorphosed Ordovician sandstones (informally referred to as the Maiden Point Formation) laying high in the adjacent hills. Here, the Crouse Harbour Formation also contains coarse-grained sandstone with conglomeratic lags that may have formed as bar-top channels. Mudstones present within this facies assemblage likely represent axial lacustrine deposits (equivalent to the Cape Rouge Formation) that inter-finger with their coarser grained equivalents (Figure 5.2). Given the presence of locally derived detrital material and the abundance of chaotic boulder conglomerates, it seems clear that this formation was deposited a short distance from its basement source and on or near the fault-margin for a half-graben depocenter. This style of deposition is apparently typical for equivalent Horton Group strata found elsewhere in the Maritimes Basin (Baird, 1966; Hamblin et al., 1995, Calder, 1998).

In contrast to the footwall deposits, Crouse Harbour strata identified from the offshore islands (Red, Pigeon, and NW Groais Island) differ from their apparently coeval deposits exposed on the isthmuses of the Cape Rouge and Conche peninsulas. The Crouse Harbour Formation, examined from these island exposures, is thought to be laying upon the hangingwall block near the eastern margin of what may be a half-graben depocenter (Figure 5.2). Here, rocks consist primarily of coarse-grained clastics representing fluvial braid plain depositional environments (Figure 5.2). On Groais Island, Crouse Harbour Formation consists of medium to coarse-grained trough-cross bedded feldspathic sandstone with scoured bases and with poorly sorted, chaotic matrix

supported boulder conglomerates of angular-to sub angular clasts. Some thin beds of freshwater limestone are exposed on Groais Island. Conglomerates of the Crouse Harbour Formation contain quartz, schists, gneisses and feldspathic sandstone clasts derived from the exposures of the adjacent Pre-Cambrian Grey-Island Schist. The coarse-grained character of this facies assemblage and the dominance of chaotic conglomerates with clasts derived from exposures of nearby rock indicate deposition in a high-energy environment laying adjacent to the source. Moreover, the abundance of trough-cross bedded sandstone beds with rip up lags and scour bases are interpreted to be deposits of a fluvial braid plain environment. This environment of deposition interpretation is similar to those made by Hamblin et al. (1995) despite visiting different outcrop locations.

#### **5.04 — Cape Rouge Formation Depositional Environment**

Lithofacies assemblages of the Cape Rouge Formation are finer grained than those of the Crouse Harbour Formation and are interpreted to represent lacustrine deposits (Figure 5.2).

Palynomorph analyses in Baird (1957, 1966), Hamblin et al. (1995) and later by Froude (2012), reported *Botryococcus* algae in Cape Rouge Formation samples, therein indicating productivity in a terrestrial, fresh to brackish water environment (Hamblin et al., 1995; Froude 2012). Likewise, in roughly coeval formations elsewhere in the Maritimes Basin, *Botryococcus* algae are found in source rock deposits of the Frederick Brook Member oil shales of the Albert Formation of New Brunswick (Chowdury et al., 1991; Utting 1987, Utting and Hamblin, 1991, Hamblin et al., 1995) and the

Strathlorne/Ainslie formations of Nova Scotia (Hamblin et al., 1995). These formations all apparently share broadly similar lacustrine environments and styles for sedimentation in this paleogeographic setting in the Early Carboniferous.

At Conche, the Cape Rouge Formation contains a variety of lithofacies with varying sedimentary structures, dominated by features suggesting lacustrine deposition. Strata are generally dominated by mud-cracked horizons infilled with ferrous dolomite, and nodular dolomite horizons. Sandstone and siltstone beds carry current, wave and planar laminations and rarely, some minor bioturbation. Dark coloured mudstones are pervasively cemented by ferrous dolomite and analcime and carry pyrite and pyrrhotite. Stromatolites are present along some bedding planes together with microbial mats. Together, the presence of zeolites, dolomite, pyrite, stromatolites, with sedimentary structures indicative of evaporation, points to a depositional environment with lake waters that had elevated alkalinity and salinity.

#### **5.04.01 Lake Style and Facies Assemblages**

Four lithofacies assemblages of the Cape Rouge Formation are viewed as distinctive stages of lacustrine basin-fill, representing varying stages of water flow and sediment dispersal. Settings range from aerially exposed mud-flats and other paralic deposits onshore, through density underflows, to open-lacustrine laminated mudstones offshore. Together these facies associations are interpreted as belonging to relatively shallow axial and also underfilled lake. The four lithofacies associations and their interpreted succession are presented below.

#### **5.04.02 Cape Rouge Assemblage 1 (CR-A1): River-Delta Stream Mouth Bars**

The Cape Rouge Facies Assemblage 1 (CR-A1) is a fine to medium-grained sandstone facies assemblage interpreted as deposits of subaqueous bars formed by unidirectional currents at the terminal ends of distributary channels. These bars are thought to form under open hydrologic conditions (wet phase) as rivers flowed into a lacustrine delta environment (Bohacs et al. 2000). This deltaic environment is likely a conduit of sediment into the lake system.

#### **5.04.03 Cape Rouge Assemblage 2 (CR-A2): Lake Margin (Plain) Facies**

The Cape Rouge Facies Assemblage 2 (CR-A2), the most distinctive facies assemblage of the Cape Rouge Formation, is characterized by an aggradational stacking pattern of interbedded grayish-red sandstone, siltstone, dolostone and carbonaceous mudstone. Sedimentary structures and other diagenetic features point to periods of lowstand (hydrologically closed) in a lacustrine environment. The sedimentary structures of this facies assemblage are typical of environments exposed to sub-aerial conditions related to episodic drying (similar examples have been presented by Bohacs et al. 2000). Such structures include desiccation cracks, microbial mats, occasional stromatolites, and ripple cross-lamination. The abundance of desiccation cracks over extensive areas and the repetitive aggradational architecture of carbonaceous-rich facies is indicative of deposition in a marginal mud-flat lacustrine environment with fluctuating water depths (see Belt, 1967).

Mudcracks are often infilled with ferrous-dolomite and associated with “globby” dolomite masses. The dolomite is most likely an early diagenetic precipitate from the breakdown of organic carbon, by methanogenic organisms, during breaks in sediment accumulation. These breaks in sediment accumulation were likely important to diffuse sufficient solutes to the precipitation sites. The mudcracks may have acted as migration pathways for fluids (carrying solutes such as Mg and Ca).

Domal stromatolites, closely associated with mud-cracked strata, are interpreted to have grown in shallow ephemeral calcium enriched waters during those short times when a closed basin developed.

Some fluvial erosion in this facies assemblage (Figure 3.5 C & D) is interpreted as climatically-driven lake level fluctuations along the margins of the lake. These events are often observed near the top of units and are interpreted to represent re-activation of streams after a closed lake basin phase ended.

In analog basins, similar facies assemblages have been observed in roughly age-equivalent and often conjugate Carboniferous rift valleys (as noted by Belt et al, 1967). Here, these lithologies have been historically called “Cementstone” facies and are seen in the Albert Formation of New Brunswick and the Spear Point and Snakes Bight formations of Newfoundland (Gesner, 1847; Belt et al., 1967, Hamblin et al., 1995). To the east in the British Isles, similar lithological assemblages have been reported in Northern Ireland and the Midland Valley of Scotland (Freshney, 1961).

Trace fossils in these rocks are limited to horizontal and resting traces. Ichnofauna include firmground traces of the *Mermia* ichnofacies, an assemblage that includes horizontal grazing and feeding traces from invertebrates, common to subaqueous

conditions in freshwater environments, and potential tetrapod trackways. Other traces include *Planolites* and *Cochlichnus anuineus* (Figure 3.7 A& B). *Cochlichnus anuineus* is also found in the Albert Formation of New Brunswick (Pickerill, 1992). The spatially isolated imprints of *Calamites*, found on the Cape Rouge Peninsula, are similar to those identified in the Blue Beach Formation, Horton Group, of Nova Scotia. Together, this low diversity trace fossil assemblage may be indicative of a stressed environment, typical to a facies assemblage alternating between sub-aerial exposure, desiccation, and saline/alkaline-rich waters.

Two sets of irregular markings, found on the Conche Peninsula, are thought to be potential candidates for tetrapod amphibian footprints. If these markings are indeed a true representation of amphibian life, these, along with other trackways found in the Blue Beach and Hurd Creek members of the Horton Bluff Formation in Nova Scotia, represent some of the oldest reported known vertebrate footprints (Martel and Gibling 1994; Hunt et al., 2004; Gibling et al., 2008). In Nova Scotia, tetrapod trackways are preserved in lacustrine/marginal marine strata Blue Beach and Hurd Creek members (Martel and Gibling 1994; Hunt et al., 2004).

#### **5.04.04 Cape Rouge Facies Assemblage 3 (CR-A3): Lake Floor Density Underflow Facies**

The Cape Rouge Assemblage 3 (CR-A3) is interpreted as lake-floor density underflows (turbidites) with an aggradation fill stacking pattern, composed dominantly of siltstone and fine-grained sandstone with minor mudstone.

Sedimentary architecture and structures are dominated by massive, contorted and, convoluted stratification together with trough-cross lamination. Convoluted beds are common in siltstone and sandstone beds, and generally grade from massive strata to contorted strata at bed tops. This facies assemblage is interpreted as a deposit originating in a high energy hypopycnal flow and likely represents one aspect of the physical expression for a highstand lake (see other examples in Renaut and Gierlowski-Kordesch, 2010).

#### **5.04.05 The Cape Rouge Assemblage 4 (CR-A4): Offshore Facies**

The Cape Rouge Assemblage 4 (CR-A4) is dominated by laminated mudstone and represents the finest grain facies assemblage of the Cape Rouge Formation, and the strata carrying the most source-potential. In appearance, it is basically a dark carbonaceous and zeolite-rich mudstone and ferroan dolostone that is rarely burrowed.

Strata of facies assemblage CR-A4 are interpreted to have been deposited in an offshore environment with both shallow banks and moderately deep basins. Whether large or small, shallow or deep, facies CR-A4 lake bottoms can show large changes in fluid flow and chemistry affecting both the process of sedimentation and the mineralogy of the material delivered to that part of a lake. Consequently, and in general, distal offshore sediment of facies CR-A4 are, to a large extent, identified by significant suspension fallout onto both oxic and anoxic lake beds.

The often fine-grain size of the inorganic matter (clay and silt size grains) and the thinly laminated character of the mudstone imply deposition largely dominated by suspension fall out. However, some lamina sets can be rippled (with silt or clay size

particles) or have beds rich in detrital material (e.g., quartz or pyrrhotite) and are therefore interpreted to be deposited by higher-energy loads. Moreover, pyrrhotite, found in thin lamina and often found as platy star-like shapes (Figure 4.4 C & D), is a mineral that occurs as a characteristic feature in this facies assemblage. It is thought to be a detrital component from metamorphic rocks of the Maiden Point or Grey-Island Schist. Radial, star-like morphologies are considered to be a function of this mineral's weakly magnetic character. Rapid transport from source to sink likely assisted with mineral preservation in an otherwise hostile geochemical setting. Similar occurrences of pyrrhotite have also been observed in the Paleogene Green River Formation (Horng and Roberts, 2005).

Mudstones are very rarely burrowed. This points to unfavourable conditions for a lake bed biome. This may include an anoxic water column (potentially representing development below a stratified water column with anoxic bottom water condition), by the presence of particularly soft soupy organic strata (Burden pers com.), or high recurrence frequencies of bed emplacement leading limiting deep faunal colonization. Miospore degradation by pyrite, reported by Froude (2012), is further evidence in support of an anoxic setting. Framboidal pyrite occurs within this facies assemblage which could suggest saline conditions as they can be generated by the reduction of sulphate in saline water by anaerobic bacteria (e.g., Postma, 1982; Cohen et al., 1984; Brown and Cohen, 1995).

Mudstones of this facies assemblage are well cemented with ferroan dolomite (due to microbial degradation of organic carbon in the methanogenic zone) and analcime, and with very minor cements from the illite/smectite clay mineral suite. Analcime is a

common authigenic silicate often associated with saline-alkaline lake environments (Hay, 1977, 1978; Sheppard, 1973; Remy, 1989). This mineral assemblage (high concentration of analcime, with low concentration of illite/smectite) suggests that detrital clays were altered to analcime as the breakdown of clays provides a source of silica and Al for the formation of analcime rich brines. Similar deposits and occurrences have been noted in the lacustrine deposits of the Green River Formation by Remy (1989).

### **5.05 — Lake Basin Type**

Stratigraphic sections examined in this thesis are interpreted to represent a lacustrine sedimentary setting that fluctuated between a wet and expansive lake and a dry and arid plain. Regional faulting in and adjacent to this ancient lake is part of a regional transtensional fault system and interpreted to be part of a rift system of grabens and half-grabens. The four major lithofacies associations represent environments that vary according to sediment and water supply and accommodation space. These facies associations represent distinct depositional settings that shift from evaporitic and mudcracked lowstand deposits to highstand hypopycnal density flows related to rejuvenation of muddy and sandy river floods (see other examples in Renault and Gierlowski-Kordesch, 2010).

Together, the combination of strata stacking patterns, sedimentary structures, lithofacies and trace fossil assemblages indicate an underfilled depositional environment (as characterized by Bohacs et al., 2000). In this type of setting and sedimentary succession, the subsidence rate exceeds the sediment fill rate (sediment + water) (Bohacs

et al., 2000; Deocampo and Jones, 2014), and results in a largely closed hydrologic system.

Facies associations are indicative of varying stages of lake development from periods of high-stand (e.g., river delta and density underflows) to low-stand (lake-plain facies; subaerial exposures). Many cycles begin and end with complete desiccation, which indicates they record the entire base-level range of the lake (Figure 5.3). Shoaling cycles, are expressed as sequences where Facies CR-A4 (mudstone) is overlain by C4-A3 (turbidites) in turn overlain by lake plain facies of CR-A2 (plain). Facies CR-A1 is rarer, representing expression of the activation of fluvial incisions, and can be found overlying facies assemblage Cr-A3 and CR-A4.

Similar to the Cape Rouge Formation, the roughly age equivalent Horton Group (preserved to the west in the Maritime Provinces), has thick successions of lacustrine facies. Moreover, like the Cape Rouge Formation, lacustrine facies of the Horton Group have been interpreted to have been deposited along the same extensional belt in similar underfilled lake-basins where strata are dominated by coarsening upward cycles (Martel & Gibling, 1991; Calder, 1990).

#### **5.06 — Source Rock Potential**

Espitalié et al., (1977, 1986, 1987) and Peters and Cassa, (1984, 1994) provide a fundamental framework for classifying “effective” source rocks from Rock-Eval Pyrolysis and organic richness analysis (TOC). This is the framework used here to determine source rock effectiveness of the Cape Rouge Formation (in Facies Assemblage

CR-A4).

### **5.06.01 Thermal Maturity**

Vitrinite samples from the Cape Rouge Formation range from late immature to late mature (0.5-1.12%  $R_o$ ). Vitrinite phytoclast samples from all localities contain a combination of autochthonous (first cycle), allochthonous (recycled) and suppressed (contaminated) phytoclasts. The autochthonous vitrinite phytoclasts range from the late immature to the late mature ( $R_o=0.5-1.01\%$ ) therein falling in the oil generation window (Table 4). The widespread, and consistent,  $R_o$  results indicate similar burial history across the study area.

Allochthonous (recycled) vitrinite phytoclasts have higher thermal maturities and are considered to be reworked. If allochthonous vitrinite grains are included in the average, thermal maturities increase but remain in the oil generation window (between late immature to late mature).

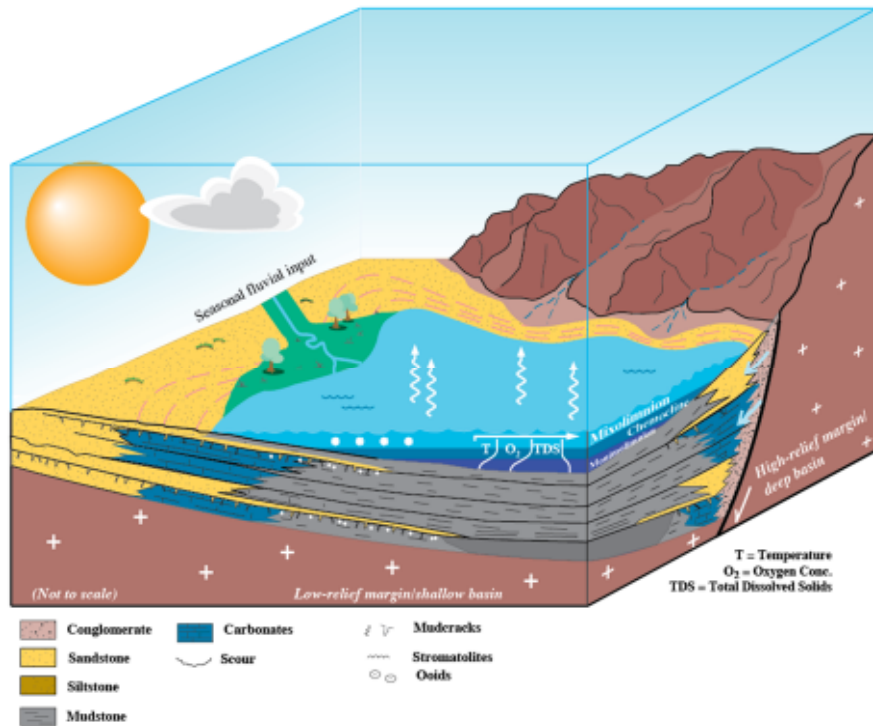


**Figure 5.3 Simplified underfilled lake model (modified from Bohacs et al., 2000)**

Thermal Alteration Index results support  $R_o$  maturation findings, with ranges in the mature zone (2 to 3- on the Conche and Cape Rouge peninsulas and 2+ to 3- on Rouge Island). Furthermore, the Pyrolysis temperature of the Rock-Eval  $S_2$  peak (known as  $T_{max}$ ) is often used as an estimate for thermal maturity for samples of similar lithology (Hackley, 2016).  $T_{max}$  for all samples analyzed ( $n=89$ ) range between 430 to 457°C (mean of 445.50 and median of 447.50), with calculated  $R_o$  range between 0.58-1.07 (very similar to actual measured  $R_o$  results), supporting thermal maturation in the oil generation window (Table 4).

### 5.06.02 Visual Kerogen

Kerogen macerals from the Cape Rouge Formation (Facies Assemblage CR-A4) are dominated by Type I macerals with lesser concentrations of Type II, III and Type IV kerogen along with solid bitumen. The concentration of kerogen macerals indicates that fresh water algae dominated productivity and organic enrichment followed by spores, pollen, woody tissue and reworked/oxidized material. Moreover, bitumen migrated through this system post deposition.

These findings support the biostratigraphic palynomorph analysis by Baird (1957, 1966), Hamblin et al. (1995) and later by Froude (2012), who reported upon the abundance of the alga (*Botryococcus*) with lesser amounts of Type II (bright orange to black spores and exinite) and Type III macerals (brown to black wood, cuticles, tracheid phytoclasts and other membranous tissue) (Froude 2012).

### 5.06.03 Source Quality and Quantity

Total Organic Carbon (TOC) concentrations for this study area (and namely from the Conche Peninsula, Cape Rouge Peninsula and Rouge Island) show a TOC range from 0.23-6.54%. Given the source rock classification scheme of Peters and Cassa (1994) (Table 2), these concentrations represent a spread from poor to excellent petroleum potential with average potential rated as fair. When analyzed by locality, samples from the Cape Rouge Peninsula have slightly higher TOC concentrations and are rated as good petroleum potential while those from the Conche Peninsula and Rouge Island have poor petroleum potential.

For all samples analyzed for TOC, 31 samples (out of 89) contain >1% TOC, a value considered by some as representing the minimum acceptable TOC for a clastic source rock (Peters and Cassa, 1994). Others, and notably some former research scientists with the GSC, believe 1.5% is a more realistic cut-off for a productive source rock (Burden pers com). This cuts the number of possible source rocks to 10 samples (out of 89).

When TOC concentrations are interrogated by specific stratigraphic sections, several localities have higher-organic concentrations than their regional counterparts. On the Conche Peninsula, and near Martinique Point, 8 of 12 mudstones contain more than 1% TOC. This 9 m black mudstone interval has TOC values ranging from 0.48-1.86% with a median of 1.08% (1.12% mean). In addition, and within this sequence, oil seeps are pervasive along cleavage planes. This indicates the presence of an active source-prone interval expelling hydrocarbons. This may be hydrocarbon seeps from migrated oil or locally derived as in-situ leakage from fractured organic-rich source rocks.

The Cape Rouge Peninsula has the highest TOC average (median of 1.16% and a mean of 1.30%) and with 54% (15/28) of the samples with TOCs > 1%. The Pyramid Point site hosts the highest TOC value collected for this study (6.54%) and represents a source rock with excellent petroleum generating potential. As with the Martinique Point mudstones, rocks at Pyramid Point are exceptionally dark in colour, with oil seeps along several bedding planes. Similar observations of oil seeps by Baird (1966) indicate the Pilier Bay area of the Cape Rouge Peninsula continues to leak small quantities of hydrocarbons. Inasmuch as these sections preserve some of the highest TOC values in

this area, their sedimentology indicates mud deposition in what may be a deeper part of this ancient lake and likely in a slightly more reducing environment, favourable for preserving organic matter.

Given that TOC is a good basic indicator of the quantity of organic matter in a rock, these results in fact represent both the “live” and “dead” carbon (kerogen and bitumen). As a consequence, TOC is not a clear indicator of the overall petroleum potential of a rock (Peters and Cassa, 1994). It should be noted that although TOCs for the Cape Rouge Formation are currently low, they were likely higher during its immature stage of burial. To find that number, a pre-burial TOC reconstruction would be necessary to understand original organic concentrations before any hydrocarbons are generated and lost. This is outside the scope of this study.

Rock-Eval Pyrolysis is another standard tool for assessing both the quantity and quality of organic matter bound in sedimentary rocks. The  $S_1$  and  $S_2$  pyrogram peaks generated from pyrolysis (measured in mgHC/g rock) represent the existing petroleum content and the remaining petroleum generating potential of kerogen bound in a sedimentary rock sample (Peters, 1986; Hunt, 1996). Given Peters and Cassa (1994) source rock metric ranking methodology (Table 2, Table 3), Rock-Eval pyrolysis results from this study show poor  $S_1$  and  $S_2$  values. The relatively low  $S_2$  values indicate the strata from the Conche Study area have, on average, little remaining potential to generate hydrocarbons. When analyzed by locality, mudstone samples from the Cape Rouge Peninsula have slightly better remaining generation potential than those on the Conche Peninsula and Rouge Island, with fair  $S_2$  values (median of 2.17 and mean of 3.86

mgHC/g rock).

Often, petroleum potential ( $S_1+S_2$ ) versus TOC plots are used to estimate the hydrocarbon producing capacity (Figure 5.4). Samples from within the zone for “good, hydrocarbon generative potential”, are all very dark, thinly laminated strata, of the deepest, most distal part of this ancient lake.

Plotting pyrolysis H1 ( $S_2/TOC \times 100$ ) with  $T_{max}$  (Figure 5.5) confirms that samples from Conche have Type I-III kerogens and they fall in the oil generation window (as validated by TAI and  $R_o$  results together with visual kerogen analysis).

### **5.07 — Controls on Organic-carbon Enrichment**

To a large degree, lake basin type greatly influences organic carbon enrichment. Organic carbon enrichment is promoted when destruction and dilution rates are minimized, and primary production maximized (Bohacs et. al., 2000). At Conche, Lower Carboniferous strata were deposited in a half-graben rift, where rapid subsidence associated with extensional tectonism provided accommodation space and an opportunity for the development of an axial lake system. Strata of this axial lake are interpreted as deposits from a warm tropical setting alternating between arid and humid cycles and with water that may be enriched in dissolved minerals or biologically productive and full of organic matter. The dilution rates for organic material are tied to alternating clastic input under high- and low-stand conditions together with early diagenesis. Large, deep lakes tend to have a larger load of organic matter than smaller, shallow lakes. Shallow lakes tend to hold desiccated, cracked and oxidized strata with little preserved organic matter.

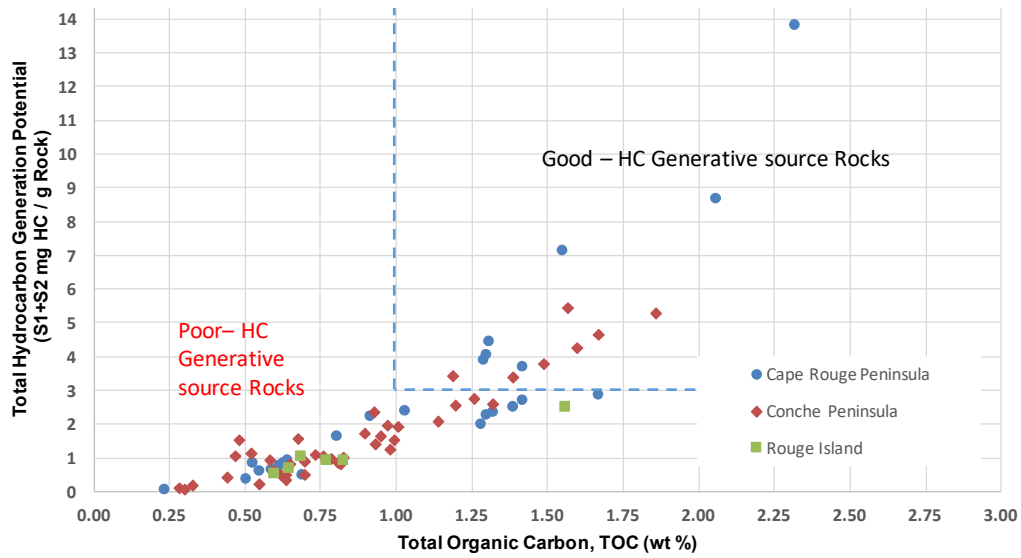


**Figure 5.4 Pyrolysis S<sub>2</sub> versus total organic carbon (TOC) plot**

Generative capacity of rocks in the Conche study area (broken out into locality, including the Cape Rouge Peninsula, Conche Peninsula, and Rouge Island.

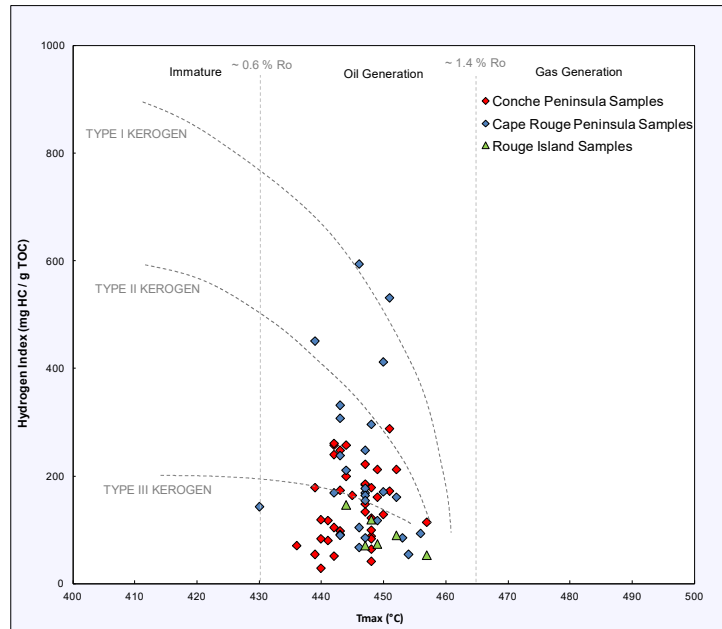


**Figure 5.5 T<sub>max</sub> and HI Plot**

Graph shows the relations of kerogen types and maturation stages with petroleum generation potential.

At Conche, the overall frequency of desiccation is thought to have oxidized and destroyed a large part of the organic matter entering the lake, leaving an abundance of lean-source rocks. Moreover, organic carbon was also hindered by methanogenic organisms during the formation of dolomite. The most organically enriched facies, thought to lie farther offshore in slightly deeper basins (e.g., at Pyramid Point), show less evidence for desiccation and perhaps some periods of complete anoxia (limiting benthic scavengers and bacterial respiration) therein preserving slightly higher concentrations of organic carbon.

#### **5.08 — Comparison with the Albert Formation**

The classic and well described source rocks of the Albert Formation, Horton Group, are the source rocks for two producing hydrocarbon fields in New Brunswick (Stoney Creek and McCully fields). The organic-rich rocks sourcing these fields are estimated to account for only a small percentage of this otherwise heterogeneous formation (~4%) (Greiner, 1962). The Albert Formation and the Cape Rouge Formation share some key similarities that may help define the prospectivity of the enigmatic St. Anthony Basin. Strata from both formations represent early fill of the Maritimes Basin (Hacquebard, 1972; Smith et al., 1991). Both formations are found in similar tectonic environments (half-graben rifts) along a shared rift system. Furthermore, both formations were deposited along similar near-equatorial paleolatitudes that likely had similar climates. The Albert Formation varies in thickness, reaching a maximum of 1500m (Smith et al., 1991), a similar thickness to that of the Cape Rouge Formation.

In the most organic-rich facies of the Albert Formation (referred to as the Frederick Brook Member), TOC values range from 0.2-29.3%, but mainly range from 3-14% (Smith et al., 1991; Follows and Tyson, 1998); prospective Cape Rouge Formation rocks range between 0.23-6.54%.

The organic-rich Frederick Brook Member is further divided into 3 distinctive organic rock types, simply named A, B & C (Macauley and Ball, 1982; Smith, 1985; Smith et al., 1991). Type C with less than 7 wt.% TOC is the leanest with respect to organic carbon-enrichment (Smith et al., 1991).

On mineralogy, the inorganic compositions of Types A & B oil shales are mainly illite, carbonates (calcite and dolomite, potentially ankerite), quartz and feldspar with minor amounts of other silicates (including analcime). In contrast, the lean Type C rocks contain higher concentrations of analcime and dolomite (Macauley and Ball, 1982; Smith, 1985; Smith et al., 1991) – a fact that makes them very similar to the fine-grained facies assemblage at Conche (CR-A4).

In many respects, the relatively lean Type C rocks/facies of the Frederick Brook Member are closely matched with the fine-grained facies at Conche, where laminated mudstones are also dominated by ferroan-dolomite and analcime cements with very minor concentrations of illite and other clay minerals. For Type C mudstones, Macauley et al. (1985), Mossman et al. (1987), and Smith et al. (1991) propose that analcime is a byproduct of the alteration of clays in sodium-rich alkaline waters, and therein a likely possibility for lake water composition for the Cape Rouge Formation.

The most organic-rich rocks (types A & B) of the Frederick Brook Member are interpreted as deposits from a “deep” offshore lacustrine sub-environment, whereas the leaner oil shales (type C) are thought to be deposits from a “shallow” offshore sub-environment with more turbulence (higher-energy setting) and therein more frequently developed oxidizing conditions. In New Brunswick, these organic-rich facies have been interpreted as rocks concentrated in a narrow structural zone (~10km), close to an active tectonic margin, where the lake was stratified and deep (>60m) (Greiner, 1962; 1974; Follows and Tyson, 1998). At Conche, the depositional center is perhaps as much as 20km wide, with most of the basin located offshore. It therefore remains a possibility that higher quality source rocks, akin to the Type A and B rocks from the Frederick Brook Member, are preserved offshore, in deeper basins of this expansive lake system.

### **5.09 — Implications for Offshore Exploration**

Carboniferous plays for the St. Anthony Basin have poorly defined hydrocarbon prospectivity. This is in large part a result of limited scientific study. Without appropriate offshore data, the successions at Conche are the closest analog for this offshore Carboniferous rift basin. In addition to the strata at Conche, the widespread occurrence of other analogous source rocks in regionally contiguous basins (Magdalen and Midland Valley) offers some hope for additional source rock being discovered in the St. Anthony Basin.

Based upon these findings from Conche, other Carboniferous strata of the nearby White Bay sub-basin and farther offshore in the St. Anthony Basin remain prospective;

however, source quality and timing for hydrocarbon generation in relation to the development of traps, seal, and reservoir are the largest risks for hydrocarbon exploration. Given maturation results from Conche, it is entirely possible that any equivalent Lower Carboniferous strata found offshore are likely also mature to over mature.

Secondary risks for offshore exploration include trap and seal elements in conjunction with source quality and generation timing. Sealing elements may include marine shales from the overlying Mesozoic-Cenozoic cover. However, these younger cover rocks are only found over part of this offshore basin. In those places, and beneath Mesozoic-Cenozoic cover strata, upper Carboniferous salt deposits and diapirs might provide complicated structural traps for hydrocarbons. Moreover, reservoir presence and quality may be among the least risky elements, given the occurrence of reservoir strata in two offshore wells - Verrazano L-77 and Hare Bay E-21 (Hu and Dietrich, 2010). From the Verrazano L-77 well, late Mississippian (Mabou Group equivalent) sandstones with porosities up to 25% and permeabilities up to 100mD are reported. The authors also report reservoir quality in the Hare Bay E-21 well with porosities up to 15% at considerable depths (4500-5000m) (Hu and Dietrich, 2010). Although these are promising results, these numbers cannot significantly de-risk such a vast basin.

Thus, it remains a possibility that if similar half-graben lake systems exist farther offshore and if they preserve deeper water lake basins with enriched source rocks (similar to the Albert Formation), the basic elements for a Carboniferous petroleum system may

yet be found. Without modern seismic data and additional boreholes, little more can be deduced regarding Carboniferous hydrocarbon prospectivity of the St. Anthony Basin.

## CHAPTER SIX: CONCLUSION

This thesis sets out to characterize depositional setting and source rock prospectivity (occurrence, distribution, quality and quantity) of lower Carboniferous (Tournaisian) strata of the Conche area of Newfoundland's Northern Peninsula. Analogous and roughly age equivalent rocks from farther west in the Maritimes Basin and east in the British Isles are from similar tectonic regimes and depositional environments, and they are known to have proven source rocks and active hydrocarbon systems. Study of the Conche strata offers insight into onshore petroleum prospects and offshore into strata of the St. Anthony Basin, an otherwise enigmatic place where few boreholes have been drilled and where relatively limited seismic records have been acquired.

Before this study, the thick clastic successions at Conche received limited attention. An earlier study by Hamblin et al., (1995) showed significant vertical and lateral facies variability and some fine-grained facies with source potential.

For this work, and to better understand the distribution of fine-grained facies and to determine a lake-basin type, stratigraphic sections were measured and fine-grained samples gathered (n=89) across the Conche area, including both the Cape Rouge and Conche peninsulas, and nearby offshore islands. Analyses, using industry standard source rock techniques (LECO TOC, Rock-Eval Pyrolysis & a range of thermal maturation analyses) have contributed to the development of a better understanding of the source rock potential for the Crouse and Cape Rouge formations.

Terrestrial, primarily lacustrine strata of the Crouse Harbour and Cape Rouge formations, are interpreted to represent the initial phase of deposition within a half-graben rift-segment where accommodation space was generated through transtension and subsidence. Terrestrial sediments are in large part sourced from hanging wall and scarp exposures of the older Maiden Point and Grey Island Schist formations. Regionally, many similarities (e.g., lithology and fill patterns) exist between the Crouse Harbour and Cape Rouge formations and roughly age equivalent Horton Group rocks from New Brunswick and Nova Scotia. These are also places where oil and gas deposits have been exploited from lacustrine source rocks. Demonstrating widespread distribution of proven source rocks in Carboniferous terrestrial successions in half-graben rift basins in the Maritimes Basin and eastward into the British Isles, highlights the importance of syndepositional tectonics for development and preservation of regionally distinctive petroleum systems.

The Crouse Harbour Formation is interpreted to be footwall scarp and to contain hanging-wall fluvial-lacustrine deposits that interfinger with the axial finer-grained lacustrine Cape Rouge Formation. On the footwall margin, the Crouse Harbour Formation is thought to be an alluvial fan, gravel-bed river deposit, sourced from proximal metamorphosed basement rock. In contrast, on the eastern margin of the depocenter, the Crouse Harbour Formation is interpreted as fluvial-deltaic, sourced from the Grey-Island Schist.

Deposited contemporaneously with, and axial to the Crouse Harbour Formation, lacustrine strata of Cape Rouge Formation are dominated by finer-grained facies

assemblages, interpreted to be deposits in a underfilled lake basin. Here, stratal stacking patterns of mixed progradation and aggradation developed under alternating wet and dry conditions.

Four distinctive facies assemblages in Cape Rouge Formation strata show distinctive stages of lacustrine basin-fill linked to variability in water, sediment supply and organic productivity. These deposits range from paralic and aeriially exposed mudflats onshore, through hypopycnal density underflows and deeper water laminated mudstones offshore. Assembled together, these facies represent deposition in a relatively shallow underfilled lake basin where accommodation rates exceed sedimentary fill rates (sediment + water) over the period of a fill sequence. This overall pattern for sedimentation and lake environment indicates a largely closed hydrologic system.

From regional paleogeographic reconstructions (e.g., Blakey, 2016), the Conche area was situated  $\sim 5\text{-}10^\circ$  south of the Carboniferous paleo-equator, and therefore in a place where sediment deposits accumulate under a relatively hot equatorial climate. Moreover, the widespread occurrence of desiccation structures and the cyclical nature of stratal stacking patterns, including high-stand deposits (fluvial input and hypopycnal flows), is indicative of a setting with significant cyclical wet and dry climatic cycles. Mineral assemblages within the fine-grained mudstones support the interpretation of an alkaline lake that was perhaps also moderately saline, common in evaporative settings.

Kerogen macerals from the Cape Rouge Formation are dominated by Type I algal material with lesser concentrations of terrestrial Type II, III and Type IV particles and

followed by solid bitumen. The concentration of kerogen macerals indicates that fresh-water algae contributed to the primary productivity and was followed by terrestrial material from a vegetated landscape and lastly, reworked/oxidized organic material. Moreover, bitumen formed and migrated through this system long after it was deposited. These findings are supported by Baird (1957, 1966), Hamblin et al., (1995) and later by Froude (2012) who reported an abundance of the algal species *Botryococcus* sp. and with lesser amounts of Type II (bright orange to black spores and exinite) and Type III macerals (brown to black wood, cuticles, tracheid phytoclasts and other membranous tissue) (Froude 2012).

A comprehensive maturation analysis, including  $R_o$ , TAI, and Rock-Eval Pyrolysis places rocks of the Cape Rouge Formation within the oil generation window.

- Autochthonous (first cycle) vitrinite phytoclasts range from the late immature to the late mature ( $R_o=0.5-1.01\%$ )
- Thermal Alteration Index results supports  $R_o$  maturation findings, with ranges in the mature zone (2 to 3-)
- $T_{max}$  ranges for all samples analyzed ( $n=89$ ) by Rock-Eval range between 430 to 457°C (mean of 445.50 and median of 447.50), with a calculated  $R_o$  laying between 0.58-1.07.

Total Organic Carbon analysis and Rock Eval pyrolysis, used to characterize source rock quality and quantity, show fine-grained strata with source potential are limited to facies association CR-A4. Within this facies association, TOC concentrations range from 0.23-6.54%, representing a poor to excellent petroleum potential with a fair

average potential. When analyzed by sample locality, mudstone samples from the Cape Rouge Peninsula have slightly higher TOC concentrations (average good petroleum potential) while those from the Conche Peninsula and Rouge Island have somewhat lower petroleum potential. Given that thermal maturities for these mudstones are all within the oil generation window, it is likely that these relatively low TOC concentrations were higher during their immature stage of development. Rock Eval Pyrolysis shows poor  $S_1$  and  $S_2$  values indicating that mudstones from Conche have little remaining potential to generate hydrocarbons.

The fine-grained facies at Conche share similarities with the lean source rocks of the Albert Formation (Type C) facies in the Moncton Sub-basin. Albert Formation Type C rocks are thought to come from deposits formed in an offshore setting in shallow to moderately deep water where significant evaporation has altered lake waters, encouraging analcime and dolomite enrichment. Thus, the depositional setting for fine-grained organic rocks at Conche is likely similar to that reported for the lean source rocks of the Albert Formation. Given common patterns for lean and rich source rocks it remains possible that higher quality organic rich strata are located offshore where deeper water lacustrine settings might have formed.

For offshore exploration, the prospect for significant Carboniferous source rocks remains hopeful. However, timing for hydrocarbon generation and seal remain significant risks.

## 6.01 — Areas for future research

The recommended areas for future research include:

- Complete an examination of existing 2D seismic data from the offshore regions of the White Bay and St. Anthony basins to assess potential trapping mechanisms and their relative ages in relation to Carboniferous strata. If new seismic data become available, it is recommended that geophysical analysis be completed for source rock detection using acoustic impedance analysis, as described by Løseth et al. (2011).
- Review validity of maturation results from drill cuttings from Verrazano L-77 by Utting et al. (1976). Currently the reference work is classified as “confidential” and is held by the INRS in Quebec, an access for information request would have to be completed to acquire the analysis. Moreover, if the Verrazon-L77 drill cuttings can be located, it is recommended that the cuttings be re-examined for maturation ( $R_o$  and TAI) to confirm results by Utting et al. (1976).
- Study the timing of generation by creating a maturation diagenesis graph for Carboniferous sediments within the St. Anthony Basin. This may help define a working hydrocarbon system within the St. Anthony Basin. To achieve this point, it is important to define a critical point for generation to understand when potential source rocks entered the oil window in relation to the availability of reservoir, trap and seal elements.
- Reconstruct original TOC concentrations for the Cape Rouge Formation.

## REFERENCES

- Anadón, P., Cabrera, L., and Kelts, K., editors, 1991, *Lacustrine Facies Analysis*: London, Blackwell Scientific Publications Ltd., International Association of Sedimentologists Series, v.30, 328 p.
- Aplin A.C., and Macquaker J.H.S, 2011, Mudstone diversity: origin and implications for source, seal and reservoir properties in petroleum systems. *AAPG Bulletin*, v. 95, p. 2031-2059
- Baird, D. M., 1950, Oil shales of the Deer Lake regions: Newfoundland Geological Survey Unpublished Report, p. 9–23.
- Baird, D. M., 1957, Carboniferous rocks of the Conche-Northern Grey Island area (part of 2L/13): Department of Mines and Resources, p. 1–25.
- Baird, D. M., 1966, Carboniferous rocks of the Conche-Groais Island area, Newfoundland: *Canadian Journal of Earth Science*, v. 3, p. 247–257.
- Barss, M. S., Bujak, J. P., and Williams, G. L., 1979, Palynological zonation and correlation of sixty-seven wells, eastern Canada: Geological Survey of Canada, p. 78-24.
- Blakey, R.C., 2016, North American Key-Time-Slice Series, a digital map database (available at: <http://deeptimemaps.com/north-america-key-time-slices-map-list/>)
- Belt, E. S., 1969, Newfoundland Carboniferous stratigraphy and its relation to the Maritimes and Ireland: *American Association of Petroleum Geologists*, p. 734–753.
- Bertani, R. T., and Carozzi, A. V., 1985, Lagoa Feia Formation (Lower Cretaceous), Campos basin, offshore Brazil: Rift valley stage lacustrine carbonate reservoirs: *Journal of Petroleum Geology*, v. 8, no. 1, p. 37–58, doi:10.1111/j.1747-5457.1985.tb00190.x.
- Bless, M. J. M., Bouckaert, J., and Parroth, E., 1987, Fossil assemblages and depositional environments: limits to stratigraphic correlations, *in* Miller, J., Adams, A.E., and Wright, V.P., ed., *European Dinantian Environments*, New York, John Wiley & Sons, p. 61-73.
- Bohacs, K. M., Carroll, A. R., Neal, J. E., 2003, Lessons from large lake systems—thresholds, nonlinearity, and strange attractors: *Geological Society of America Special Paper 370*, p. 75–90.
- Bohacs, K. M., Carroll, A. R., Neal, J. E., and Mankiewicz, P. J., 2000, Lake-basin type,

source potential, and hydrocarbon character: an integrated sequence-stratigraphic-geochemical framework: Lake Basins through Space and Time: American Association of Petroleum Geologists Studies in Geology, v. 46, p. 3–34.

Bohacs, K.M., Grabowski, G.J. and Carroll, A.R., 2005, Production, destruction, and dilution- the many paths to source-rock development: SEPM Special Publication No. 82, p. 61-101.

Bordenave, M.L., Espitalie, J., Leplat, P., Oudin, J.L., Van-denbroucke, M., 1993, Screening techniques for source rock evaluation, *in* Bordenave, M.L., ed., Applied Petroleum Geochemistry, Paris, Editions Technip, 524 p.

BP et al., 2007, Hare Bay E-21 Schedule of Wells Newfoundland and Labrador Offshore Area, Canada-Newfoundland and Labrador Offshore Petroleum Board: <http://www.cnlopb.ca/pdfs/wells/well61.pdf> (accessed July 2018).

Bradley, W. H., 1931, Origin and microfossils of the oil shale of the Green River Formation of Colorado and Utah: United States Geological Survey Paper 168, 58 p.

Bradley, W. H., 1964, Geology of Green River Formation and associated Eocene rocks in southwestern Wyoming and adjacent parts of Colorado and Utah: United States Geological Survey, p. 496–A.

Calder, J.H., 1998, The Carboniferous evolution of Nova Scotia, *in* Blundell, D. J. & Scott, A.C. eds., *Lyell: The Past is the Key to the Present*, London, Geological Society, p. 261-302.

Carroll, A.R., and Bohacs, K.M., 1999, Stratigraphic classification of ancient lakes: balancing tectonic and climatic controls: *Geology*, v. 27, p. 99–102.

Carroll, A.R., and Bohacs, K.M., 2001, Lake-type controls on petroleum source rock potential in non-marine basins: *AAPG bulletin*, v. 85, doi: 10.1306/8626CA5F-173B-11D7-8645000102C1865D.

Carruthers, R. G., Cadell, H. M., and Wilson Grant, J. S., 1912, The oil-shales of the Lothians: Edinburgh, HMSO, Memoir of the Geological Survey of Scotland, 314 p.

Carter, D.C. and Pickerill, R.K., 1985, Lithostratigraphy of the Late Devonian-Early Carboniferous Horton Group of the Moncton sub-basin, southern New Brunswick, Maritime Sediments and Atlantic Geology, v.21, p. 11-24.

Christiansen, F. G., Olsen, H., Piasecki, S., and Stemmerik, L., 1990, Organic geochemistry of Upper Paleozoic lacustrine shales in the East Greenland basin: *Organic Geochemistry*, v. 16, p. 287–294.

Cole, G. A., 1979, *Textbook of Limnology* (2nd ed.): St. Louis, C.V. Mosby, 426 p.

- Conybeare, C., and Crook, K., 1968, Manual of sedimentary structures: Commonwealth of Australia Department of National Development Bulletin No.102.
- Dean, M.T., Browne, M.A.E., Waters, C.N., Powell, J.H., 2011, A lithostratigraphical framework for the Carboniferous successions of northern Great Britain (onshore), British Geologic Survey, Research Report RR/10/07
- Demaison, G. J., and Moore, G. T., 1980, Anoxic environments and oil source bed genesis: *Organic Geochemistry*, v. 2, no. 1, p. 9–31.
- Deocampo, D.M., and Jones, B.F., 2014, Geochemistry of saline lakes, *in* Drever, J.I., ed., *Treatise on geochemistry*, Volume 7, Laramie, WY, Elsevier, 644 p.
- Department of Mines and Energy, 2000, Sedimentary basins and hydrocarbon potential of Newfoundland and Labrador: Government of Newfoundland and Labrador, Energy Branch, p. 1–71.
- Desheng, L., Renqi, J., and Katz, B.J., 1995, Petroleum generation in the nonmarine Qingshankou Formation (Lower Cretaceous), Songliao Basin, China, *in* Katz, B.J. ed., *Petroleum source rocks*, Heidelberg, Springer-Verlag, 7 p.
- Desilva, N. R., 1999, Sedimentary basins and petroleum systems offshore Newfoundland and Labrador, *in* *Petroleum geology conference series*: London, Geological Society of London, p. 501–515, doi:10.1144/0050501.
- Dietrich, J., Lavoie, D., Hannigan, P., Pinet, N., Castonguay, S., Giles, P., and Hamblin, A. P., 2011, Geological setting and resource potential of conventional petroleum plays in Paleozoic basins in eastern Canada: *Bulletin of Canadian Petroleum Geology*, v. 59, no. 1, p. 54–84.
- Eastcan et al., 2013, Verrazano L-77 Schedule of Wells Newfoundland and Labrador Offshore Area, Canada-Newfoundland and Labrador Offshore Petroleum Board: <http://www.cnlopbc.ca/pdfs/wells/well54.pdf> (accessed October 2016).
- Encyclopedia Britannica, 2009, Carboniferous period, *in* *Britannica Concise Encyclopedia*: Britannica Digital Learning.
- Espitalie, J., Deroo, G., and Marquis, F., 1986, La pyrolyse rock-eval et ses applications Partie 3: *Revue de l'Institut Francais du Petrole*, v. 41, p. 73–89.
- Espitalie, J., La Porte, J.L, Madec, M., Marquis, F., Le Plat, P., Paulet, J., and Boutefeu, A., 1977, Méthode rapide de caractérisation des roches mères de leur potentiel pétrolier et de leur degré d'évolution: *Revue de l'Institut Francais du Pétrole*, v. 32, p. 23–41.

- Espitalie, J., Marquis, F., and Sage, L., 1987, Organic geochemistry of the Paris basin, *in* Brooks, J., Glennie, K., eds., *Petroleum geology of northwest Europe*, London, Graham and Totman, p. 71–86.
- Follows, B., and Tyson, R. V., 1998, Organic facies of the Asbian (Early Carboniferous) Queensferry beds, Lower Oil Shale Group, South Queensferry, Scotland, and a brief comparison with other Carboniferous North Atlantic oil shale deposits: *Organic Geochemistry*, v. 29, no. 4, p. 821–844.
- French Shore Historical Society, 2011, *Map of Conche Newfoundland: Québec-Labrador Foundation*.
- Froude, G. P., 2012, Thermal maturation and preservation comparisons of Carboniferous (Mississippian) palynomorphs from Conche and Deer Lake areas, Newfoundland and Albert County, New Brunswick: Memorial University of Newfoundland, 1 p.
- Gibling, M. R., Culshaw, N., Rygel, M. C., and Pascucci, V., 2008, The Maritimes basin of Atlantic Canada: Basin creation and destruction in collisional zone of Pangea: *Sedimentary Basins of the World*, v. 5, p. 211–244, doi:10.1016/S1874-5997(08)00006-3.
- Gluyas, J., and Swarbrick, R., 2004, *Petroleum Geoscience: Teaching in Earth Sciences*, v. 28, p. 41-42.
- Greensmith, J. T., 1968, Palaeogeography and rhythmic deposition in the Scottish oil-shale group *in* United Nations symposium on the development and utilisation of oil shale resources: Tallinn, USSR, p. 16.
- Greiner, H. R., 1962, Facies and sedimentary environments of Albert shale, New Brunswick: *Bulletin of the American Association of Petroleum Geologists*, v. 46, p. 219–234.
- Greiner, H. R., 1974, The Albert Formation of New Brunswick: a Paleozoic lacustrine model: *Geologische Rundschau*, v. 63, no. 3, p. 1102–1113, doi:10.1007/BF01821325.
- Hackley P.C., and Cardott, B.J., 2016, Applications of organic petrography in North American Shale petroleum systems: a review: *International Journal of Coal Geology*, v. 163, p. 8–51.
- Hamblin, A. P., 1992, Half-graben lacustrine sedimentary rocks of the Lower Carboniferous Strathlorne Formation, Horton Group, Cape Breton Island, Nova Scotia, Canada: *Sedimentology*, v. 39, p. 263-284.
- Hamblin, A. P., and Rust, B. R., 1989, Tectono-sedimentary analysis of alternate-polarity half-graben basin-fill successions: Late Devonian-Early Carboniferous Horton

Group, Cape Breton Island, Nova Scotia: Basin Research, v. 2, no. 4, p. 239–255, doi:10.1111/j.1365-2117.1989.tb00038.x.

Hamblin, A. P., Fowler, M. G., and Utting, J., 1995, Sedimentology, palynology and source rock potential of Lower Carboniferous (Tournaisian) rocks, Conche area, Great Northern Peninsula, Newfoundland: Bulletin of Canadian Petroleum Geology, v. 43, no. 1, p. 1–19.

Hay, R. L., 1977, Geology of zeolites in sedimentary rocks, *in* Mumpton, F. A., ed., Mineralogy and geology of natural zeolites, Reviews in Mineralogy, Volume 4: Washington, D.C., Mineralogical Society of America, p. 53-64.

Hay, R. L., 1978, Geologic occurrence of zeolites, *in* Sand, L. B., and Mumpton, F. A., eds, Natural zeolites: occurrence properties use: Elmsford, New York, Pergamon Press, p. 135-143.

Horng, C., and Roberts, A. P., 2006, Authigenic or detrital origin of pyrrhotite in sediments?: Resolving a paleomagnetic conundrum: Earth and Planetary Sciences, v. 241, p. 750-762.

Hu, K., and Dietrich, J., 2010, Petroleum reservoir potential of Upper Paleozoic sandstones in the offshore Maritimes basin, eastern Canada: Geological Survey of Canada, Open File 6679, p. 1–16.

Hunt, A. P., Lucas, S. G., Calder, J. H., van Allen, H. E. K., George, E., Gibling, M. R., Hebert, B. L., Mansky, C., and Reid, D., 2004, Tetrapod footprints from Nova Scotia: the Rosetta Stone for carboniferous tetrapod ichnology: Geological Society of America Annual Meeting Abstracts, v. 36, p. 66.

Hunt, J.M., 1996, Petroleum geochemistry and geology, 2nd Edition; New York, W H Freeman & Co, p. 743.

Hussey, D., 2011, An investigation of fundamental controls on lithofacies variability in mud-dominated, Anguille Group, Mississippian strata on the Northern Peninsula, Newfoundland and Labrador: Memorial University of Newfoundland, 1 p.

Hyde, R. S., 1979, Geology of Carboniferous strata in portions of the Deer Lake Basin, western Newfoundland: Newfoundland Department of Mines and Energy Report 79-6, p. 43.

Hyde, R. S., Miller, H. G., Hiscott, R. N., and Wright, J. A., 1988, Basin architecture and thermal maturation in the strike-slip Deer Lake basin, Carboniferous of Newfoundland: Basin Research, p. 85–105.

Jarvie, D.M., 1991, Total organic carbon (TOC) analysis, *in* Merrill, R.K. ed., Source and migration processes and evaluation techniques, Tulsa, OK, The American

Association of Petroleum Geologists Bulletin, p. 113-118.

- Jarvie, D.M., Claxton, B.L., Henk, F., Breer, J.T., 2001, Oil and shale gas from the Barnett Shale, Fort Worth Basin, Texas: American Association of Petroleum Geologists Bulletin, v. 85, p. A100.
- Katz, B.J., Xingcai, L., 1998, Summary of the AAPG Research Symposium on Lacustrine Basin Exploration in China and Southeast Asia, AAPG Bulletin, v. 82, no. 7, p. 1300-1307.
- Keighley, D., 2008, A lacustrine shoreface succession in the Albert Formation, Moncton Basin, New Brunswick: Bulletin of Canadian Petroleum Geology, v. 56, p. 235–258.
- Keighley, D.G., and Pickerill, R.K., 1998, Systematic ichnology of the Mabou and Cumberland groups (Carboniferous) of western Cape Breton Island, eastern Canada, 2: surface markings: Atlantic Geology, v. 34, doi: 10.4138/2041.
- Kelts, K., 1988, Environments of deposition of lacustrine petroleum source rocks: an introduction, *in* Fleet, A. J., Kelts, K., and Talbot, M. R., eds., Lacustrine petroleum source rocks: Geological Society Special Publication, Volume 40: Oxford, Blackwells, p. 3–26.
- Kerr, D., 1994, Shale Oil Scotland: The World's Pioneering Oil Industry. Scotch Publishing, Edinburg
- Kirkland, D. W., and Evans, R., 1981, Source-rock potential of evaporitic environment: AAPG bulletin, v. 65, no. 2, p. 181–190.
- Knight, I., 1983, Geology of the Carboniferous Bay St. George sub basin, western Newfoundland: Newfoundland Department of Mines and Energy, Memoir 1, 1 p.
- Laracy, M., 2012, An assessment of fundamental controls on petrophysical variability of organic carbon rich mudstones: an integrated wireline log lithofacies study of Jurassic (Toarcian) shales [Master's Thesis]: Memorial University of Newfoundland, 240 p.
- Lavoie, D., Pinet, N., Dietrich, J. R., Hannigan, P. K., Castonguay, S., Hamblin, A. P., & Giles, P. S., 2009, Petroleum Resource Assessment, Paleozoic successions of the St. Lawrence Platform and Appalachians of eastern Canada: Geological Survey of Canada, Open File 6174; 275 p. DOI 10.4095/248071
- Leeder, M.R., and Gawthorpe, R.L., 1987, Sedimentary models for extensional tilt-block/half-grabins: Geological Society, London, Special Publications, v.28, p.139-152, doi: 10.1144/GSL.SP.1987.028.01.11
- Lomando, A.J., 1996, Exploration for lacustrine carbonate reservoirs: Insights from West

Africa: AAPG bulletin, v. 80.

Løseth, H., Wensaas, L., Gading, M., Duffaut, K., and Springer, M., 2011, Can hydrocarbon source rocks be identified on seismic data?: *Geology*, v.39, no. 12, p 1167–1170, DOI 10.1130/G32328.1.

MacQuaker, J. H. S., and Adams, A., 2003, Maximizing information from fine-grained sedimentary rocks: an inclusive nomenclature for mudstones: *Journal of Sedimentary Research*, v. 73, no. 5, p. 735–744.

MacQuaker, J. H. S., and Bohacs, K. M., 2007, On the accumulation of mud: *Science*, v. 318, p. 1734–1735.

MacQuaker, J. H. S., and Howell, J. K., 1999, Small-scale (<5.0m) vertical heterogeneity in mudstones: implications for high-resolution stratigraphy in mudstone siliciclastic successions: *Journal of the Geological Society*, v. 156, no. 1, p. 105–112, doi:10.1144/gsjgs.156.1.0105.

Macquaker, J. H. S., and Jones, C. R., 2002, A sequence-stratigraphic study of mudstone heterogeneity: A combined petrographic/wireline log investigation of Upper Jurassic mudstones from the North Sea (U.K.): *AAPG Methods in Exploration*, p. 123–141.

Magoon, L. B., and Dow, W. G., 1994, *The petroleum system - from source to trap: Tulsa: The Association of Petroleum Geologists, AAPG Memoir 60.*

Martel, A.T., and Gibling, M.R., 1996, Stratigraphy and tectonic history of the Upper Devonian to Lower Carboniferous Horton Bluff Formation, Nova Scotia: *Atlantic Geology*, v. 32, doi: 10.4138/2076.

Martel, A.T., 1990, Stratigraphy, fluviolacustrine sedimentology and cyclicity of the Late Devonian/Early Carboniferous Horton Bluff Formation, [Unpublished Ph.D. thesis]: Dalhousie University.

McWhae, J. R. H., Elie, R., Laughton, K. C., and Gunther, P. R., 1980, Stratigraphy and petroleum prospects of the Labrador Shelf: *Bulletin of Canadian Petroleum Geology*, v. 28, p. 460–488.

Miller, H. G., and Wright, J. A., 1984, Gravity and magnetic interpretation of the Deer Lake basin, Newfoundland: *Canadian Journal of Earth Sciences*, v. 21, no. 1, p. 10–18, doi:10.1139/e84-002.

Morel, P., and Irving, E., 1978, Tentative paleocontinental maps for the Early Phanerozoic and Proterozoic: *The Journal of Geology*, v. 86, no. 5, p. 535–561.

Mossman, D. J., 1992, Carboniferous source rocks of the Canadian Atlantic margin: *Geological Society, London, Special Publications*, v. 62, no. 1, p. 25–33,

doi:10.1144/GSL.SP.1992.062.01.05.

Murphy, J. B., and Rice, R. J., 1998, Stratigraphy and depositional environment of the Horton Group in the St. Mary's Basin, central mainland Nova Scotia: *Atlantic Geology*, v. 34, no. 1, doi:10.4138/2037.

Murray, A., Howley, J.P., 1881, Reports of the geological survey of Newfoundland 1864-1880. Stanford, London.

Murray, A., Howley, J.P., 1918, Reports of the geological survey of Newfoundland, 1881-1909. Robinson St. John's.

Paproth, E., 1983, Bio- and lithostratigraphic subdivisions of the Dinantian in Belgium, a review: *Annales de la Société Géologique de Belgique*, v. 106, p. 185–259.

Parnell, J., 1988, Lacustrine petroleum source rocks in the Dinantian Oil Shale Group, Scotland: a review: *Geological Society, London, Special Publications*, v. 40, no. 1, p. 235–246, doi:10.1144/GSL.SP.1988.040.01.20.

Parnell, J., 1991, Hydrocarbon Potential of Northern Ireland: Part 1. Burial histories and source-rock potential: *Journal of Petroleum Geology*, v. 14, no. 1, p. 65–78, doi:10.1111/j.1747-5457.1991.tb00299.x.

Peters, K.E., 1986, Guidelines for evaluating petroleum source rock using programmed pyrolysis: *The American Society of Petroleum Geologists Bulletin*, v. 70, No. 3, p. 318-329.

Peters, K.E., and Cassa, M.R., 1994, *Applied Source Rock Geochemistry*, Chapter 5: Petroleum system - from source to trap: AAPG Memoir 60.

Peters, K.E., Walters, C.C., and Moldowan, J.M., 2004, *The Biomarker Guide: Volume 1, Biomarkers and Isotopes in the environment and human History*, 2<sup>nd</sup> Edition: Cambridge, England, Cambridge University Press, 490 p.

Piasecki, S., Christiansen, F. G., and Stemmerik, L., 1990, Depositional history of an Upper Carboniferous organic-rich lacustrine shale from east Greenland: *Bulletin of Canadian Petroleum Geology*, v. 38, no. 3, p. 273–287.

Pickerill, R.K., 1992, Carboniferous nonmarine invertebrate ichnocoenoses from southern New Brunswick, eastern Canada: *Ichnos*, v. 2, p. 21–35, doi:10.1080/10420949209380072.

Plasse, D., and Graves, M., 1985, Index of commercially acquired potential field data in the Canadian East coast offshore: *Geological Survey of Canada Paper no. 85-1B*, p. 428.

- Powell, T. G., 1986, Petroleum geochemistry and depositional setting of lacustrine source rocks: *Marine and Petroleum Geology*, v. 3, no. 3, p. 200–219, doi:10.1016/0264-8172(86)90045-0.
- Prothero, D.R., and Schwab, F., 2004, *Sedimentary geology - an introduction to sedimentary rocks and stratigraphy*: New York, W.H. Freeman and Company, 593 p.
- Remy, R.R., and Ferrell, R.E., 1989, Distribution and origin of analcime in marginal lacustrine mudstones of the Green River Formation, South-Central Uinta Basin, Utah: *Clays and Clay Minerals*, v. 37, no. 5, p. 419-432.
- Rietveld, H.M., 1969, A profile refinement method for nuclear and magnetic structures: *Journal of Applied Crystallography*, v 2, p. 64.
- Renaut, R. W., and Gierlowski-Kordesch, E. H., 2010, Lakes, *in* N. P. James, and Dalrymple, R. W., eds., *Facies Models 4: St. John's, NL*, Geological Association of Canada, p. 541–575.
- Rojas, K. M. K., Niemann, M., Palmowski, D., Peters, K., and Stankiewicz, A., 2013, Basic Petroleum Geochemistry for Source Rock Evaluation: *Oilfield Review* Schlumberger, p. 32–43.
- Schieber, J., and Southard, J. B., 2009, Bedload transport of mud by floccule ripples - Direct observation of ripple migration processes and their implications: *Geology*, v. 37, no. 6.
- Schieber, J., Southard, J., and Thaisen, K., 2007, Accretion of mudstone beds from migrating floccule ripples: *Science*, v. 318, issue 5857, p. 1760-1763.
- Schliche, R.W. and Olsen, P.E., 1990, Quantitative filling model for continental extensional basins with applications to Early Mesozoic rifts of eastern North America: *Journal of Geology*, v. 98, p. 135-155.
- Senftle, J.T., and Landis, C.R., 1991, Vitrinite reflectance as a tool to assess thermal maturity, *in* Merrill, K.R. ed., *Source and migration processes and evaluation techniques: AAPG Treatise of Petroleum Geology, Handbook of Petroleum Geology*, p. 119-125.
- Sheppard, R.A., 1973, *Zeolites in sedimentary rocks*: U.S. Geological Survey Professional Paper 820, p. 689-695.
- Sinclair, I.K., 1990, A Review of the Upper Precambrian and Lower Paleozoic Geology of Western Newfoundland and the Hydrocarbon Potential of the Adjacent Offshore Area of the Gulf of St. Lawrence, C-NOPB Report GLCNOPB-90-1
- Smith, W. D., and Gibling, M. R., 1987, Oil shale composition related to depositional

setting: a case study from the Albert Formation, New Brunswick, Canada: *Bulletin of Canadian Petroleum Geology*, v. 35, p. 469–487.

Smith, W. D., St Peter, C. J., Naylor, R. D., Mukhopadhyay, P. K., Kalkreuth, W. D., Ball, F. D., and Macauley, G., 1991, Composition and depositional environment of major eastern Canadian oil shales: *International Journal of Coal Geology*, v. 19, no. 1-4, p. 385–438, doi:10.1016/0166-5162(91)90028-H.

Spackman, W., 1958, The maceral concept and the study of modern environments as a means of understanding the nature of coal: *Transactions of the New York Academy of Sciences*, v.20, issue 5, series II, p. 411–423.

St. Peter, C. J., and Johnson, S. C., 2009, Stratigraphy and structural history of the late Paleozoic Maritimes Basin in southeastern New Brunswick, Canada: *New Brunswick Department of Natural Resources, Memoir 3*, p. 348.

Stow, D., 2006, *Sedimentary Rocks in the Field, a Colour Guide*: London, Manson Publishing, 320 p.

Suárez-Ruiz, I., Flores, D., Mendonça Filho, J.G., and Hackley, P.C., 2012, Review and update of the applications of organic petrology: Part 1, geological applications: *International Journal of Coal Geology*, v. 99, p. 54–112, doi: 10.1016/j.coal.2012.02.004.

Tissot, B.P., and Welte, D.H., 1984, *Petroleum formation and occurrence*: New York, Springer-Verlag, 702 p.

Tourtelot, H., 1979, Black shale: its deposition and diagenesis: *Clays and Clay Minerals*, v. 27, no. 5, p. 313-321.

Trindade, L.A.F., Dias, J.L., and Mello, M.R., 1995, Sedimentological and geochemical characterization of the Lagoa Feia Formation, rift phase of the Campos Basin, Brazil, *in* Katz, B. J., ed., *Petroleum Source Rocks, Casebooks in Earth Sciences*: Berlin, Springer, p.149–165.

Tyson, R.V., 1995, *Sedimentary organic matter: organic facies and palynofacies*: London, Chapman & Hall, 615 p.

Utting, J., Keppie, J. D., and Giles, P. S., 1989, Palynology and stratigraphy of the Lower Carboniferous Horton Group, Nova Scotia, *in* Reynolds, L., ed., *Contributions to Canadian Paleontology, Geological Survey of Canada Bulletin 396*: Ottawa, Canadian Government Publishing Centre, p.117–143.

Utting, J., Mamet, B. L., and Heroux, Y., 1976, Investigation of samples from Verrazano L-77 (Eastcan et al.) (52° 20' 36.5' N. Lat., 54° 11' 52.6' W. Long.): Quebec, QC, INRS-Petrole, p. 14.

- Van der Zwan, C. J., Boulter, M. C., and Hubbard, R. N. L. B., 1985, Climatic change during the Lower Carboniferous in Euramerica, based on multivariate statistical analysis of palynological data: *Palaeogeography, Palaeoclimatology, Palaeoecology*, v. 52, no. 1-2, p. 1–20, doi:10.1016/0031-0182(85)90028-8.
- Van der Zwan, C. J., Boulter, M. C., and Hubbard, R. N. L. B., 1985. Climatic change during the Lower Carboniferous in Euramerica, based on multivariate statistical analysis of palynological data: *Paleogeography, Palaeoclimatology, Palaeoecology*, v. 52, p. 20
- Warren, J. K., 1986, Shallow-water evaporitic environments and their source rock potential: *Journal of Sedimentary Petrology*, v. 56, no. 3, p. 442–454.
- Williams, E. P., 1973, The Quebec and Maritimes Basin, *in* McCrossan, R. G., ed., *The future of petroleum provinces of Canada: Canadian Society of Petroleum Geology, Memoir 1*, p. 561–588.
- Zhai, G., Wang, S., and Li, G., 1984, Characteristics of sedimentary basins in China and its oil and gas distribution, *in* Beijing Petroleum Geology Symposium, Beijing, p. 37.
- Ziegler, P. A., 1988, Evolution of the Arctic-North Atlantic and the western Tethys: AAPG Memoir 43, p. 164–196.

**APPENDIX 1: GEOCHEMICAL RESULTS**

## Appendix 1 Cape Rouge Formation Geochemical Results (Rock-Eval, %Ro, TAI) (Page 1/3)

Field Data						Leco		Rock-Eval			Tmax (°C)	Thermal Maturity			Rock-Eval					Lab Notes:
Sample Name	Sample Number	Strat Section	Sample Location	Sample Region	GPS Location (UTM NAD27)	% Carb. (wt%)	Leco TOC (wt% HC)	S1 (mg HC/g)	S2 (mg HC/g)	S3 (mg CO2/g)		%Ro (Mean)	Calc. (RE TMAX)	TAI	HI (S2x100/TOC)	OI (S3x100/TOC)	S2/S3 (mg HC/mg CO2)	SI/TOC Norm. Oil Content	Production Index (S1/(S1+S2))	Low Temp S2 Shoulder?
Lnl2090-A	1	1	Pyramid Point	CRP	21 U 582525 5646050	21.81	0.62	0.23	0.55	0.16	443		0.81		89	26	3	37	0.29	
Lnl2091-A1	2	1	Pyramid Point	CRP	21 U 582514 5646049	42.52	1.67	0.08	2.81	0.32	447		0.89		168	19	9	5	0.03	
Lnl2091-A2	3	1	Pyramid Point	CRP	21 U 582514 5646049	24.65	0.96	0.15	0.94	0.56	446		0.87		98	58	2	16	0.14	Yes
Lnl2091-B	4	1	Pyramid Point	CRP	21 U 582514 5646049	31.94	6.54	0.40	34.74	0.64	451	1.01	0.96	3- to 3	531	10	54	6	0.01	
Lnl2091-C	5	1	Pyramid Point	CRP	21 U 582514 5646049	28.54	1.30	0.17	2.13	0.47	447	0.77	0.89	2+ to 3-	164	36	5	13	0.07	
Lnl2092	6	1	Pyramid Point	CRP	21 U 582509 5646015	32.87	1.32	0.11	2.25	0.38	450		0.94		170	29	6	8	0.05	
Lnl2092-D	7	1	Pyramid Point	CRP	21 U 582509 5646015	25.43	0.69	0.14	0.38	0.14	454		1.01		55	20	3	20	0.27	
Lnl2077-A	8	1	Pyramid Point	CRP	21 U 582388 5645949	17.66	0.23	0.04	0.02	0.06	0		-7.16		9	26	0	17	0.67	
Lnl2077-B	9	1	Pyramid Point	CRP	21 U 582388 5645949	30.99	0.55	0.11	0.51	0.15	456		1.05		93	27	3	20	0.18	
Lnl2077-C	10	1	Pyramid Point	CRP	21 U 582388 5645949	16.37	0.59	0.19	0.50	0.08	453		0.99		85	14	6	32	0.28	
Lnl2077-D	11	1	Pyramid Point	CRP	21 U 582388 5645949	24.51	1.29	0.08	3.82	0.19	448	0.69	0.90	2 to 2+	296	15	20	6	0.02	
Lnl2077-E	12	1	Pyramid Point	CRP	21 U 582388 5645949	31.34	2.32	0.08	13.77	0.36	446	0.73	0.87	2+ to 3-	594	16	38	3	0.01	
Lnl2077-F	13	1	Pyramid Point	CRP	21 U 582388 5645949	18.99	0.63	0.13	0.74	0.33	449		0.92		117	52	2	21	0.15	
Lnl2077-G1	14	1	Pyramid Point	CRP	21 U 582388 5645949	26.30	1.30	0.08	3.99	0.27	443		0.81		307	21	15	6	0.02	
Lnl2077-G2	15	1	Pyramid Point	CRP	21 U 582388 5645949	25.90	0.53	0.06	0.82	0.21	447		0.89		155	40	4	11	0.07	
Lnl2077-H	16	1	Pyramid Point	CRP	21 U 582388 5645949	25.73	0.92	0.07	2.18	0.05	443		0.81		238	5	44	8	0.03	
E10069-5	17	N/A	Truite Point	CRP	21 U 580993 5641559	36.92	1.55	0.16	6.98	0.33	439		0.74		450	21	21	10	0.02	
E10068-7	18	N/A	Truite Point	CRP	21 U 580823 5641572	16.78	0.60	0.13	0.51	0.13	447		0.89		86	22	4	22	0.20	
E10068-8	19	N/A	Truite Point	CRP	21 U 580823 5641572	31.49	0.81	0.30	1.36	0.12	442		0.80		169	15	11	37	0.18	
E10070-1	20	N/A	Truite Point	CRP	21 U 580910 5641555	23.90	1.31	0.13	4.35	0.23	443		0.81		332	18	19	10	0.03	
E10070-4	21	N/A	Truite Point	CRP	21 U 580910 5641555	17.54	0.64	0.28	0.67	0.11	446		0.87		104	17	6	44	0.29	
E10070-5	22	N/A	Truite Point	CRP	21 U 580910 5641555	11.92	0.50	0.05	0.34	0.16	446		0.87		67	32	2	10	0.13	
E11308-1	-	N/A	Truite Point	CRP	21 U 580808 5641594	N/A	N/A	N/A	N/A	N/A	N/A	0.60	N/A	2 to 2+	N/A	N/A	N/A	N/A	N/A	
Lnl2059-A	23	N/A	West of Truite Pt.	CRP	21 U 581668 5641548	31.97	1.28	0.21	1.82	0.13	430		0.58		142	10	14	16	0.10	
Lnl2059-B	24	N/A	West of Truite Pt.	CRP	21 U 581668 5641548	24.06	1.42	0.19	3.52	0.06	447		0.89		248	4	59	13	0.05	
E10065-3	25	N/A	Goguelin Point	CRP	21 U 580000 5642571	12.97	1.03	0.22	2.17	0.20	444		0.83		211	19	11	21	0.09	
Lnl2054-A	26	N/A	Grande Pt. Area	CRP	21 U 582422 5642211	42.00	2.06	0.21	8.50	0.20	450		0.94		413	10	43	10	0.02	
Lnl2054-B	27	N/A	Grande Pt. Area	CRP	21 U 582422 5642211	20.79	1.42	0.23	2.50	0.21	447		0.89		176	15	12	16	0.08	
Lnl2054-C	28	N/A	Grande Pt. Area	CRP	21 U 582422 5642211	30.85	1.39	0.29	2.23	0.12	452		0.98		160	9	19	21	0.12	

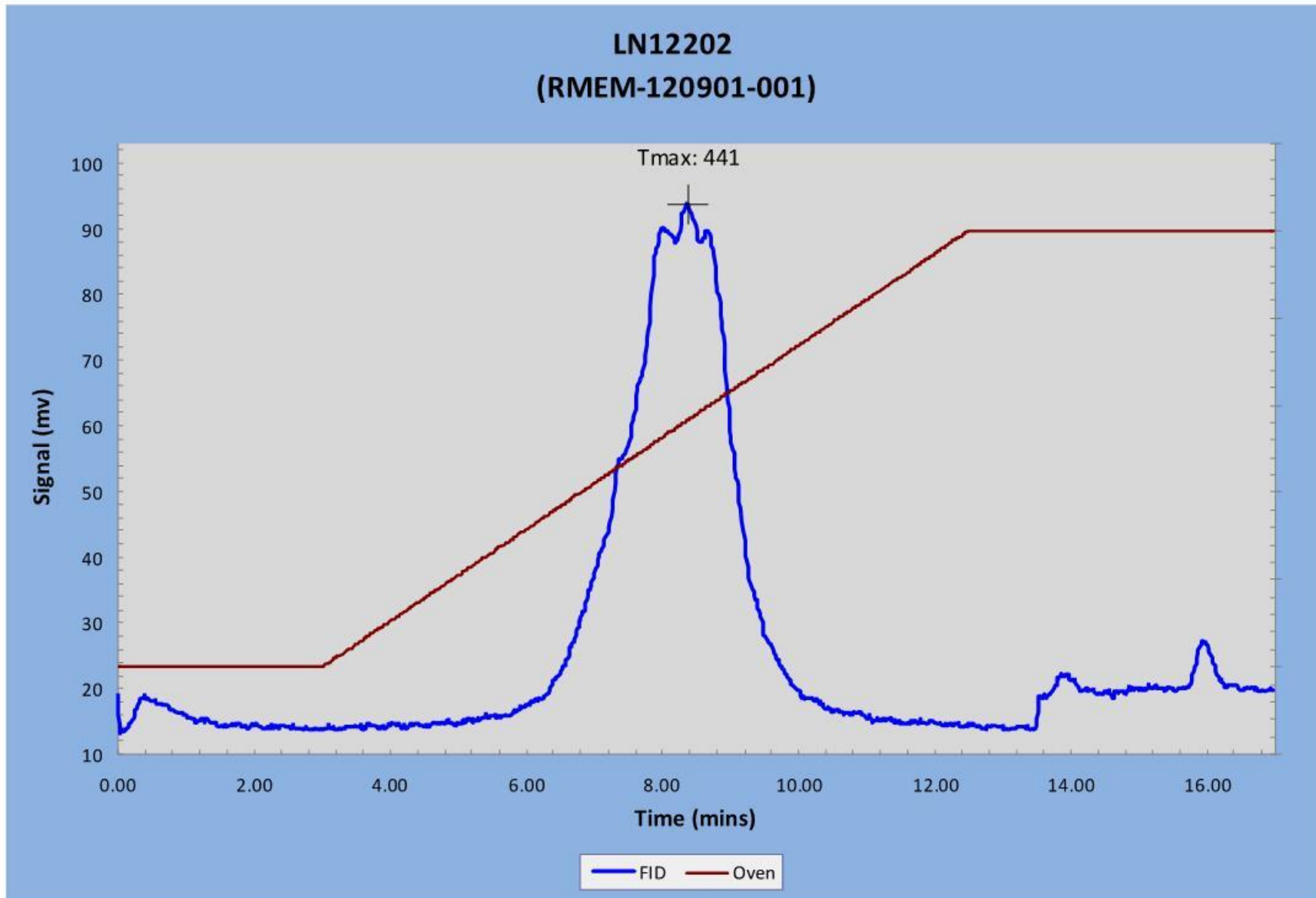
### Appendix 1 Cape Rouge Formation Geochemical Results (Rock-Eval, %Ro, TAI) (Page 2/3)

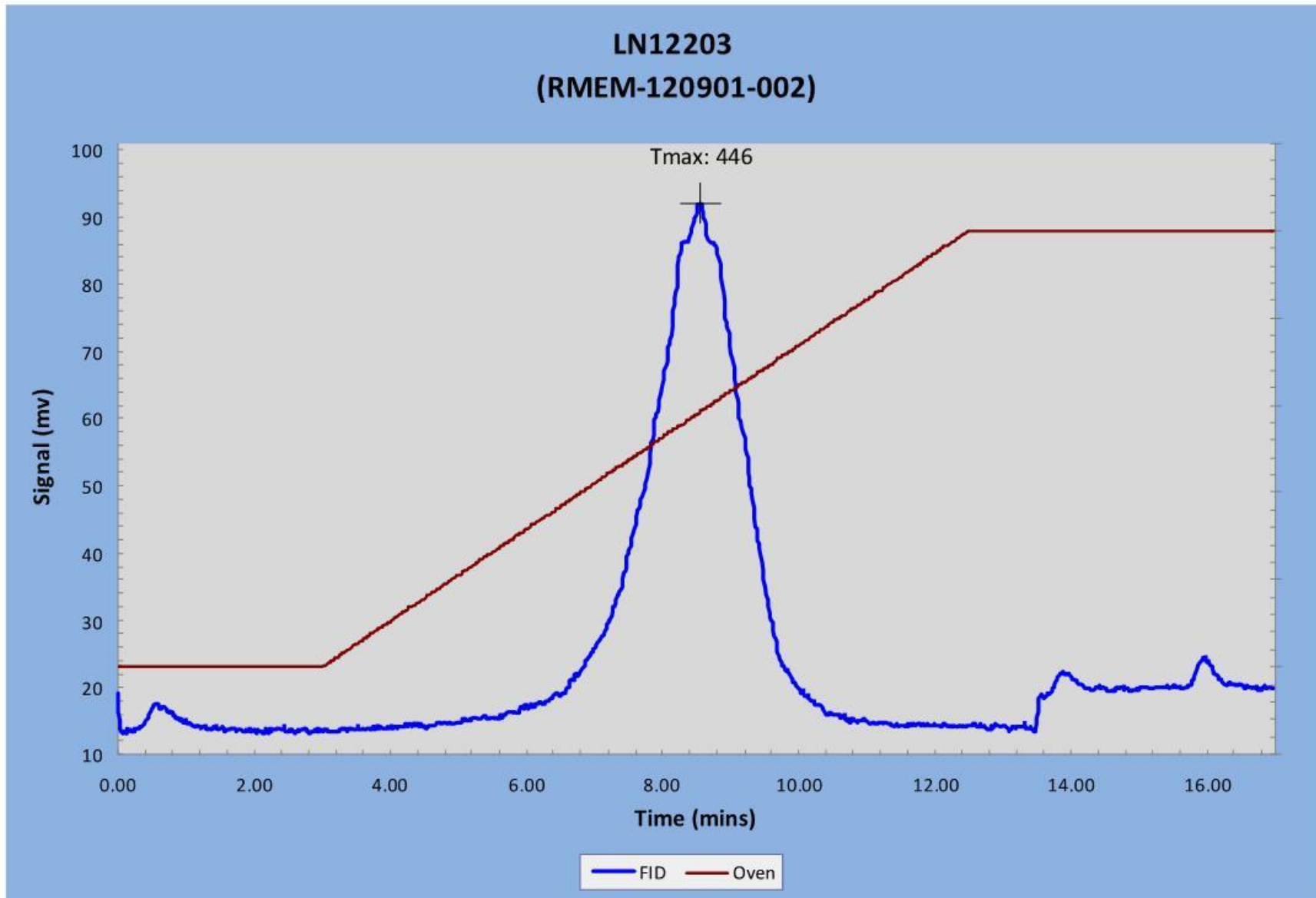
Field Data						Rock-Eval			Thermal Maturity			Rock-Eval								
Sample Name	Sample Number	Strat Section	Sample Location	Sample Region	GPS Location (UTM NAD27)	% Carb.	Leco TOC (wt% HC)	S1 (mg HC/g)	S2 (mg HC/g)	S3 (mg CO2/g)	Tmax (°C)	%Ro (Mean)	Calc. %Ro (RE TMAX)	TAI	HI (S2x100/TOC)	OI (S3x100/TOC)	S2/S3 (mg HC/mg CO2)	SI/TOC Norm. Oil Content	Production Index (S1/(S1+S2))	Lab Notes: Low Temp S2 Shoulder?
Lnl2006-A	29	N/A	Chest Head	CP	21 U 577375 5636850	82.65	0.47	0.21	0.84	0.33	439	0.74			179	70	3	45	0.20	
Lnl2006-B1	30	N/A	Chest Head	CP	21 U 577375 5636850	11.01	0.55	0.08	0.16	0.16	440	0.76			29	29	1	15	0.33	
Lnl2006-B2	31	N/A	Chest Head	CP	21 U 577375 5636850	13.16	0.64	0.17	0.35	0.18	439	0.74			55	28	2	27	0.33	
Lnl2006-B3	32	N/A	Chest Head	CP	21 U 577375 5636850	14.95	0.81	0.20	0.67	0.40	440	0.76			83	49	2	25	0.23	
Lnl2016-A	33	2	Martinique Point	CP	21 U 577462 5636353	15.31	0.93	0.28	1.39	0.27	448	0.90			149	29	5	30	0.17	Yes
Lnl2016-B	34	2	Martinique Point	CP	21 U 577462 5636353	15.98	0.82	0.17	0.65	0.49	441	0.78			79	60	1	21	0.21	
Lnl2016-C	35	2	Martinique Point	CP	21 U 577462 5636353	16.44	1.32	0.32	2.29	0.40	443	0.68	0.81	2 to 2+	173	30	6	24	0.12	
Lnl2016-D	36	2	Martinique Point	CP	21 U 577462 5636353	12.69	0.82	0.17	0.97	0.16	447	0.89			118	19	6	21	0.15	Yes
Lnl2016-E	37	2	Martinique Point	CP	21 U 577462 5636353	18.55	0.98	0.13	1.15	0.36	441	0.78			117	37	3	13	0.10	
Lnl2016-F	38	2	Martinique Point	CP	21 U 577462 5636353	21.61	0.93	0.20	1.24	0.40	447	0.89			133	43	3	21	0.14	
Lnl2016-G	39	2	Martinique Point	CP	21 U 577462 5636353	20.83	0.97	0.18	1.79	0.18	447	0.89			184	19	10	19	0.09	
Lnl2016-H	40	2	Martinique Point	CP	21 U 577462 5636353	21.58	1.49	0.20	3.58	0.23	442	0.50	0.80	2 to 2+	240	15	16	13	0.05	
Lnl2016-I	41	2	Martinique Point	CP	21 U 577462 5636353	49.08	0.90	0.13	1.6	0.31	448	0.51	0.90	2 to 2+	178	34	5	14	0.08	
Lnl2016-Ia	42	2	Martinique Point	CP	21 U 577462 5636353	17.68	0.76	0.15	0.93	0.25	448	0.90			122	33	4	20	0.14	
Lnl2016-Ib	43	2	Martinique Point	CP	21 U 577462 5636353	16.50	1.39	0.33	3.08	0.26	447	0.89			222	19	12	24	0.10	
Lnl2016-J	44	2	Martinique Point	CP	21 U 577462 5636353	80.63	0.81	2.91	4.08	0.51	422	0.44			506	63	8	361	0.42	Yes
Lnl2016-K	45	2	Martinique Point	CP	21 U 577462 5636353	74.40	0.68	0.12	1.44	0.34	452	0.98			213	50	4	18	0.08	
Lnl2021	46	2	Martinique Point	CP	21 U 577482 5636378	56.66	0.44	0.08	0.37	0.20	448	0.90			83	45	2	18	0.18	
Lnl2021-A	47	2	Martinique Point	CP	21 U 577482 5636378	22.53	0.79	0.20	0.77	0.25	443	0.81			98	32	3	25	0.21	
Lnl2021-B	48	2	Martinique Point	CP	21 U 577482 5636378	22.35	0.70	0.15	0.36	0.13	442	0.80			52	19	3	21	0.29	
Lnl2021-C	49	2	Martinique Point	CP	21 U 577482 5636378	31.66	0.70	0.28	0.64	0.14	443	0.81			92	20	5	40	0.30	
Lnl2021-D	50	2	Martinique Point	CP	21 U 577482 5636378	13.94	0.62	0.12	0.4	0.12	448	0.90			65	19	3	19	0.23	
Lnl2021-F	51	2	Martinique Point	CP	21 U 577482 5636378	15.92	0.72	0.14	0.44	0.23	442	0.80			61	32	2	19	0.24	Yes
Lnl2021-G	52	2	Martinique Point	CP	21 U 577482 5636378	27.07	0.64	0.08	0.33	0.14	452	0.98			51	22	2	12	0.20	Yes
Lnl2021-H	53	2	Martinique Point	CP	21 U 577482 5636378	19.96	0.74	0.08	0.30	0.28	452	0.75	0.98	2 to 3-	41	38	1	11	0.21	Yes
Lnl2014	54	2	Martinique Point	CP	21 U 577485 5636278	64.52	0.93	0.38	1.98	0.57	449	0.92			213	61	3	41	0.16	
Lnl2014-A	55	2	Martinique Point	CP	21 U 577485 5636278	11.88	1.14	0.23	1.86	0.37	445	0.85			163	32	5	20	0.11	
Lnl2014-B	56	2	Martinique Point	CP	21 U 577485 5636278	9.20	1.20	0.37	2.19	0.47	447	0.89			183	39	5	31	0.14	
Lnl2014-C	57	2	Martinique Point	CP	21 U 577485 5636278	14.99	0.65	0.26	0.57	0.72	448	0.90			88	111	1	40	0.31	
Lnl2014-D	58	2	Martinique Point	CP	21 U 577485 5636278	12.55	1.00	0.26	1.28	0.54	450	0.94			128	54	2	26	0.17	
Lnl2014-E	59	2	Martinique Point	CP	21 U 577485 5636278	85.80	1.01	4.88	2.44	0.76	430	0.58			242	75	3	483	0.67	Yes

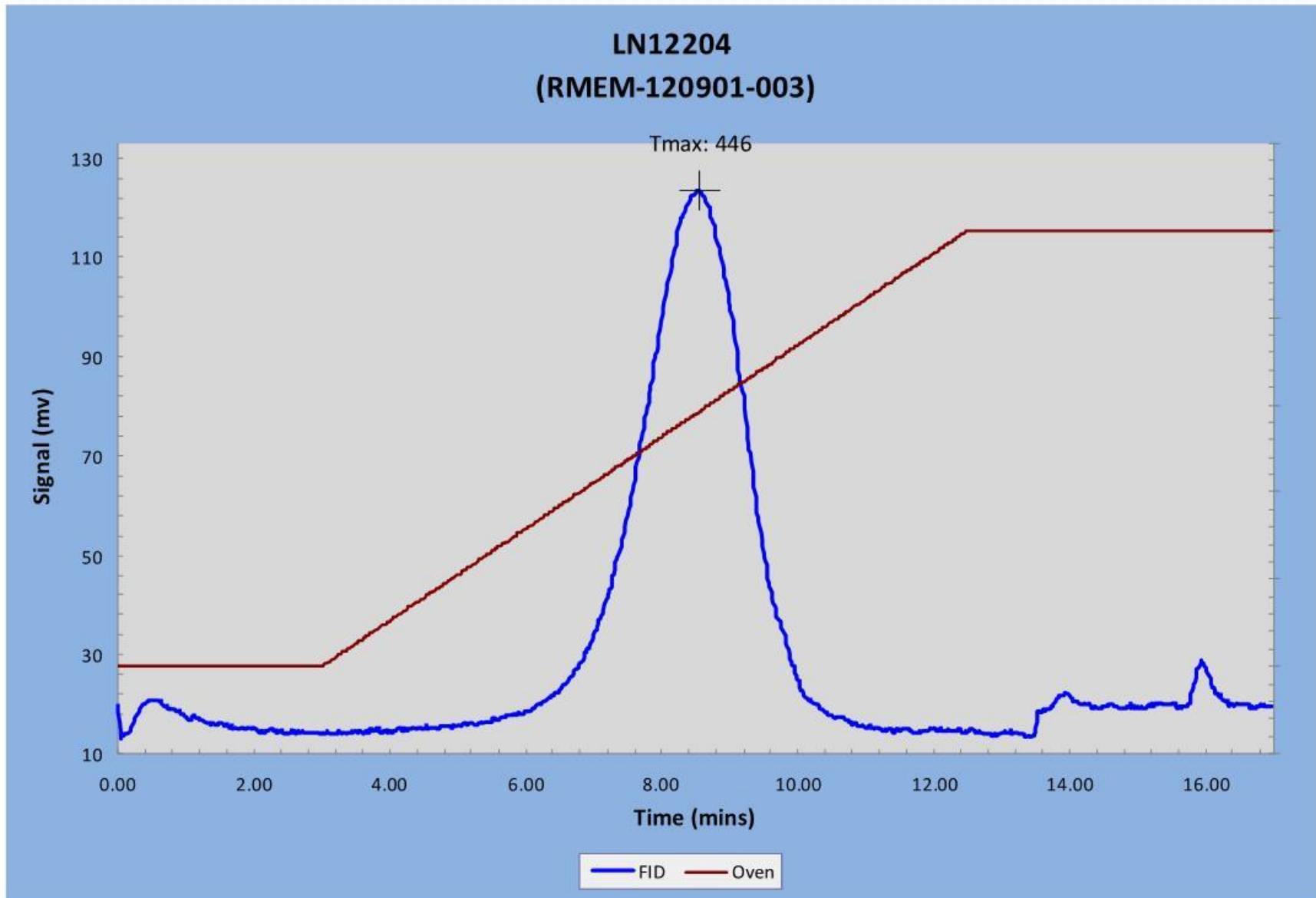
## Appendix 1 Cape Rouge Formation Geochemical Results (Rock-Eval, %Ro, TAI) (Page 3/3)

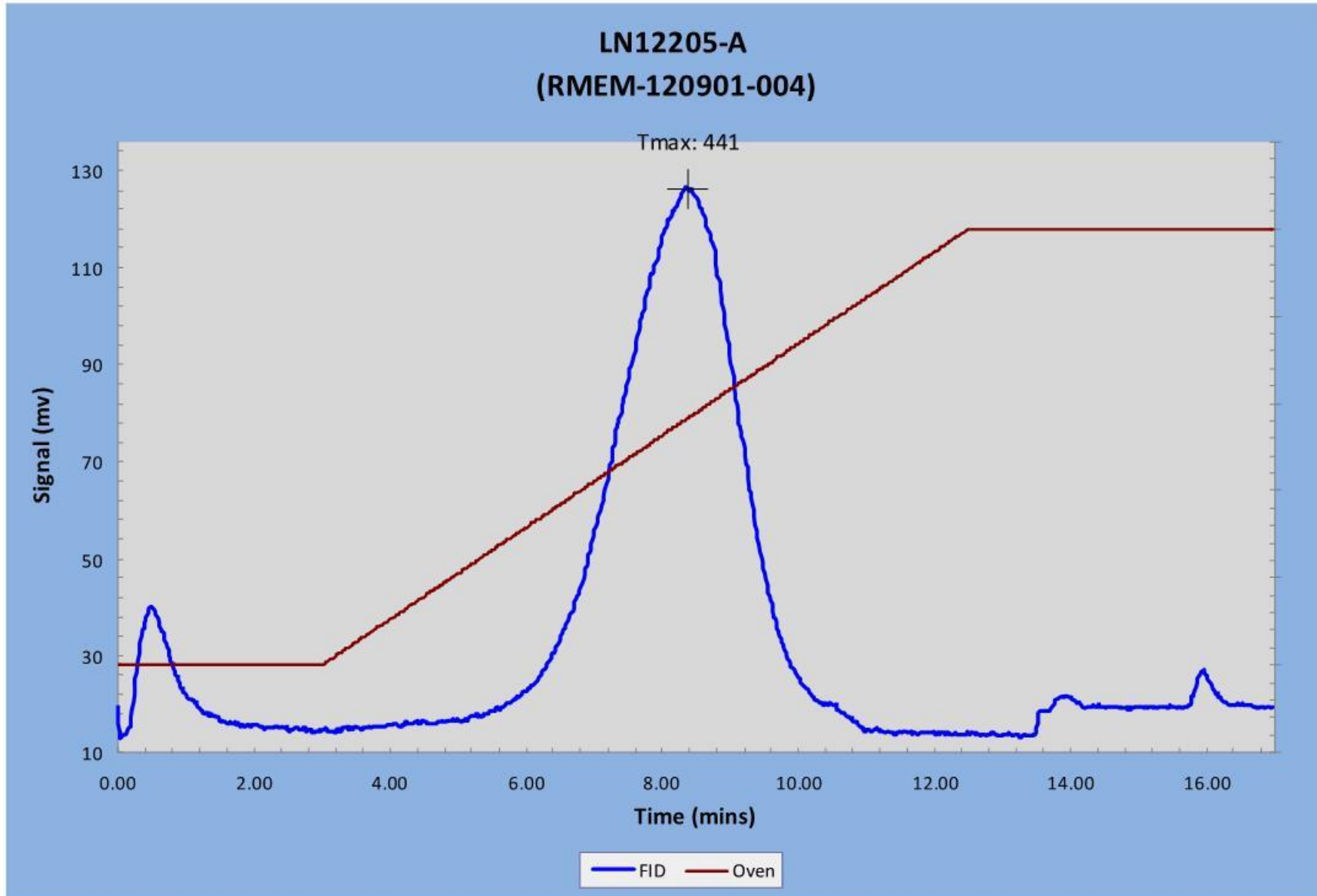
Field Data						Rock-Eval		Rock-Eval				Thermal Maturity			Rock-Eval					Lab Notes:
Sample Name	Sample Number	Strat Section	Sample Location	Sample Region	GPS Location (UTM NAD27)	% Carb.	Leco TOC	S1 (mg HC/g)	S2 (mg HC/g)	S3 (mg CO2/g)	Tmax (°C)	%Ro (Mean)	Calc. (RE TMAX)	TAI	HI (S2x100/TOC)	OI (S3x100/TOC)	S2/S3 (mg HC/mg CO2)	S1/TOC Norm. Oil Content	Production Index (S1/(S1+S2))	Low Temp S2 Shoulder?
Lnl2014-E1	60	2	Martinique Point	CP	21 U 577485 5636278	10.26	1.26	0.24	2.51	0.20	444	0.83			199	16	13	19	0.09	
Lnl2014-F	61	2	Martinique Point	CP	21 U 577485 5636278	28.71	1.67	0.36	4.31	0.34	444	0.83			258	20	13	22	0.08	
Lnl2014-G1	62	2	Martinique Point	CP	21 U 577485 5636278	27.08	1.86	0.52	4.78	0.71	442	0.52	0.80	2	257	38	7	28	0.10	
Lnl2014-H	63	2	Martinique Point	CP	21 U 577485 5636278	18.03	0.64	0.11	0.26	0.17	448	0.90			41	27	2	17	0.30	
Lnl2014-I	64	2	Martinique Point	CP	21 U 577485 5636278	86.08	0.48	1.05	0.48	0.76	448	0.90			100	158	1	218	0.69	
Lnl2014-J	65	2	Martinique Point	CP	21 U 577485 5636278	37.27	1.57	0.91	4.53	0.64	451	0.96			289	41	7	58	0.17	
Lnl2034	66	3	Cape Fox	CP	21 U 577917 5634710	77.23	0.77	0.25	1.77	0.44	439	0.74			231	57	4	33	0.12	Yes
Lnl2034-A	67	3	Cape Fox	CP	21 U 577917 5634710	14.92	1.01	0.32	1.63	0.14	449	0.92			161	14	12	32	0.16	
Lnl2034-B1	68	3	Cape Fox	CP	21 U 577917 5634710	69.92	0.52	0.26	0.90	0.26	451	0.96			172	50	3	50	0.22	
Lnl2034-B	69	3	Cape Fox	CP	21 U 577917 5634710	18.56	0.95	0.26	1.40	0.11	447	0.89			147	12	13	27	0.16	
Lnl2034-E	70	3	Cape Fox	CP	21 U 577917 5634710	23.58	0.74	0.22	0.88	0.08	452	0.98			119	11	11	30	0.20	Yes
Lnl2034-F	71	3	Cape Fox	CP	21 U 577473 5636667	31.86	0.58	0.28	0.66	0.16	457	1.07			113	27	4	48	0.30	
Lnl2037-A1	72	3	Cape Fox	CP	21 U 577834 5634761	10.52	0.33	0.10	0.09	0.07	0	0.00			27	21	1	30	0.53	
Lnl2037-B1	73	3	Cape Fox	CP	21 U 577834 5634761	8.53	1.19	0.35	3.09	0.08	442	0.60	0.80	2 to 2+	260	7	39	29	0.10	
Lnl2037-C1	74	3	Cape Fox	CP	21 U 577834 5634761	11.43	0.60	0.23	0.42	0.10	436	0.69			70	17	4	38	0.35	
Lnl2106-A	75	N/A	Northern Coast	CP	21 U 578239 5639349	23.31	1.60	0.3	3.97	0.1	443	0.81			248	6	40	19	0.07	
Lnl2107-A	76	N/A	Northern Coast	CP	21 U 578272 5639394	16.05	0.30	0.05	0.02	0.07	0	0.00			7	23	0	17	0.71	
Lnl2107-C	77	N/A	Northern Coast	CP	21 U 578272 5639394	15.44	0.29	0.05	0.07	0.01	0	0.00			24	3	7	17	0.42	
Lnl2108-B	78	N/A	Northern Coast	CP	21 U 578688 5639573	21.13	0.73	0.23	0.87	0.05	440	0.76			119	7	17	31	0.21	
Lnl2108-C	79	N/A	Northern Coast	CP	21 U 578688 5639573	13.60	0.83	0.14	0.87	0.07	442	0.80			105	8	12	17	0.14	
Lnl2109-B	80	N/A	Point Dos Cheval	CP	21 U 579565 5640029	28.26	1.30	0.61	3.66	0.21	446	0.87			282	16	17	47	0.14	Yes
E12209	-	N/A	Frauderesse Point	CP	21 U 580579 5639969	N/A	N/A	N/A	N/A	N/A	N/A	0.80	N/A	3-	N/A	N/A	N/A	N/A	N/A	
Lnl2051-A	81	4	West Coast	RI	21 U 586519 5639223	15.06	0.82	0.35	0.75	0.18	443	0.81			92	22	4	43	0.32	Yes
Lnl2051-B	82	4	West Coast	RI	21 U 586519 5639223	43.28	0.69	0.26	0.82	0.18	448	0.90			120	26	5	38	0.24	
Lnl2051-C	83	4	West Coast	RI	21 U 586519 5639223	27.70	0.96	0.59	1.13	0.28	446	0.87			118	29	4	61	0.34	Yes
Lnl2051-D	84	4	West Coast	RI	21 U 586519 5639223	18.99	0.65	0.25	0.45	0.22	447	0.89			70	34	2	39	0.36	
Lnl2051-E	85	4	West Coast	RI	21 U 586519 5639223	9.59	0.83	0.33	0.61	0.18	449	0.92			74	22	3	40	0.35	
Lnl2051-F	86	4	West Coast	RI	21 U 586519 5639223	14.12	0.90	0.52	0.80	0.35	447	0.89			89	39	2	58	0.39	Yes
Lnl2051-G	87	4	West Coast	RI	21 U 586519 5639223	34.47	1.56	0.23	2.29	0.15	444	0.75	0.83	2+ to 3-	147	10	15	15	0.09	
Lnl2051-G3	-	4	West Coast	RI	21 U 586519 5639223	N/A	N/A	N/A	N/A	N/A	N/A	0.73	N/A	2+ to 3-	N/A	N/A	N/A	N/A	N/A	
E10077-2	88	4	West Coast	RI	21 U 586505 5639254	26.15	0.77	0.24	0.69	0.15	452	0.98			90	19	5	31	0.26	
E10077-3	89	4	West Coast	RI	22 U 586505 5639254	11.37	0.60	0.25	0.32	0.2	457	1.07			53	33	2	42	0.44	

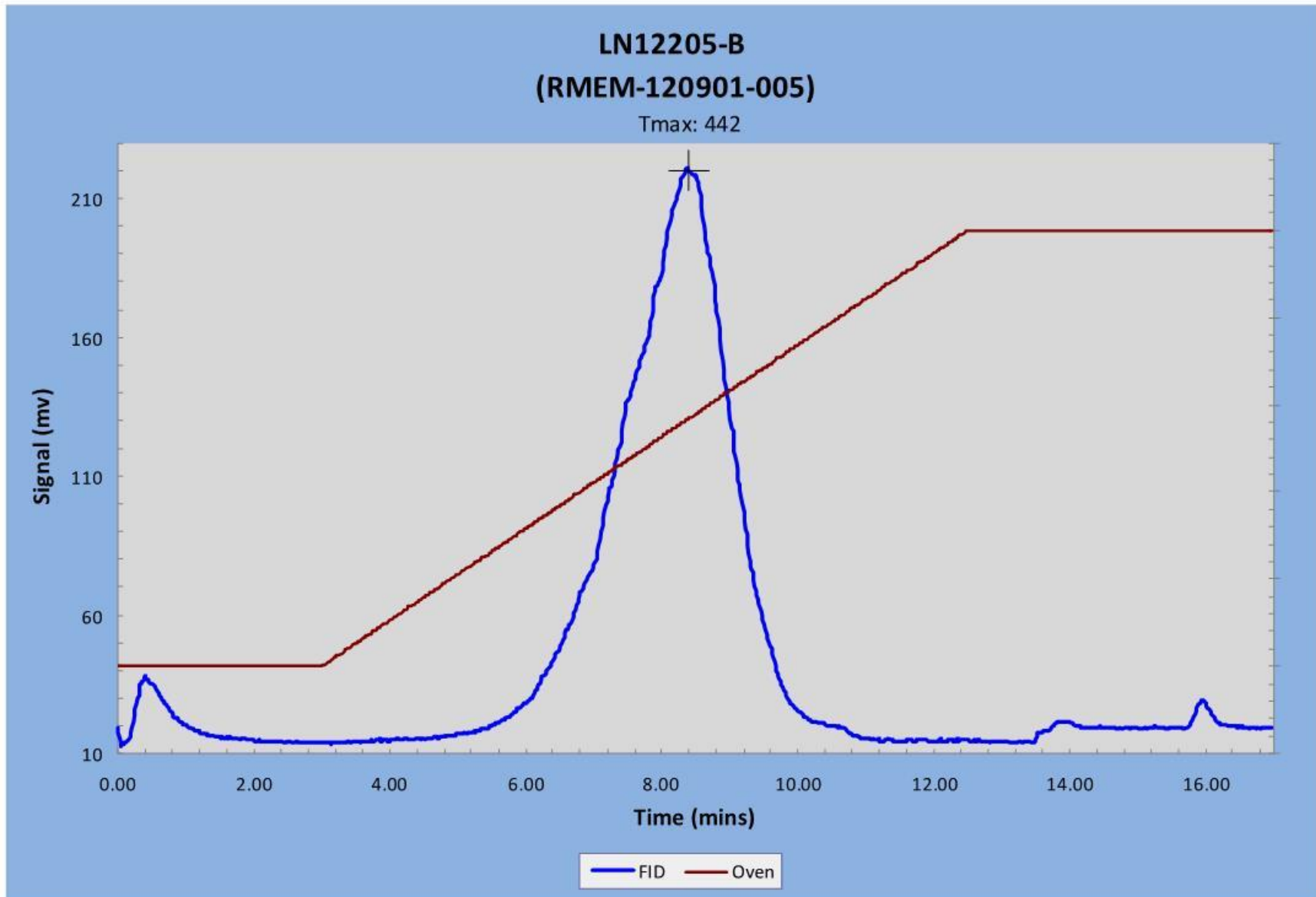
**APPENDIX 2: ROCK-EVAL PYROLYSIS PYROGRAMS**

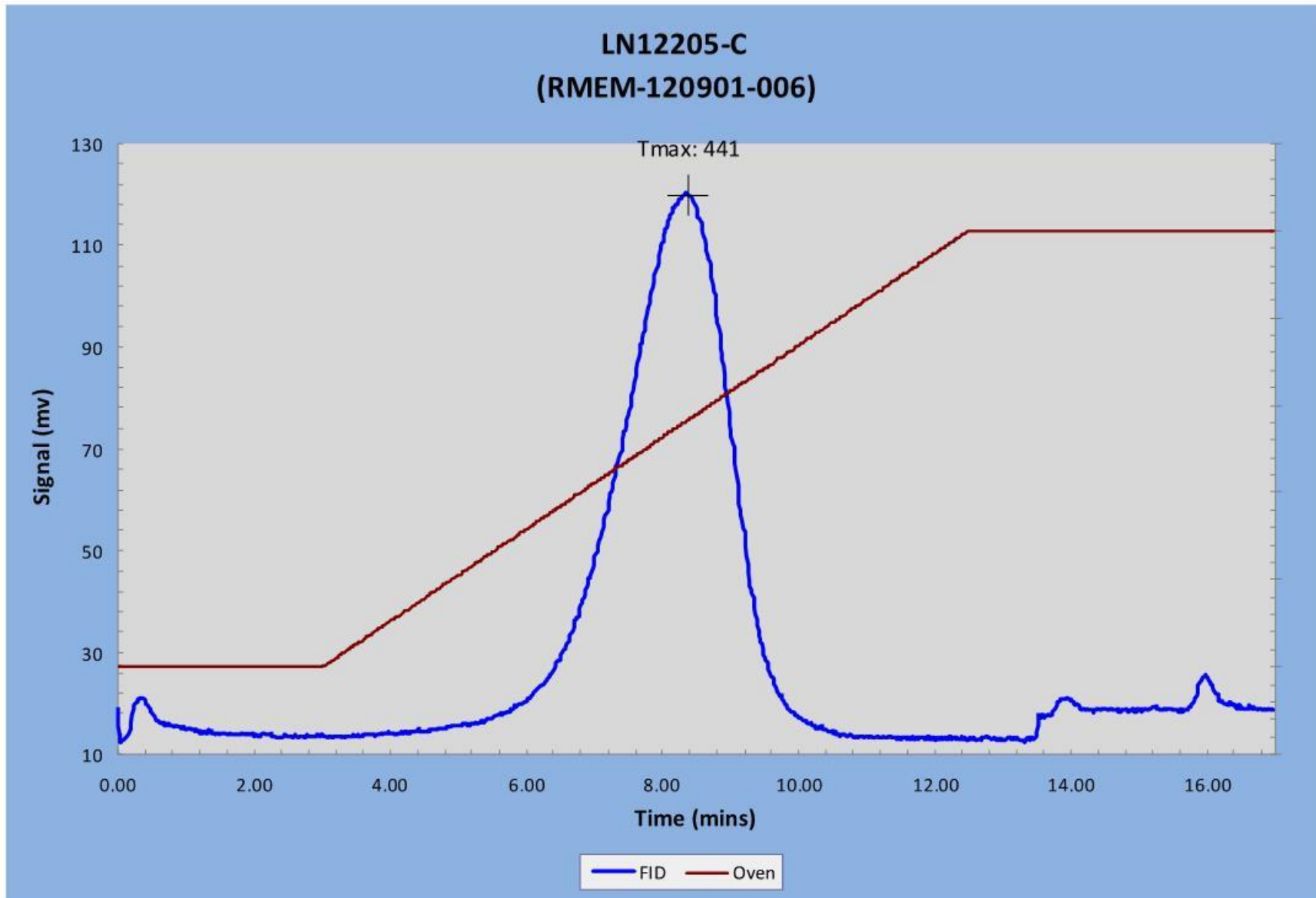


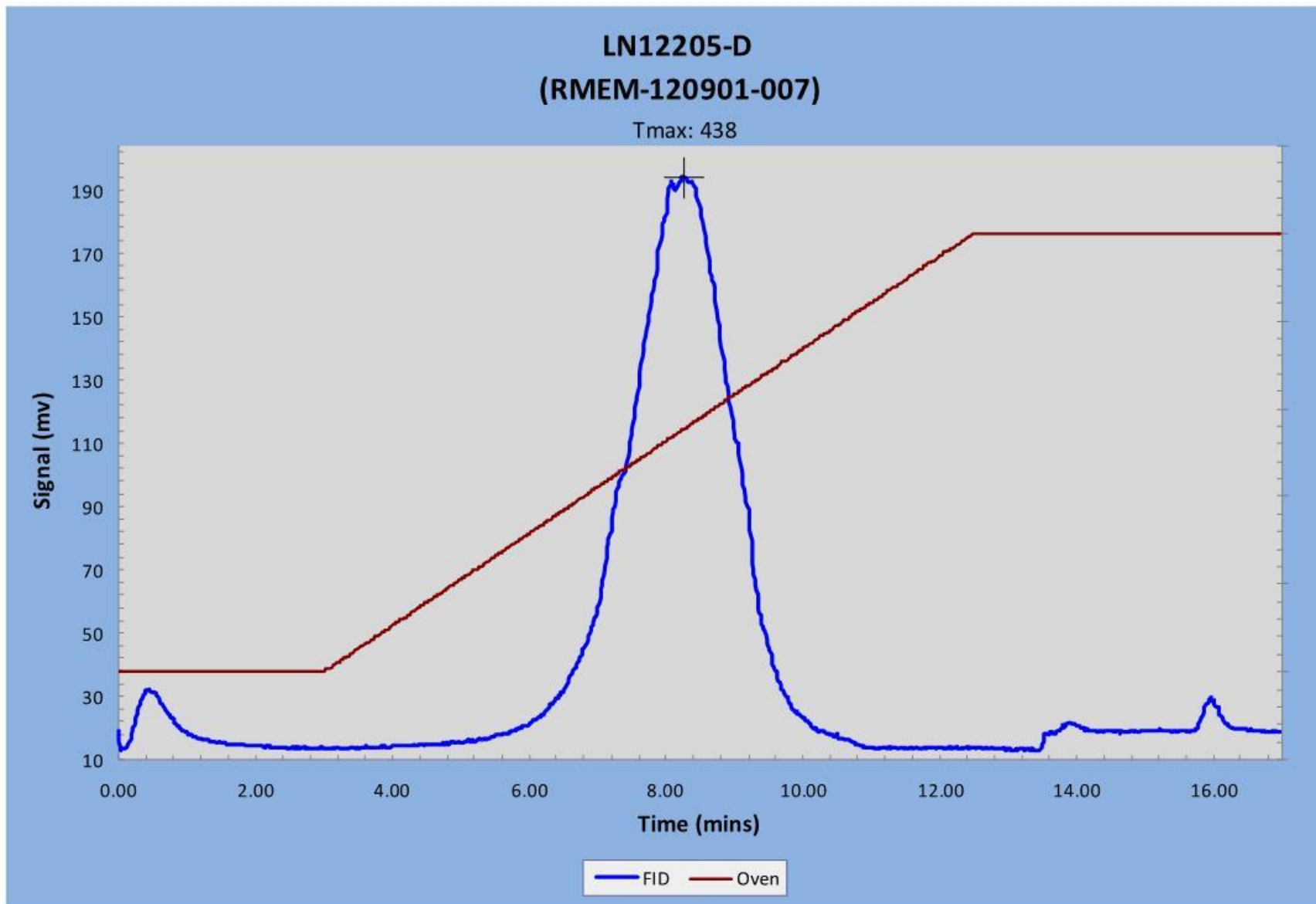


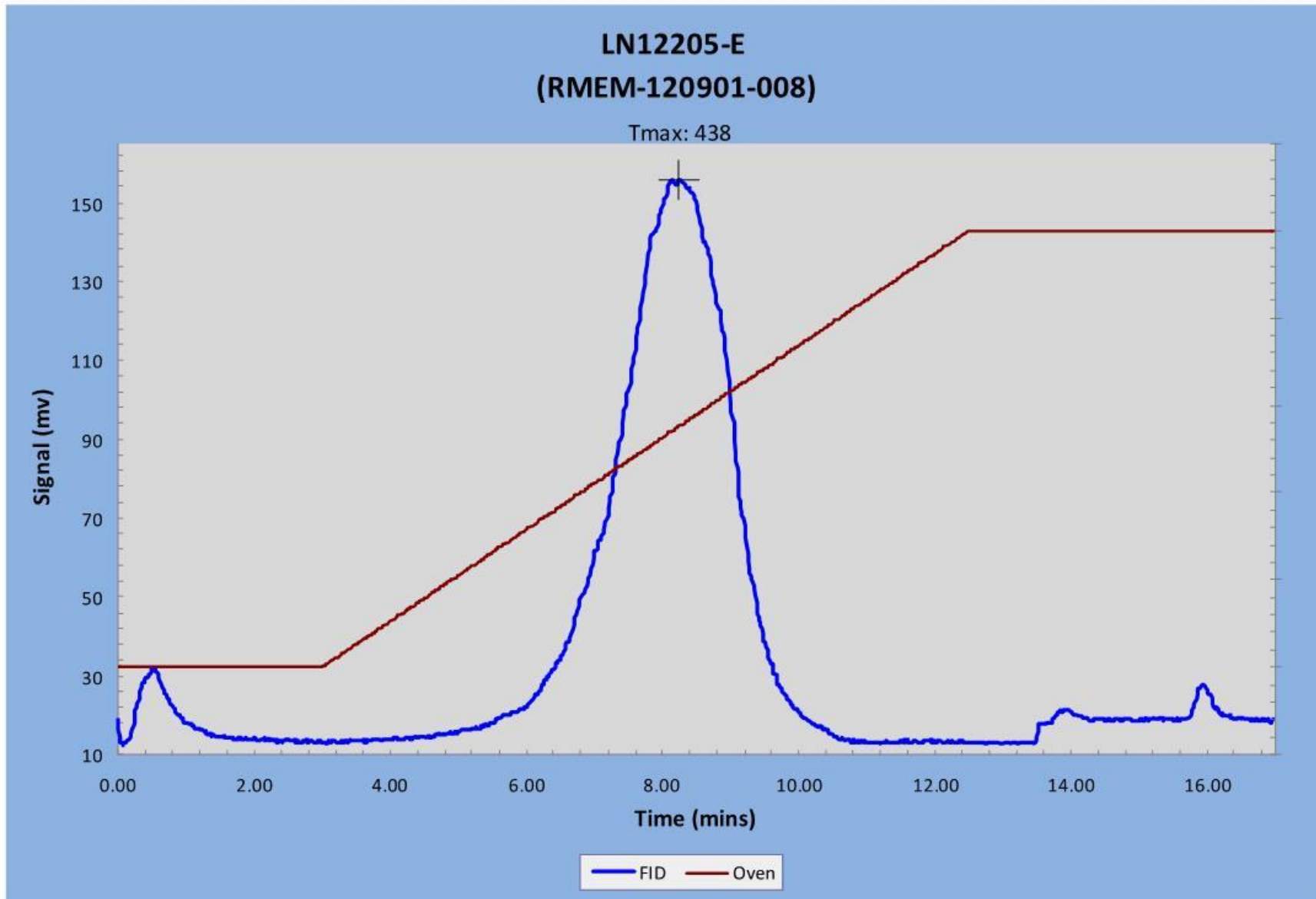




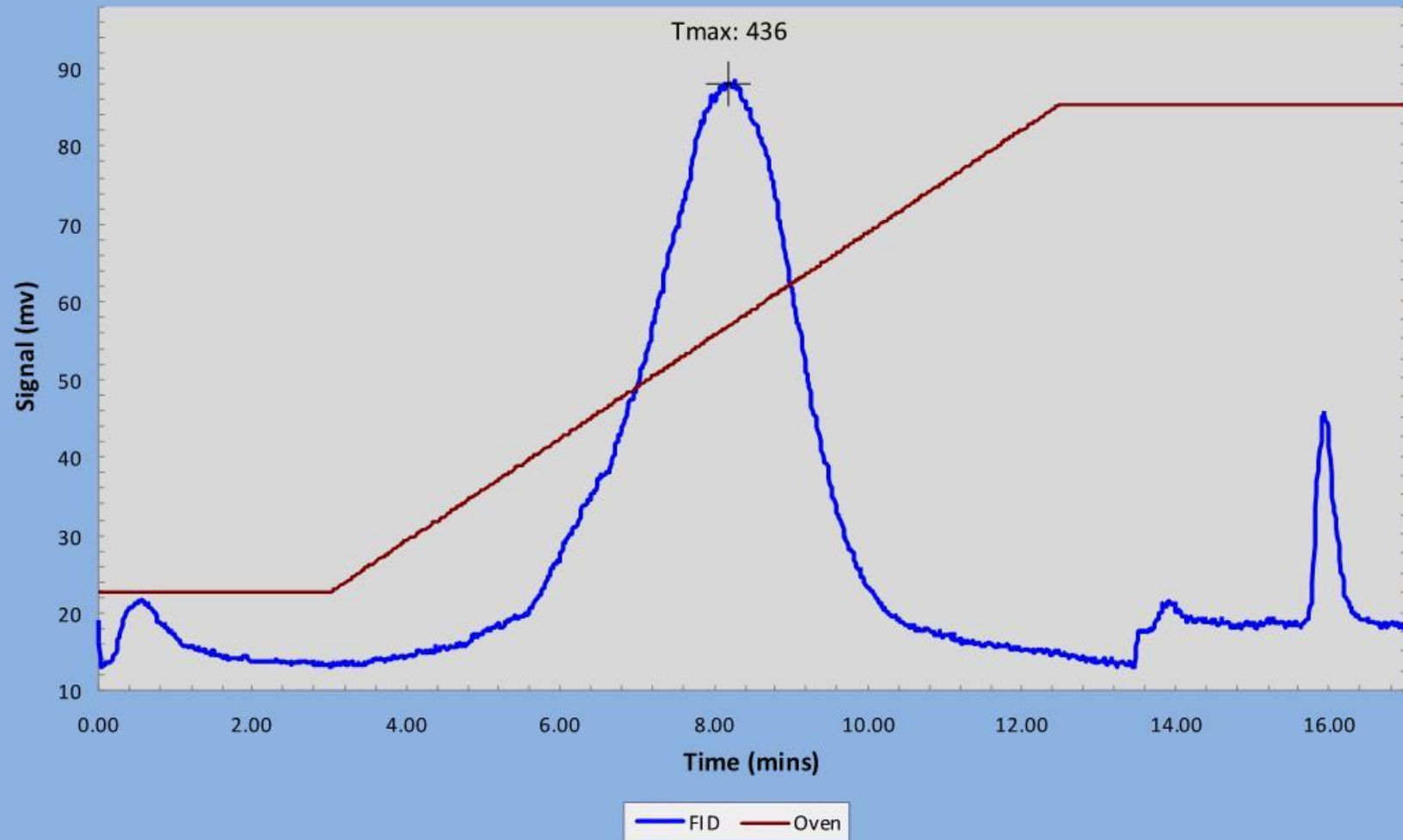


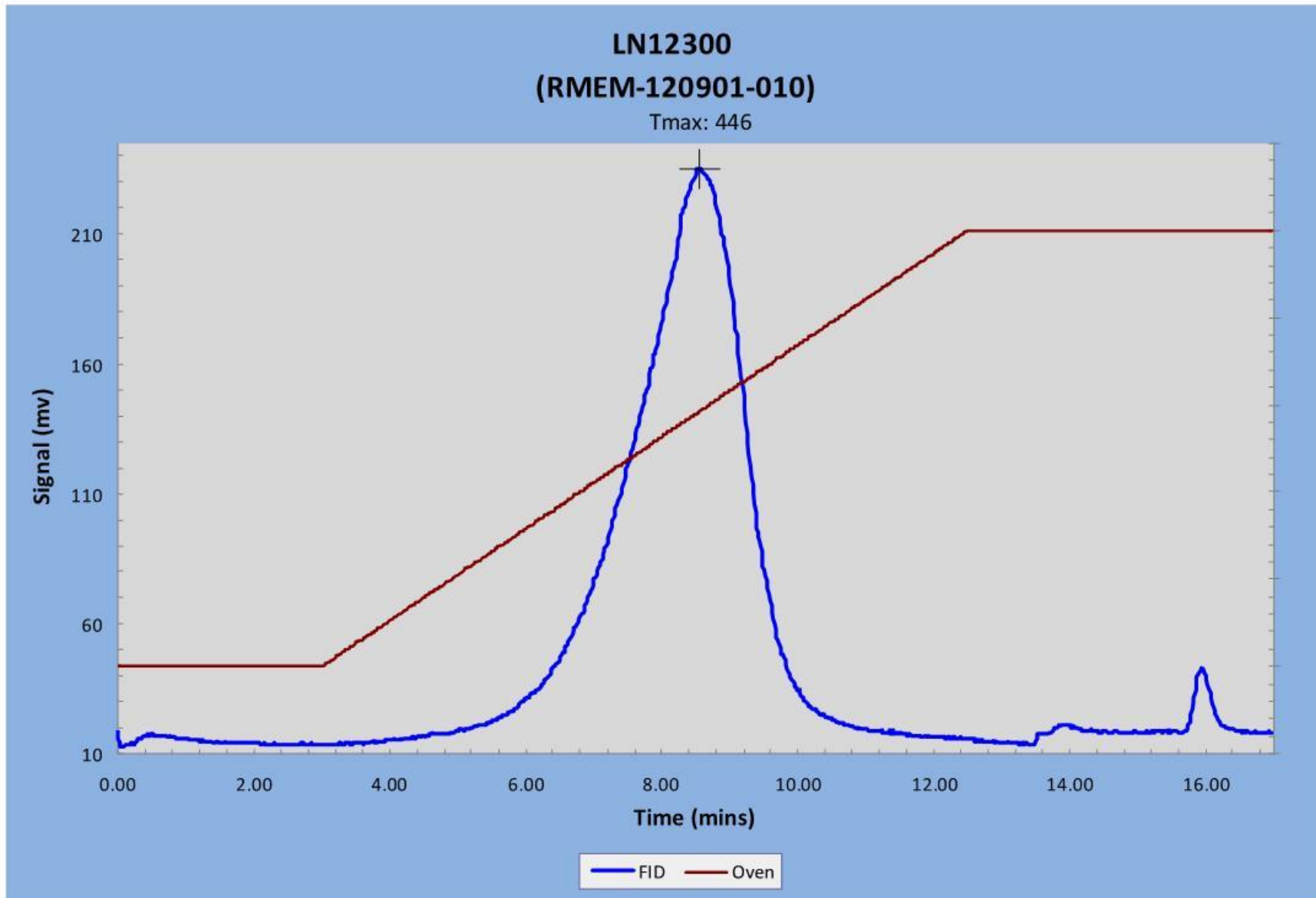




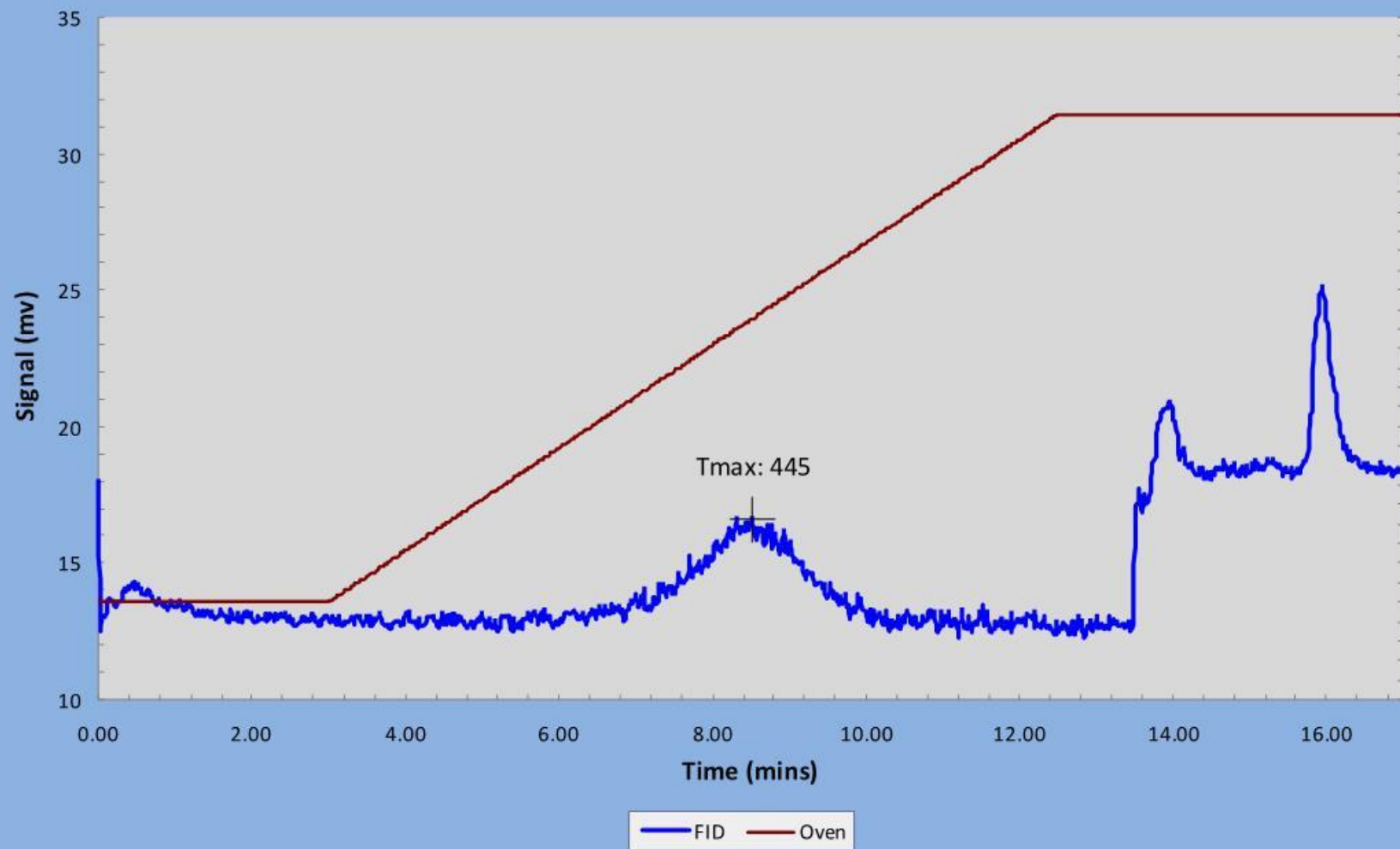


LN12205-F  
(RMEM-120901-009)

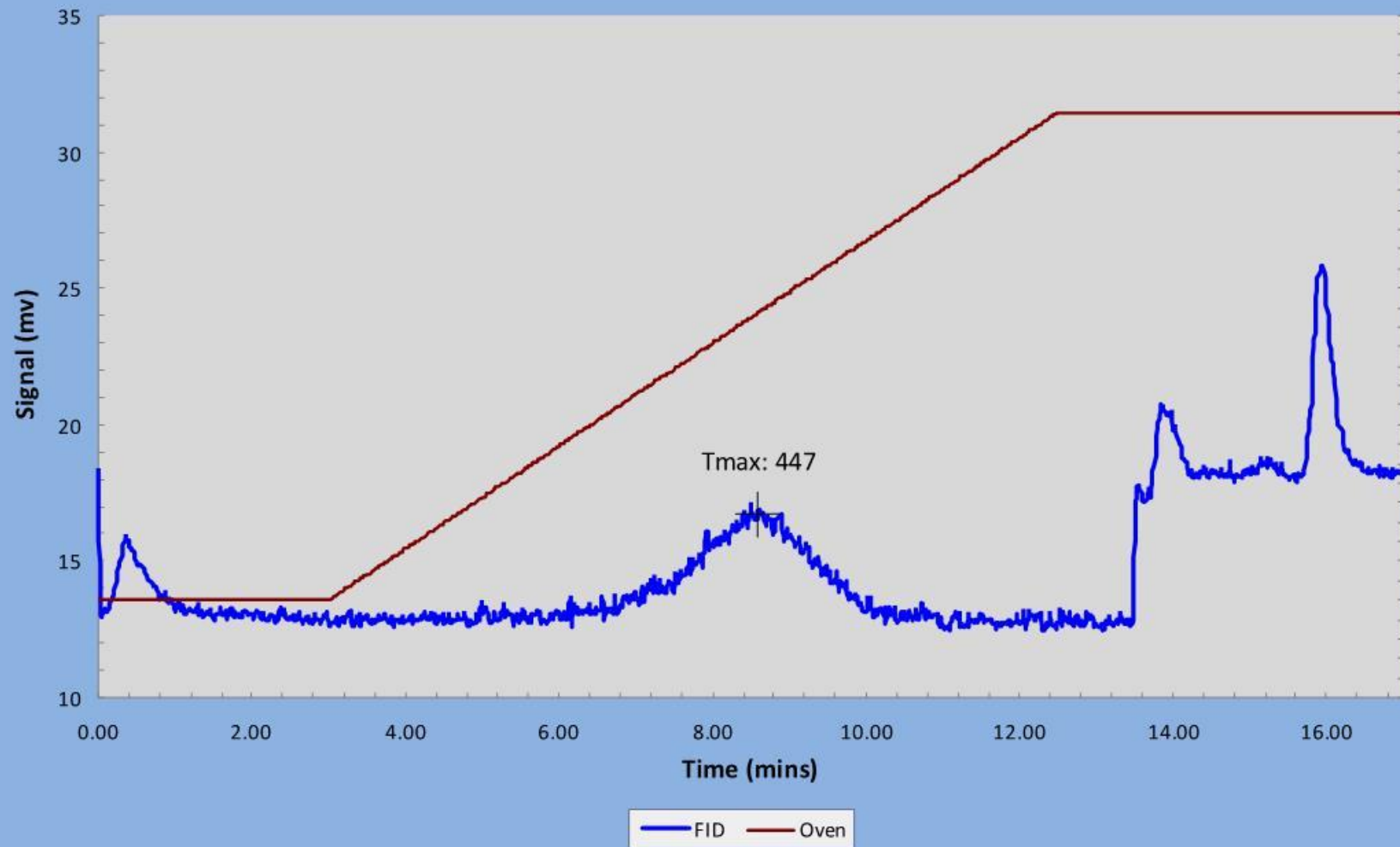




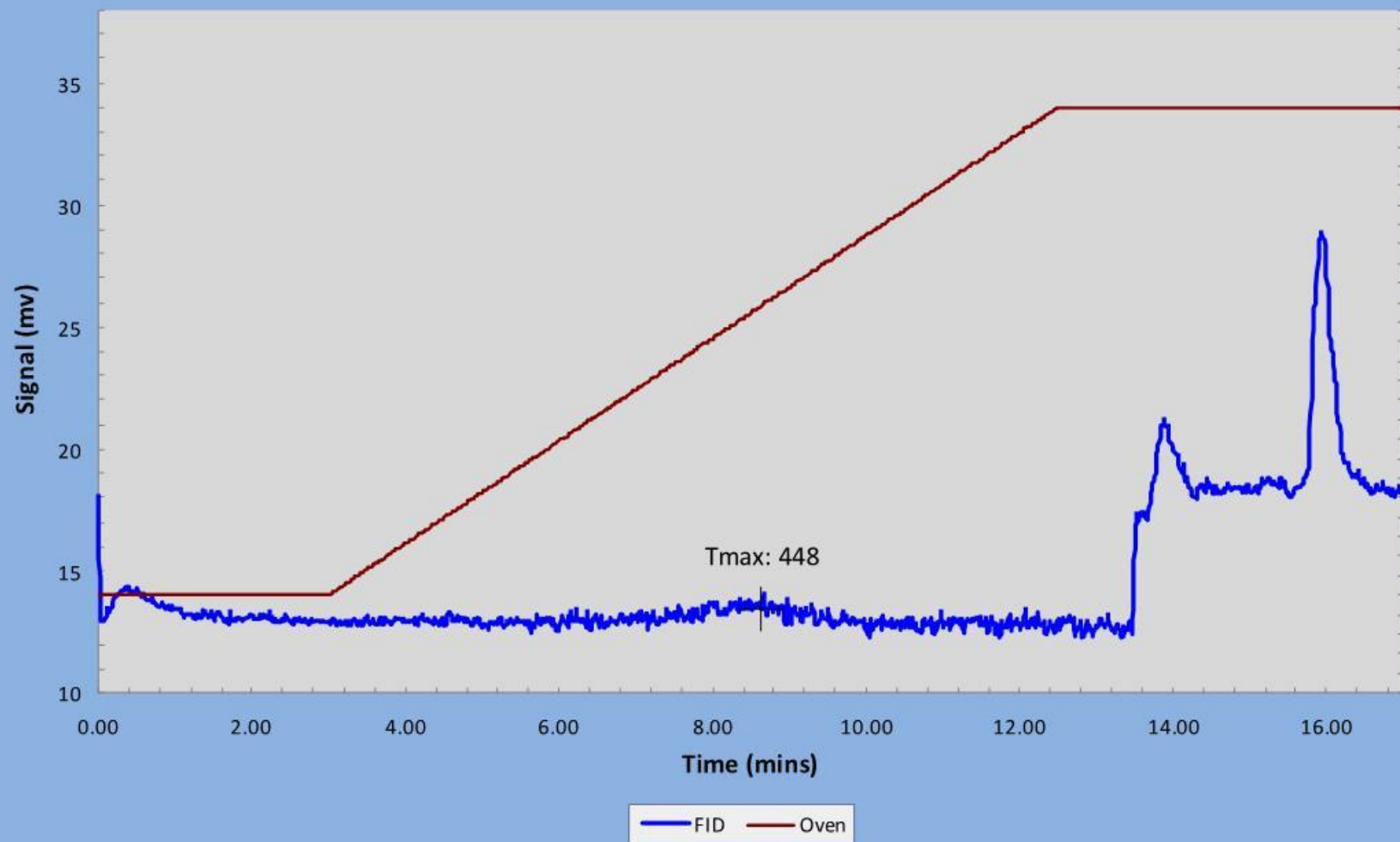
LN12014-A  
(RMEM-120901-011)



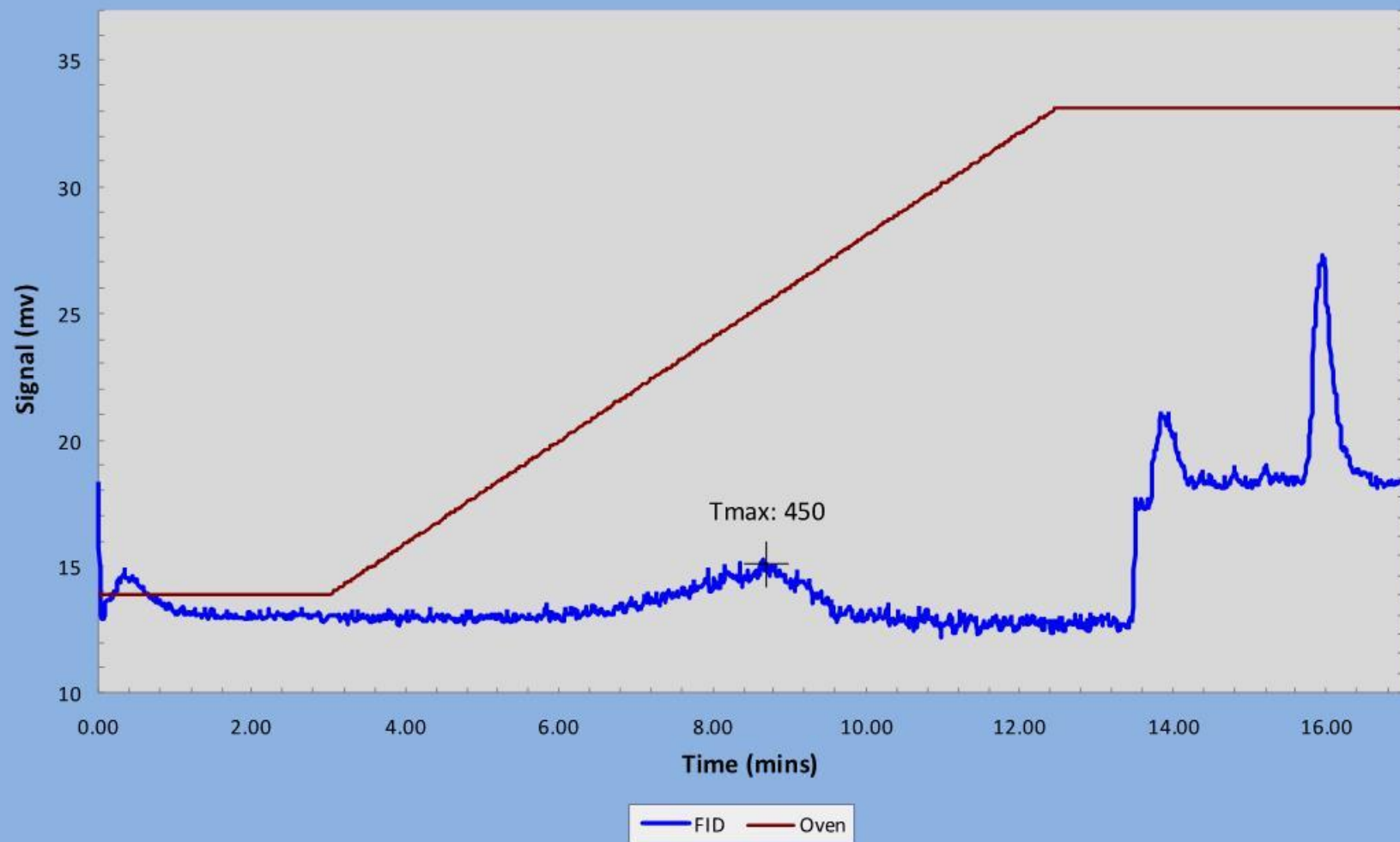
LN12014-B  
(RMEM-120901-012)



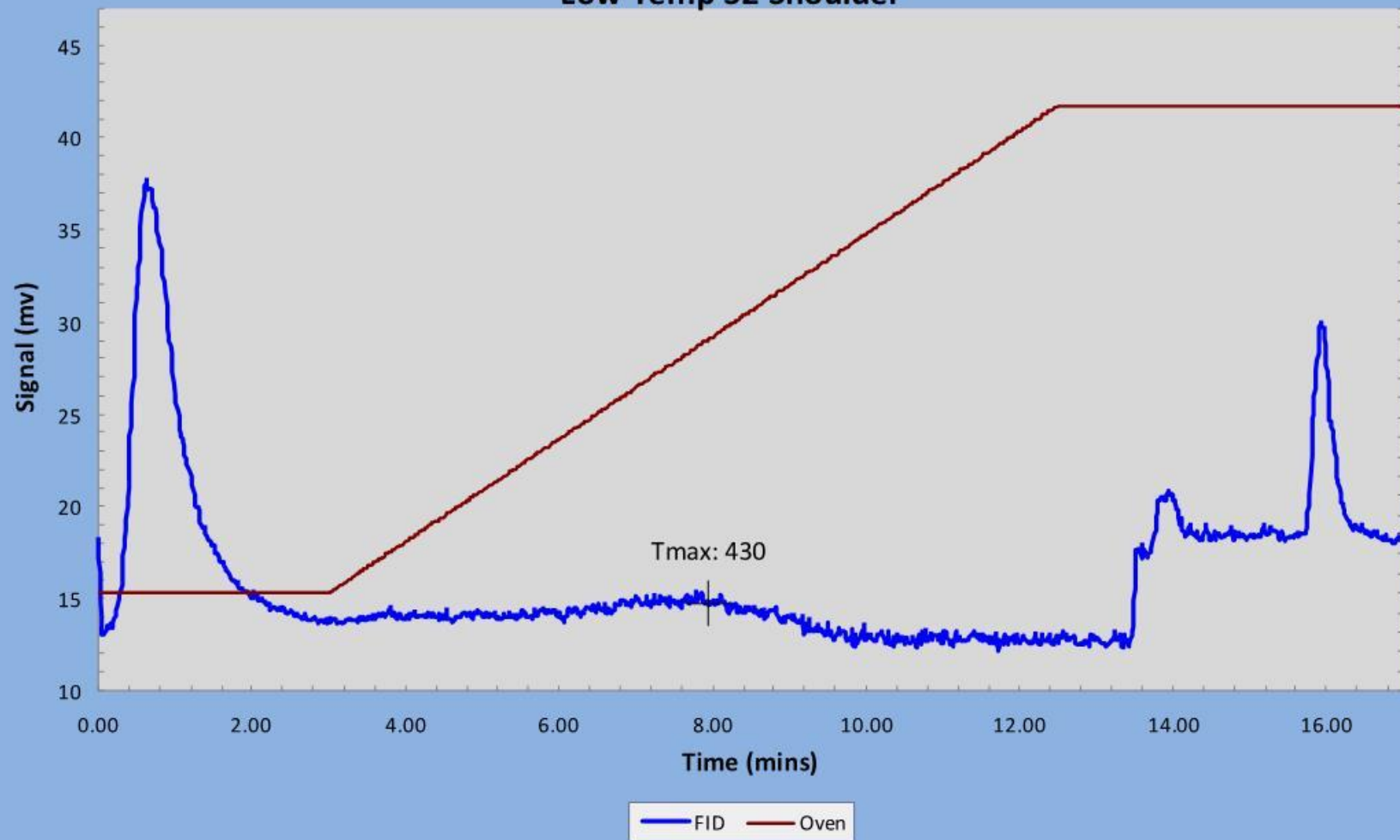
LN12014-C  
(RMEM-120901-013)



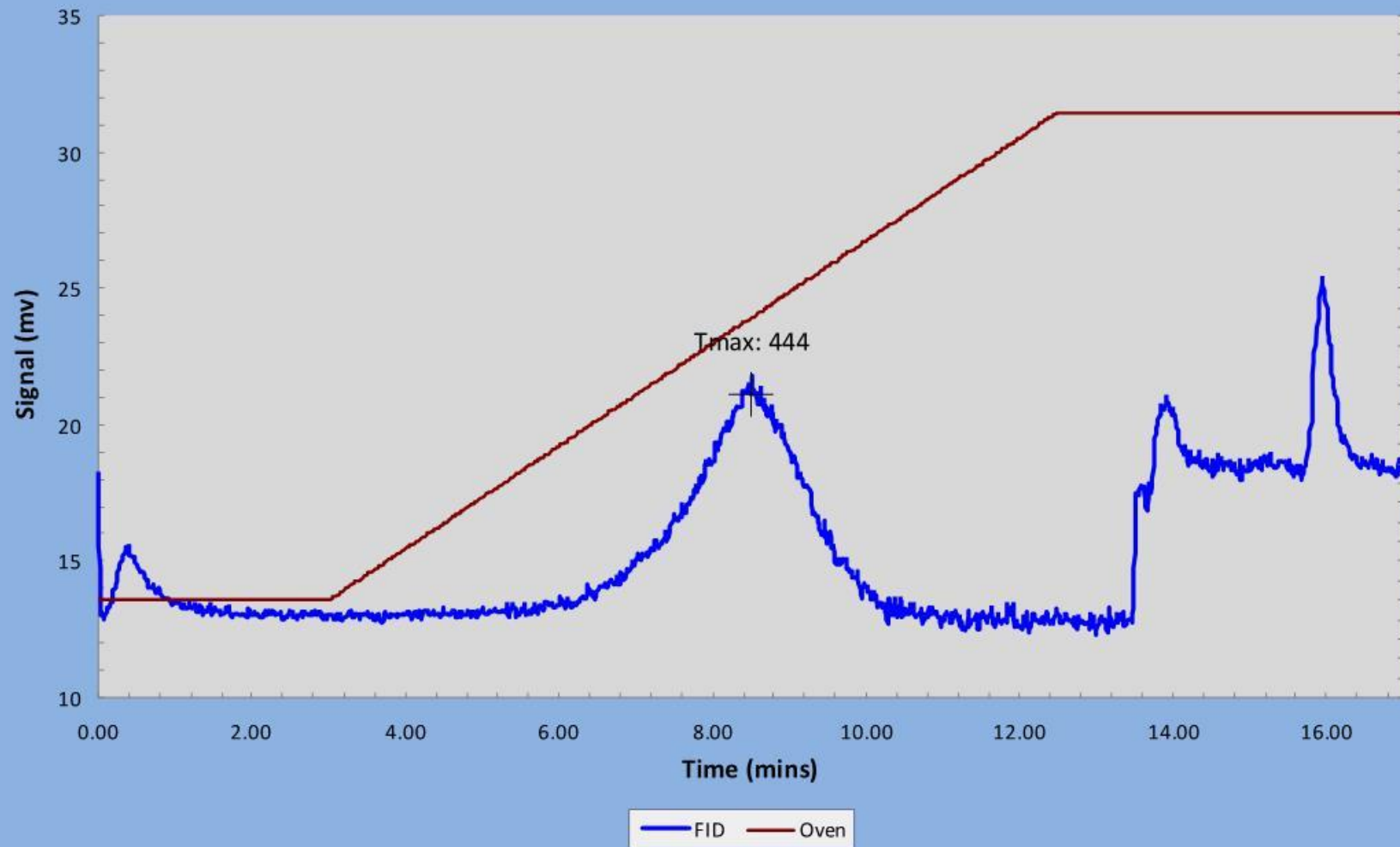
LN12014-D  
(RMEM-120901-014)



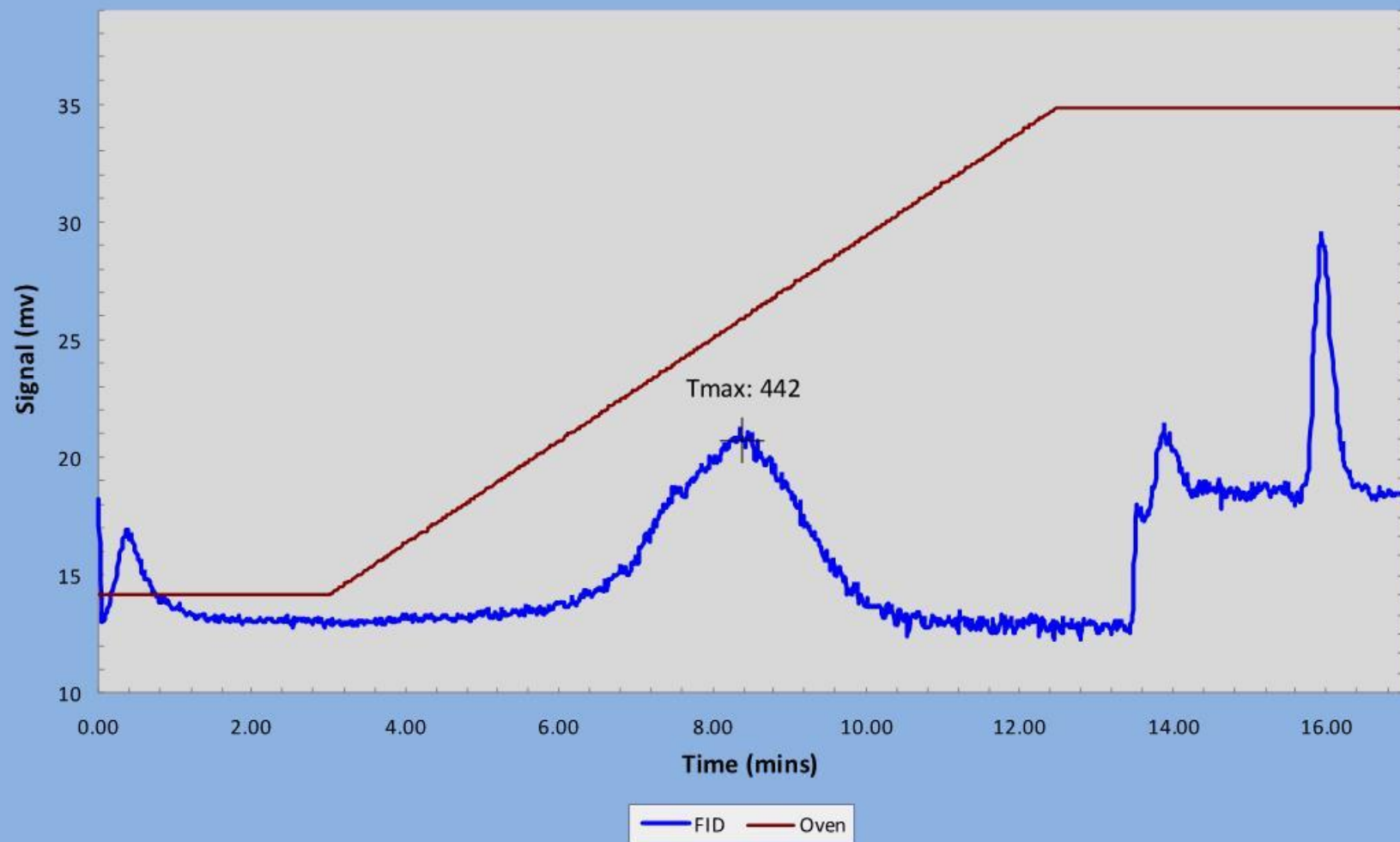
LN12014-E  
(RMEM-120901-015)  
Low Temp S2 Shoulder



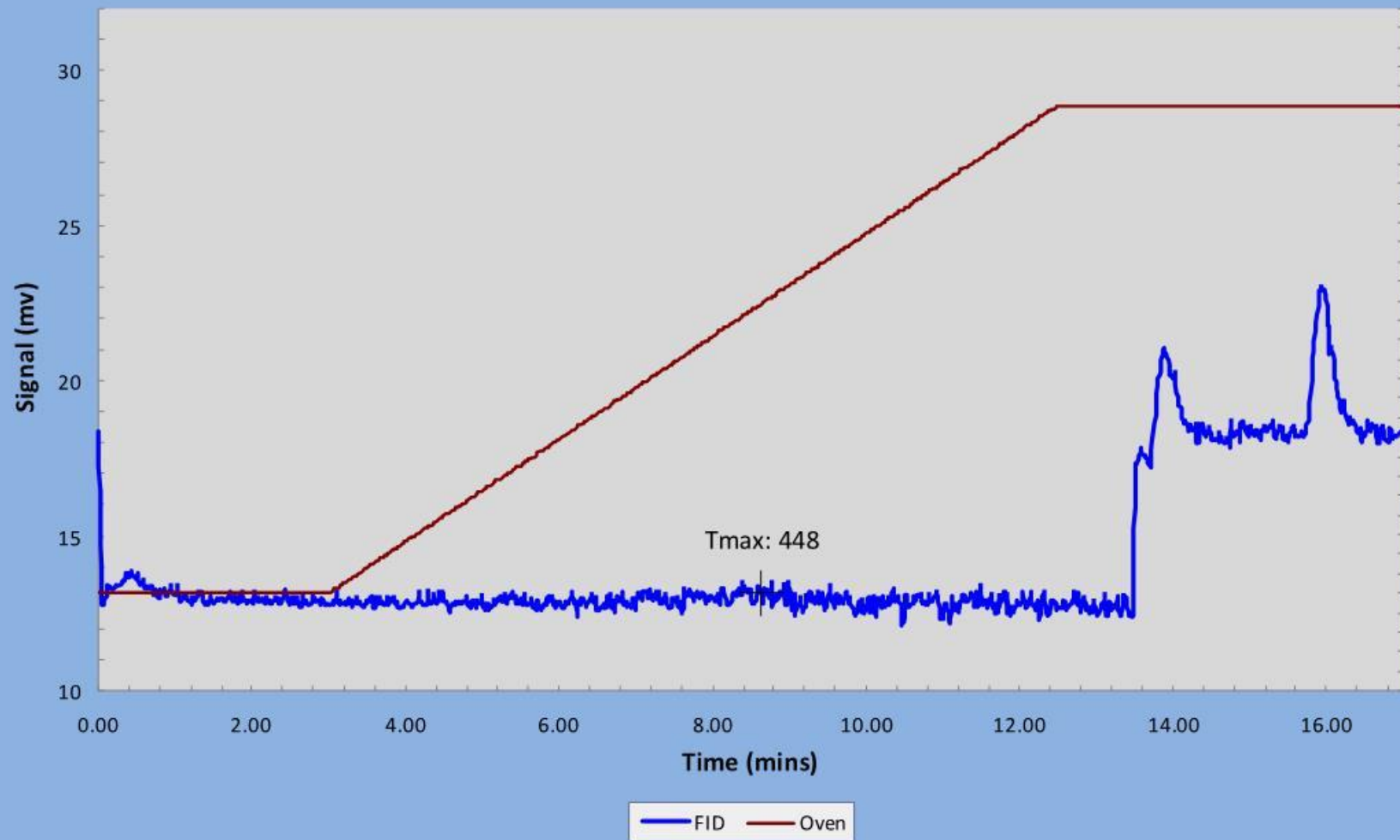
LN12014-F  
(RMEM-120901-016)



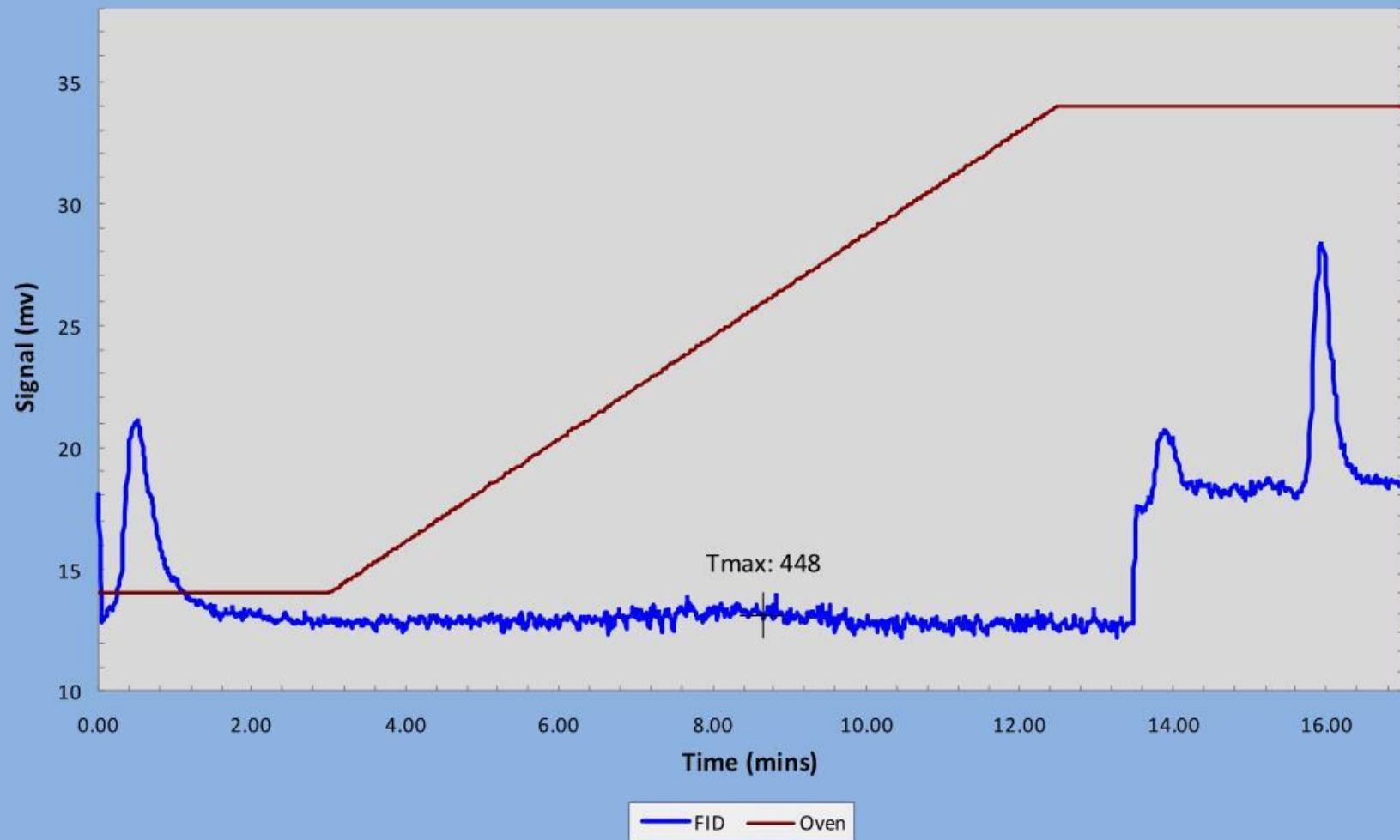
LN12014-G1  
(RMEM-120901-017)



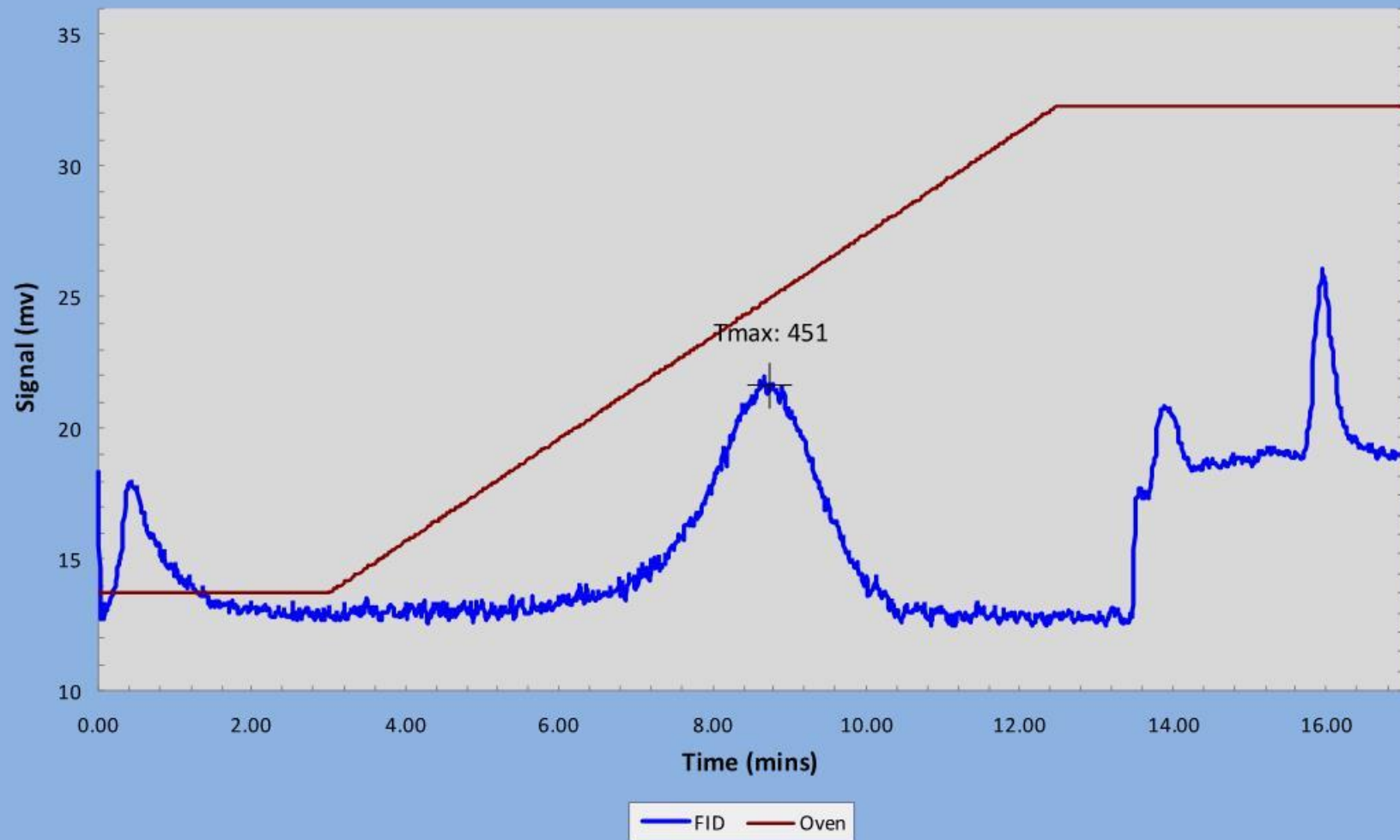
LN12014-H  
(RMEM-120901-018)



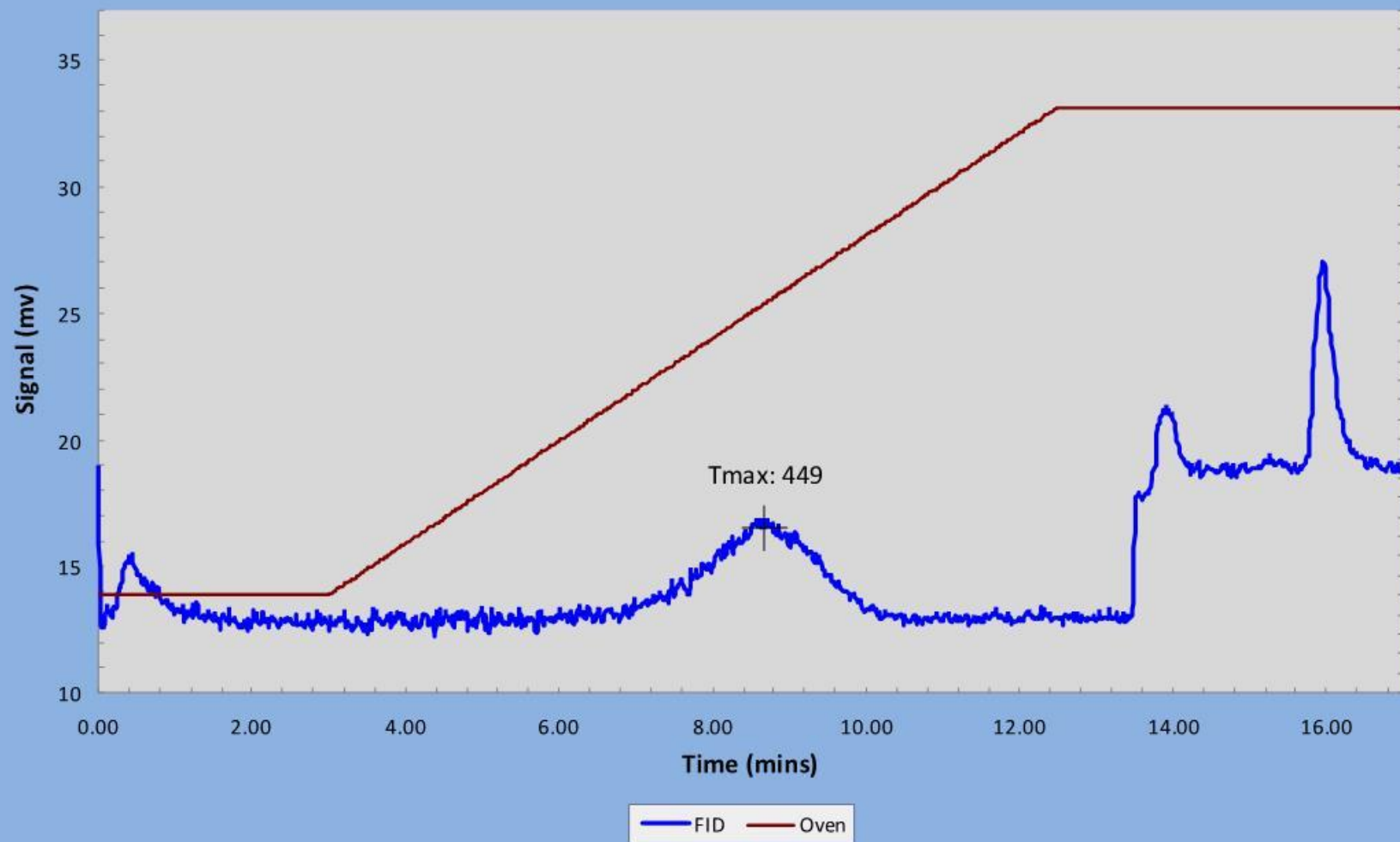
LN12014-I  
(RMEM-120901-019)



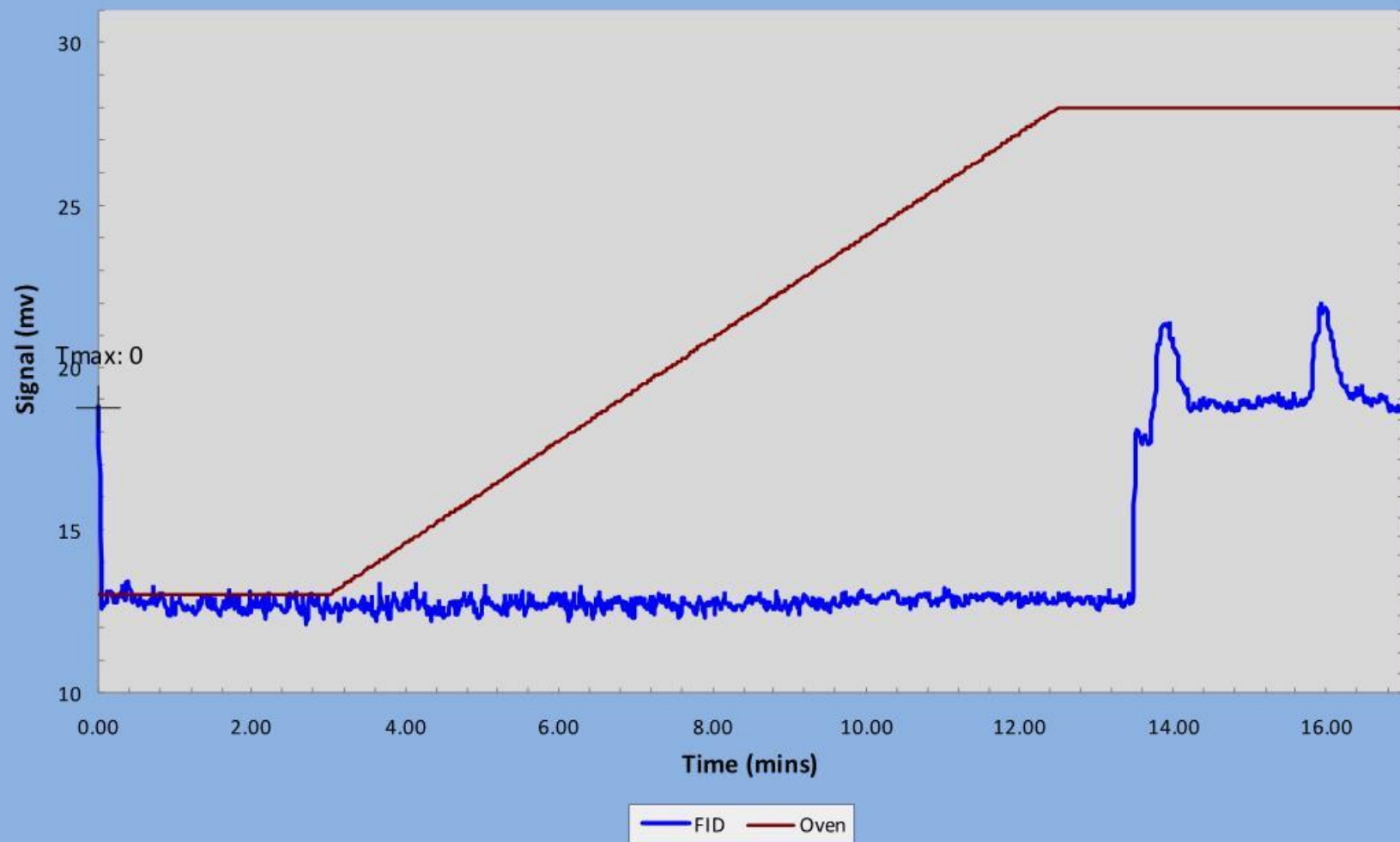
LN12014-J  
(RMEM-120901-020)



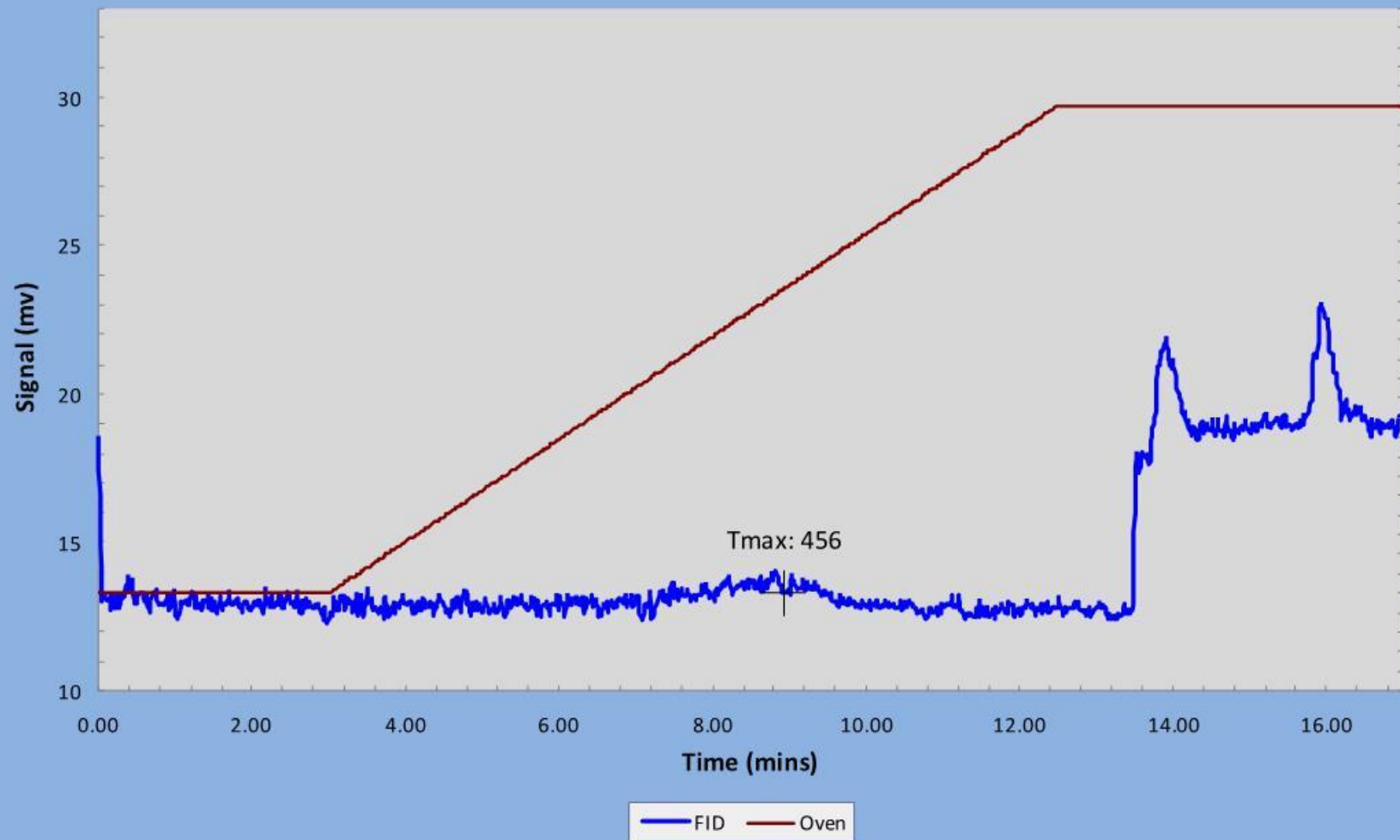
LN12014  
(RMEM-120901-021)



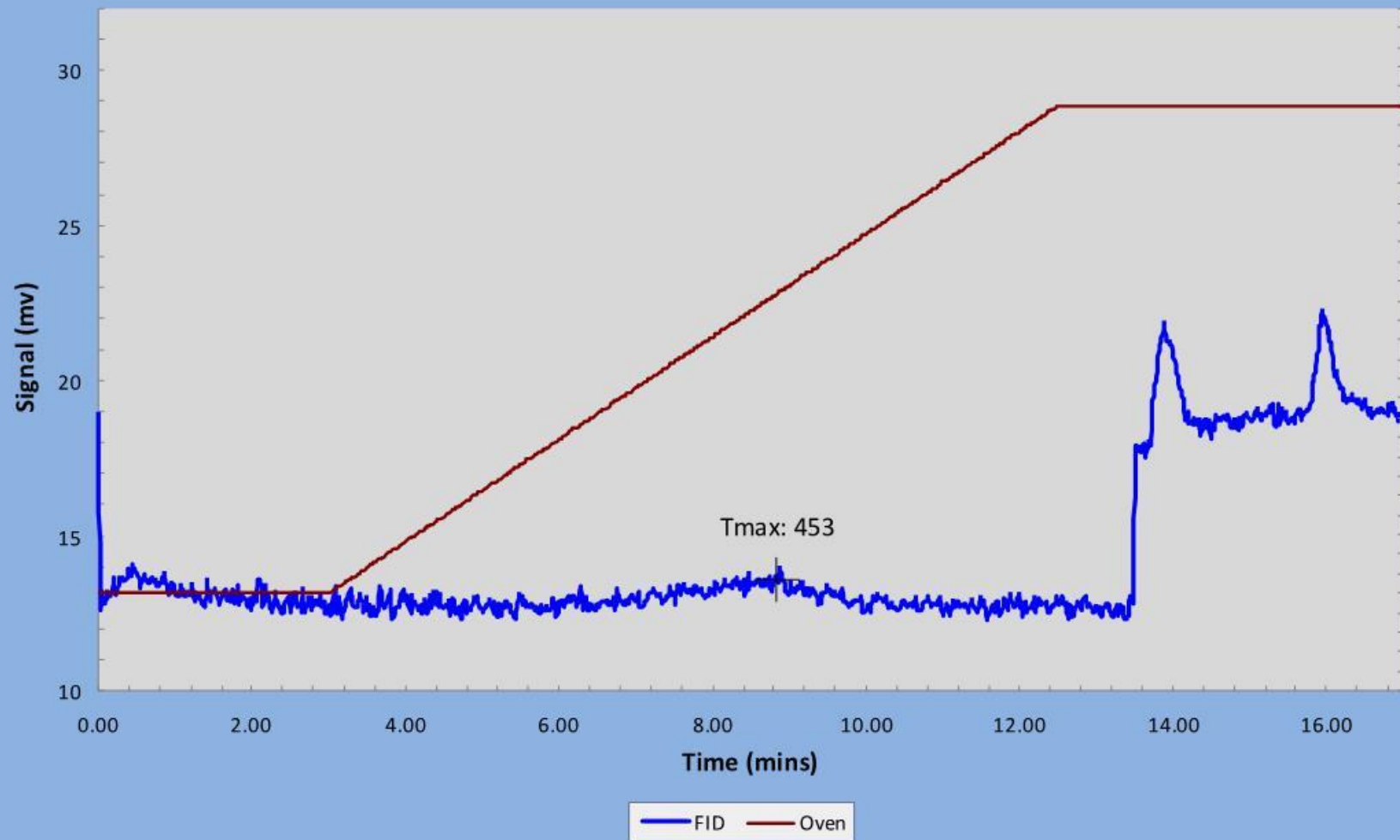
LN12077-A  
(RMEM-120901-022)



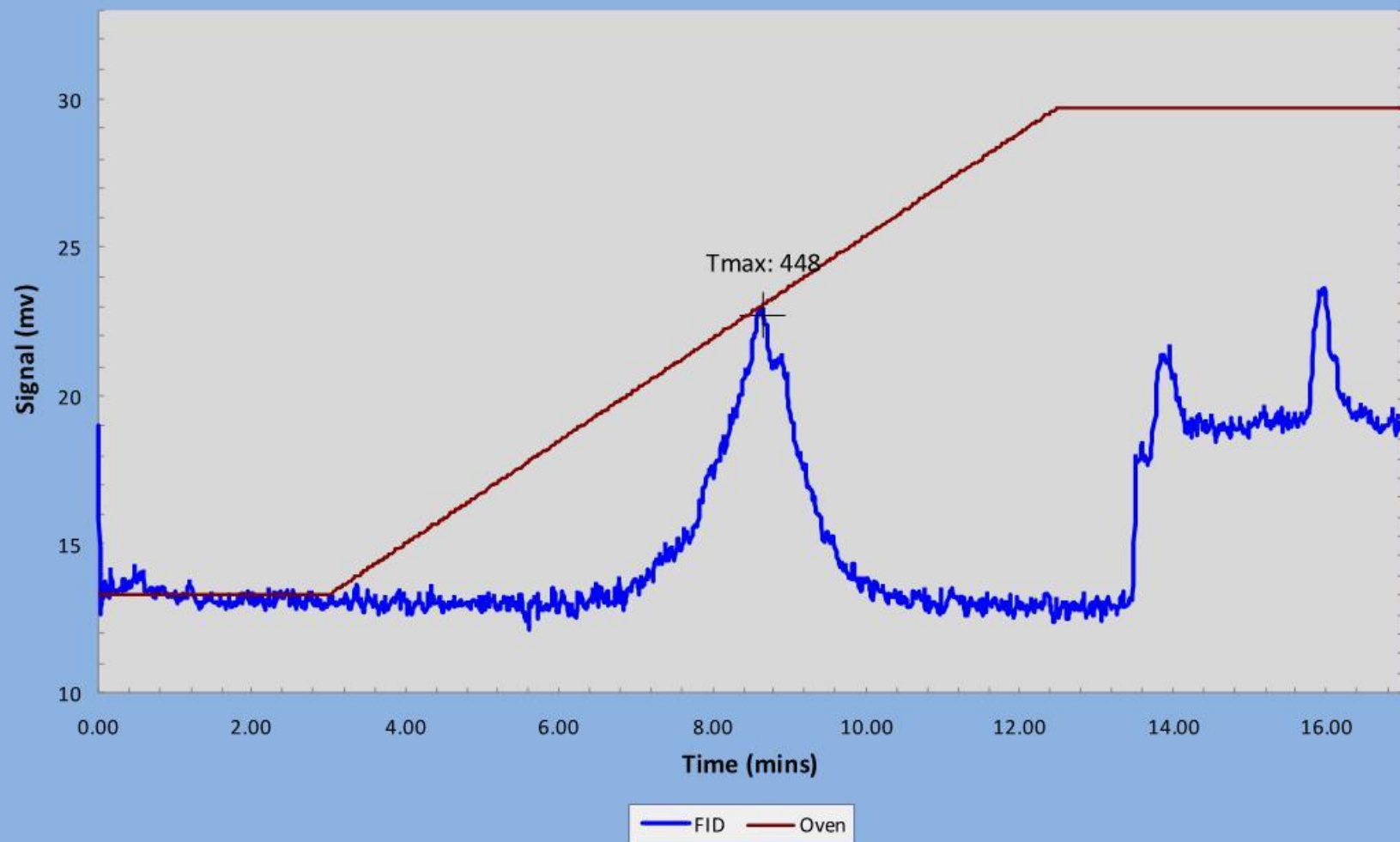
LN12077-B  
(RMEM-120901-023)



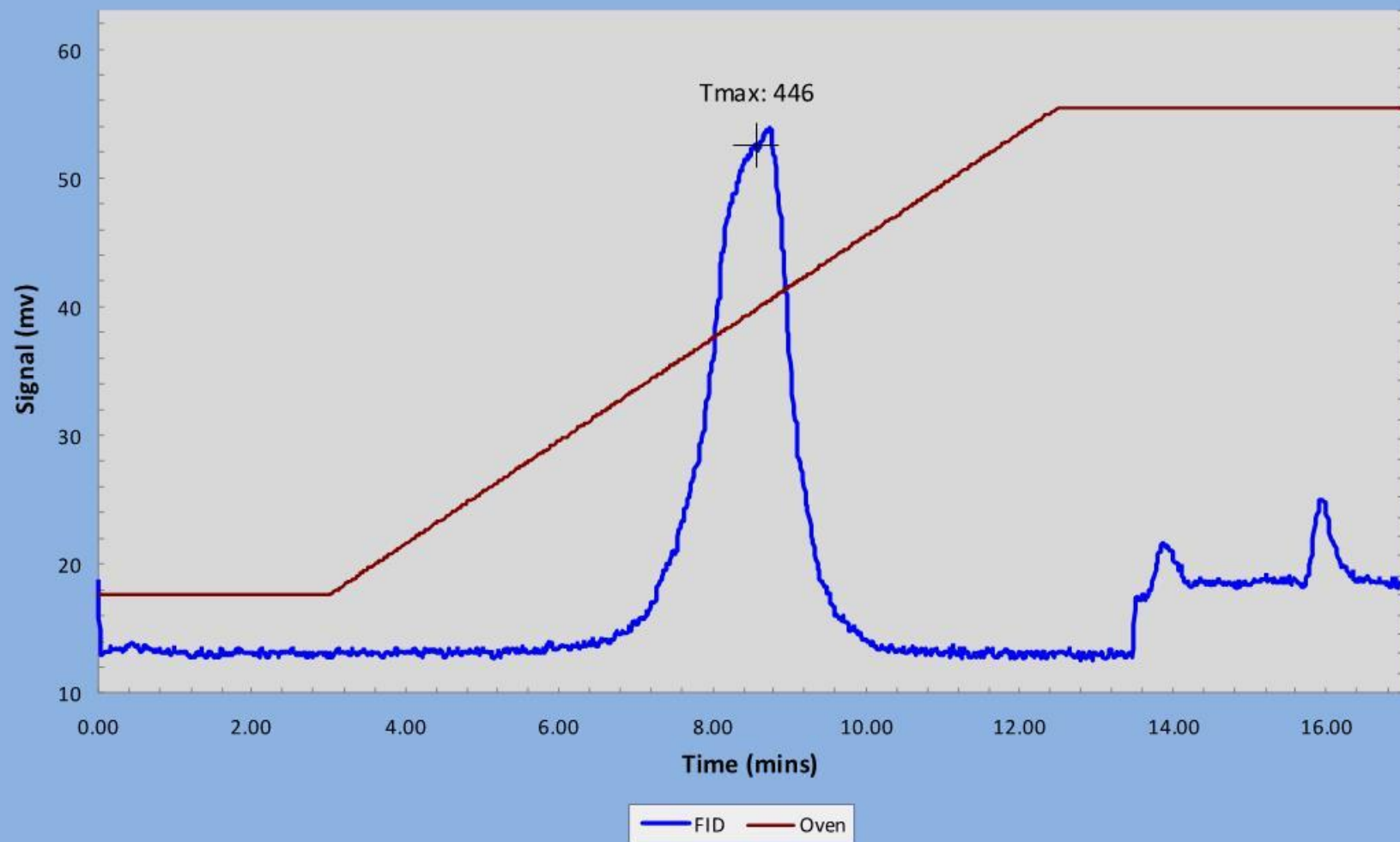
LN12077-C  
(RMEM-120901-024)



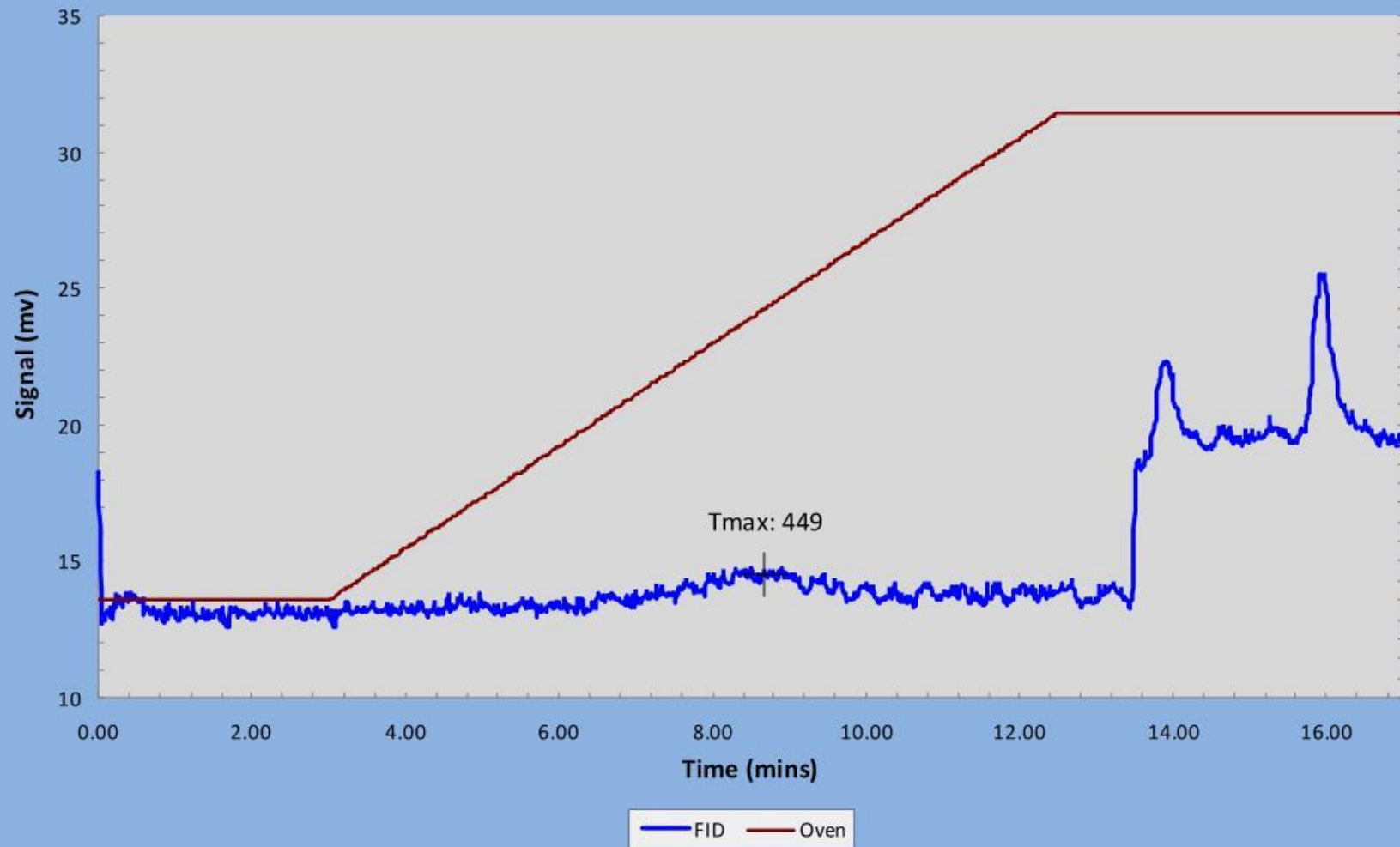
LN12077-D  
(RMEM-120901-025)



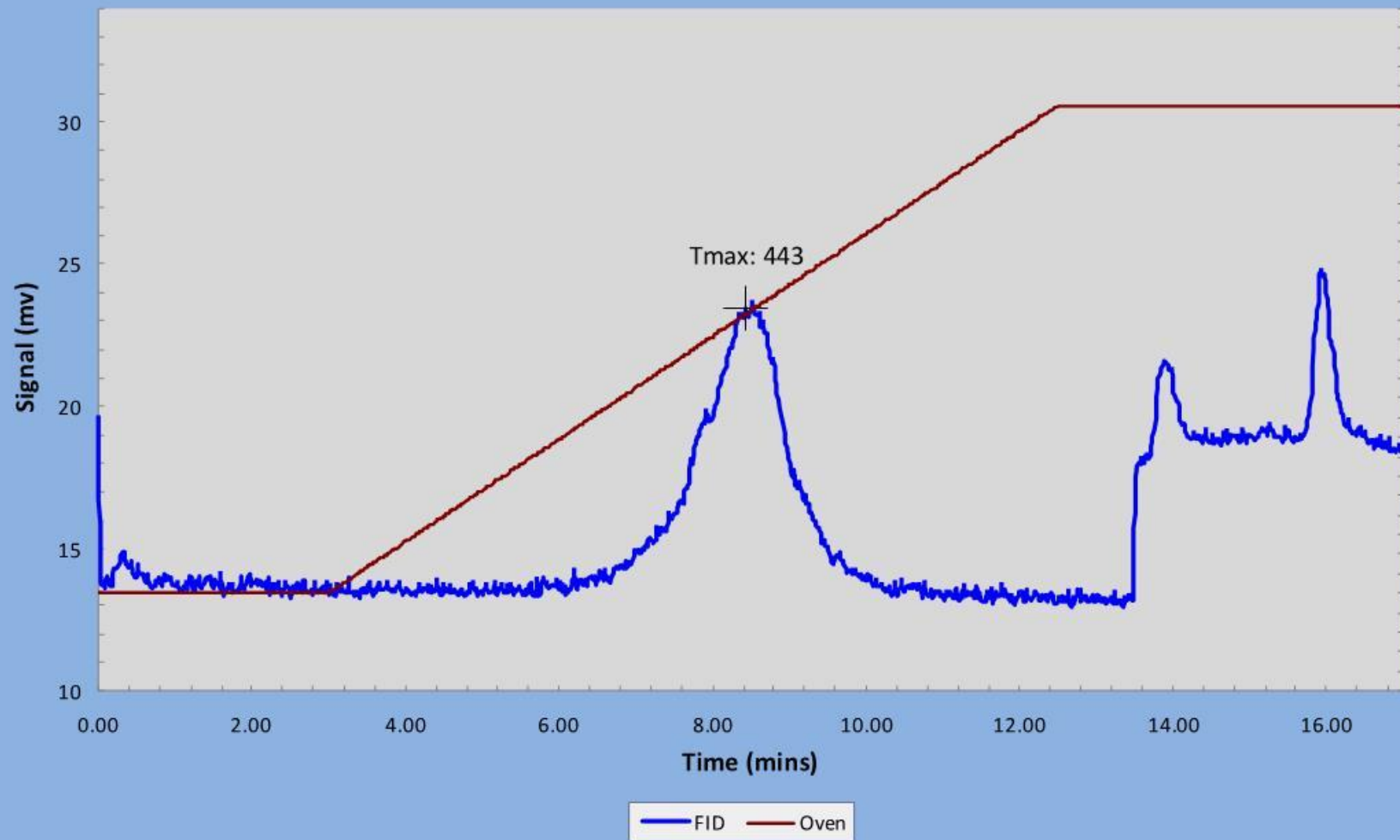
LN12077-E  
(RMEM-120901-026)



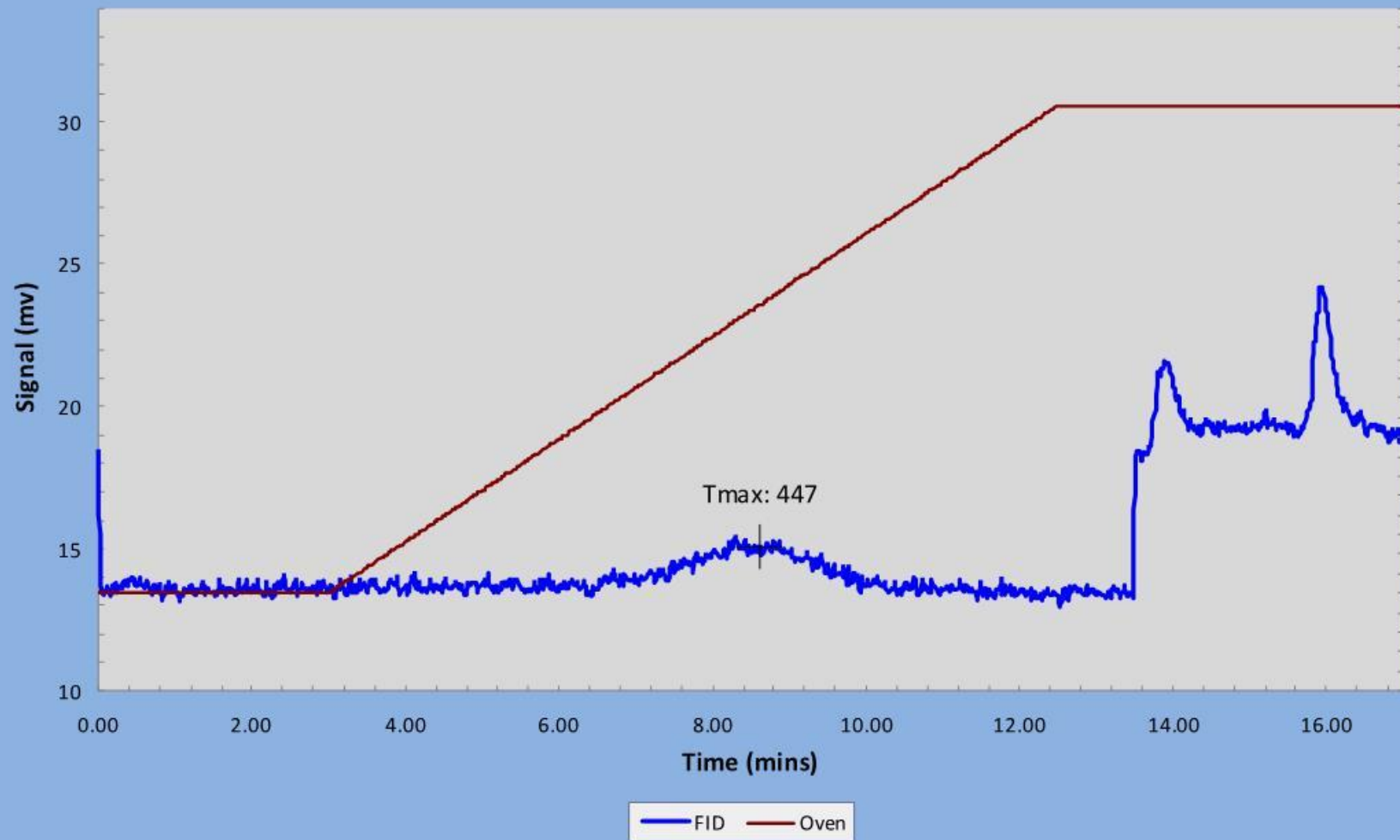
LN12077-F  
(RMEM-120901-027)



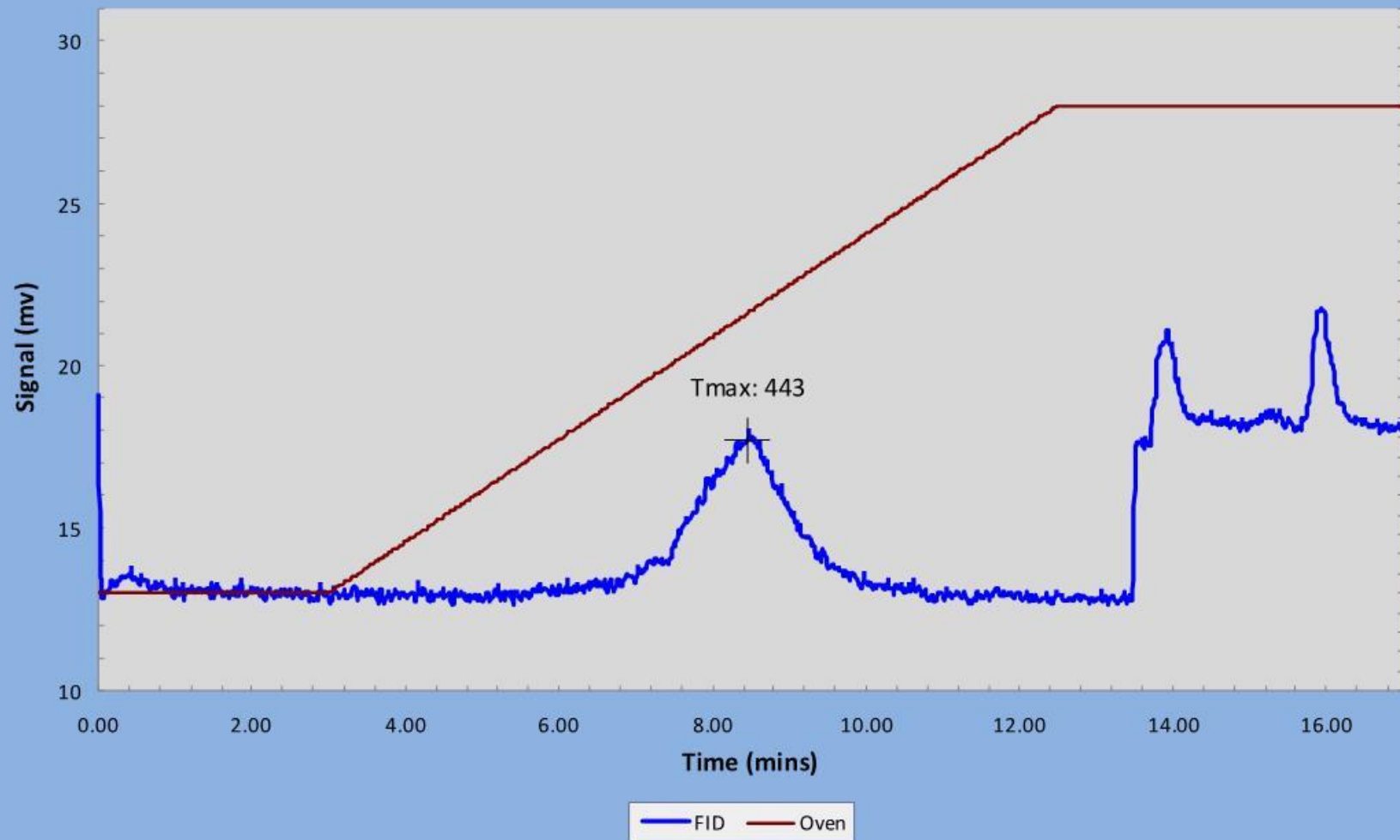
LN12077-G1  
(RMEM-120901-028)



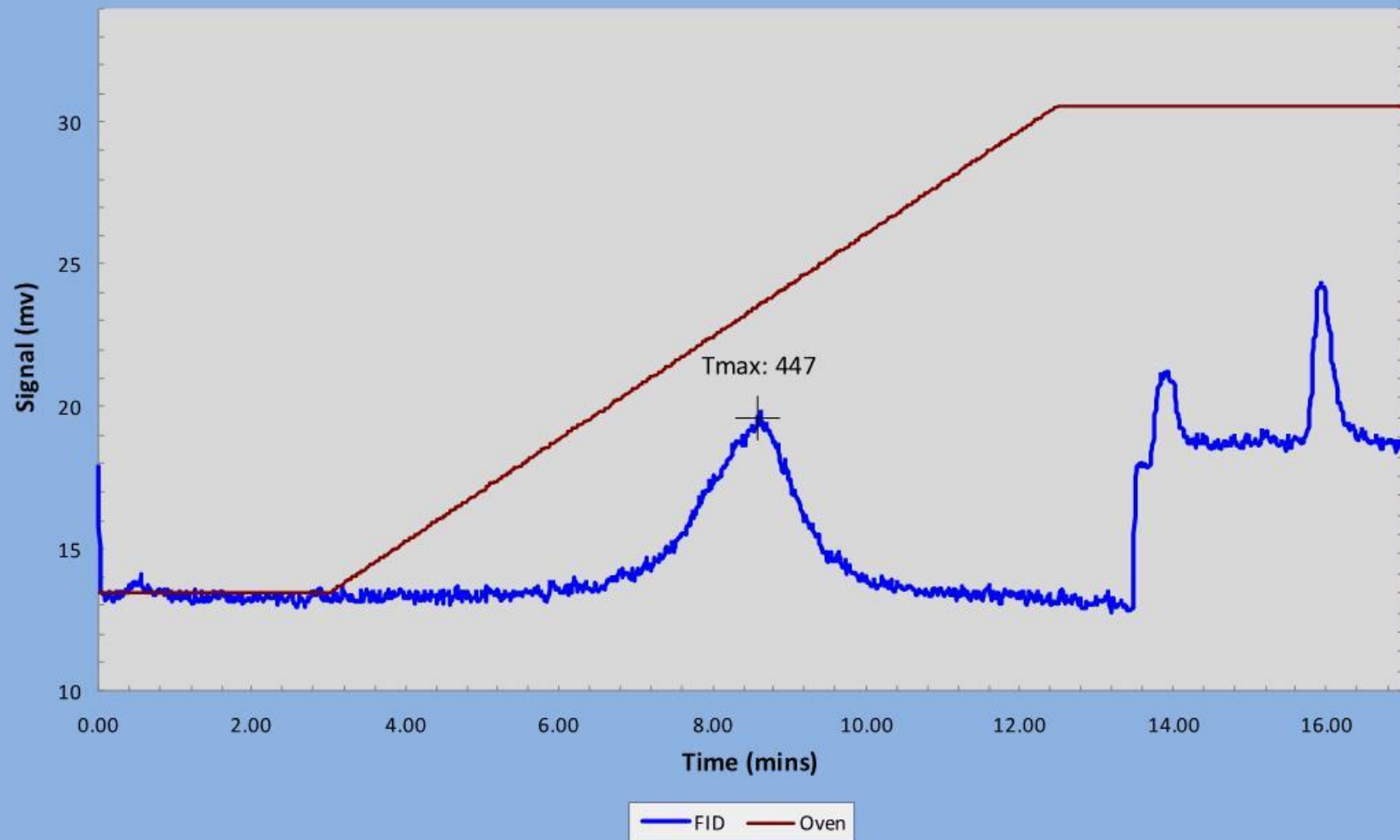
LN12077-G2  
(RMEM-120901-029)



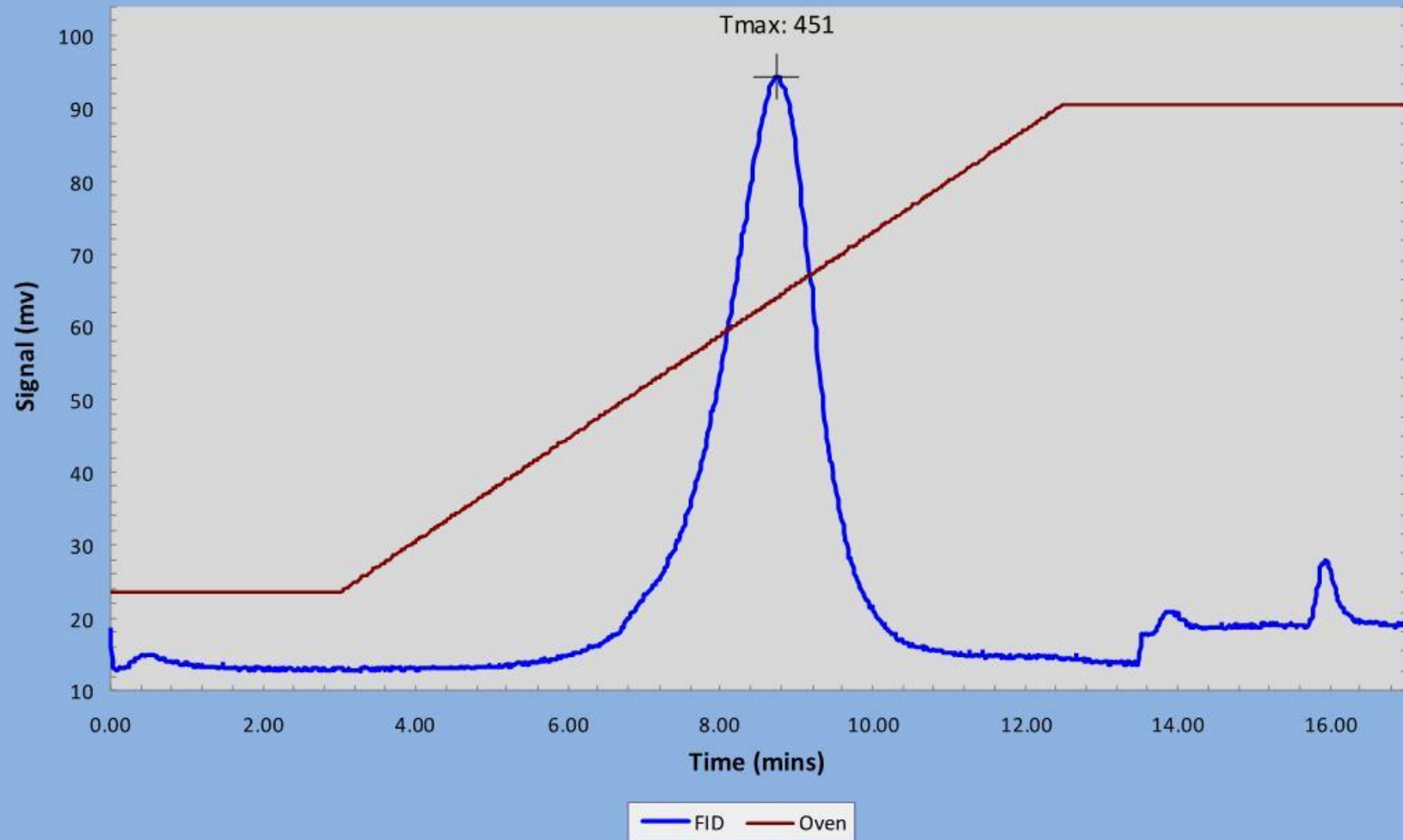
LN12077-H  
(RMEM-120901-030)



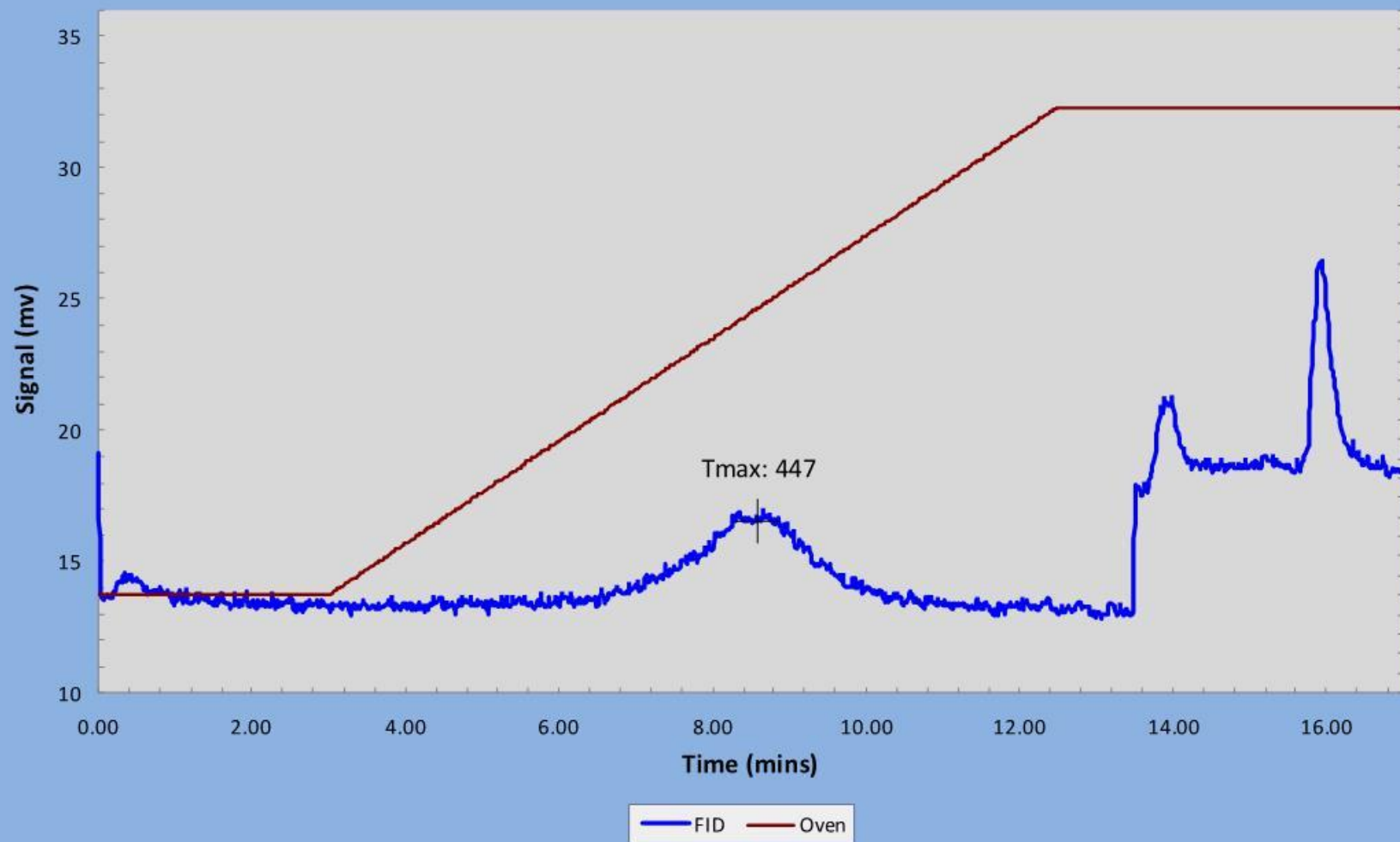
LN12091-A  
(RMEM-120901-031)



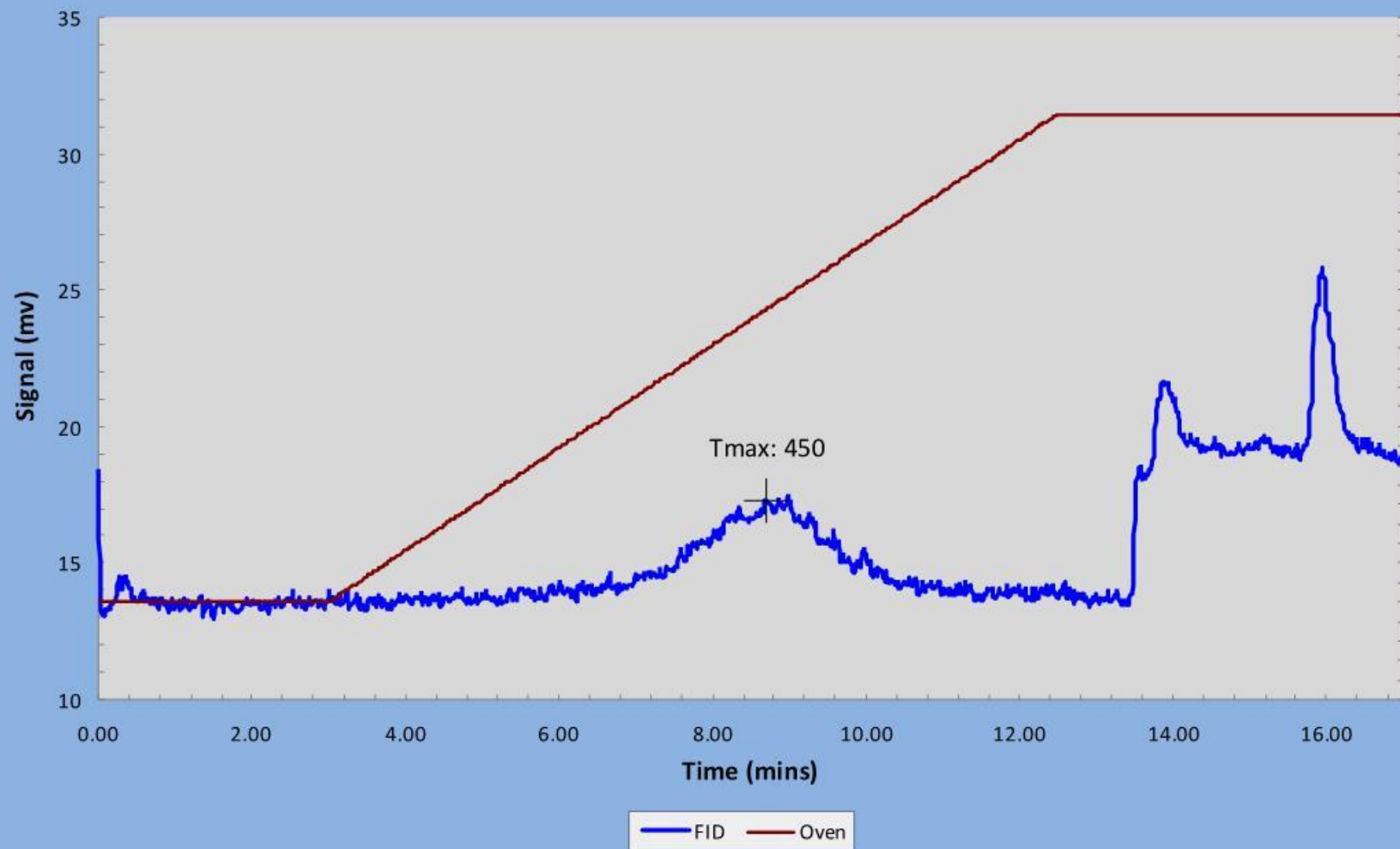
**LN12091-B**  
**(RMEM-120901-032)**



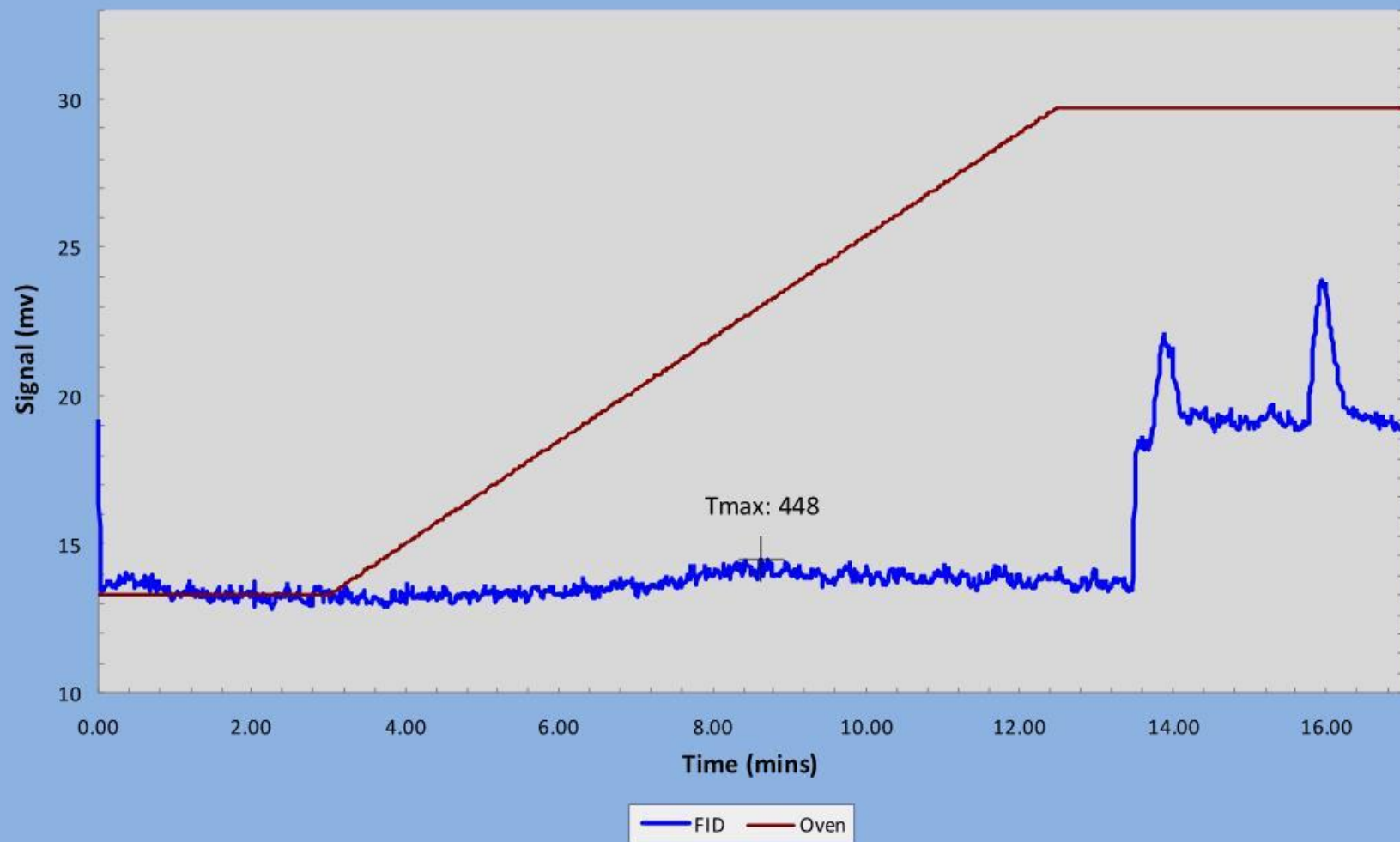
LN12091-C  
(RMEM-120901-033)



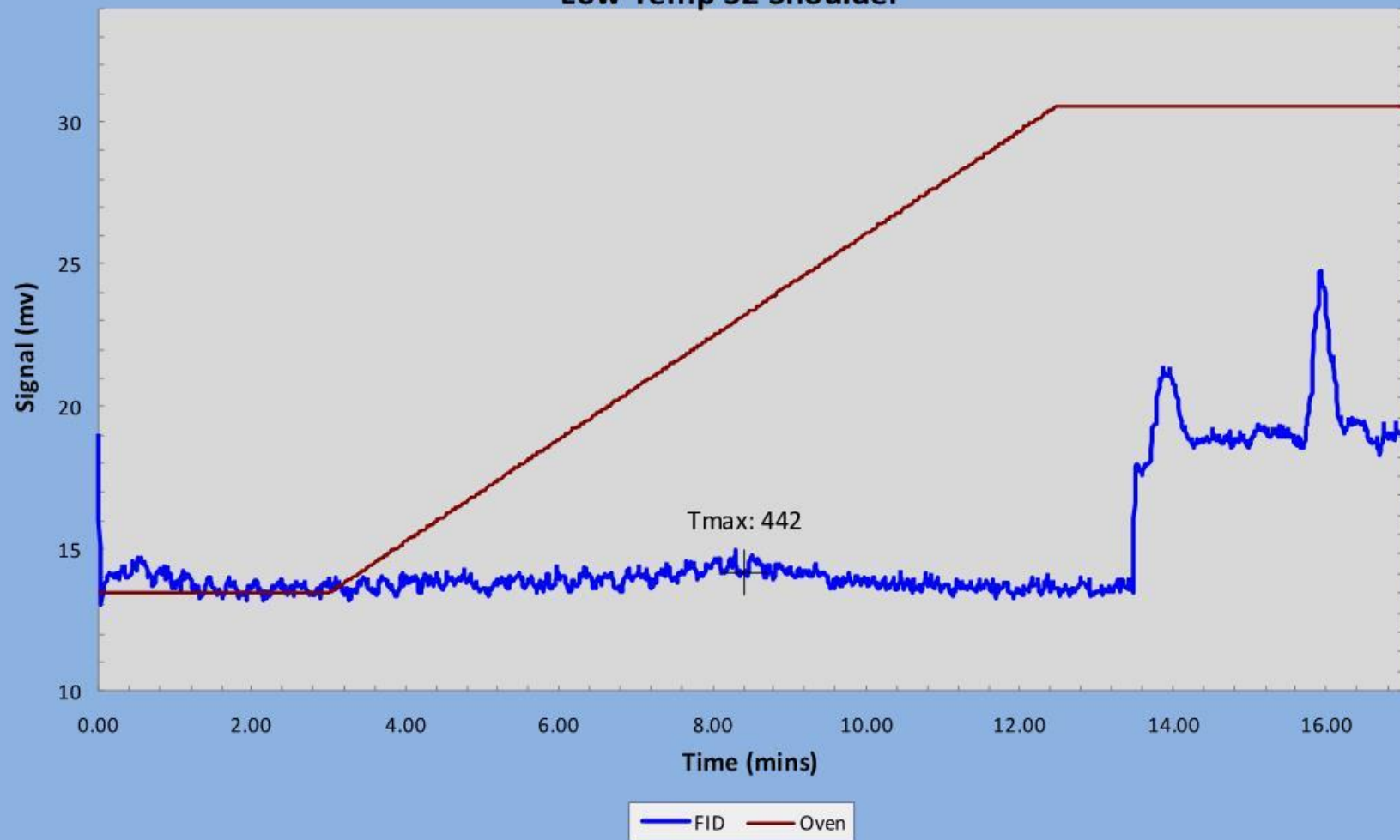
LN12092  
(RMEM-120901-034)



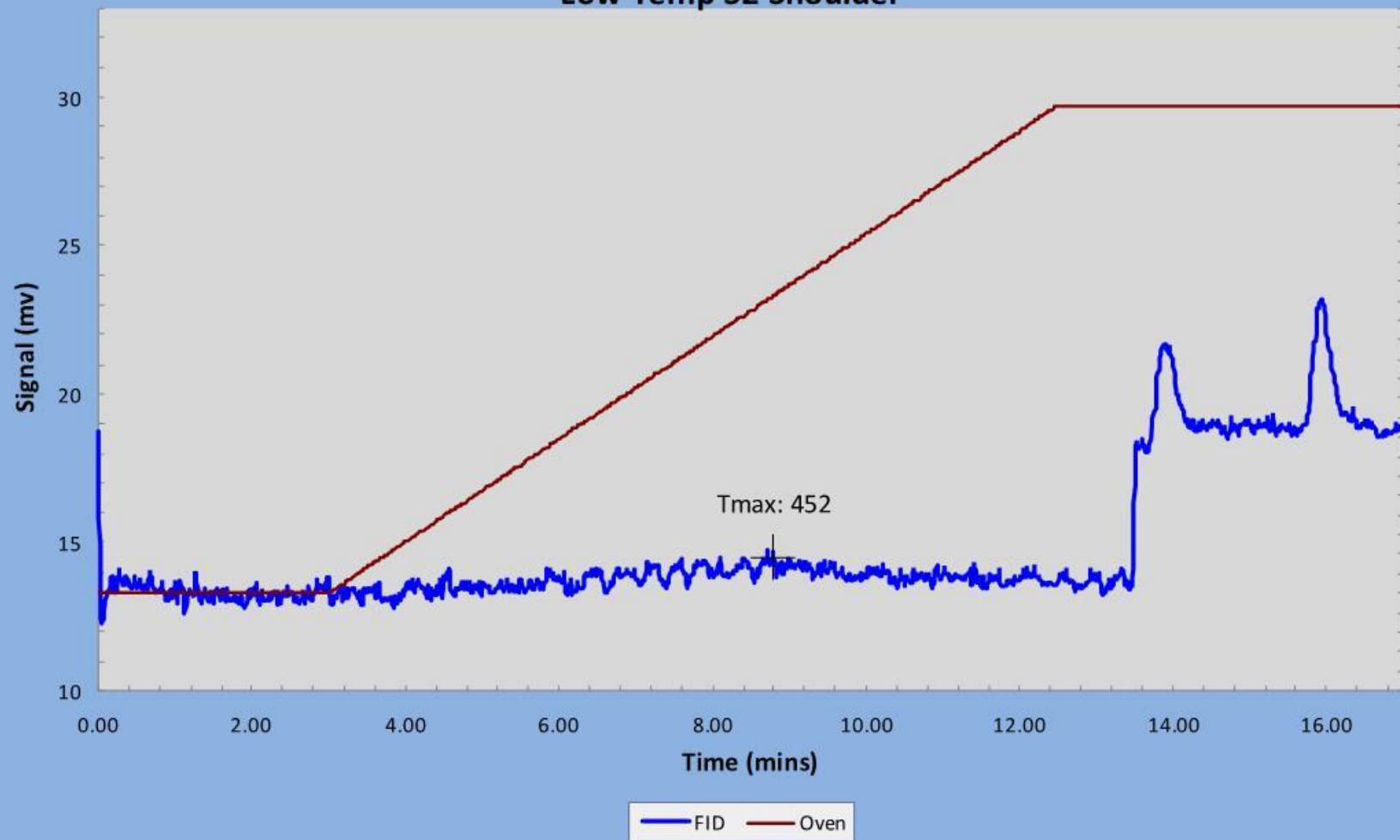
LN12021  
(RMEM-120901-035)



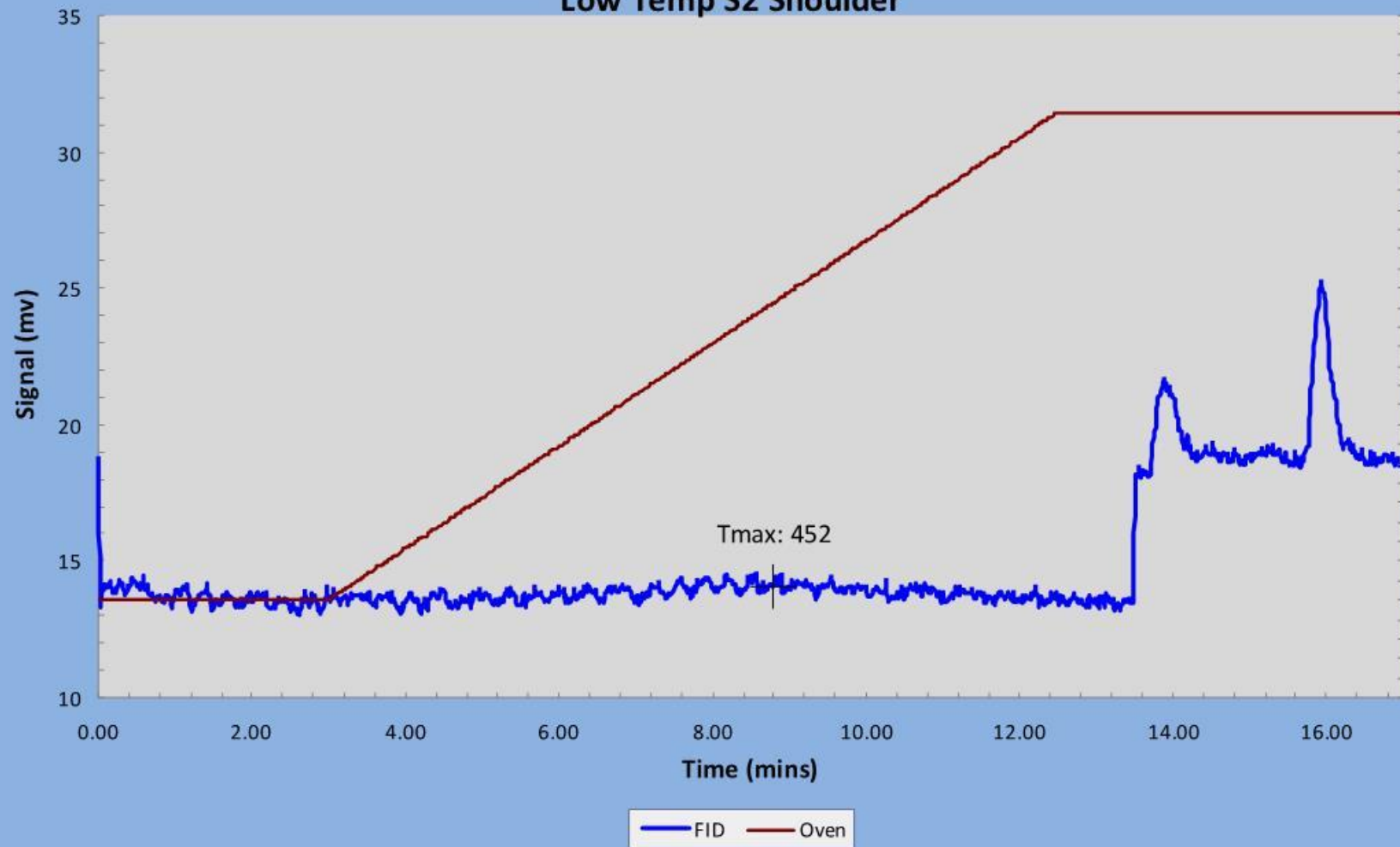
LN12021-F  
(RMEM-120901-036)  
Low Temp S2 Shoulder



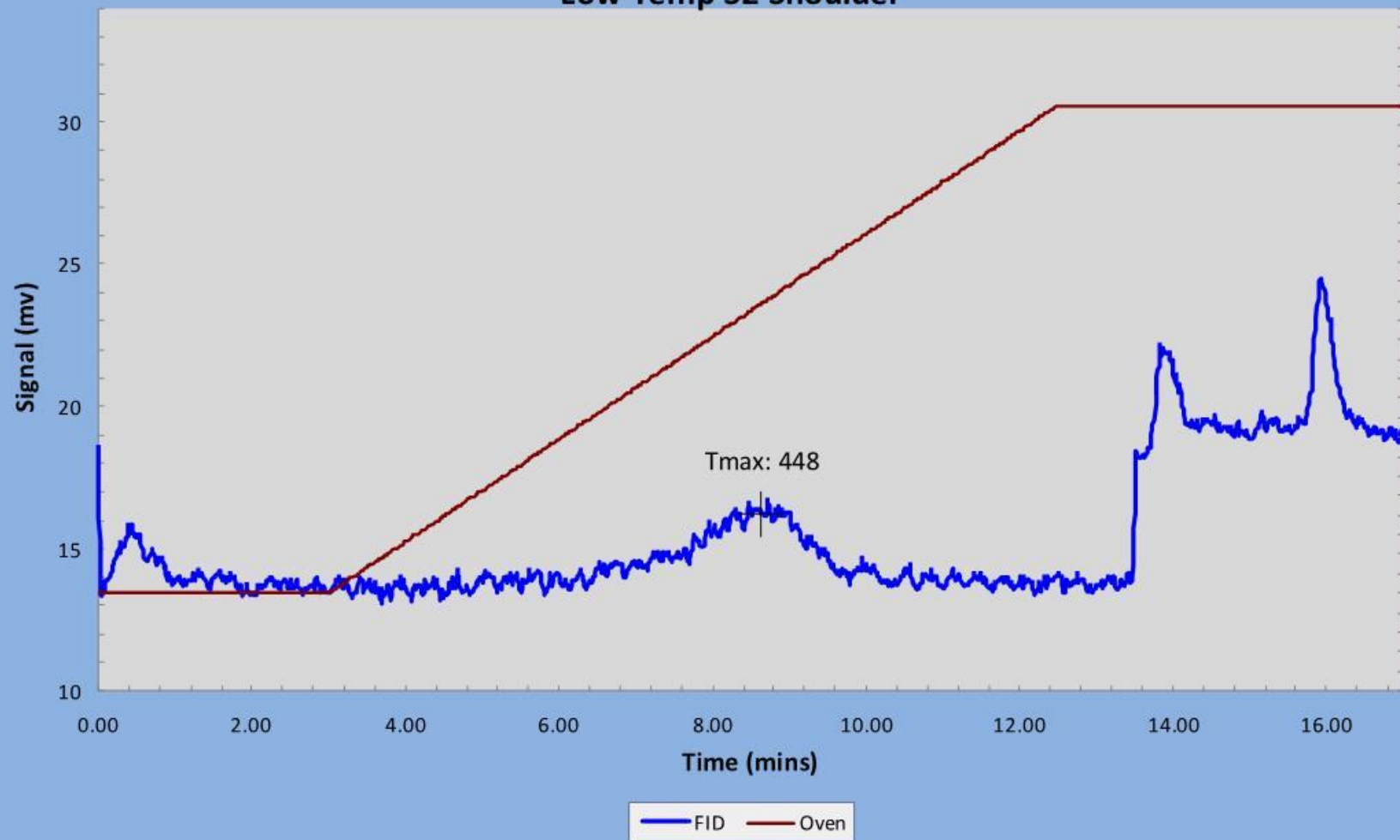
LN12021-G  
(RMEM-120901-037)  
Low Temp S2 Shoulder



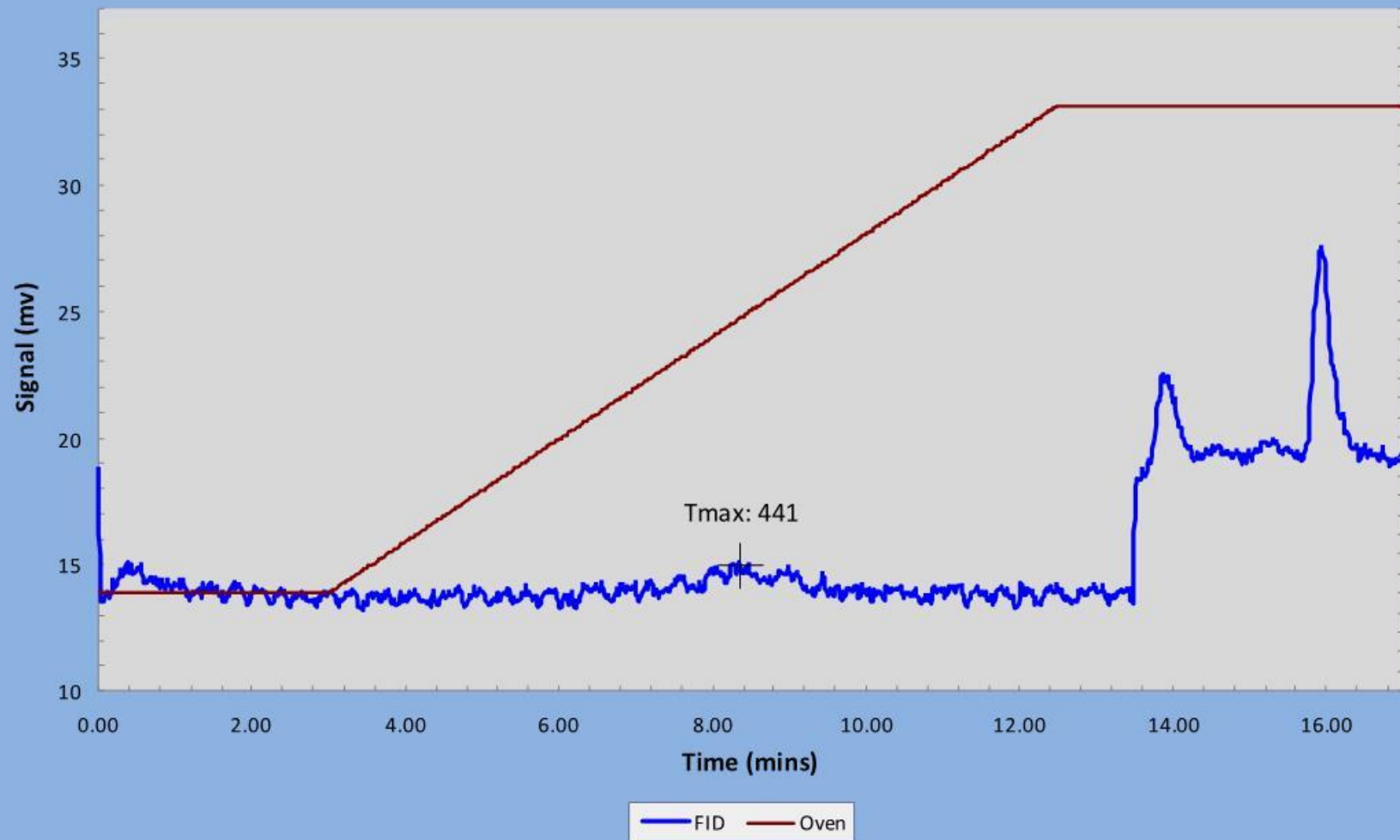
LN12021-H  
(RMEM-120901-038)  
Low Temp S2 Shoulder



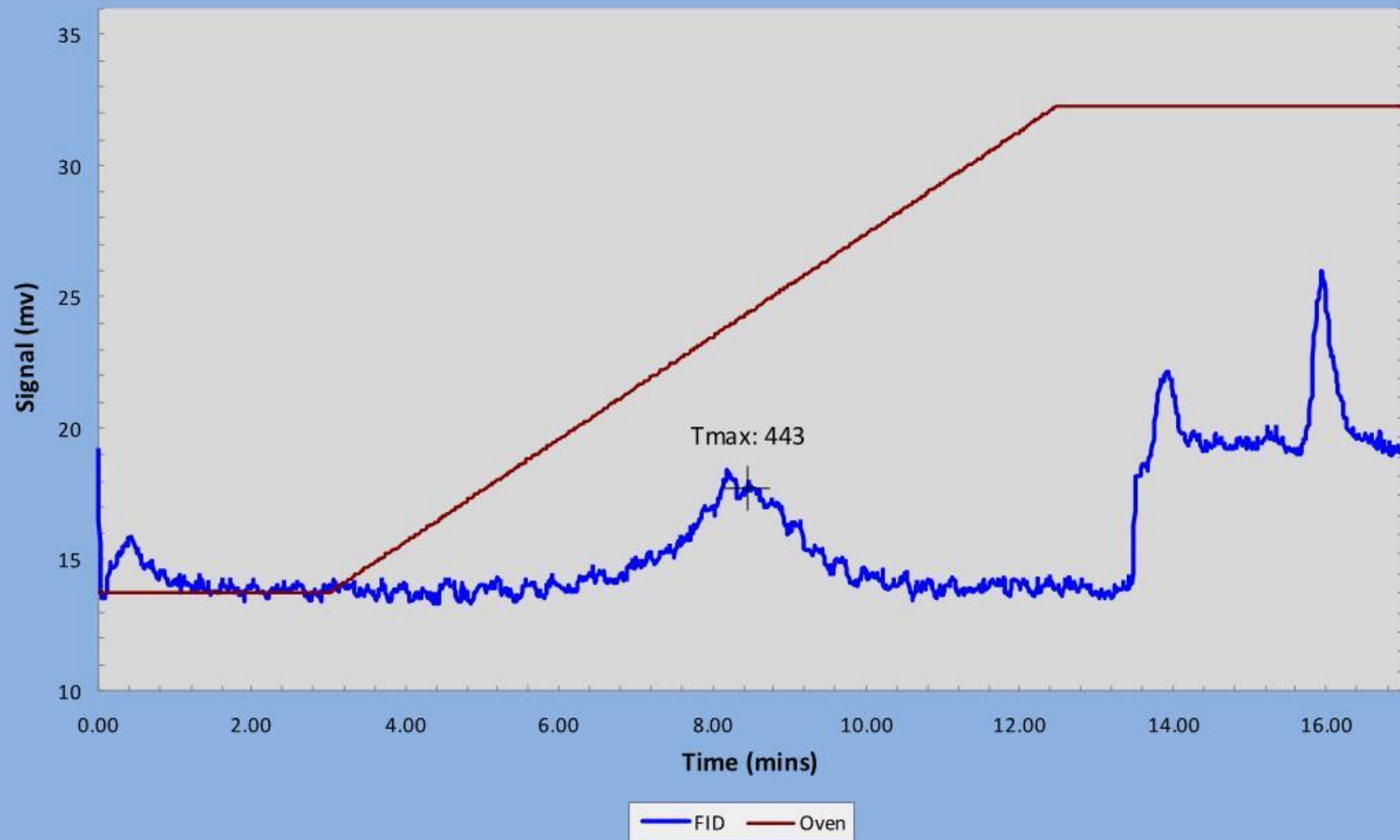
LN12016-A  
(RMEM-120901-039)  
Low Temp S2 Shoulder



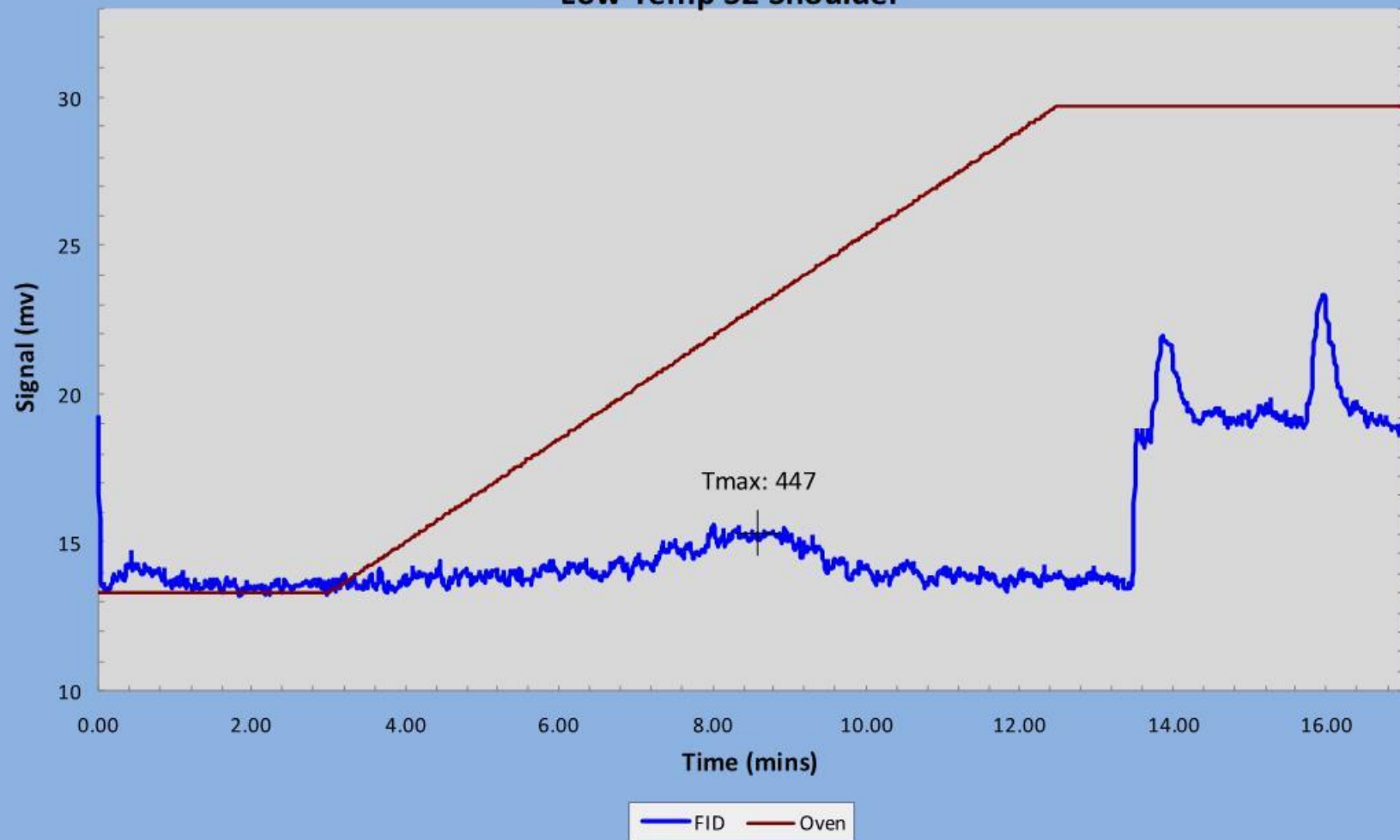
LN12016-B  
(RMEM-120901-040)



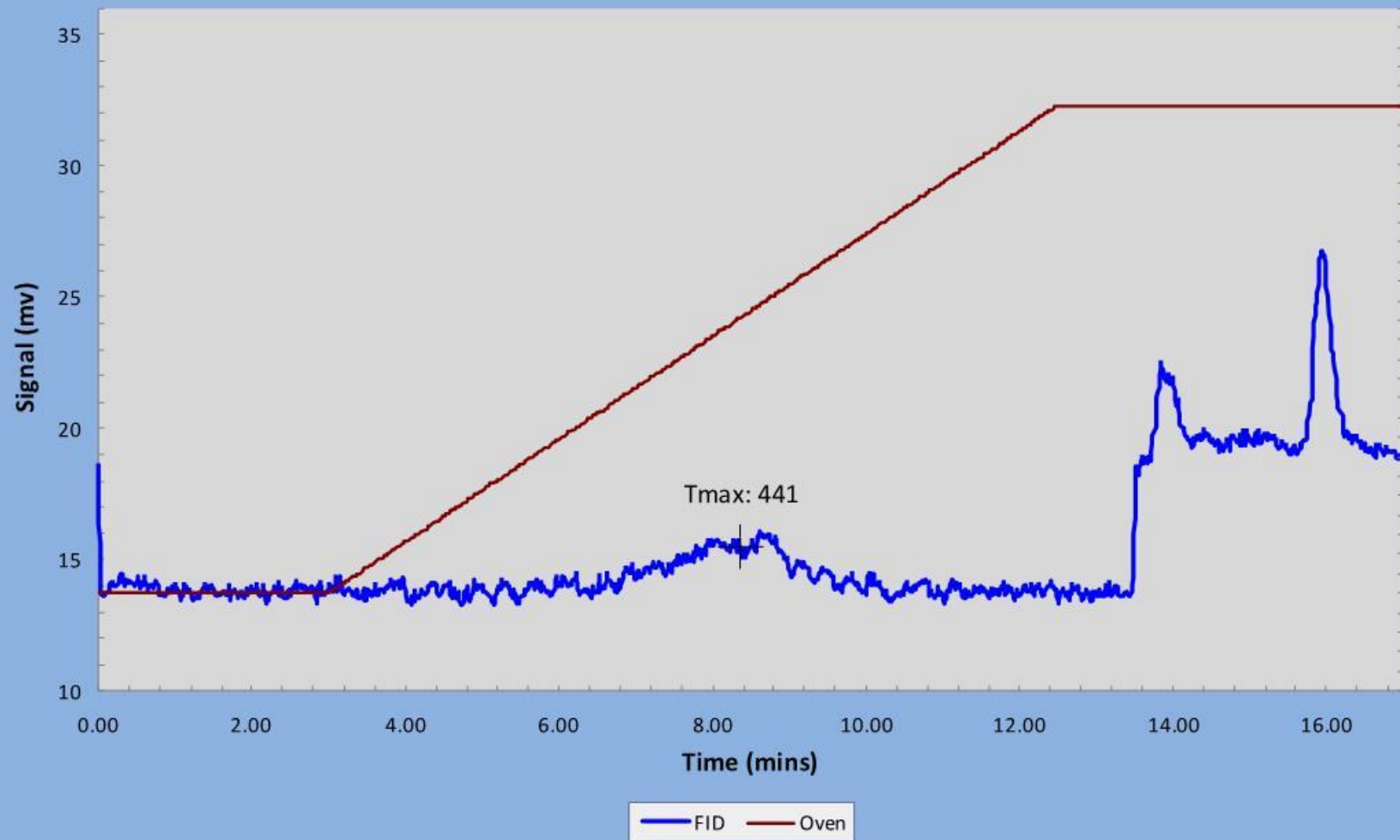
LN12016-C  
(RMEM-120901-041)



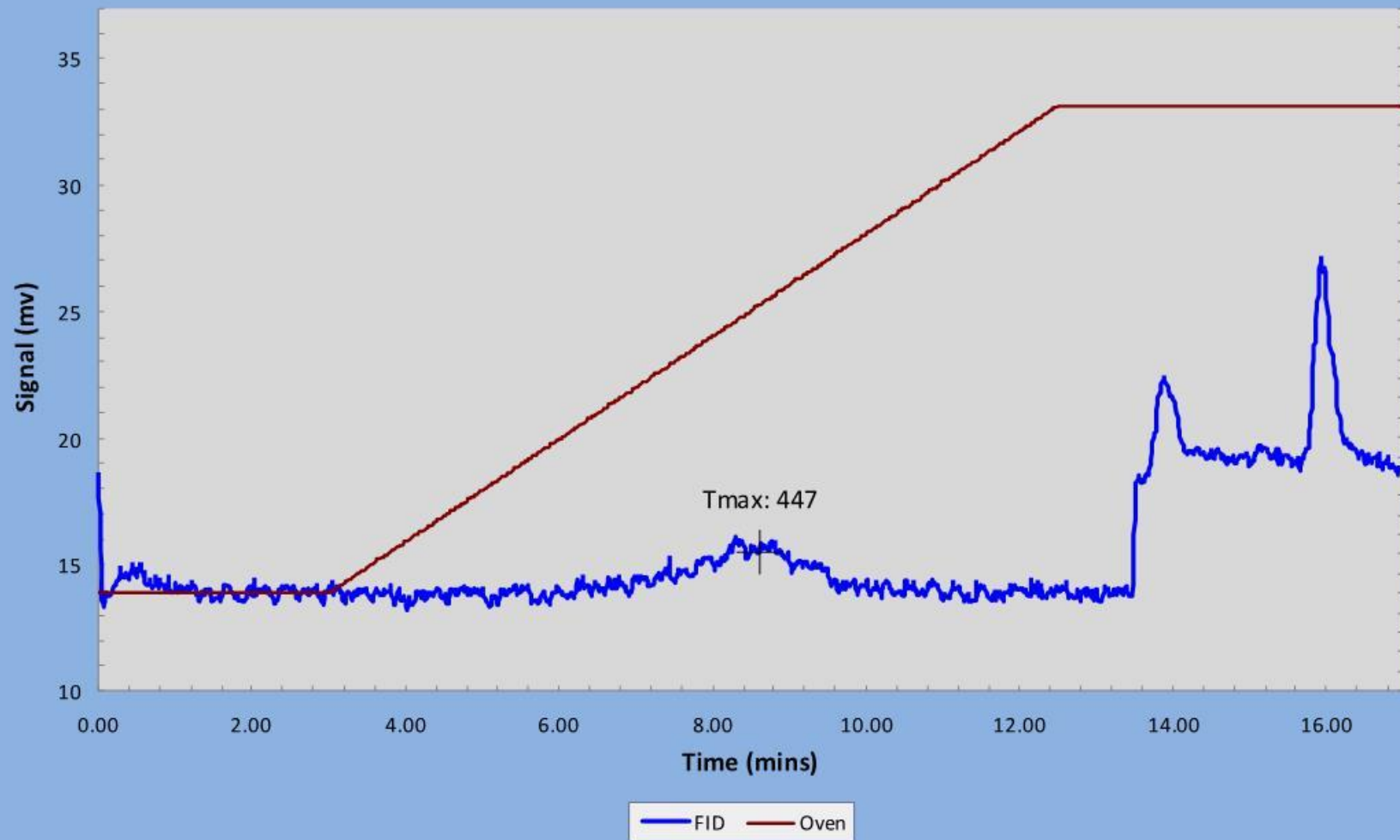
LN12016-D  
(RMEM-120901-042)  
Low Temp S2 Shoulder



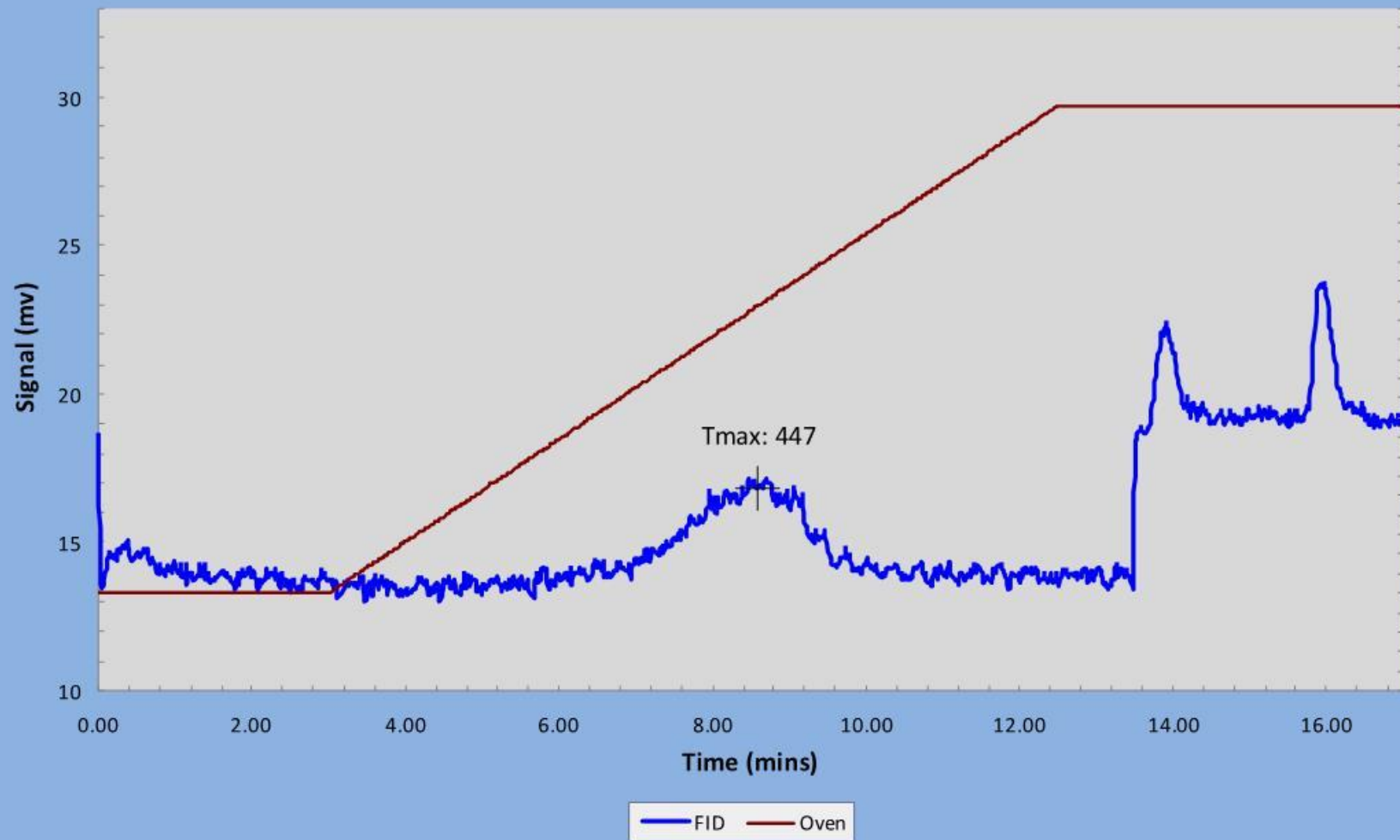
LN12016-E  
(RMEM-120901-043)



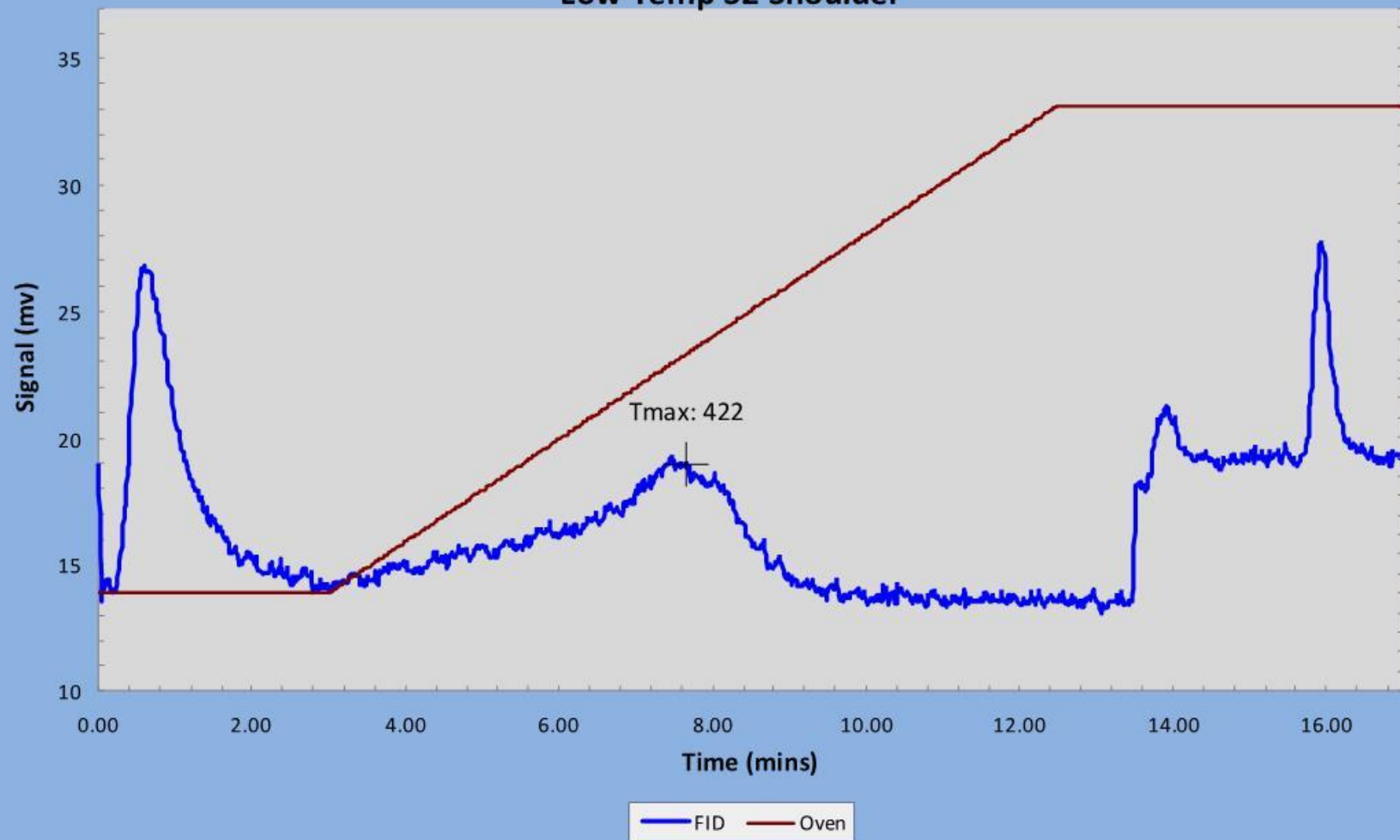
LN12016-F  
(RMEM-120901-044)

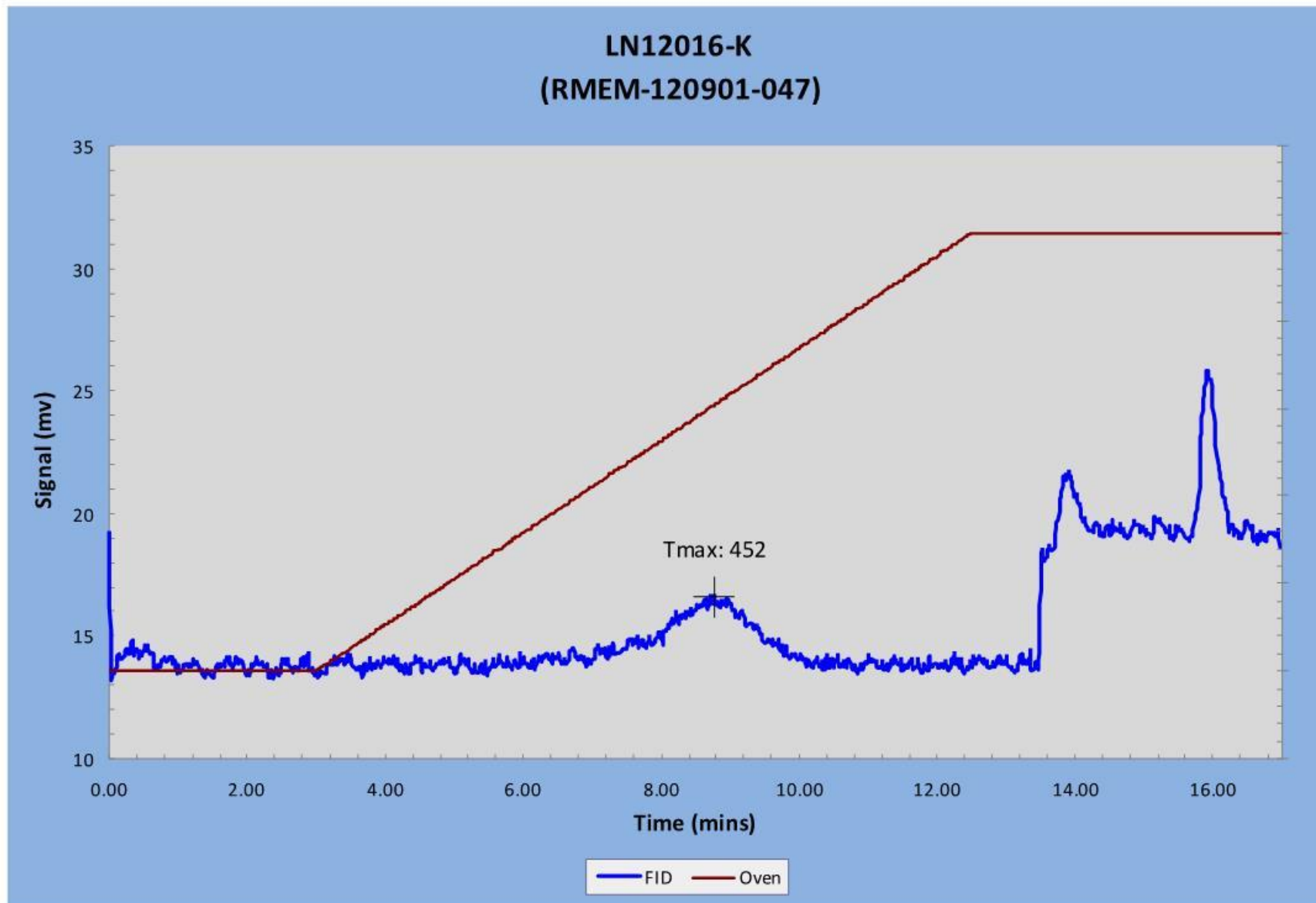


LN12016-G  
(RMEM-120901-045)

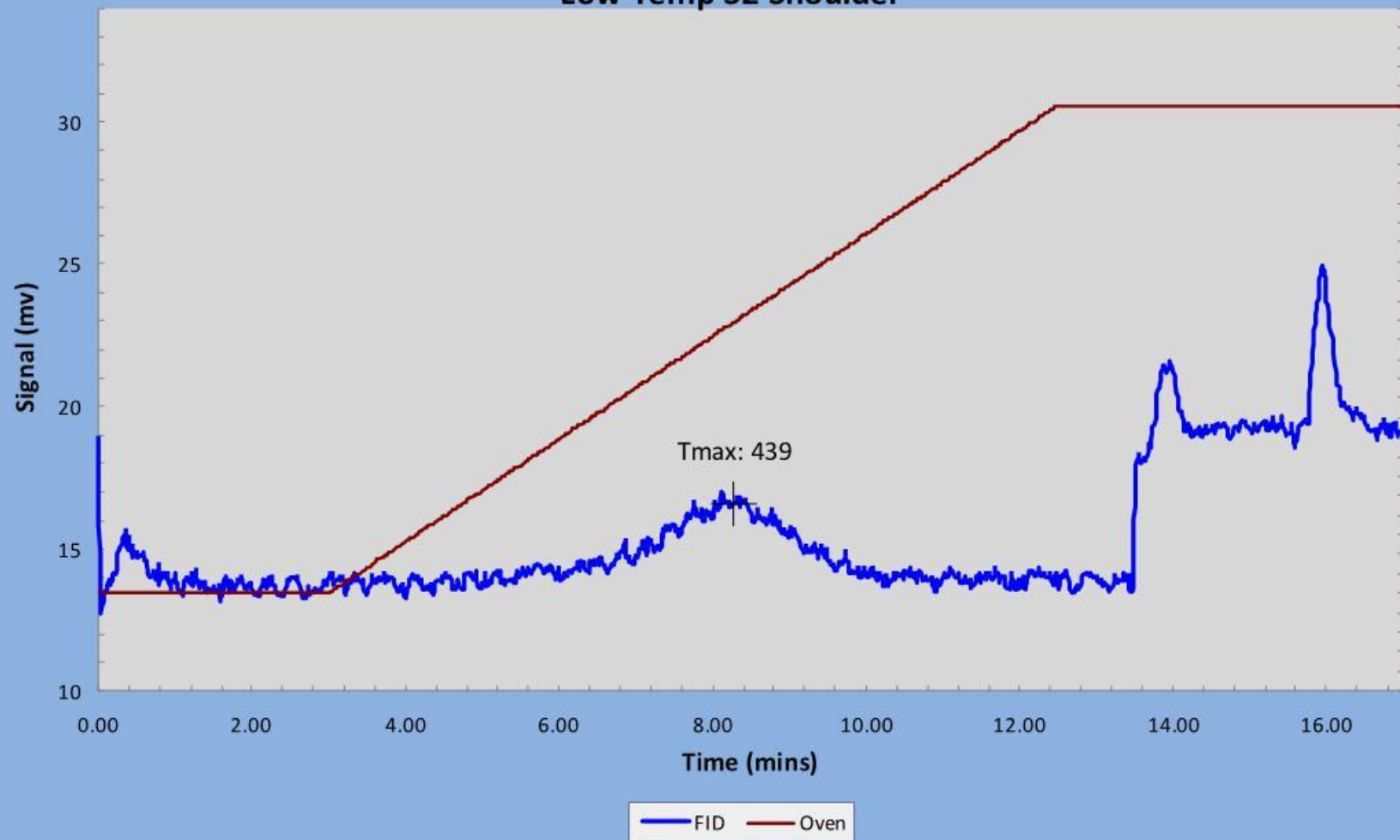


LN12016-J  
(RMEM-120901-046)  
Low Temp S2 Shoulder

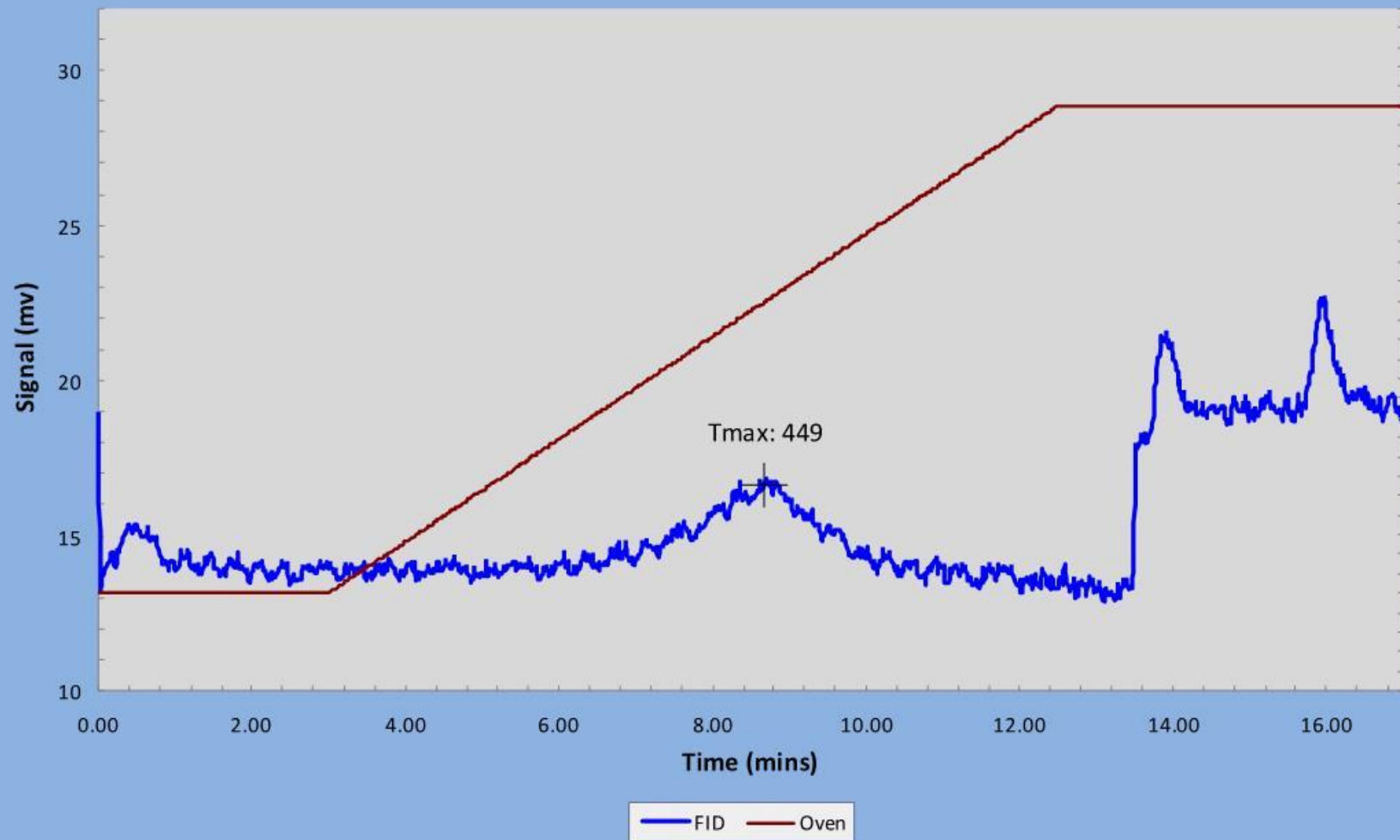




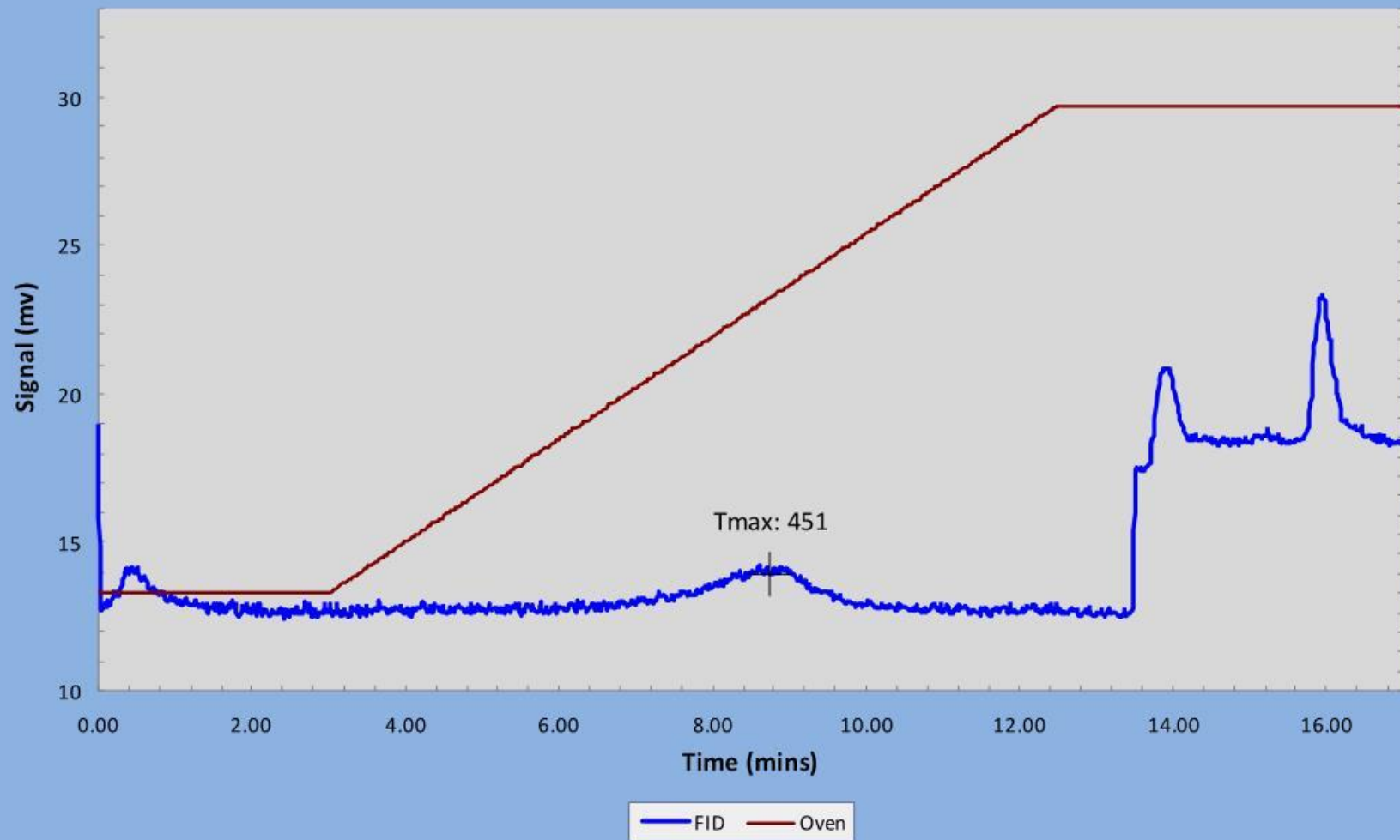
LN12034  
(RMEM-120901-048)  
Low Temp S2 Shoulder



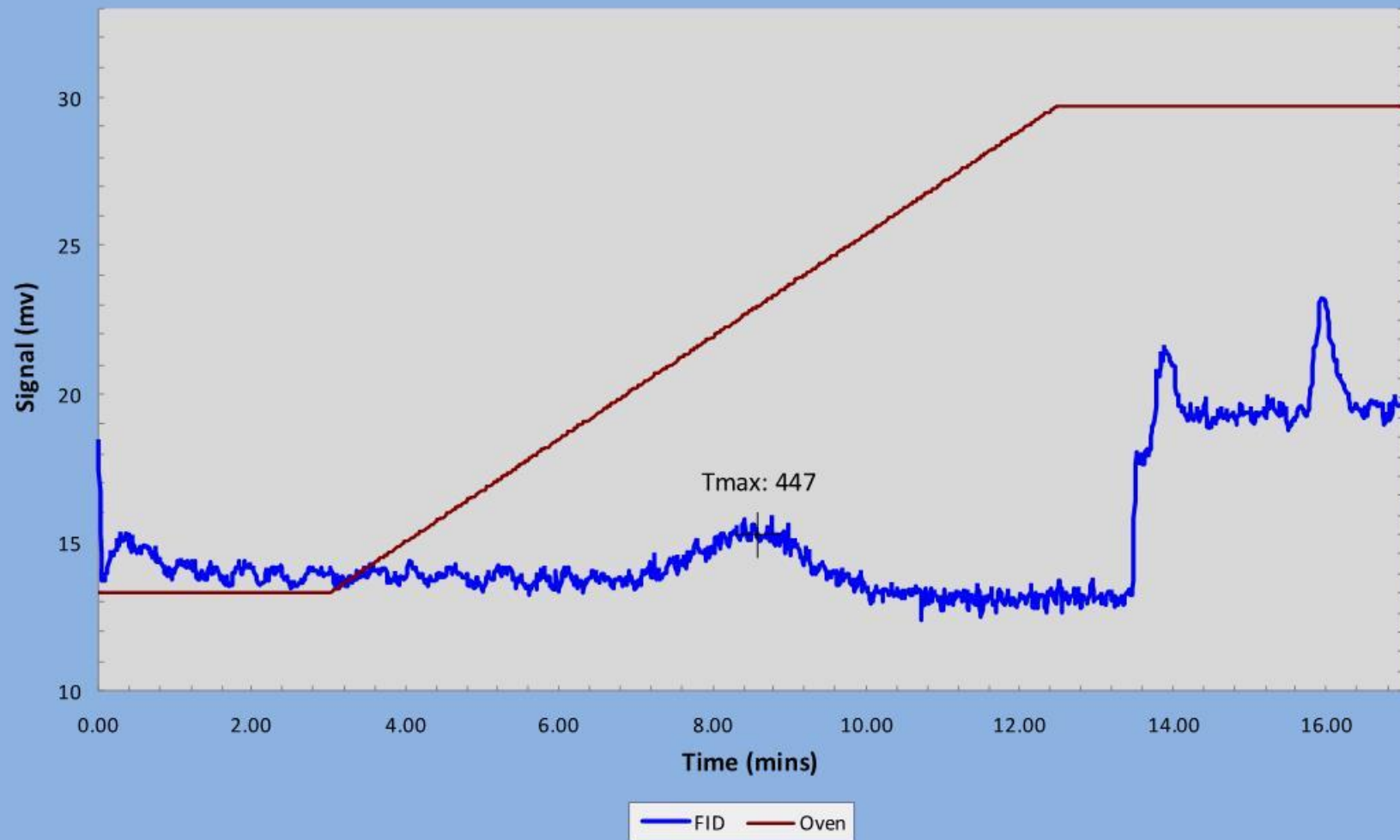
LN12034-A  
(RMEM-120901-049)



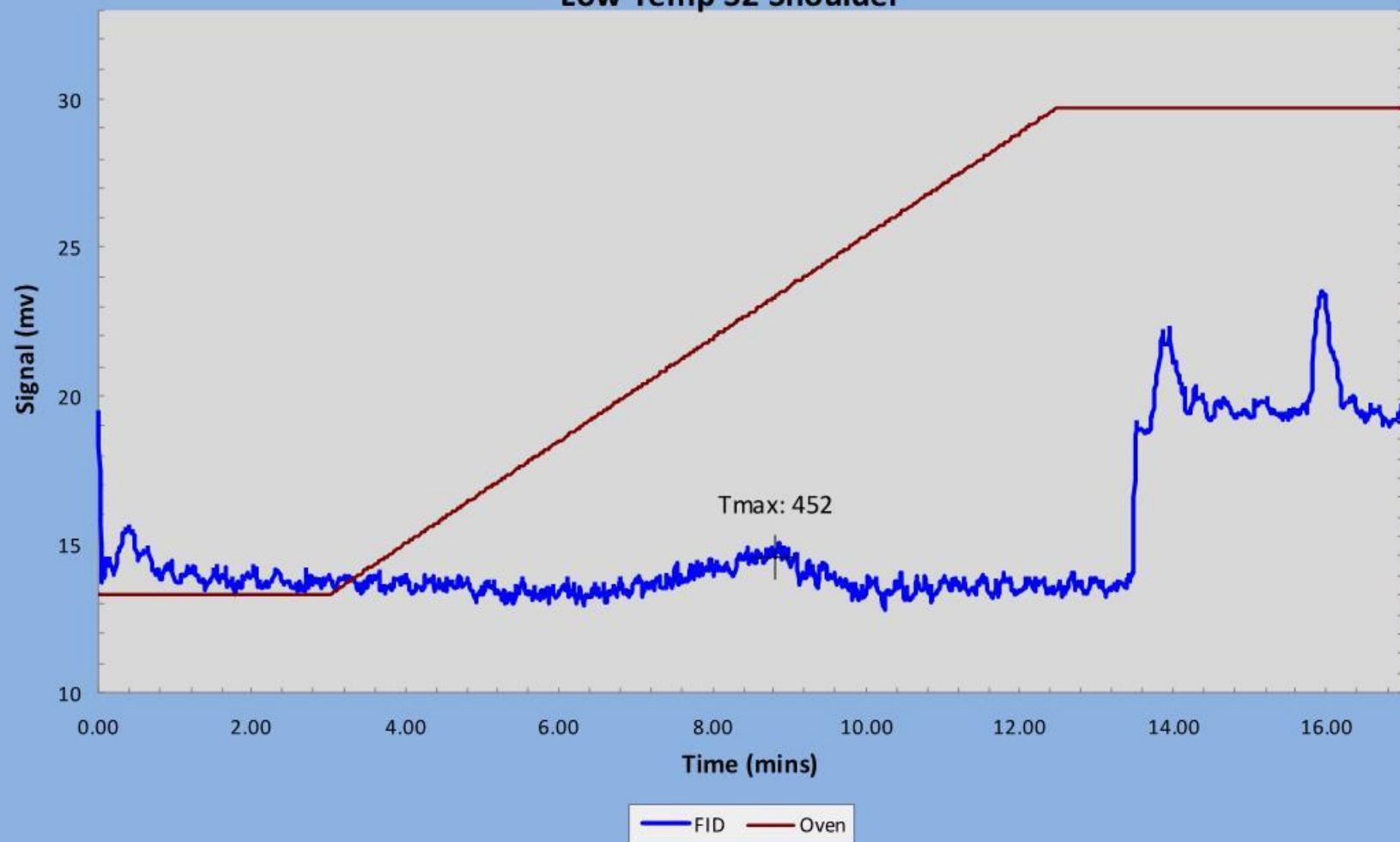
LN12034-B1  
(RMEM-120901-050)



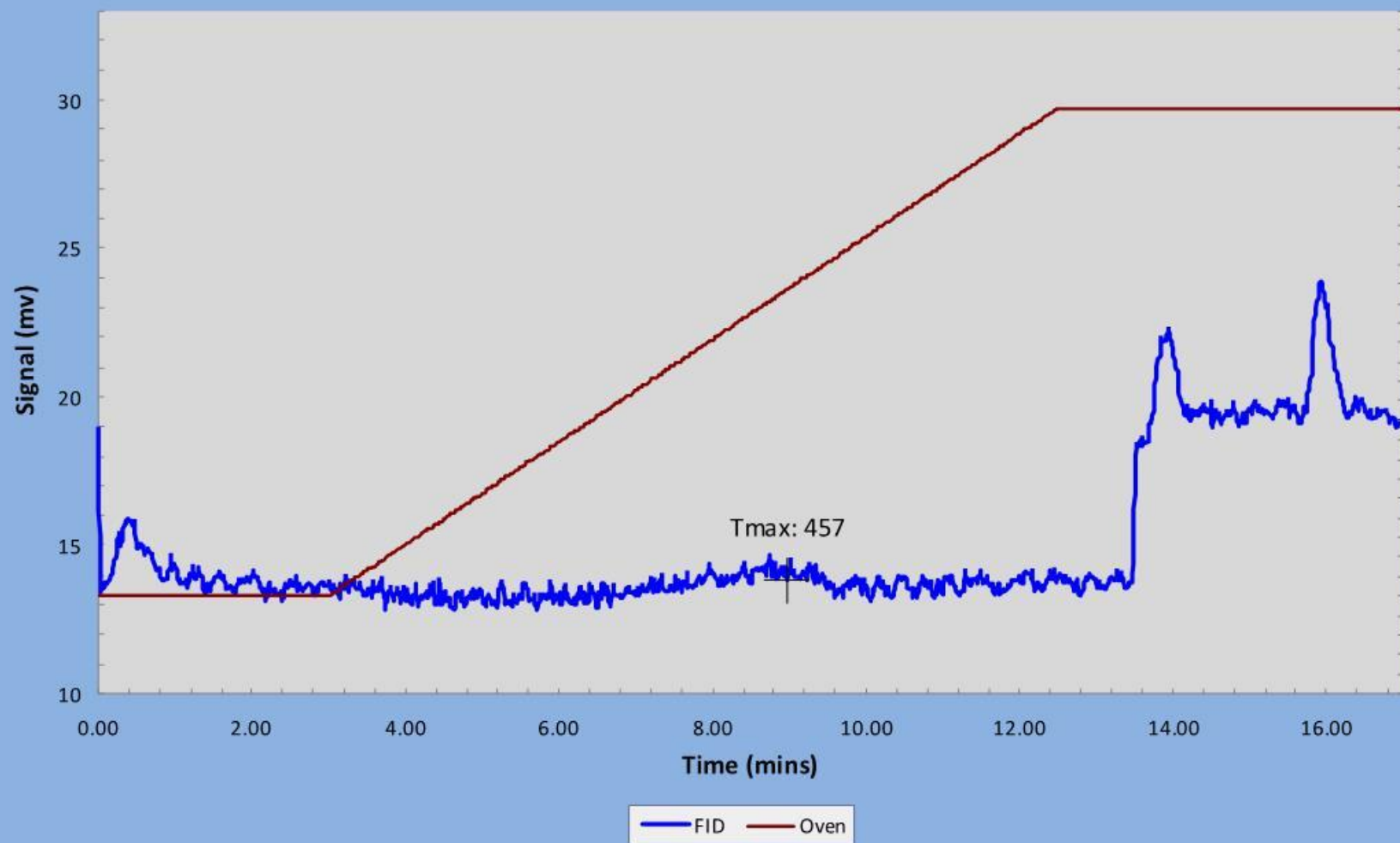
LN12034-B  
(RMEM-120901-051)



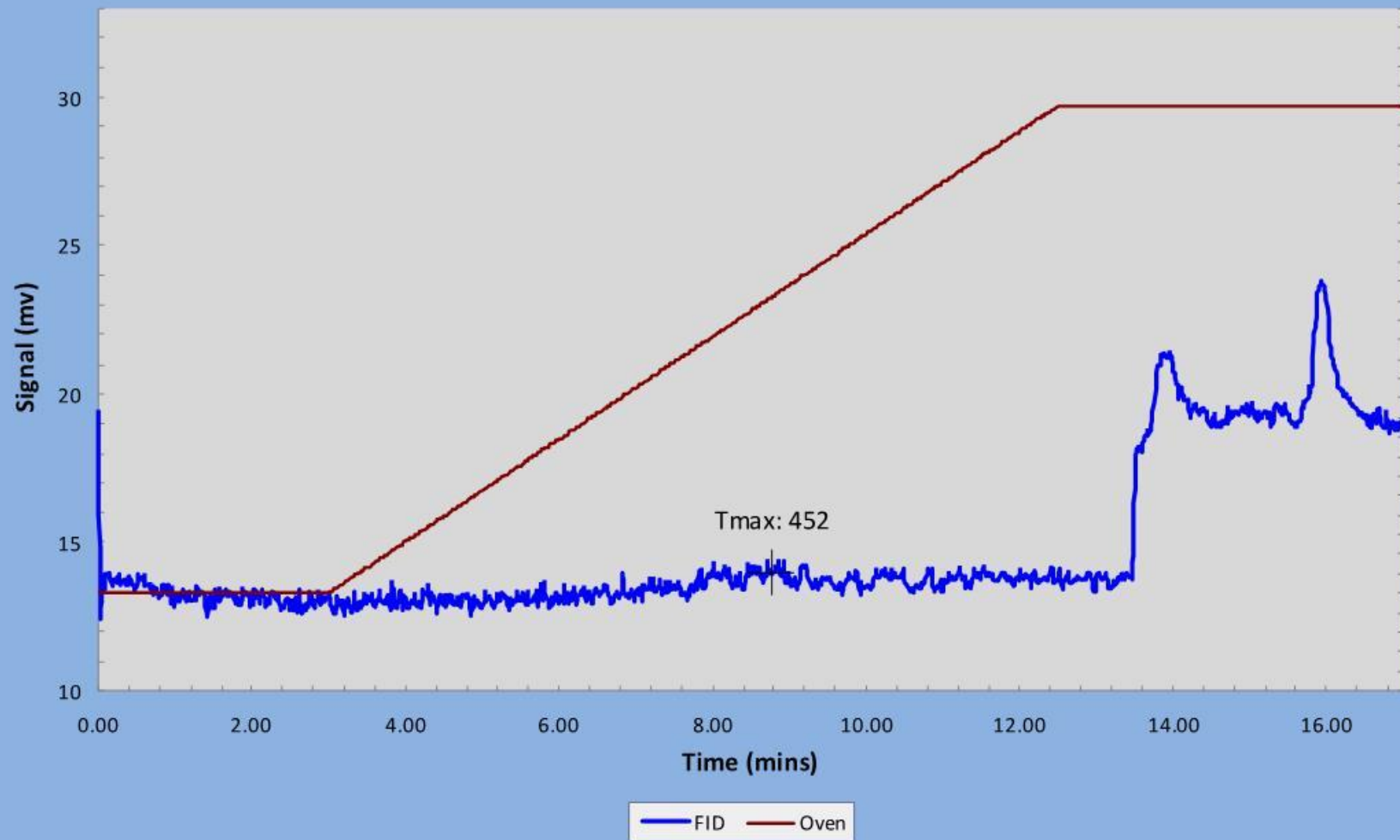
LN12034-E  
(RMEM-120901-052)  
Low Temp S2 Shoulder



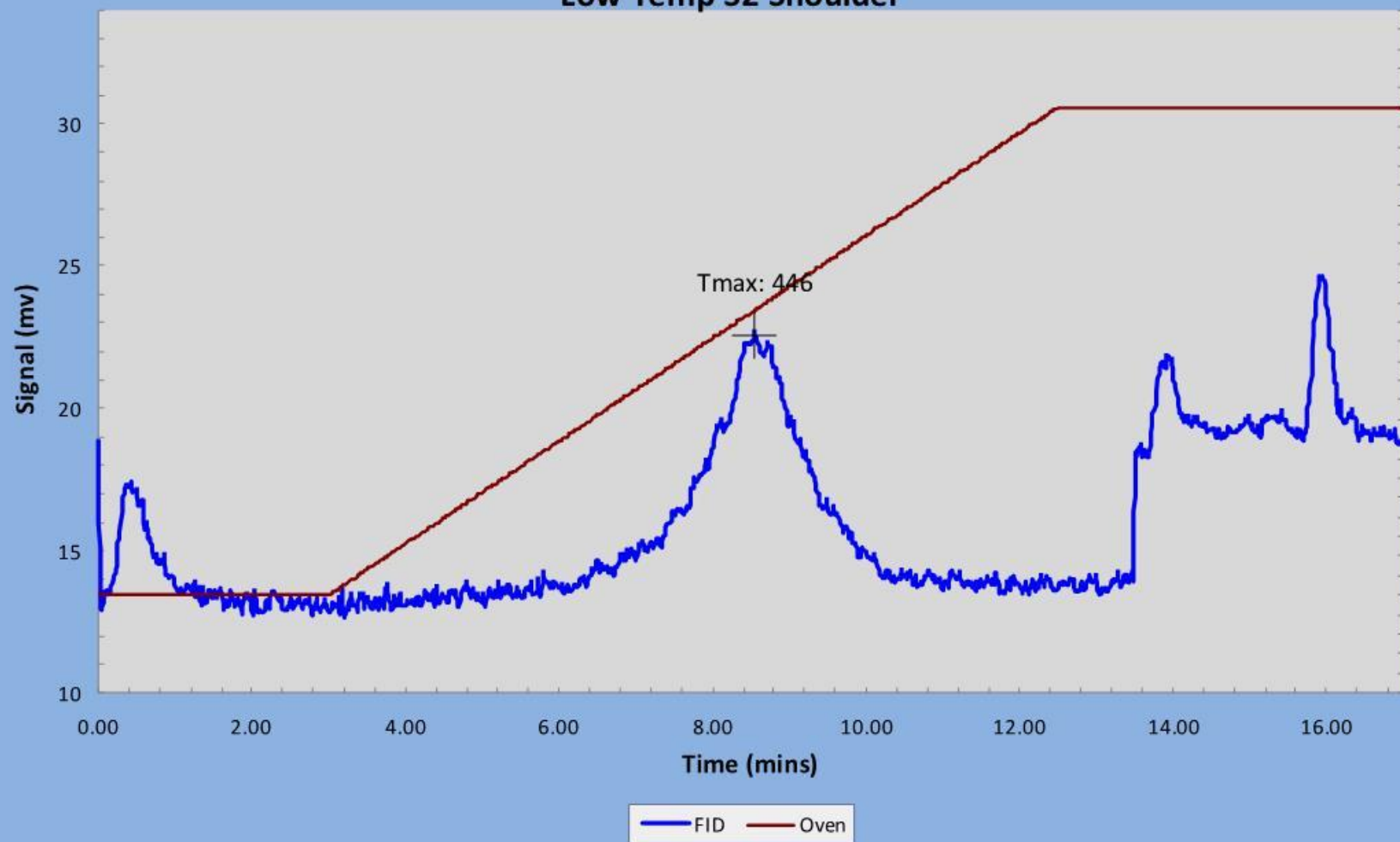
LN12034-F  
(RMEM-120901-053)

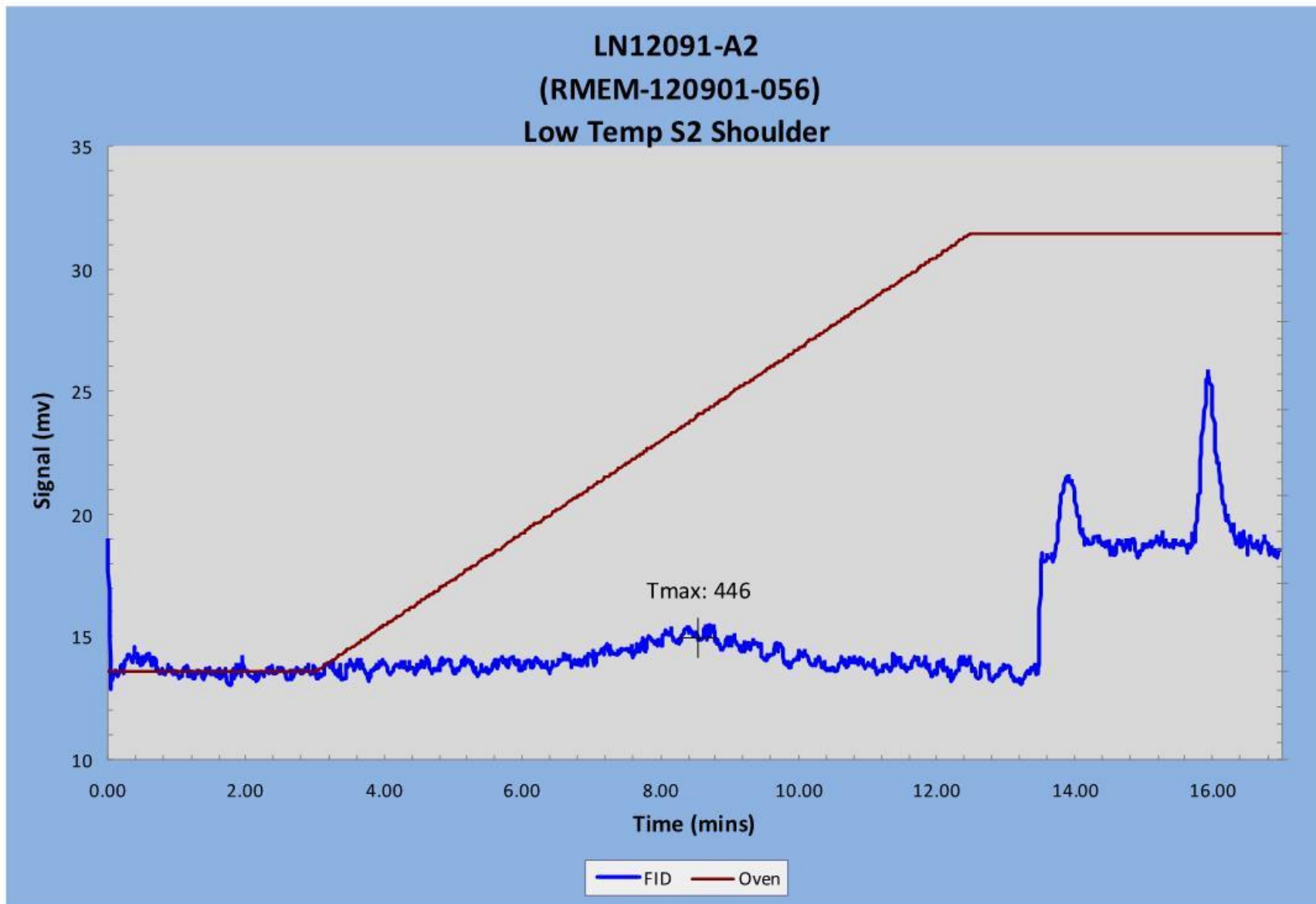


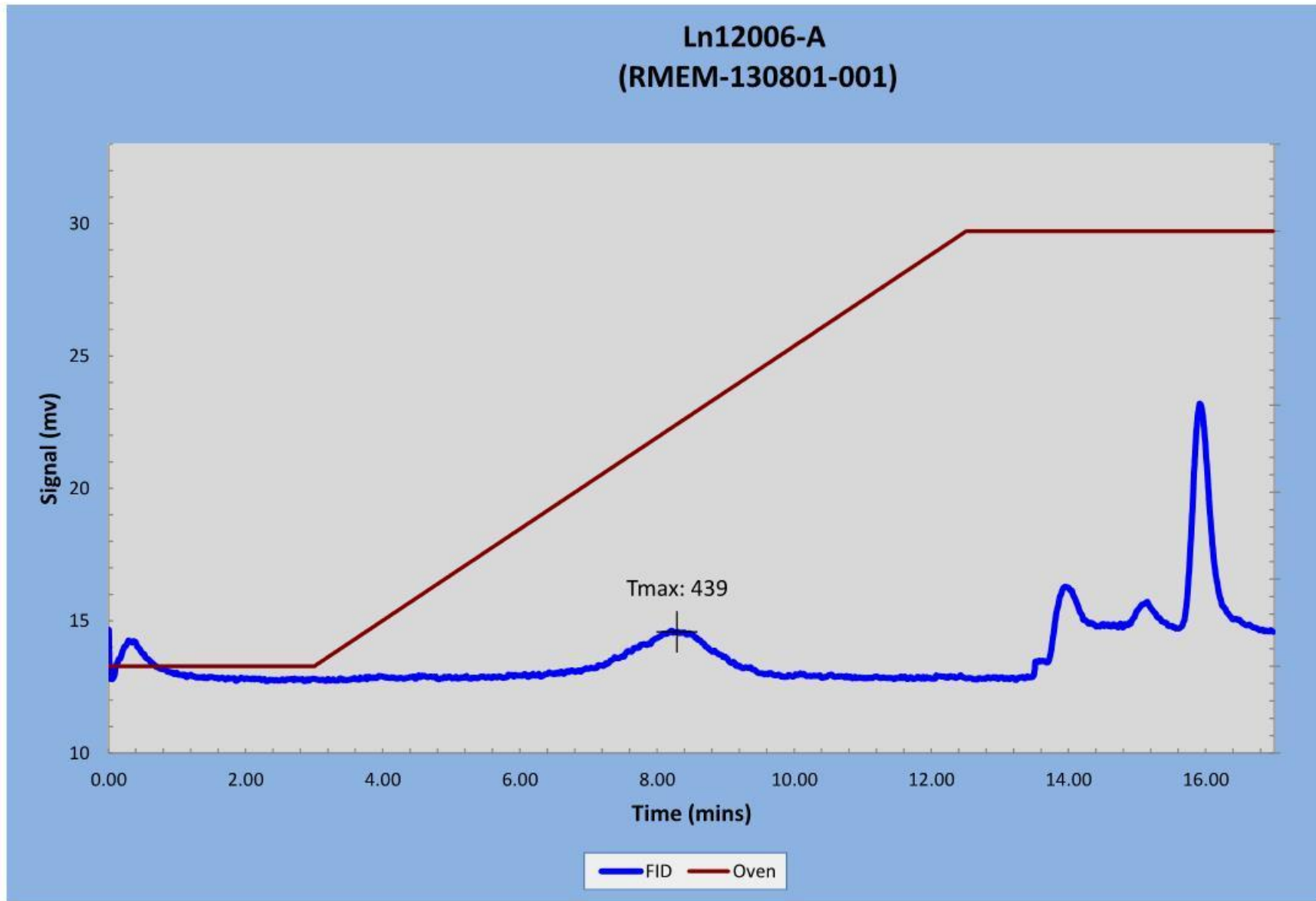
LN12006-A  
(RMEM-120901-054)

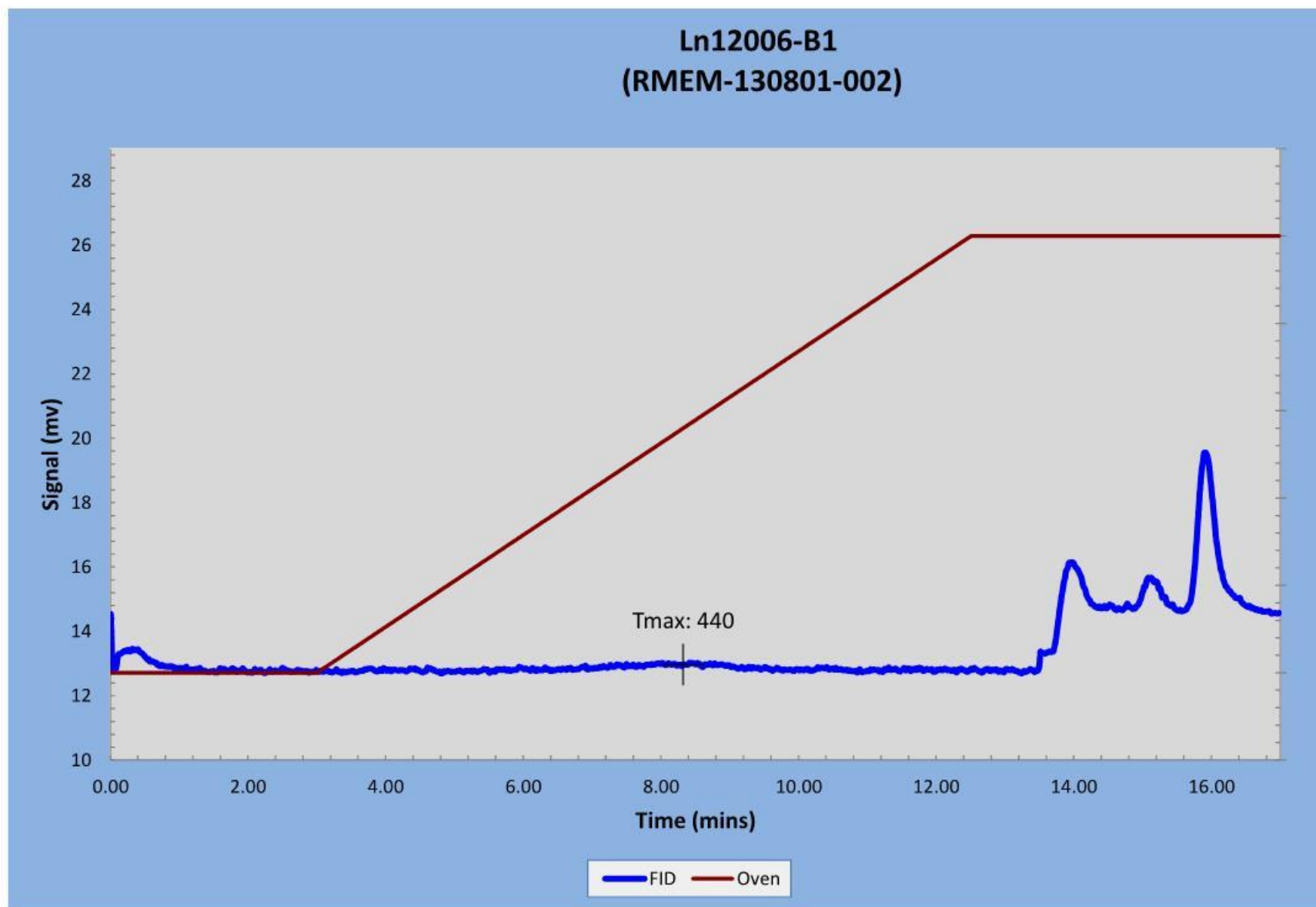


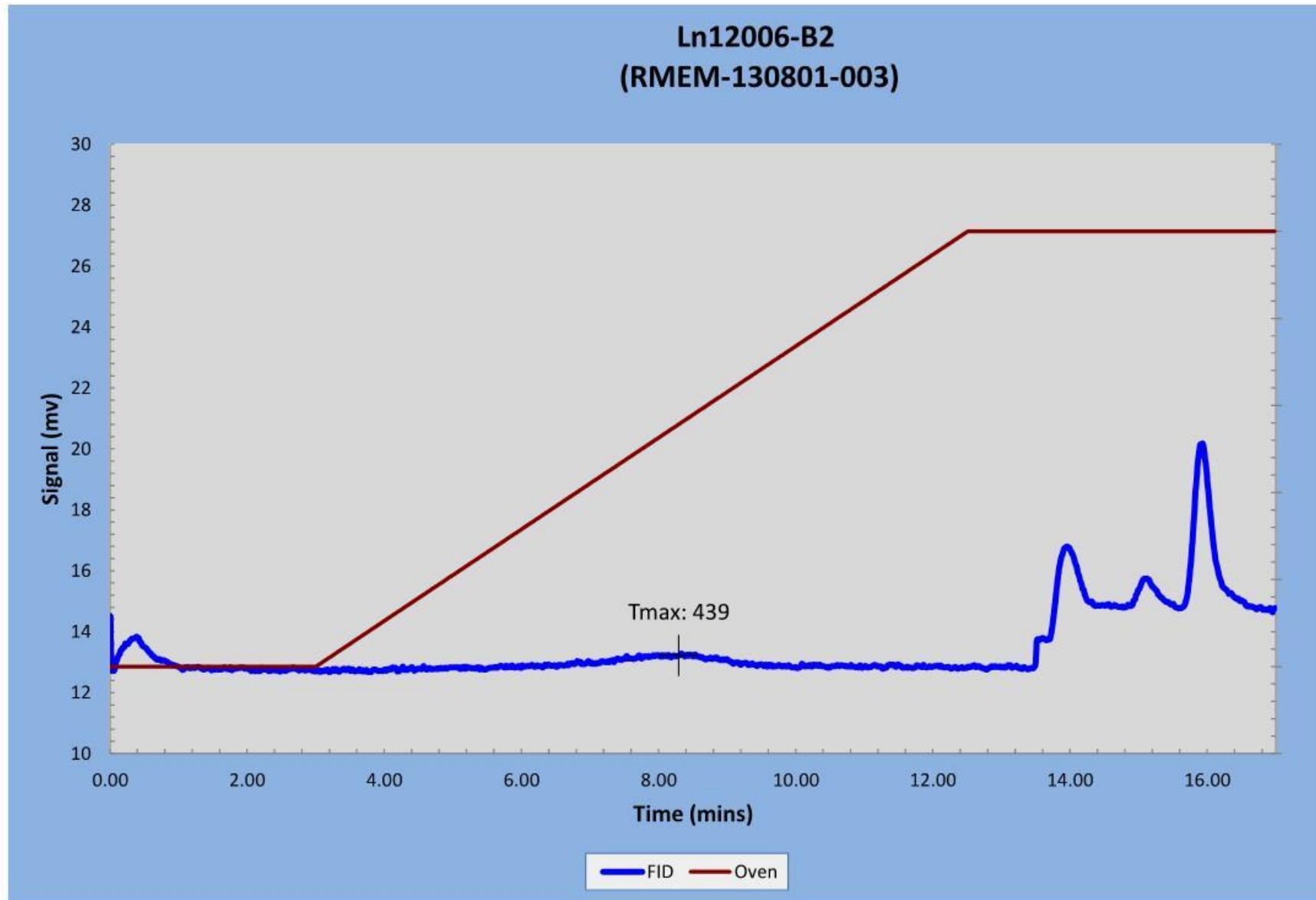
LN12109-B  
(RMEM-120901-055)  
Low Temp S2 Shoulder

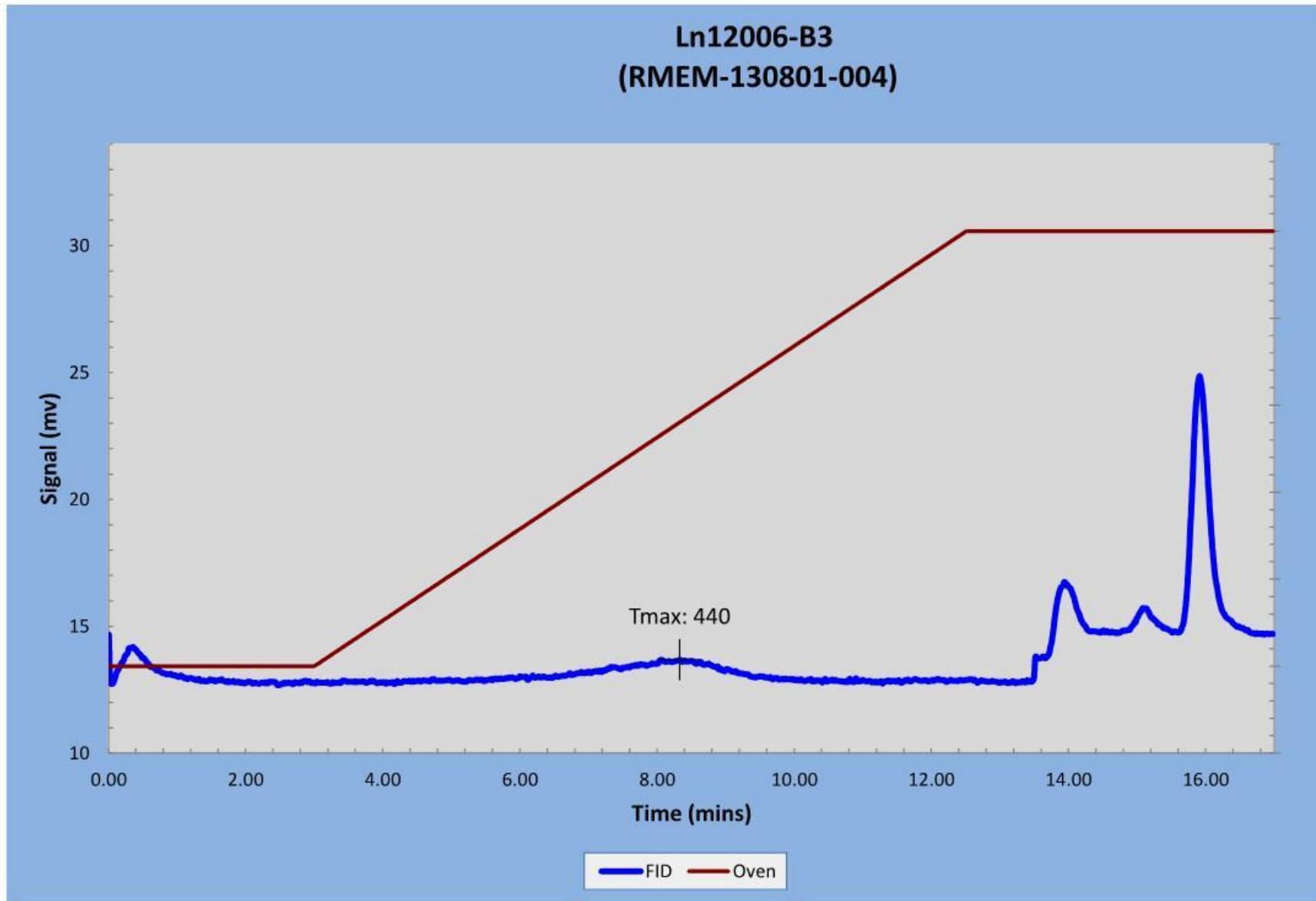


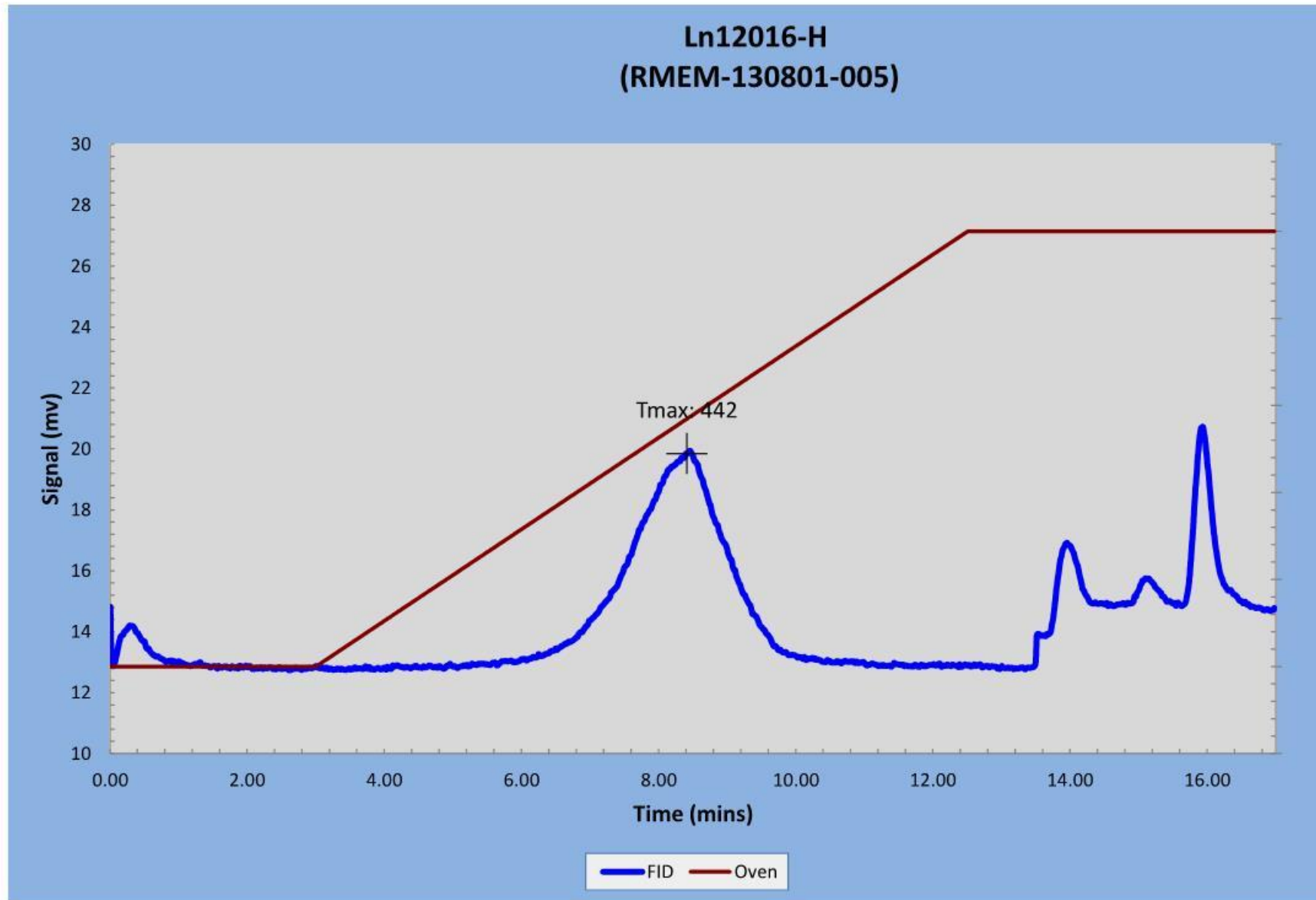


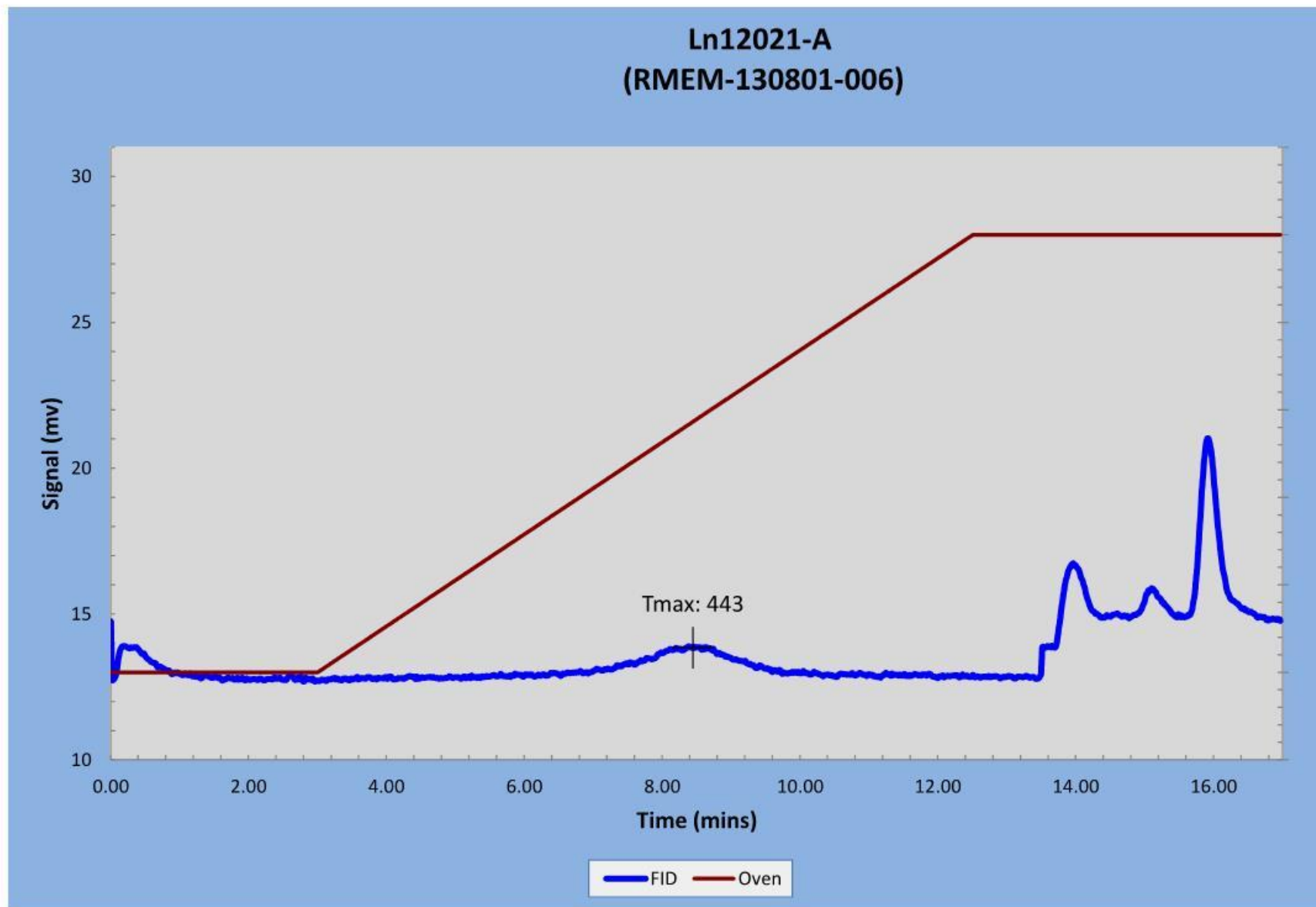




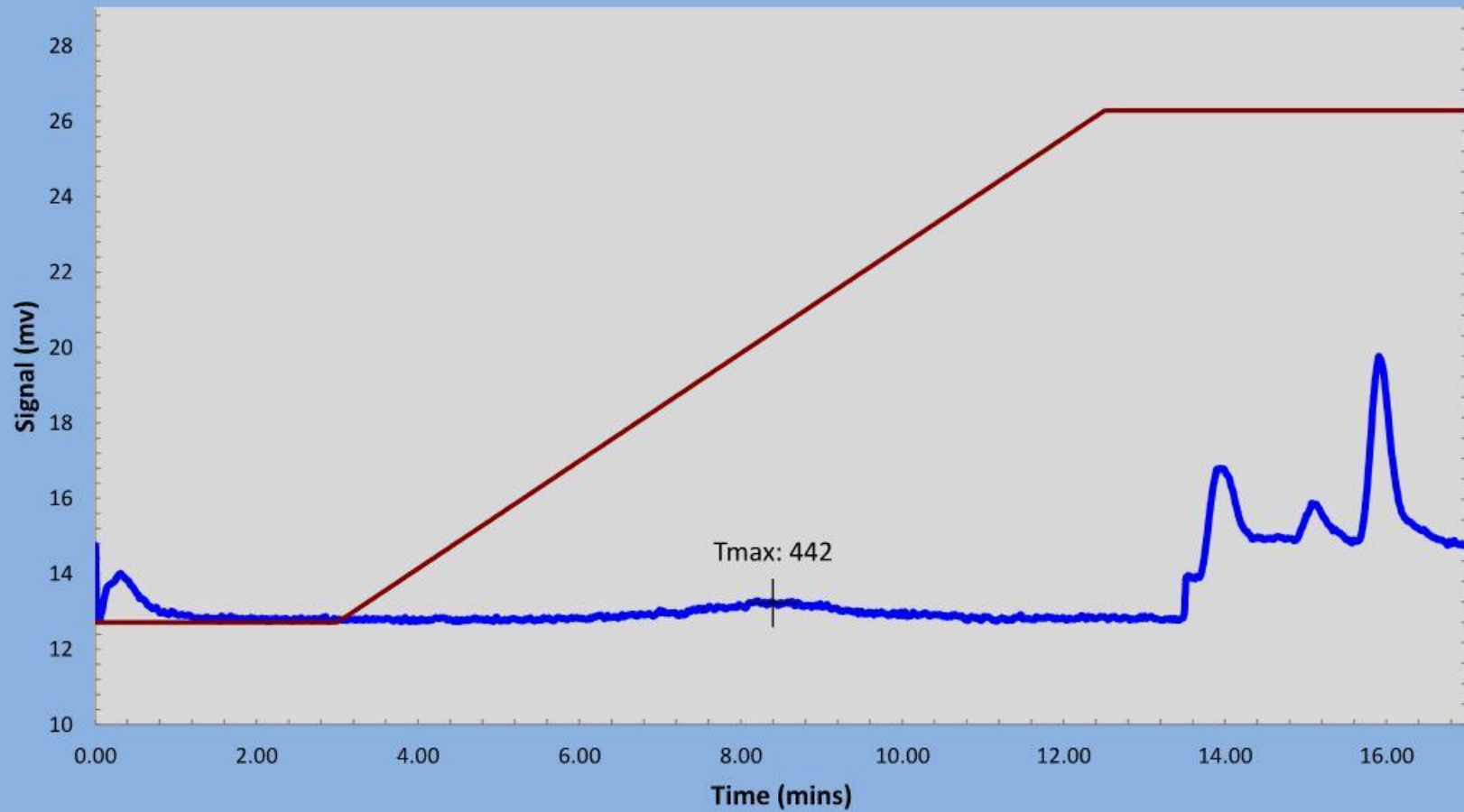




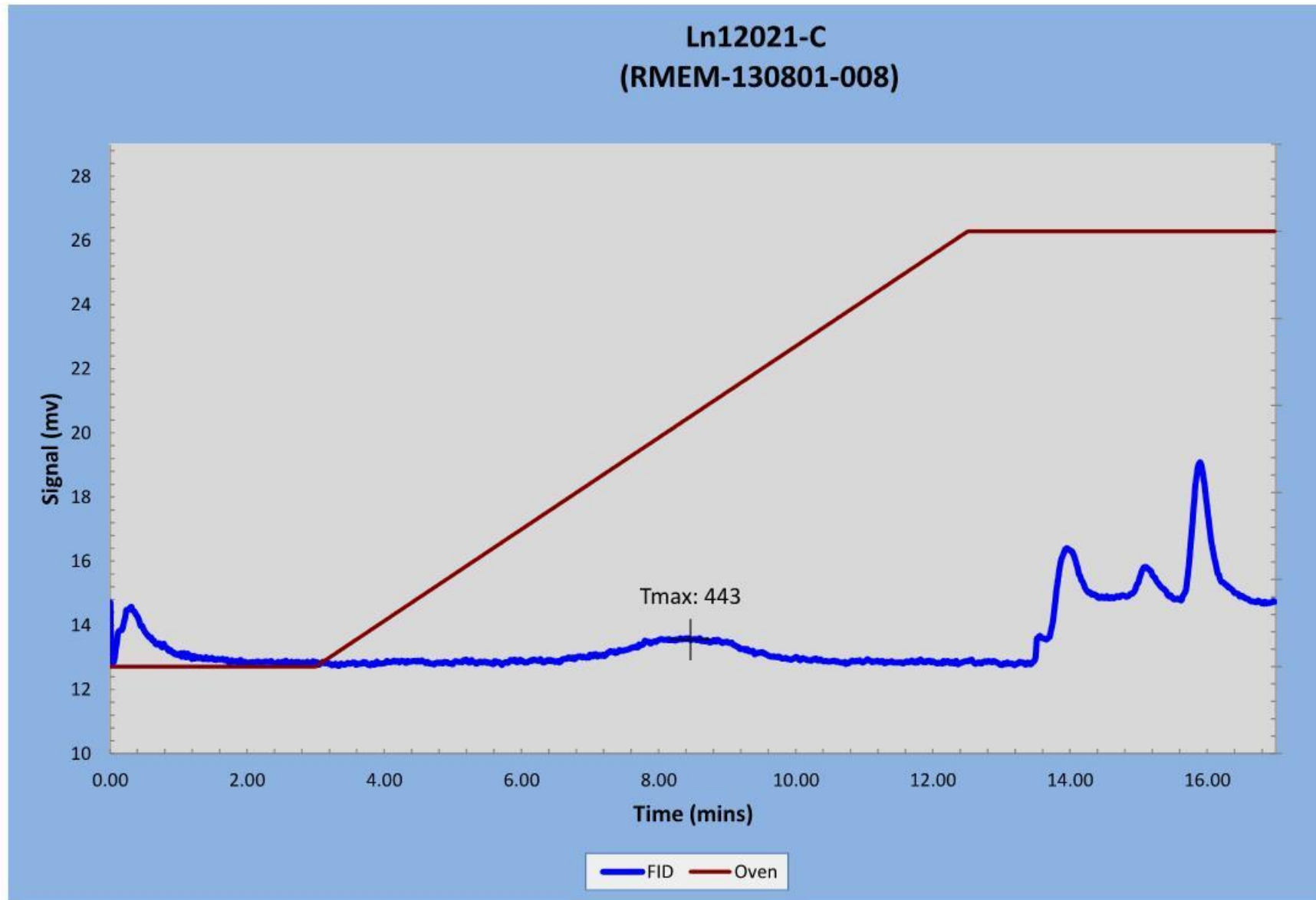




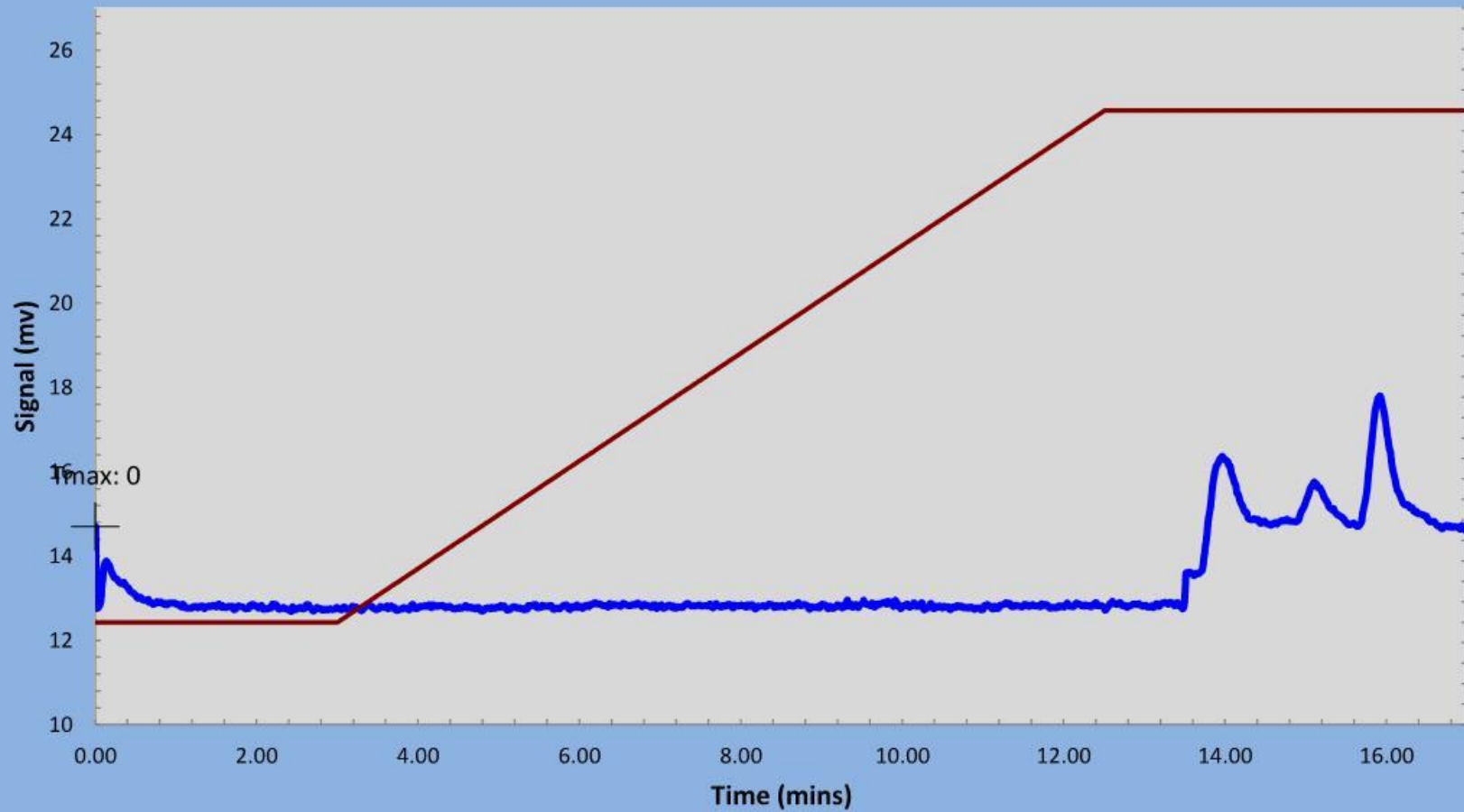
### Ln12021-B (RMEM-130801-007)



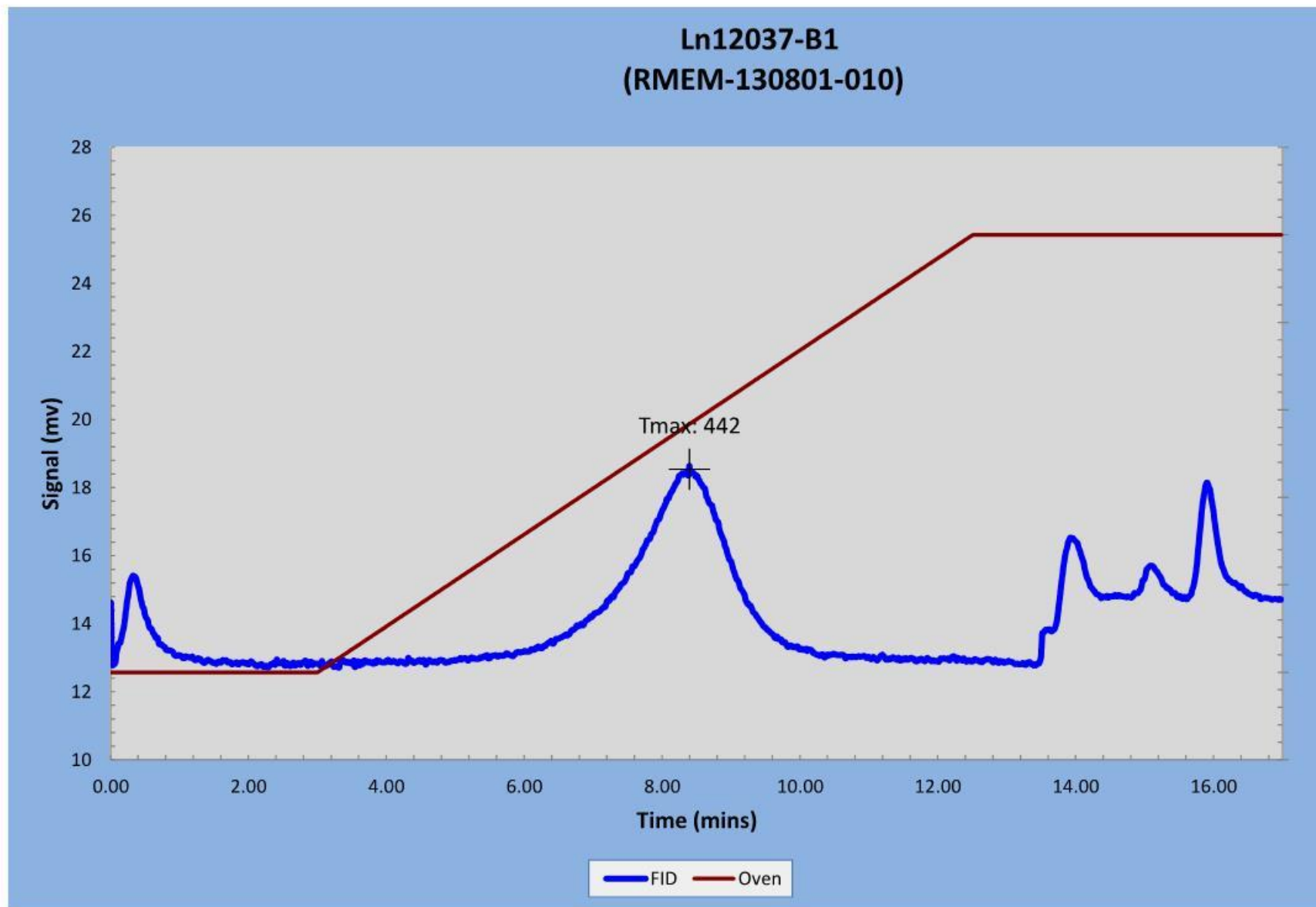
— FID — Oven

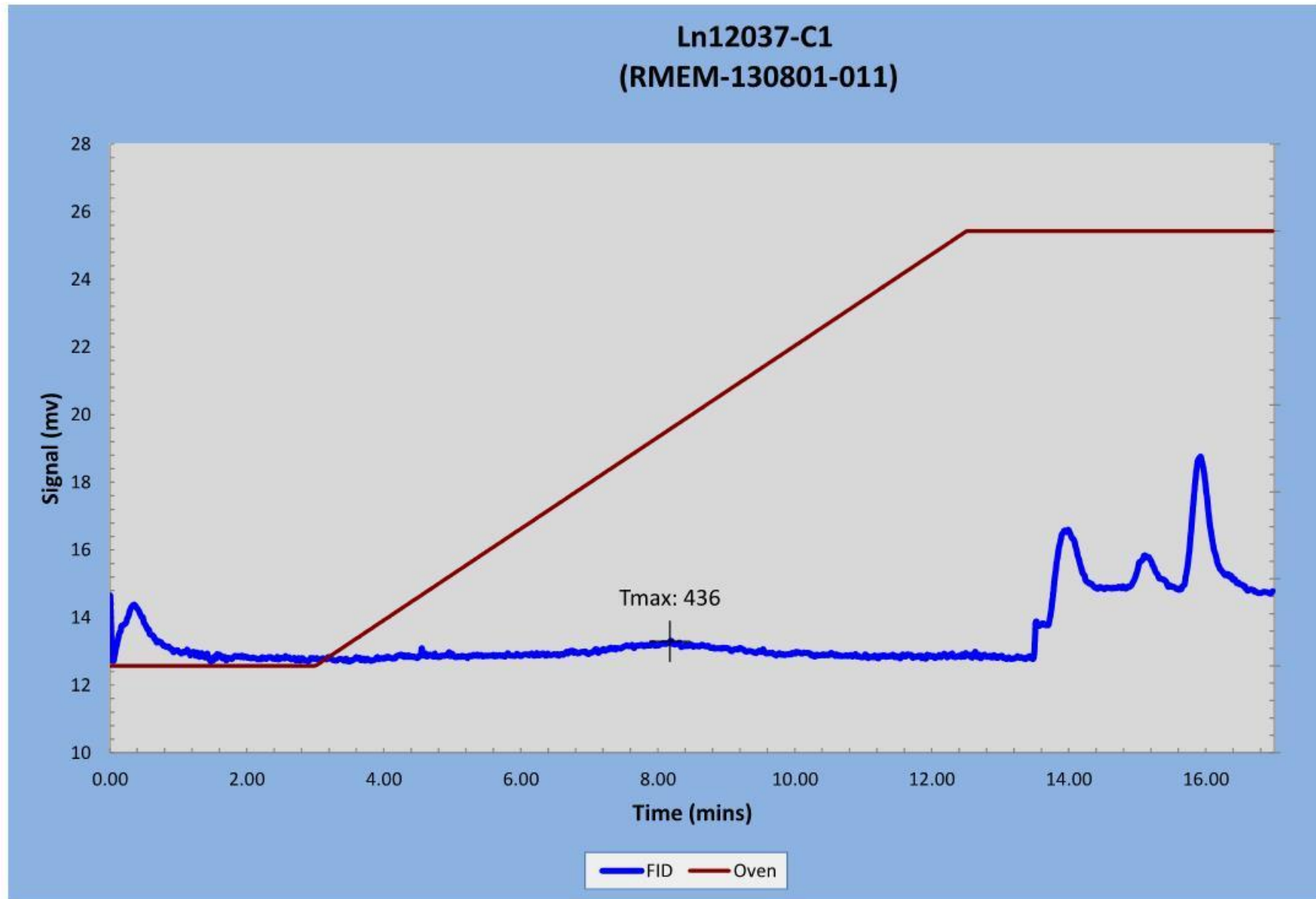


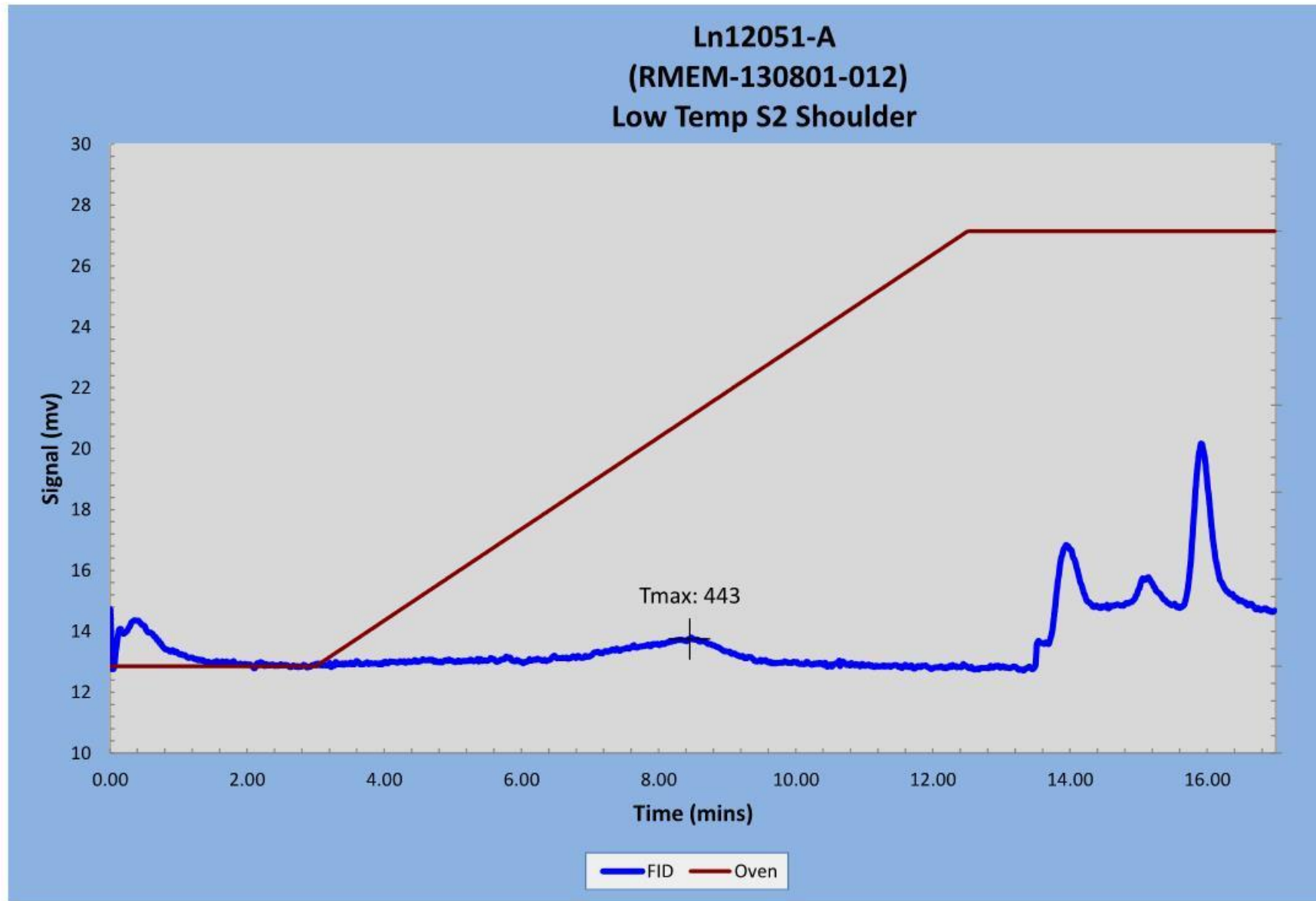
Ln12037-A1  
(RMEM-130801-009)

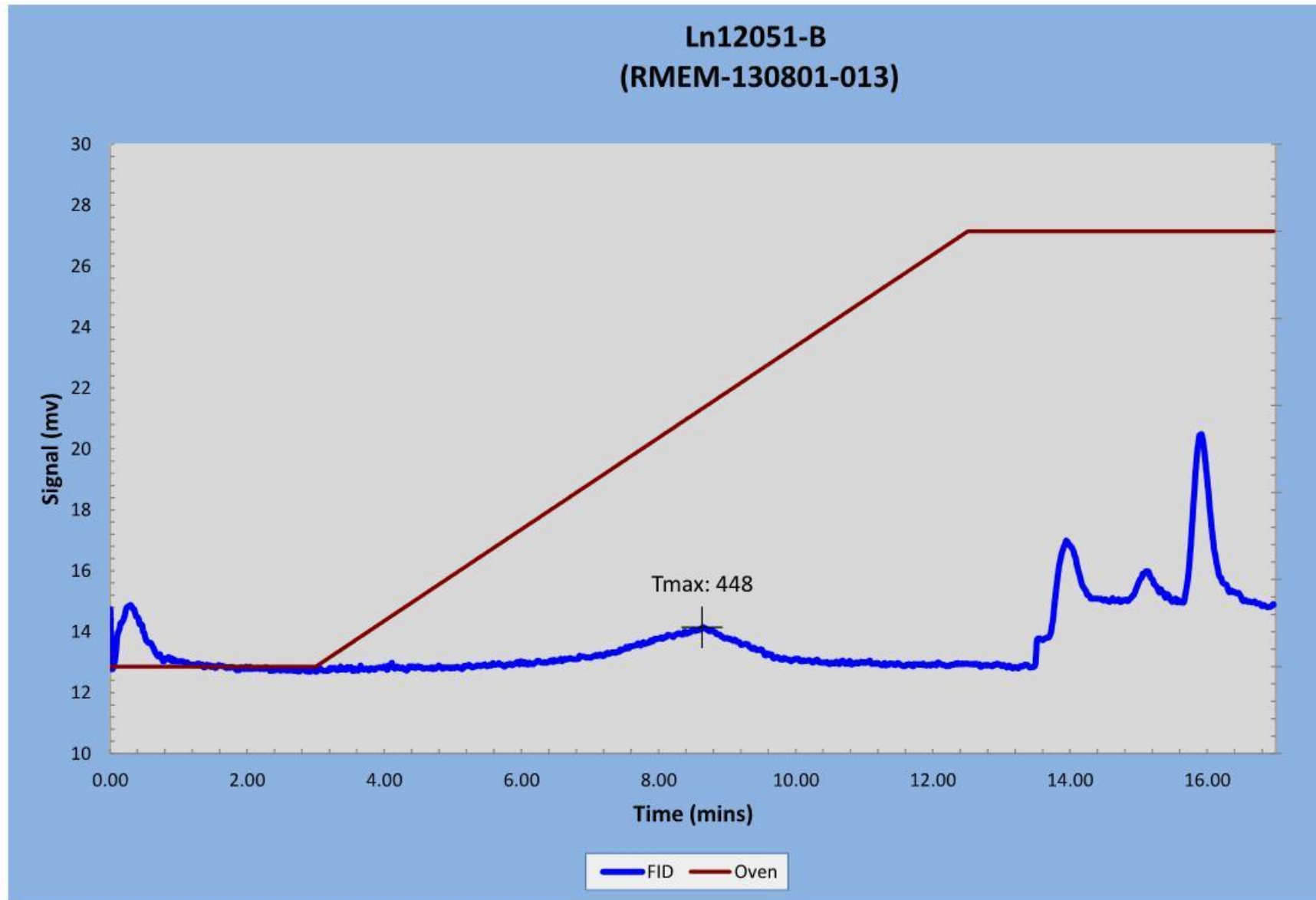


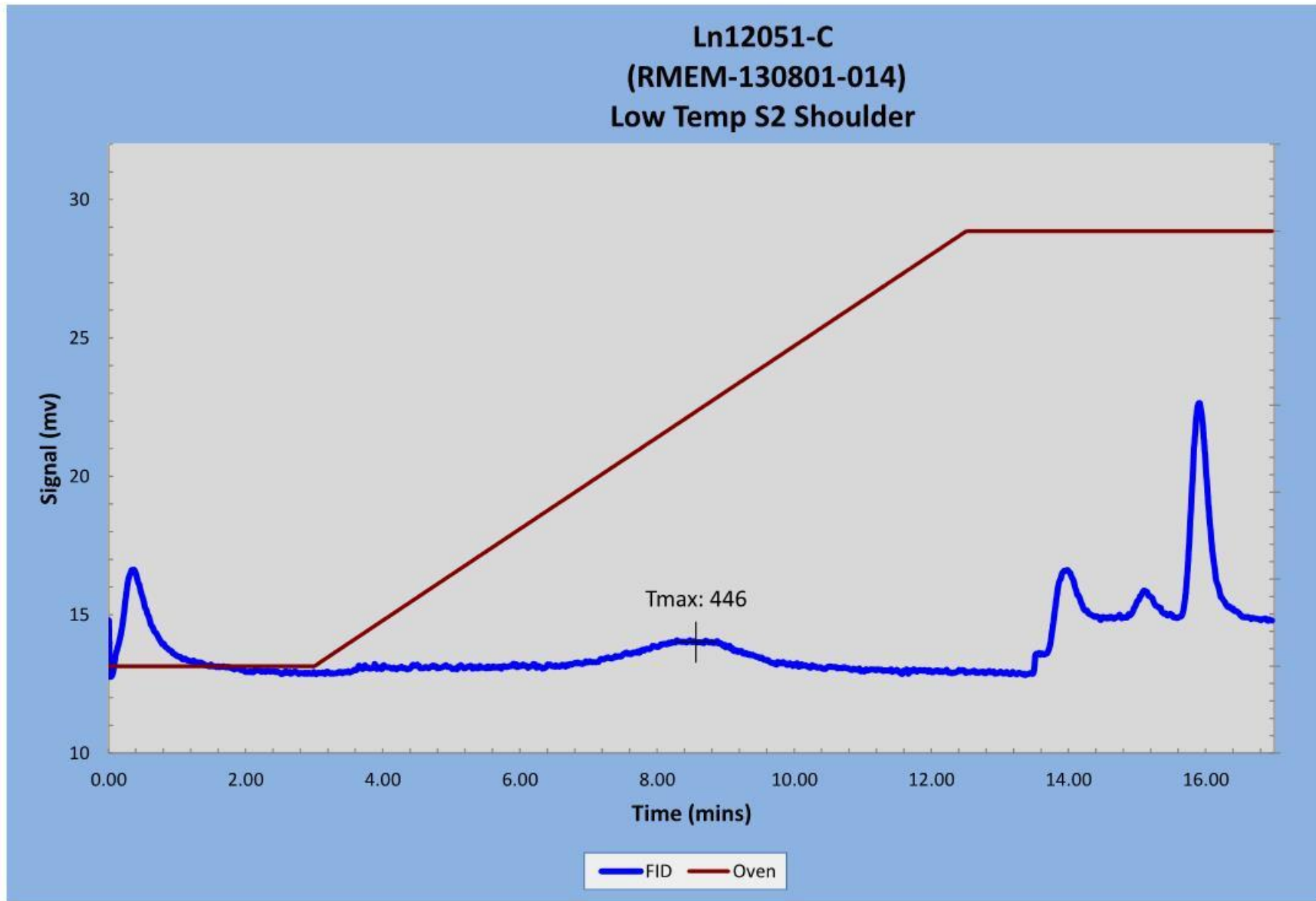
FID Oven

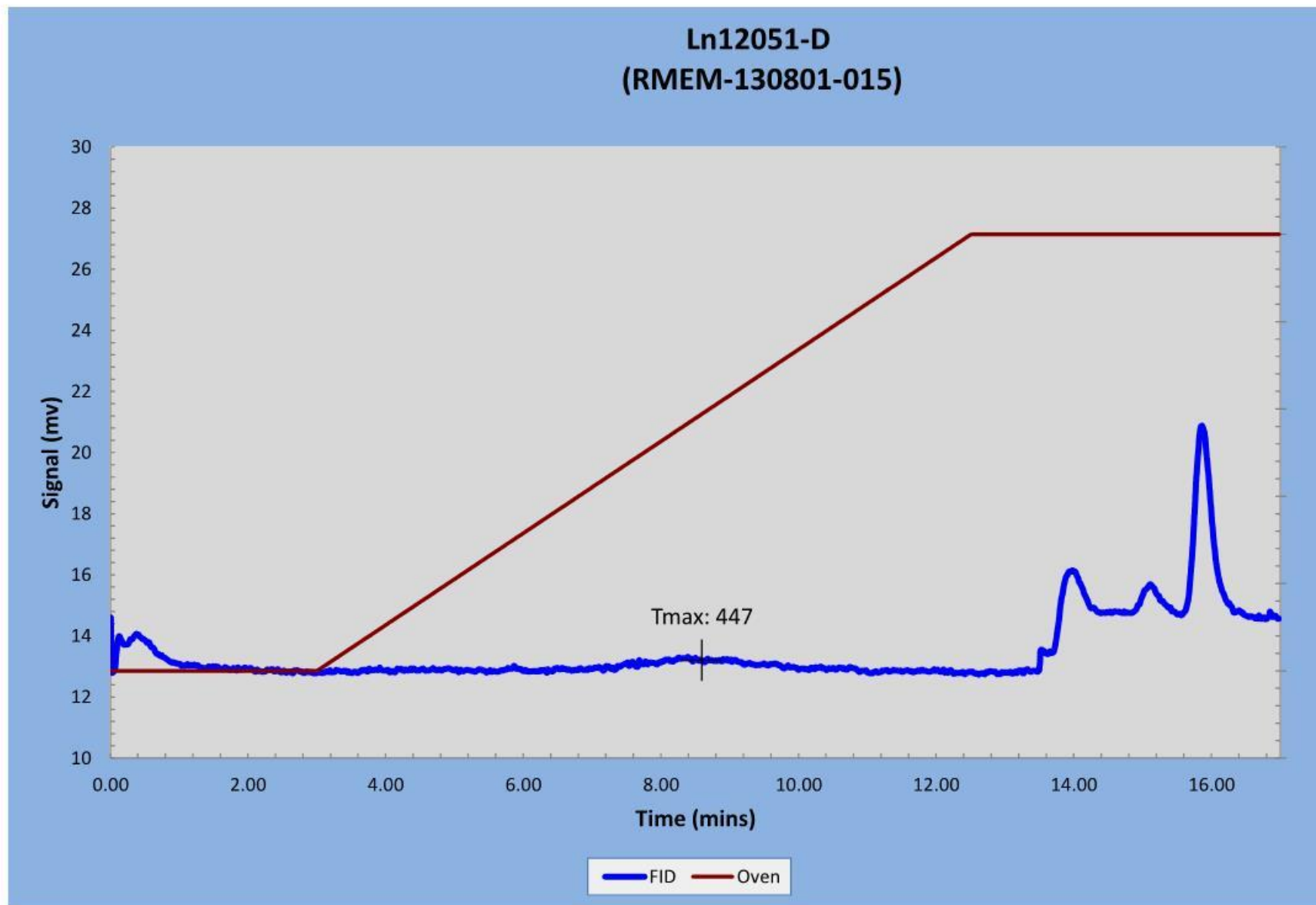


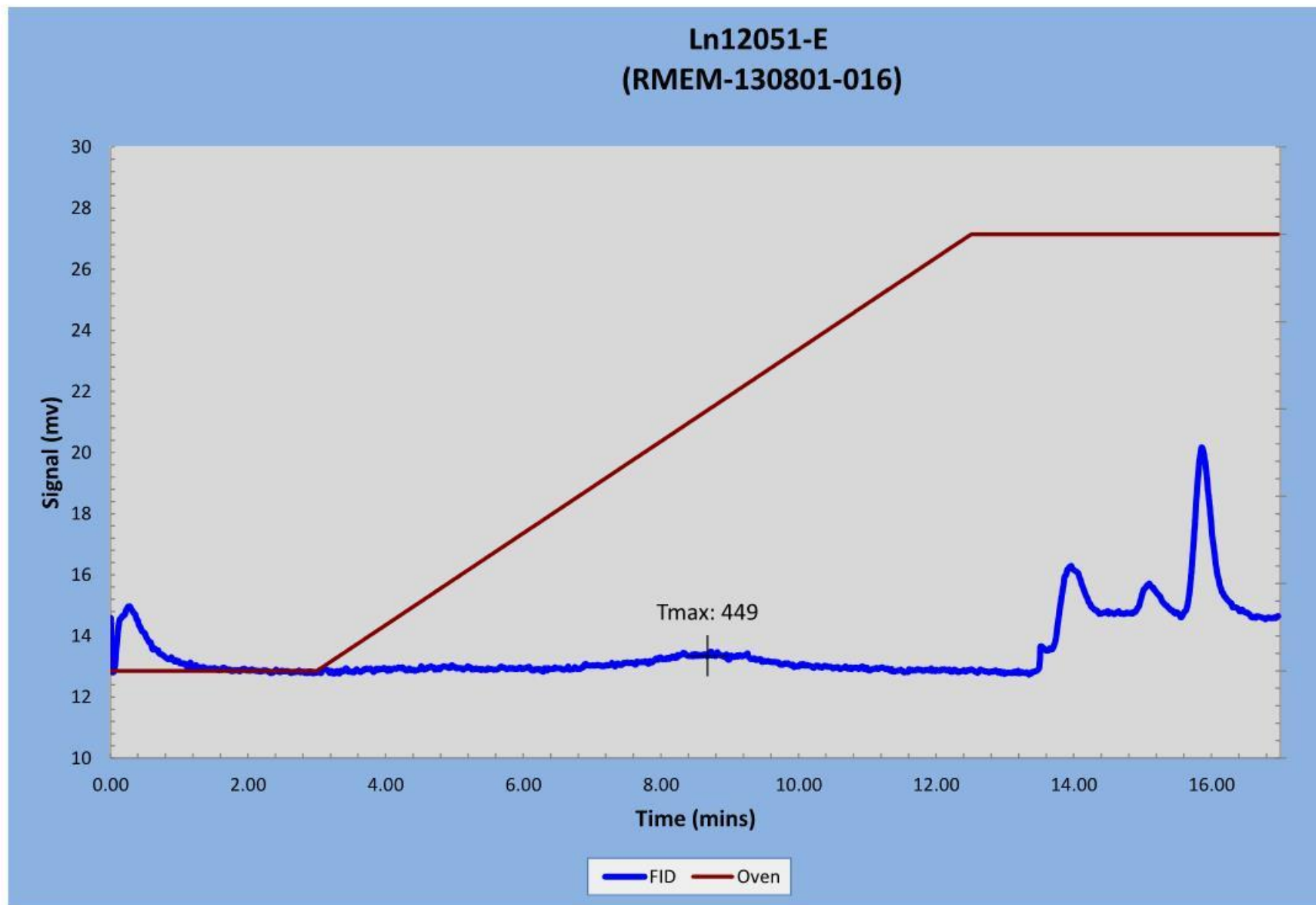




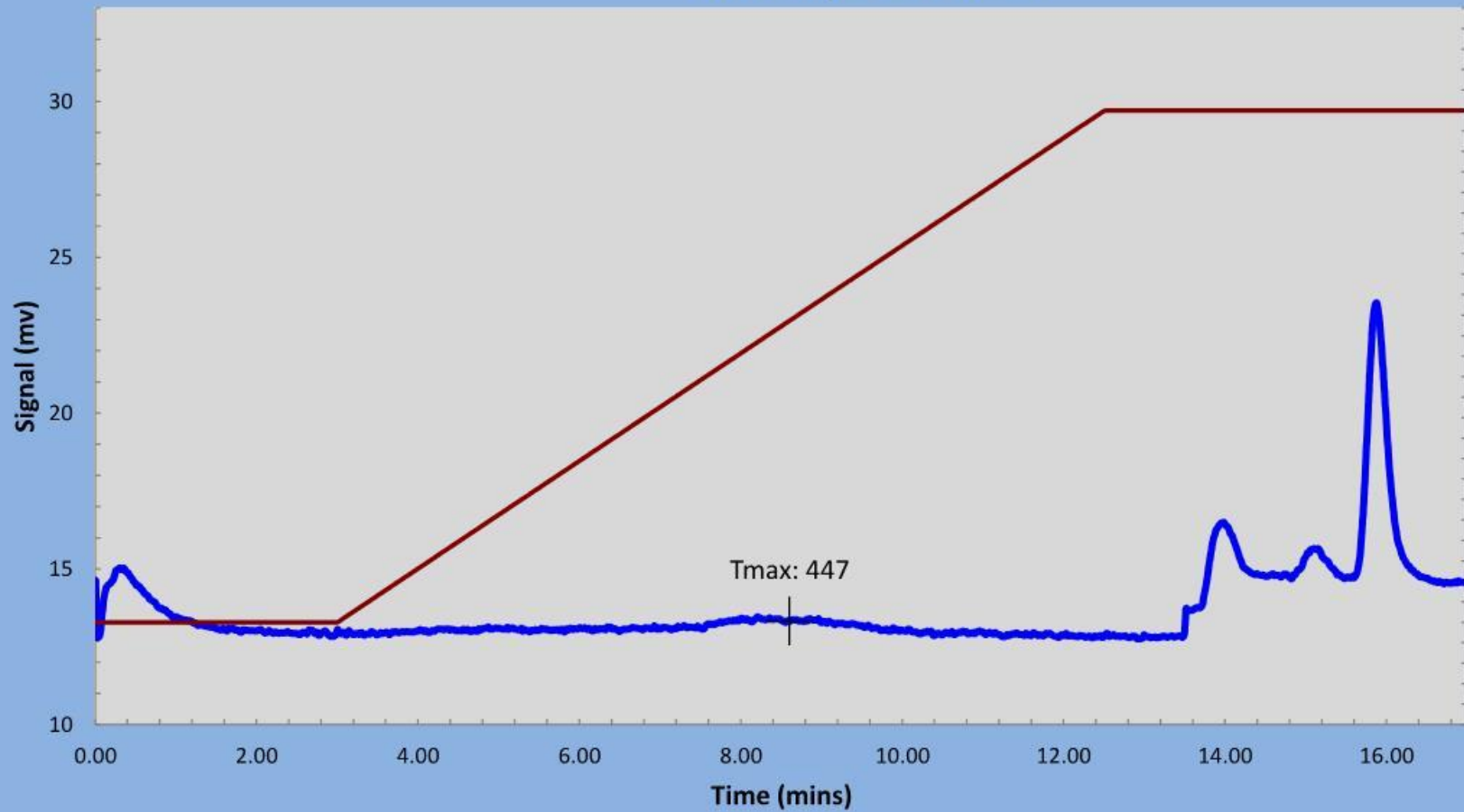




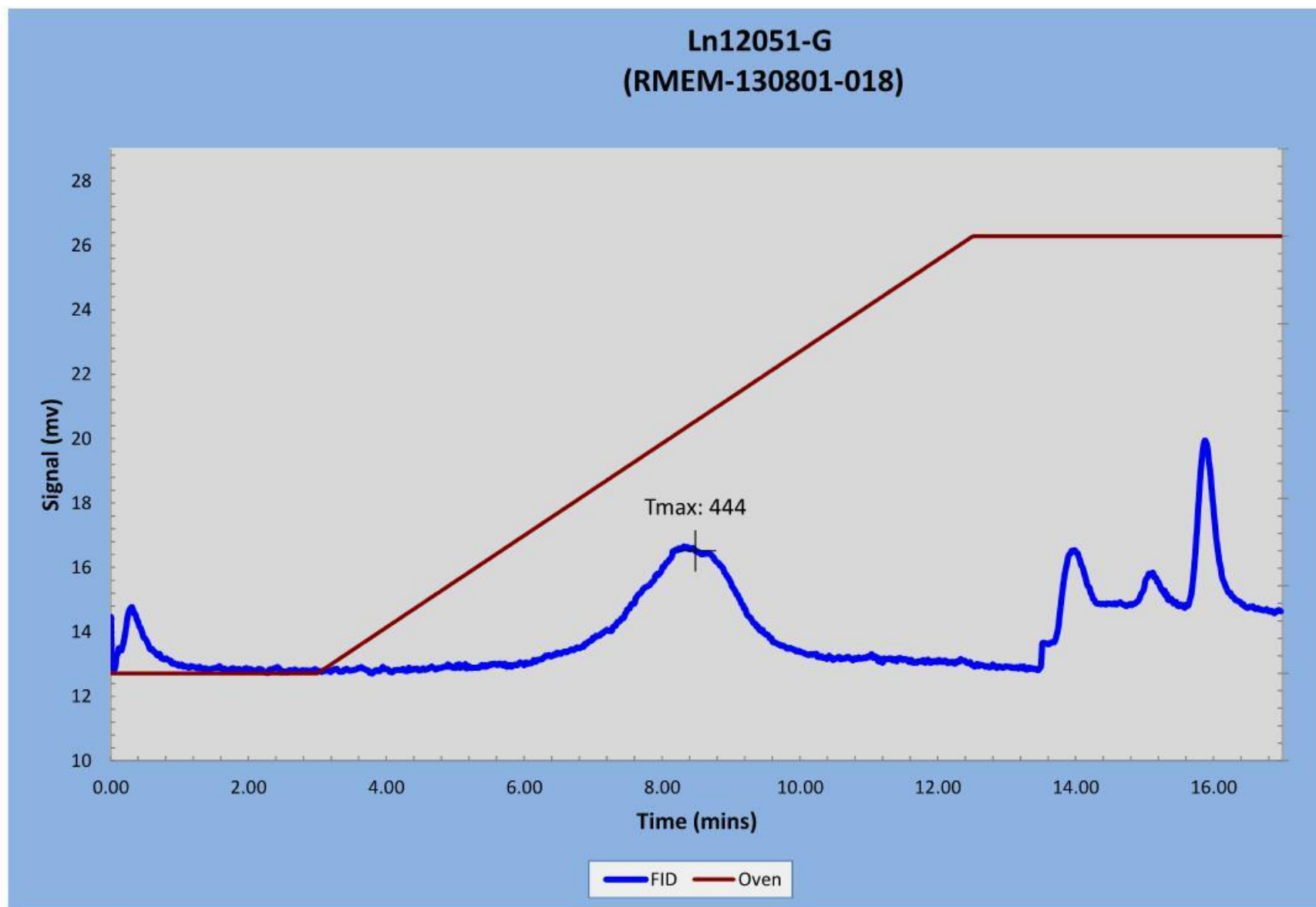


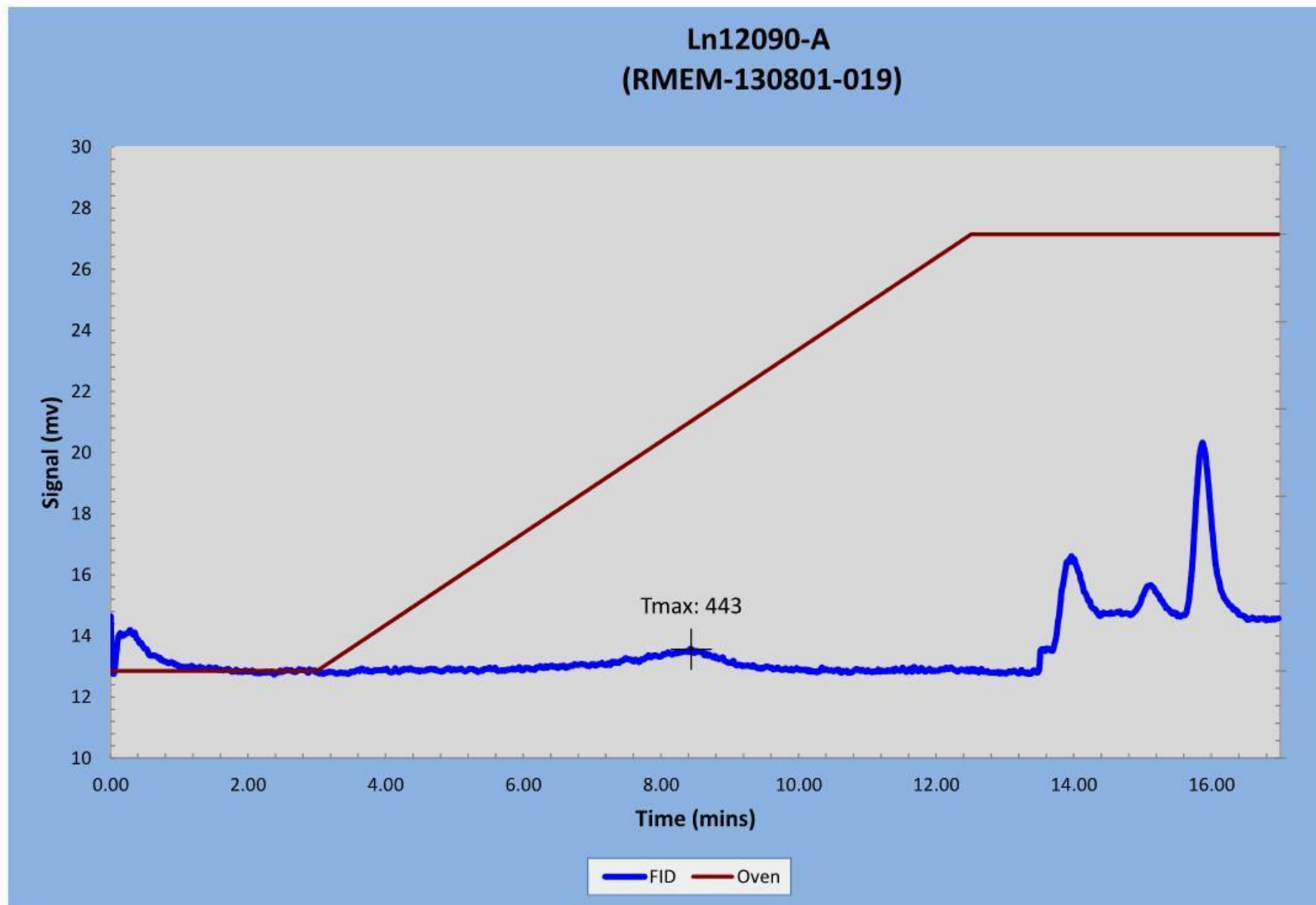


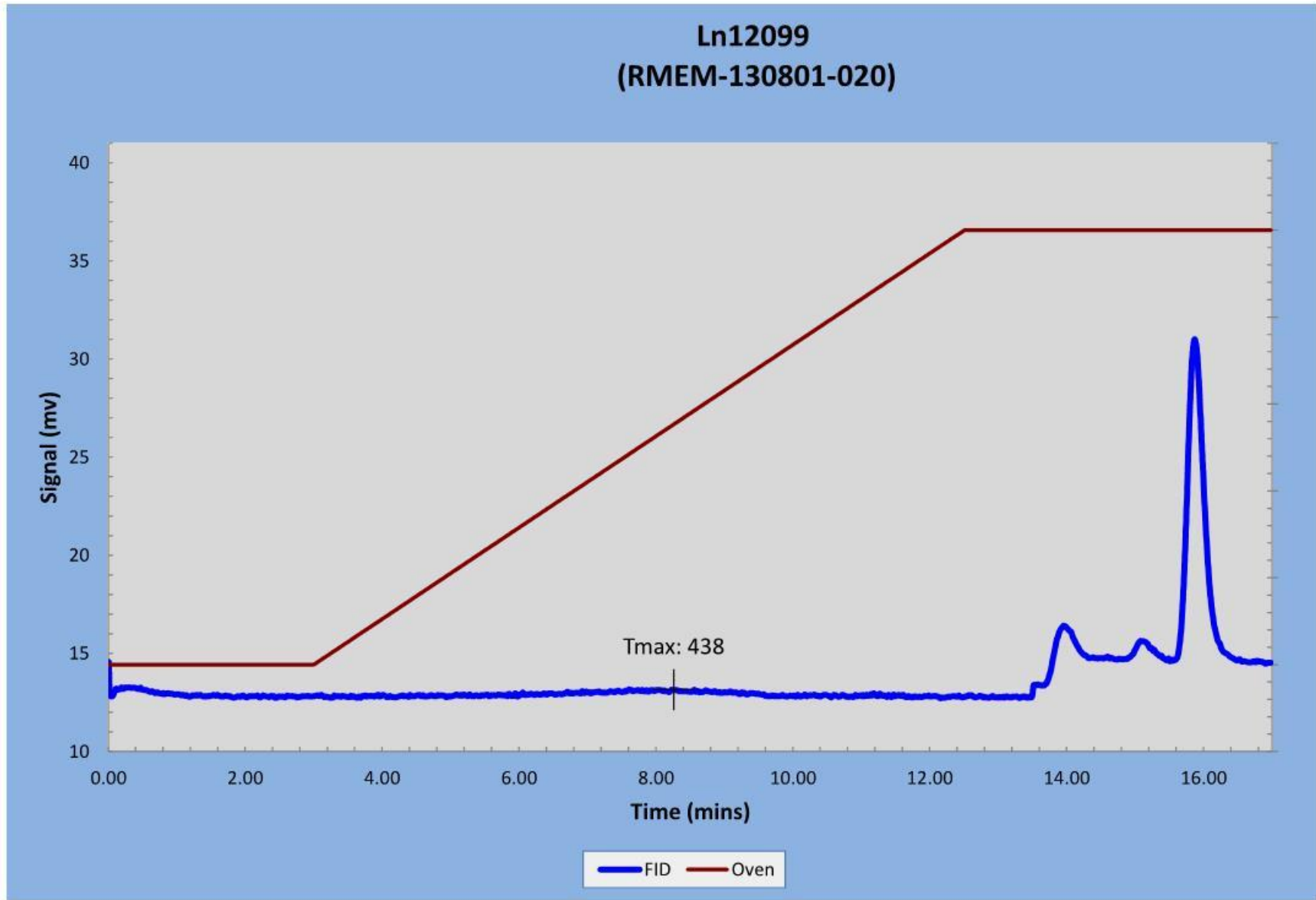
**Ln12051-F**  
**(RMEM-130801-017)**  
**Low Temp S2 Shoulder**



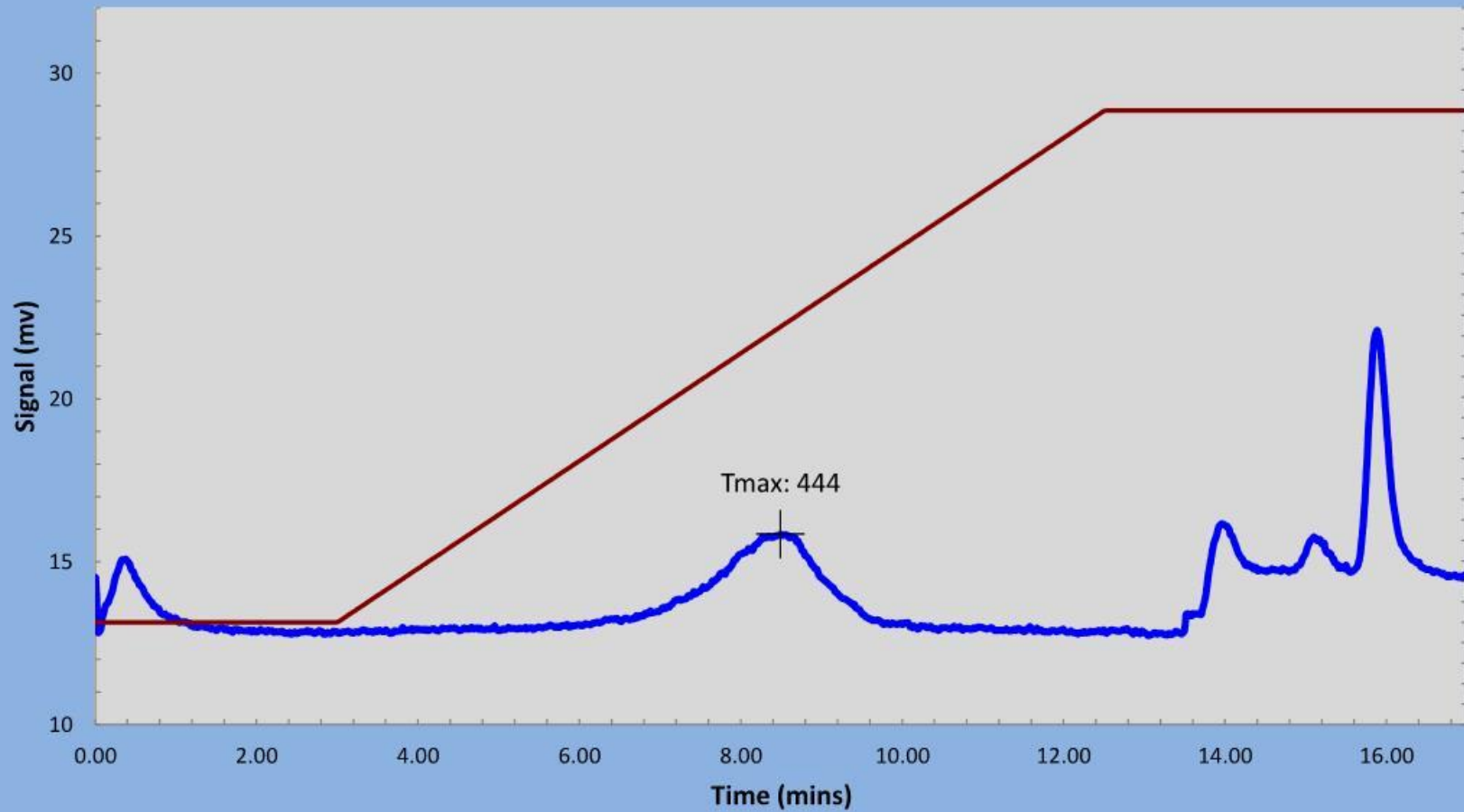
— FID — Oven



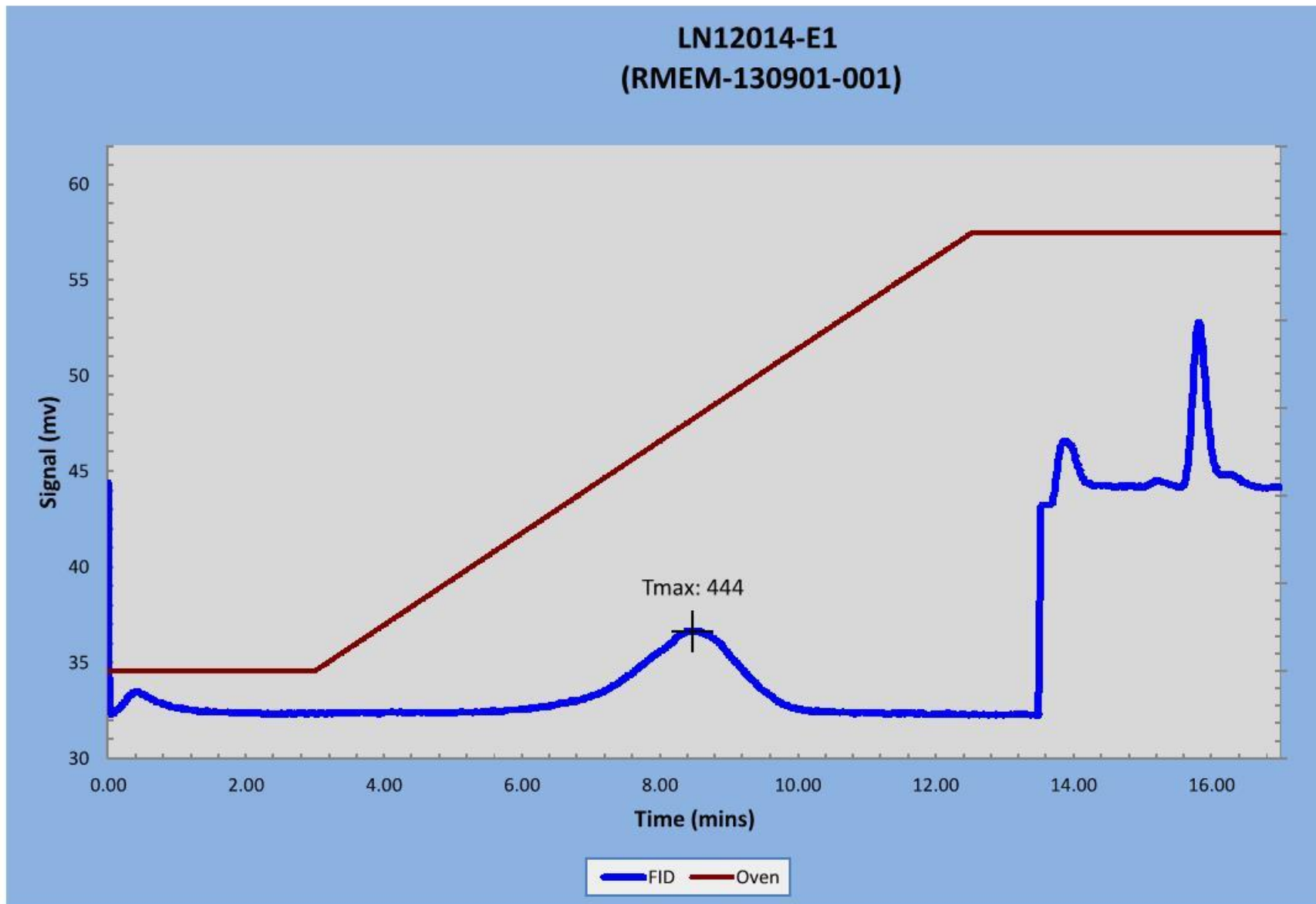


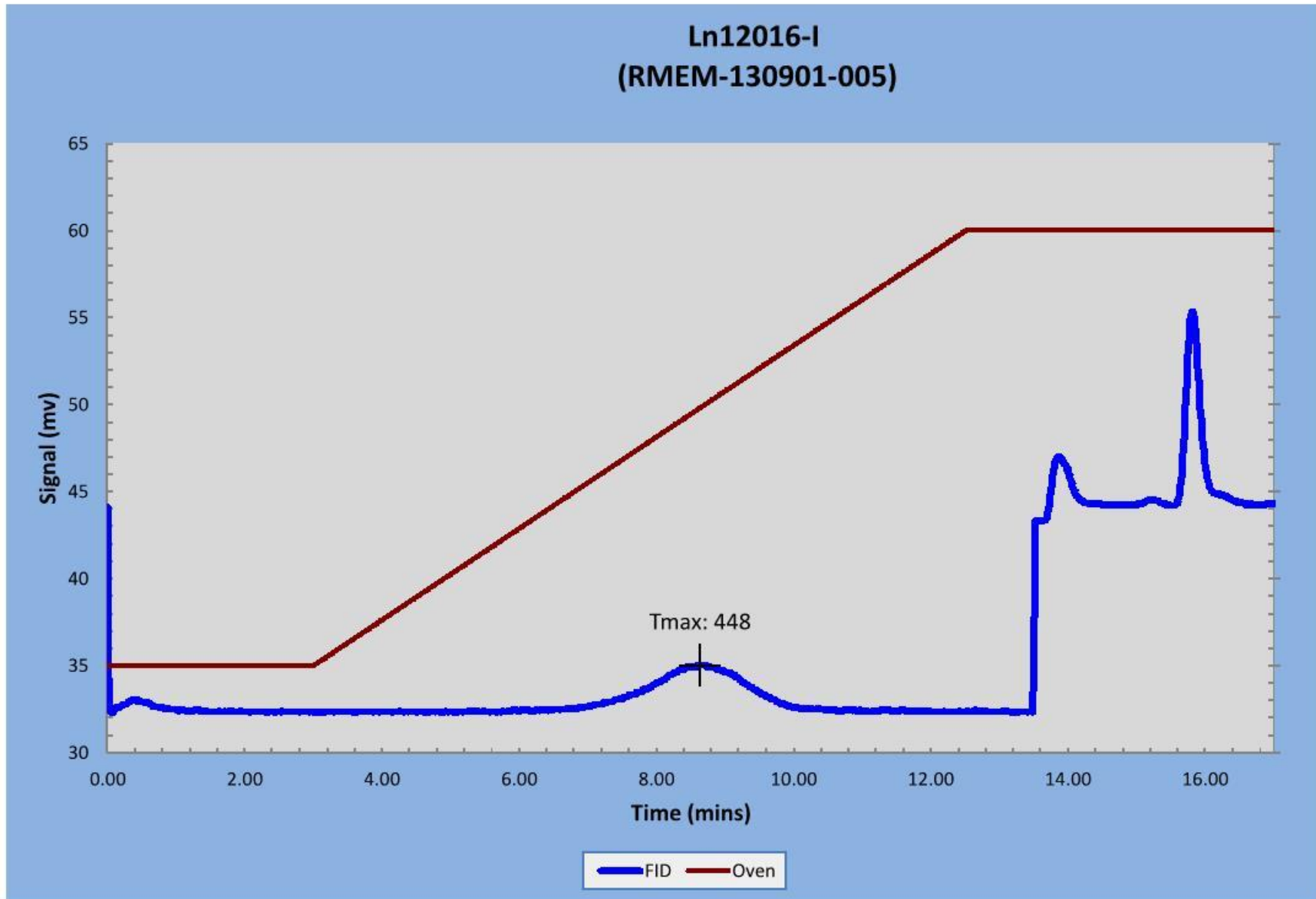


**Ln12099-B  
(RMEM-130801-021)**

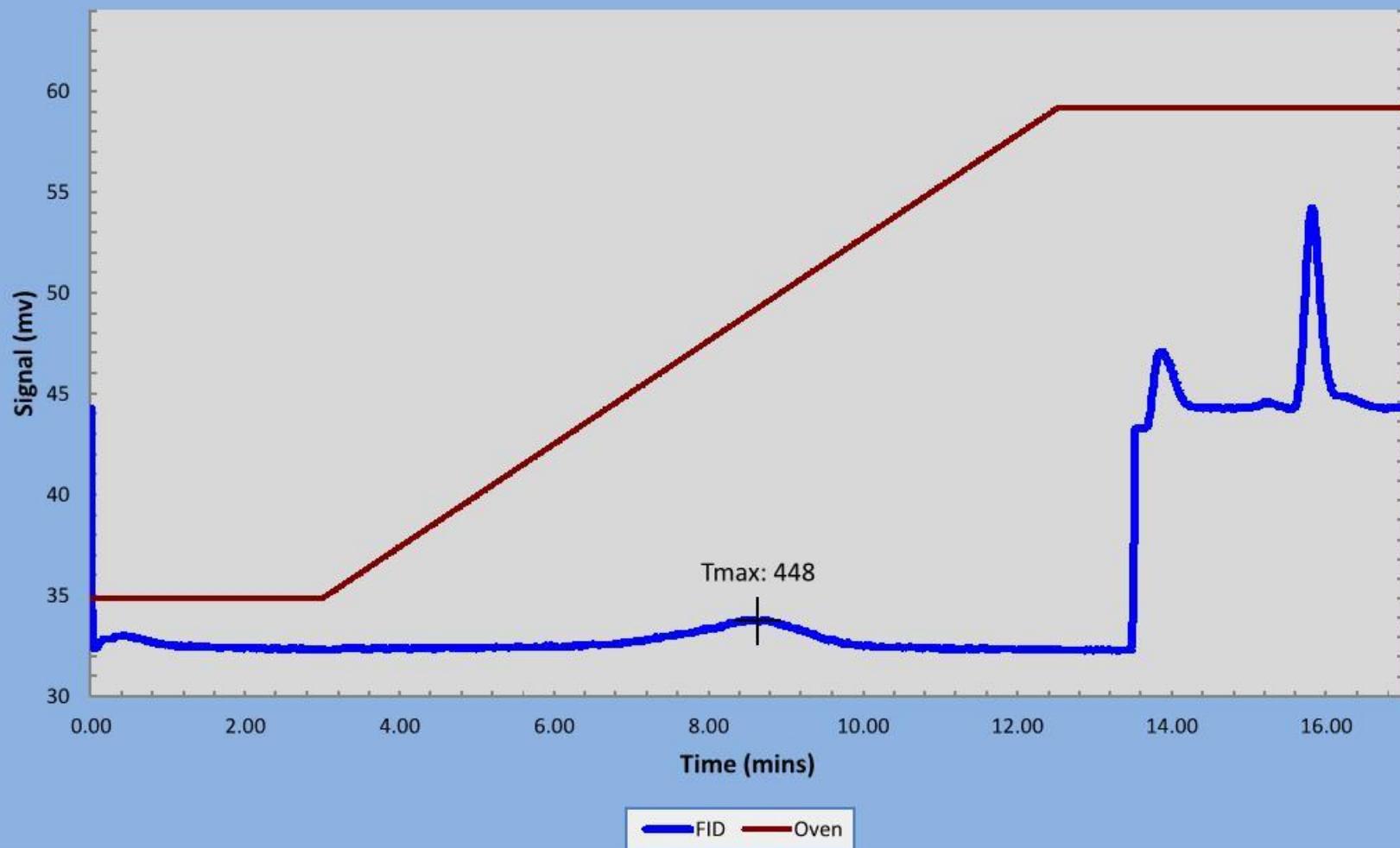


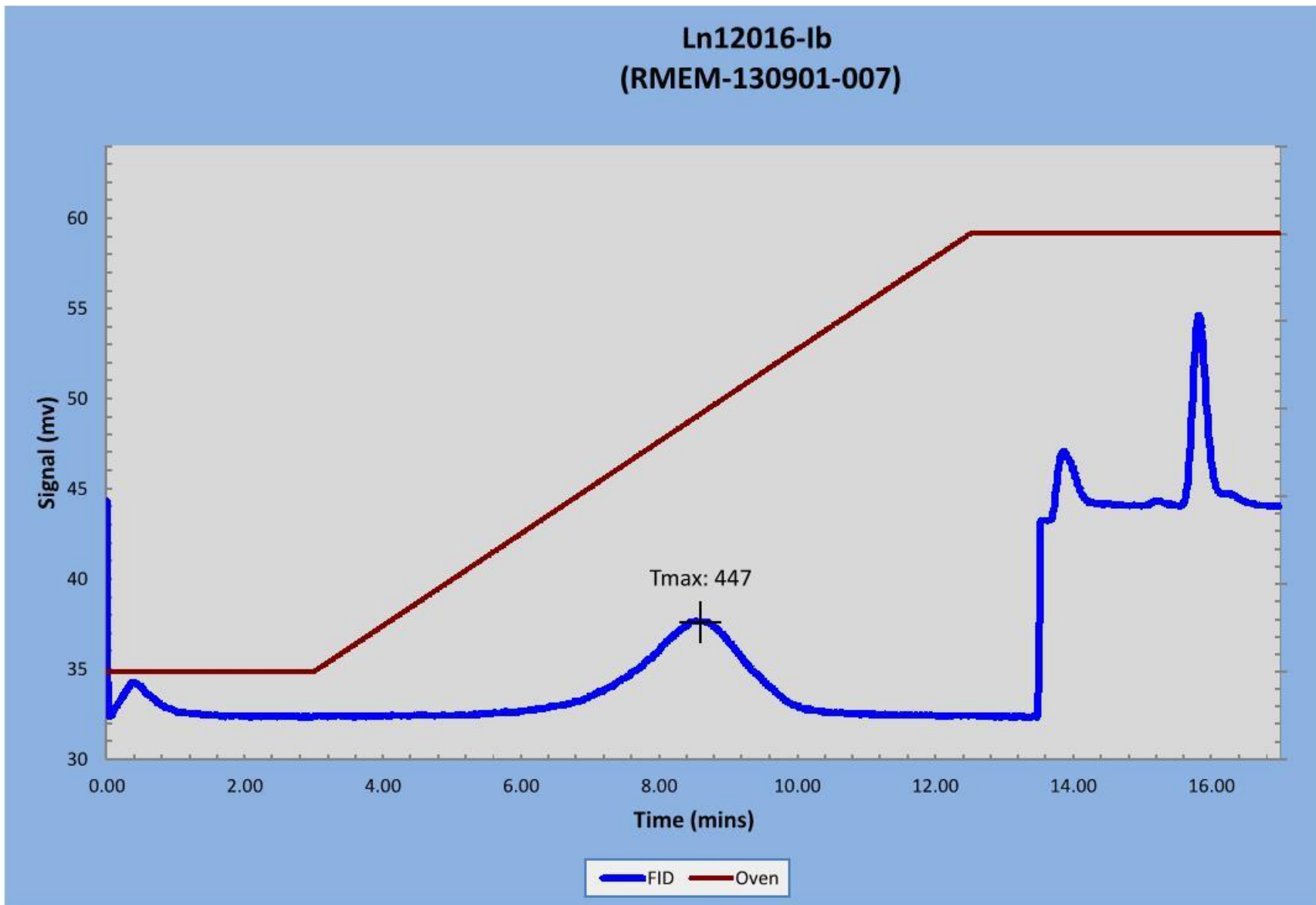
— FID — Oven

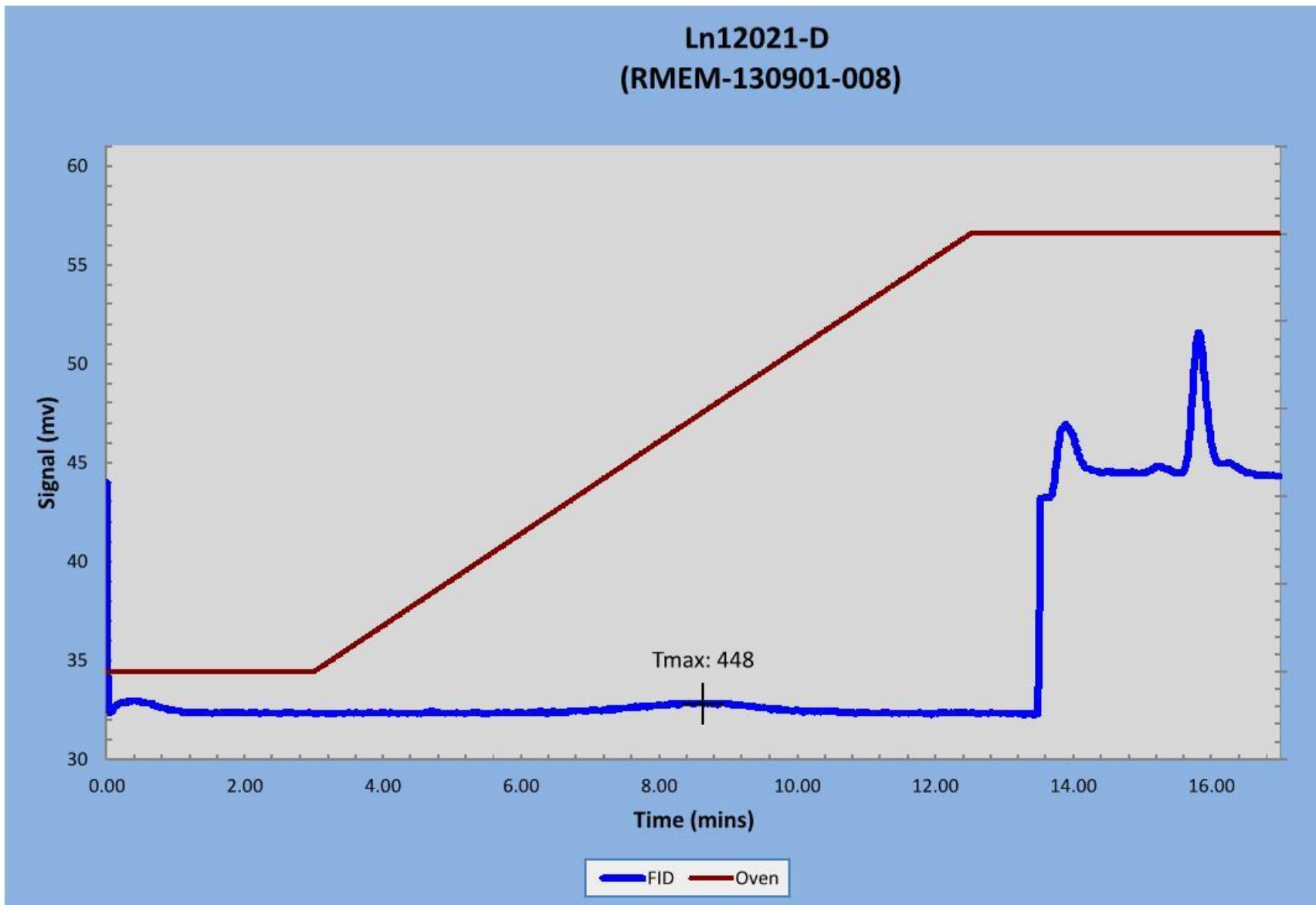




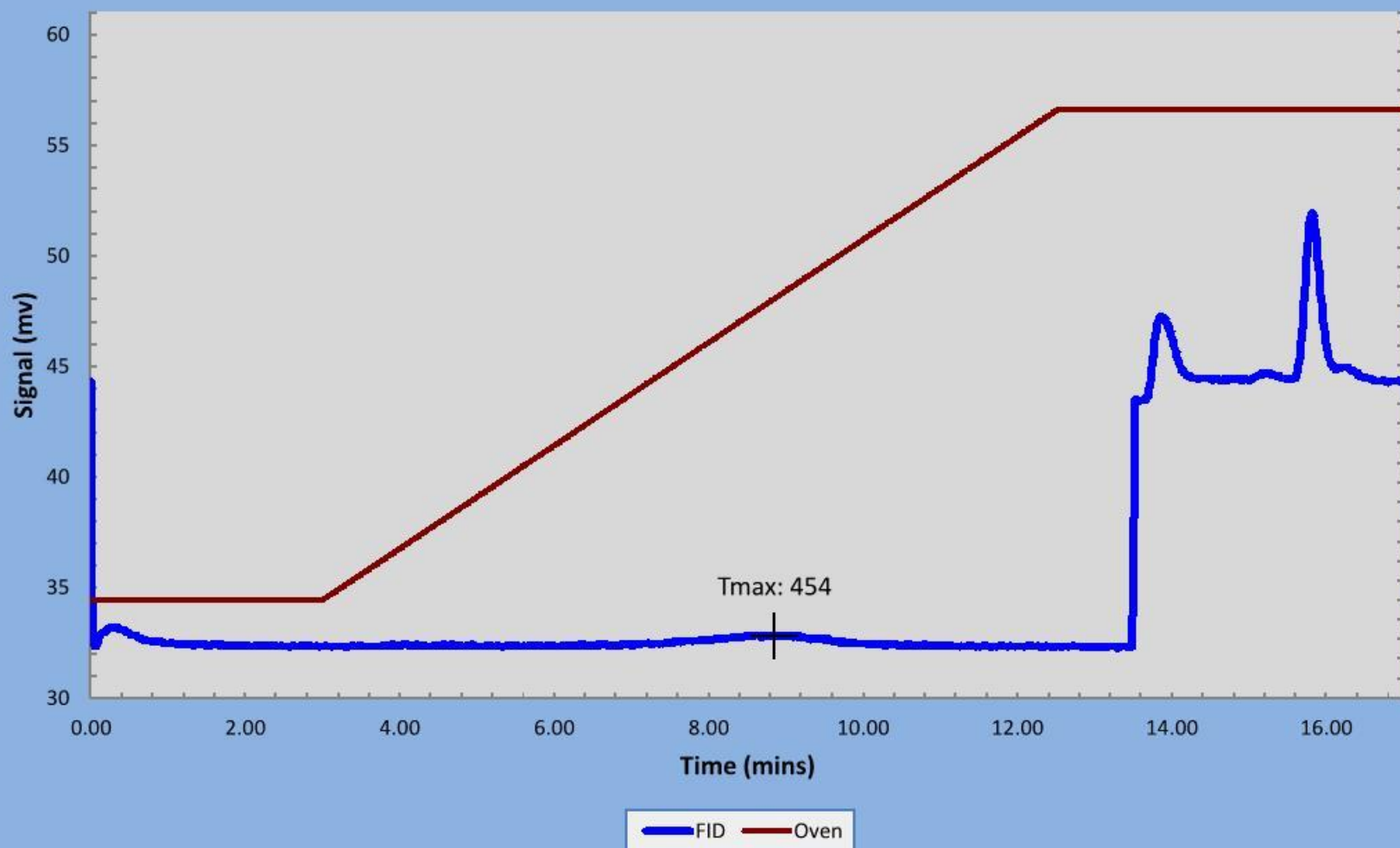
Ln12016-la  
(RMEM-130901-006)



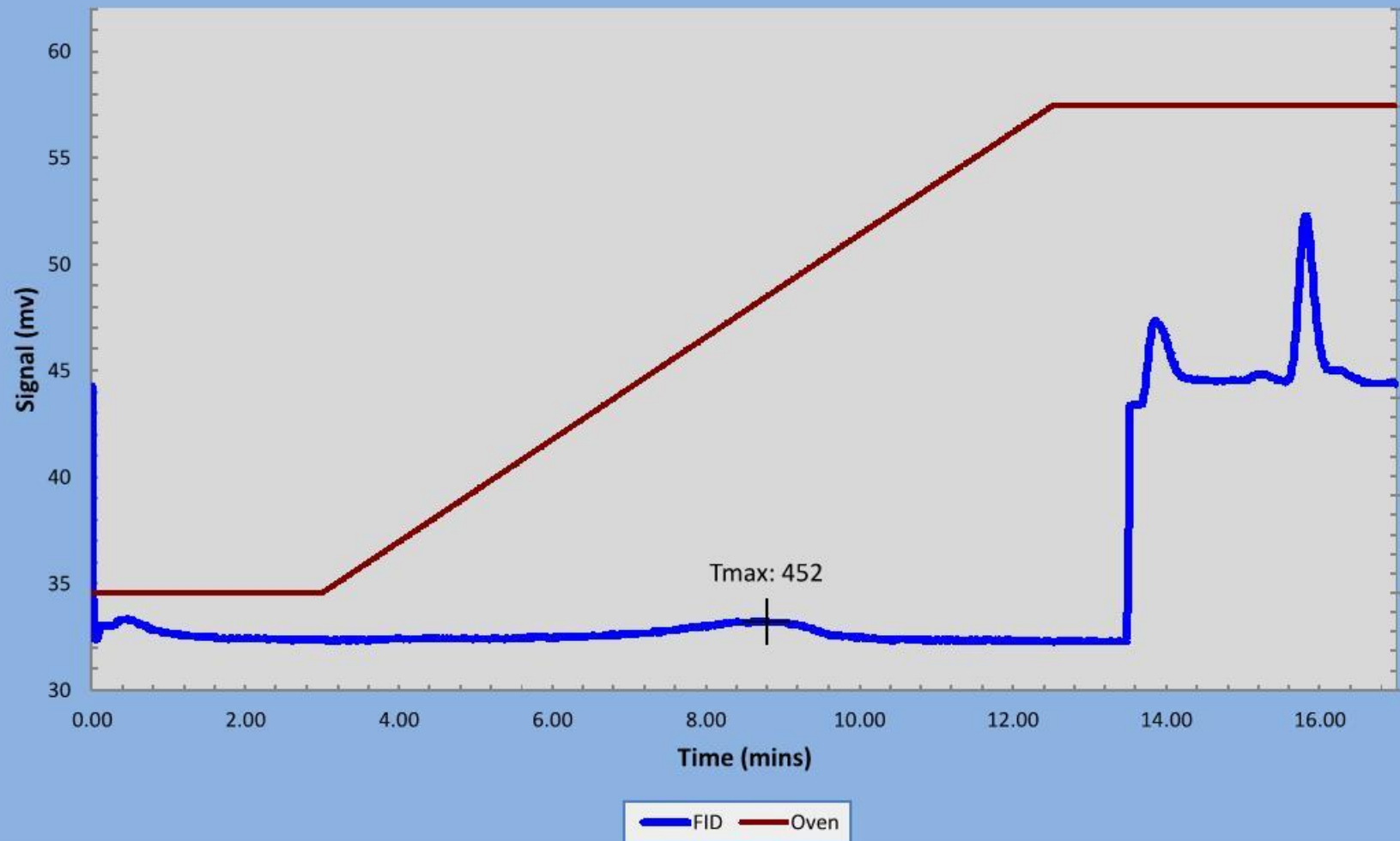




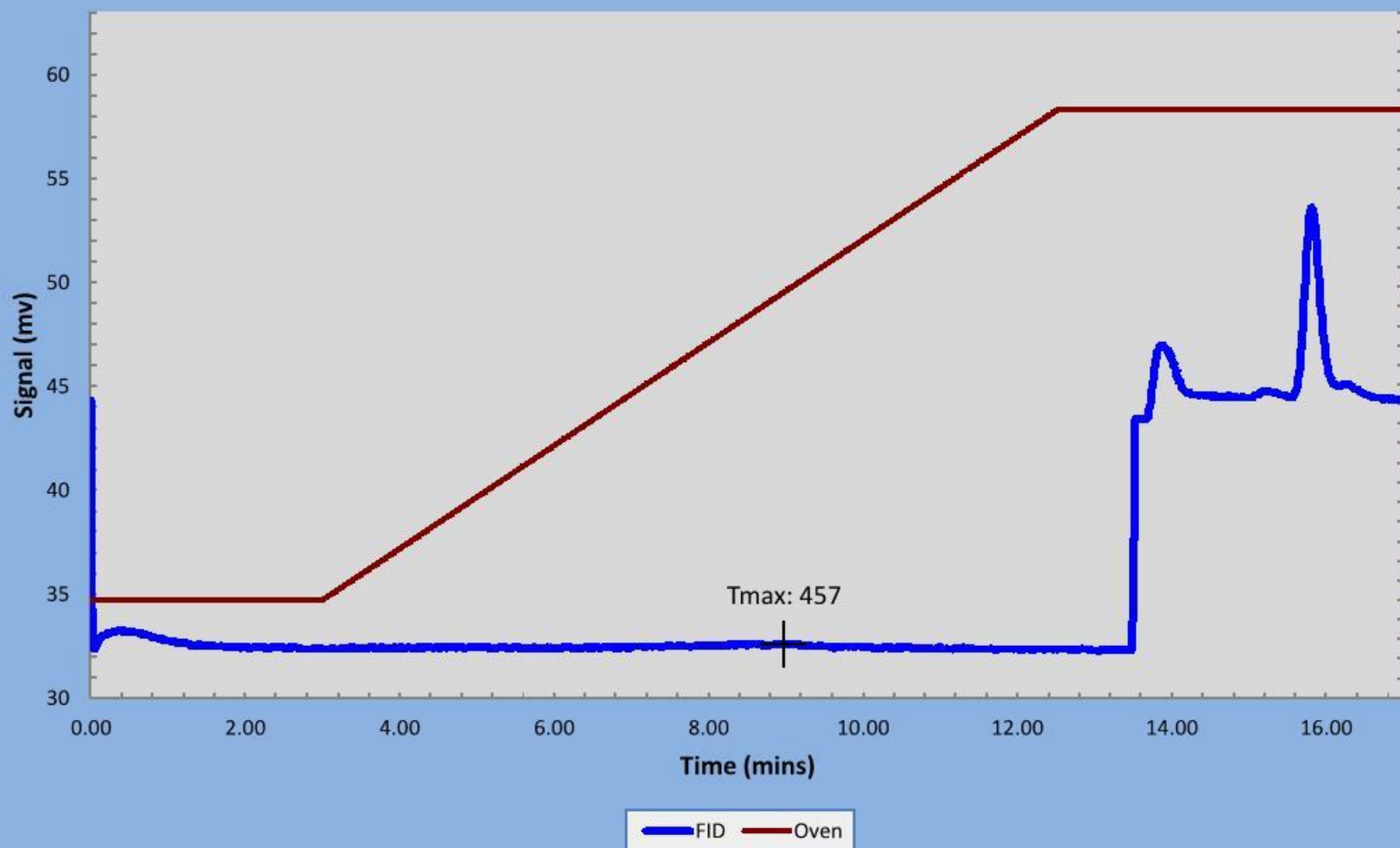
Ln12092-D  
(RMEM-130902-003)

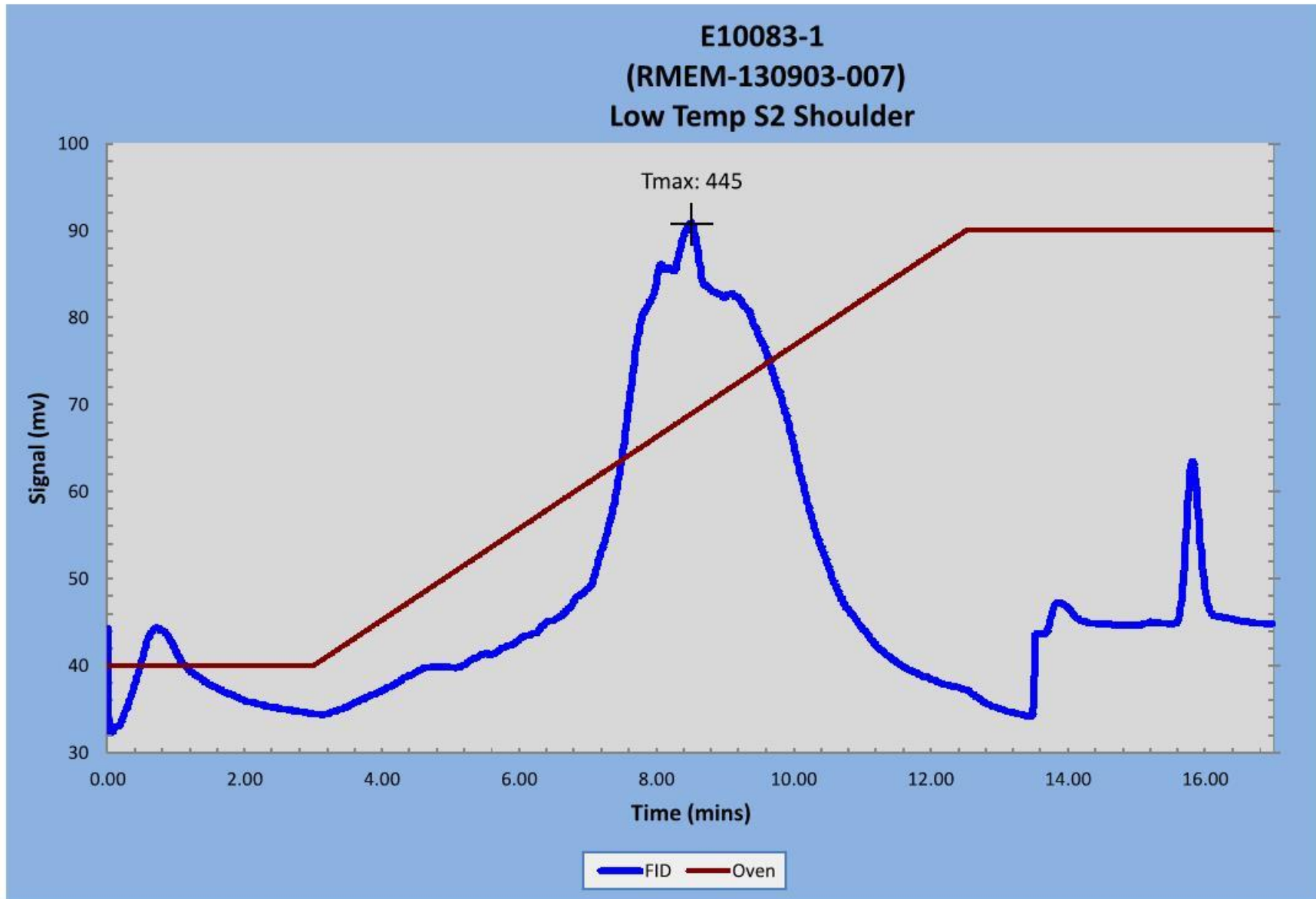


E10077-2  
(RMEM-130903-004)

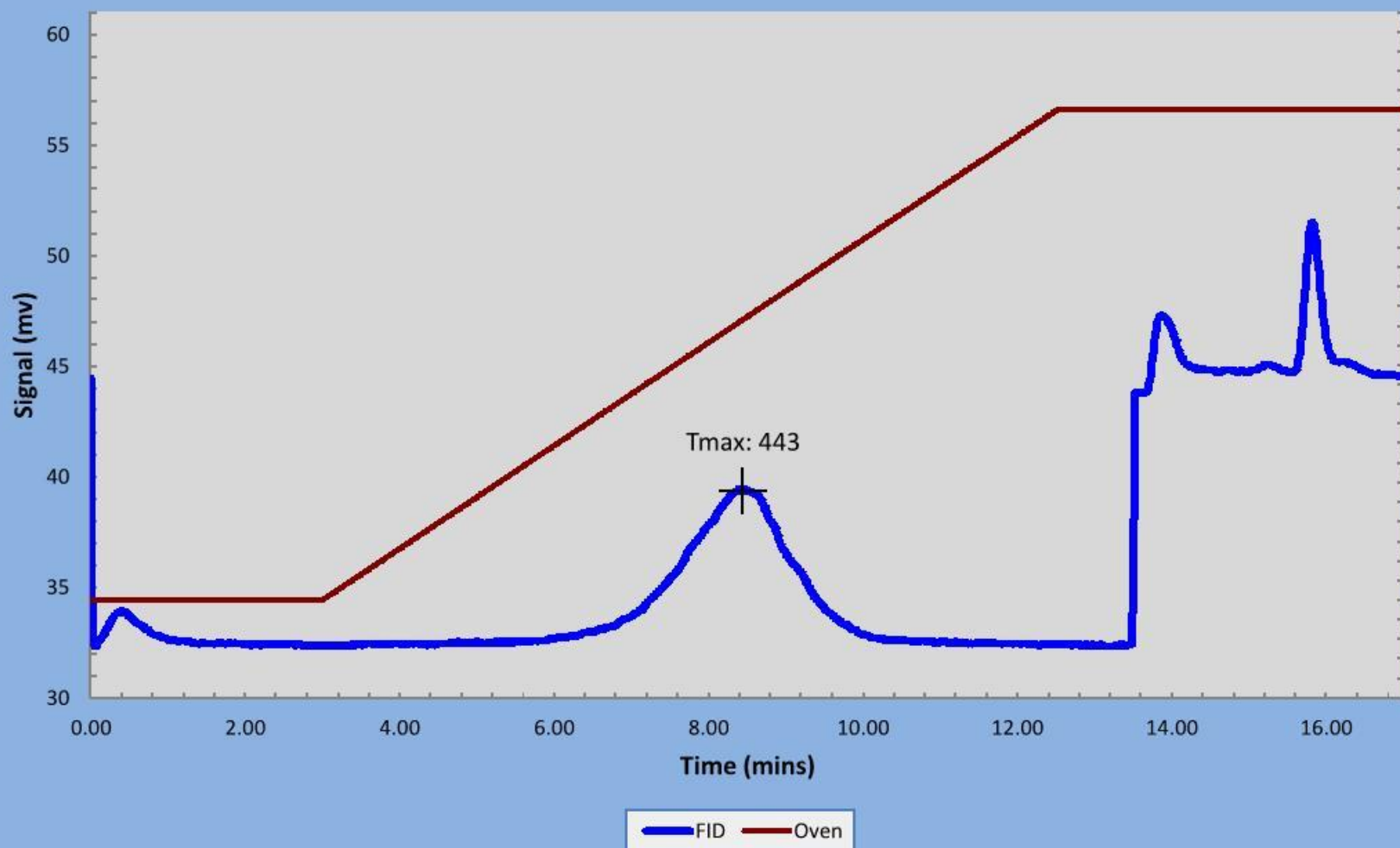


E10077-3  
(RMEM-130903-005)

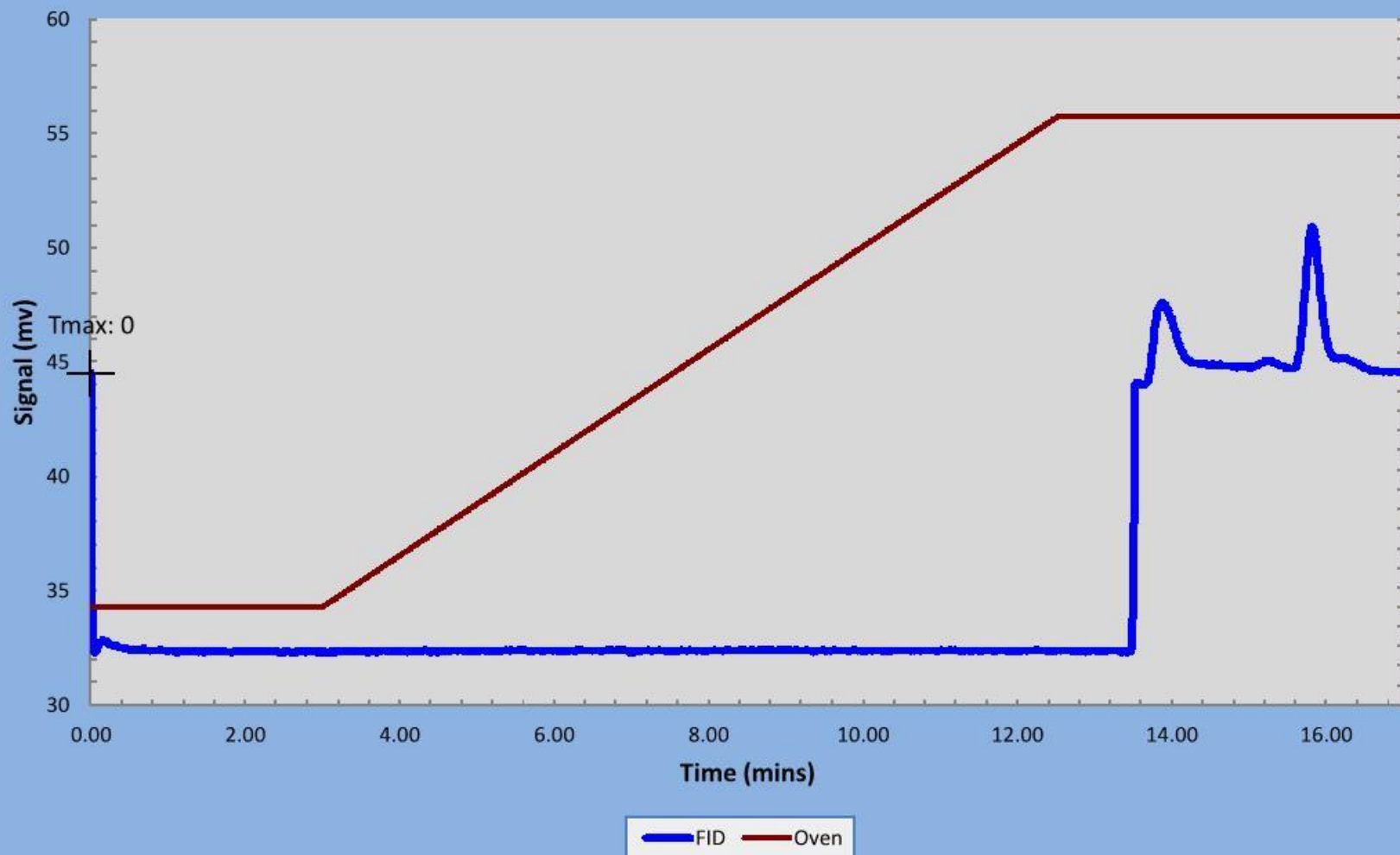




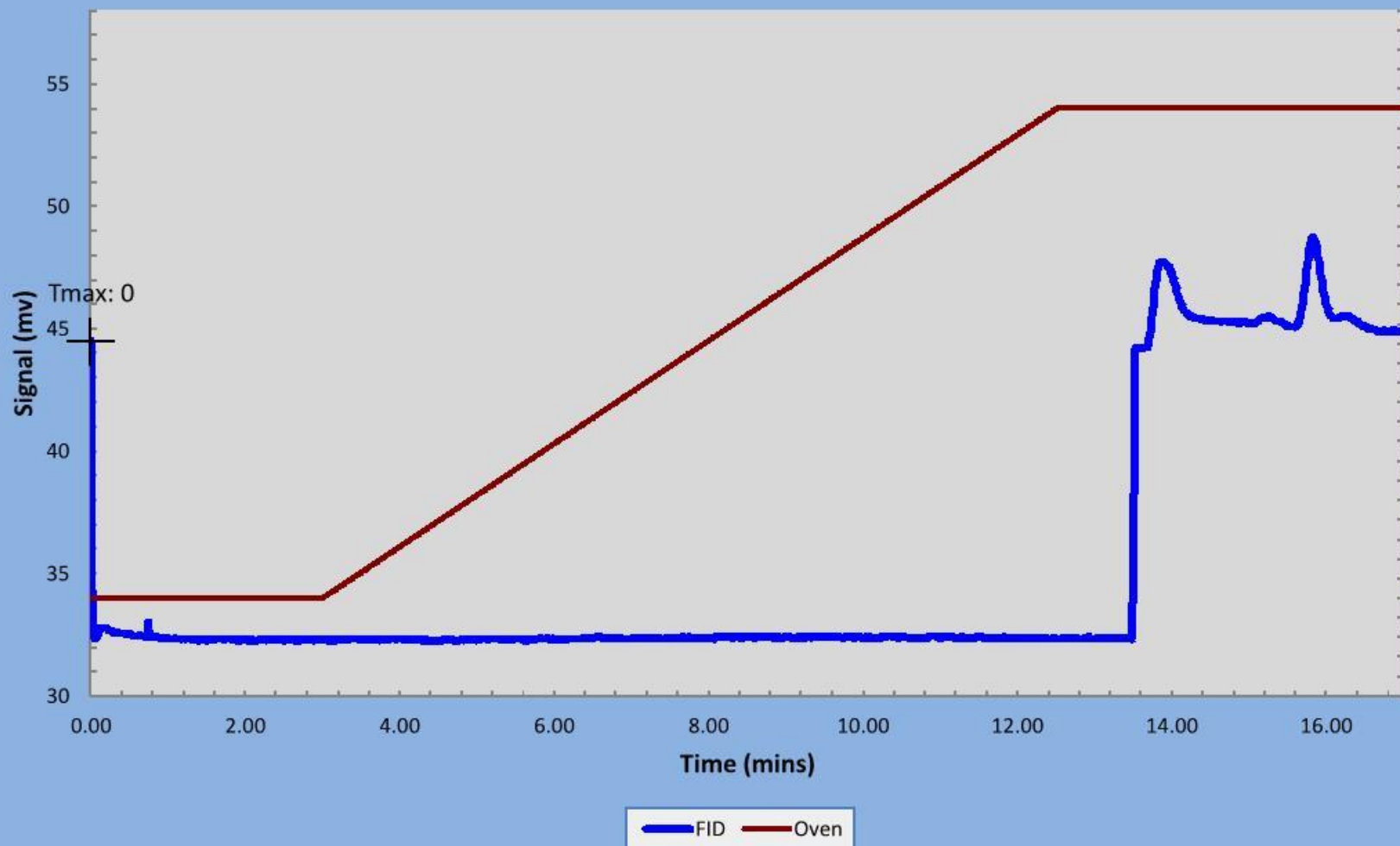
Ln12106-A  
(RMEM-130904-001)



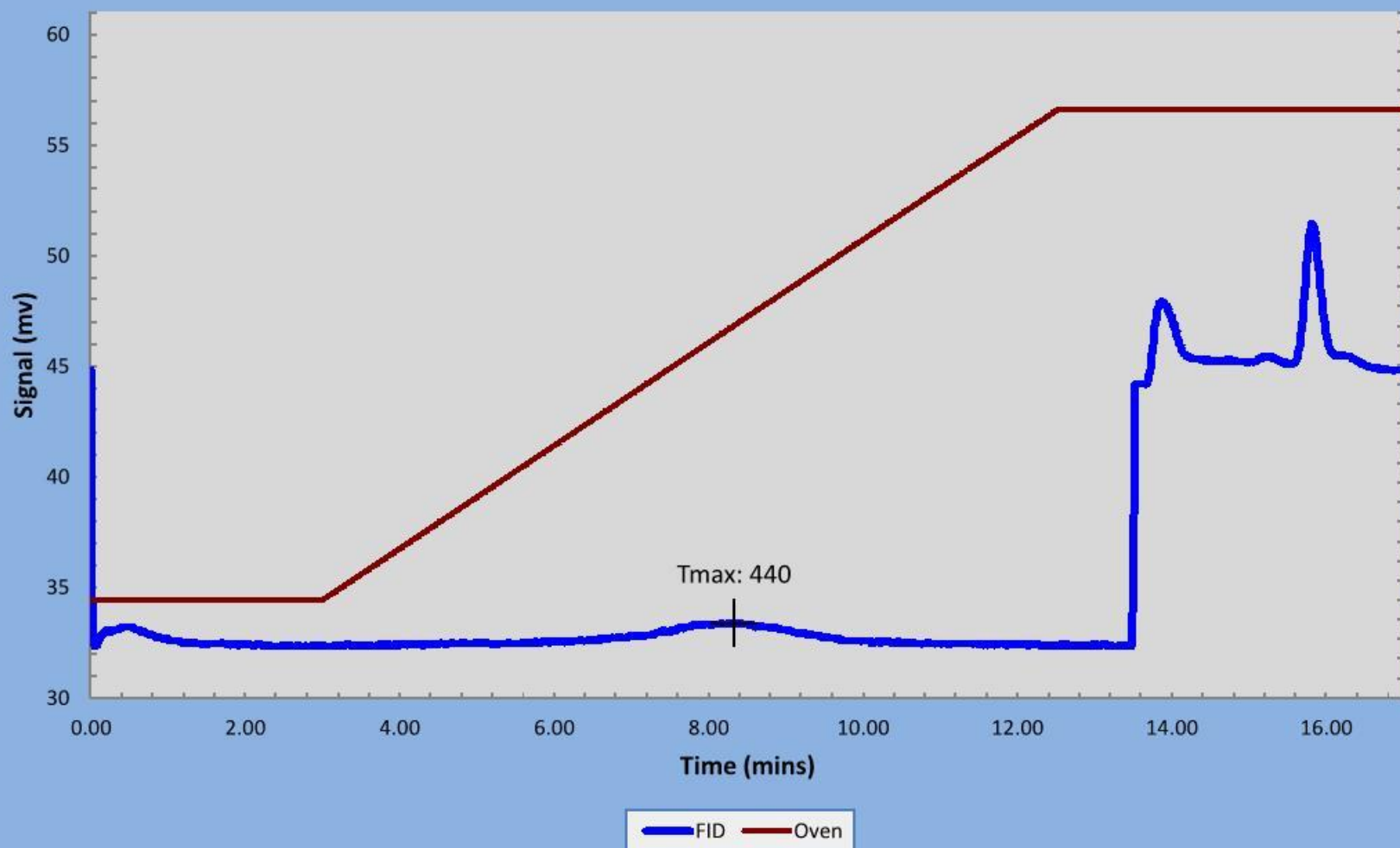
Ln12107-A  
(RMEM-130904-002)



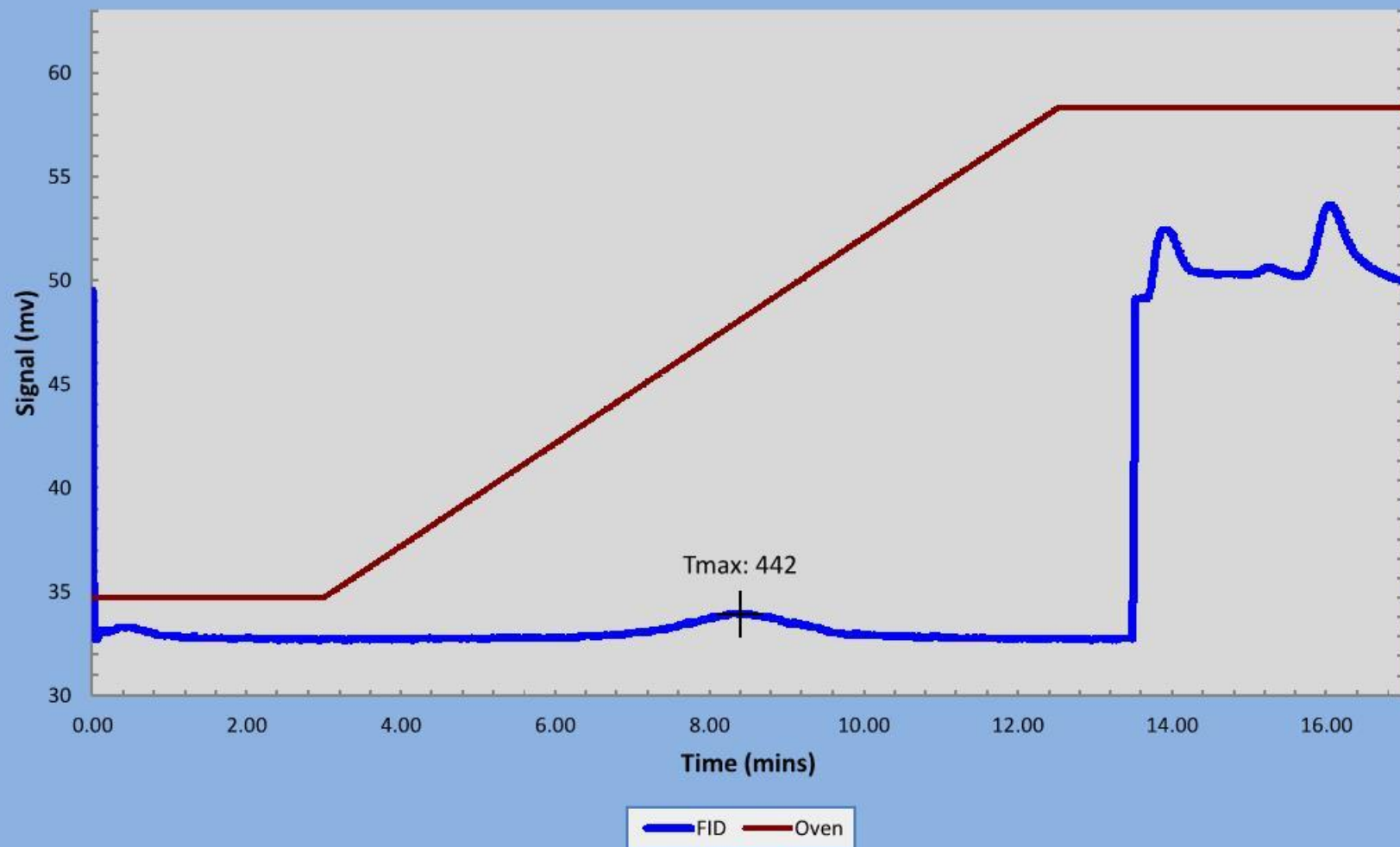
Ln12107-C  
(RMEM-130904-003)



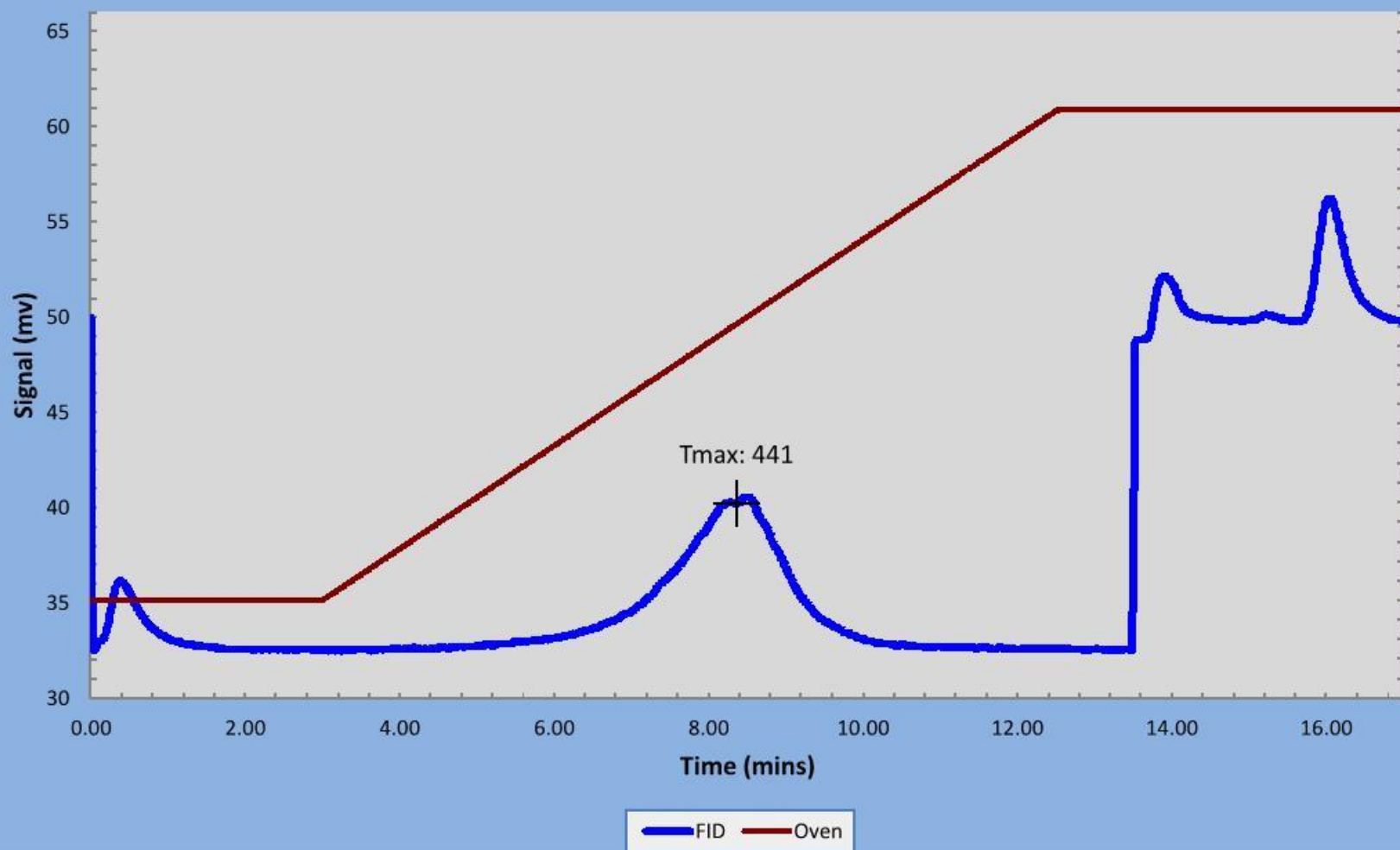
Ln12108-B  
(RMEM-130904-004)

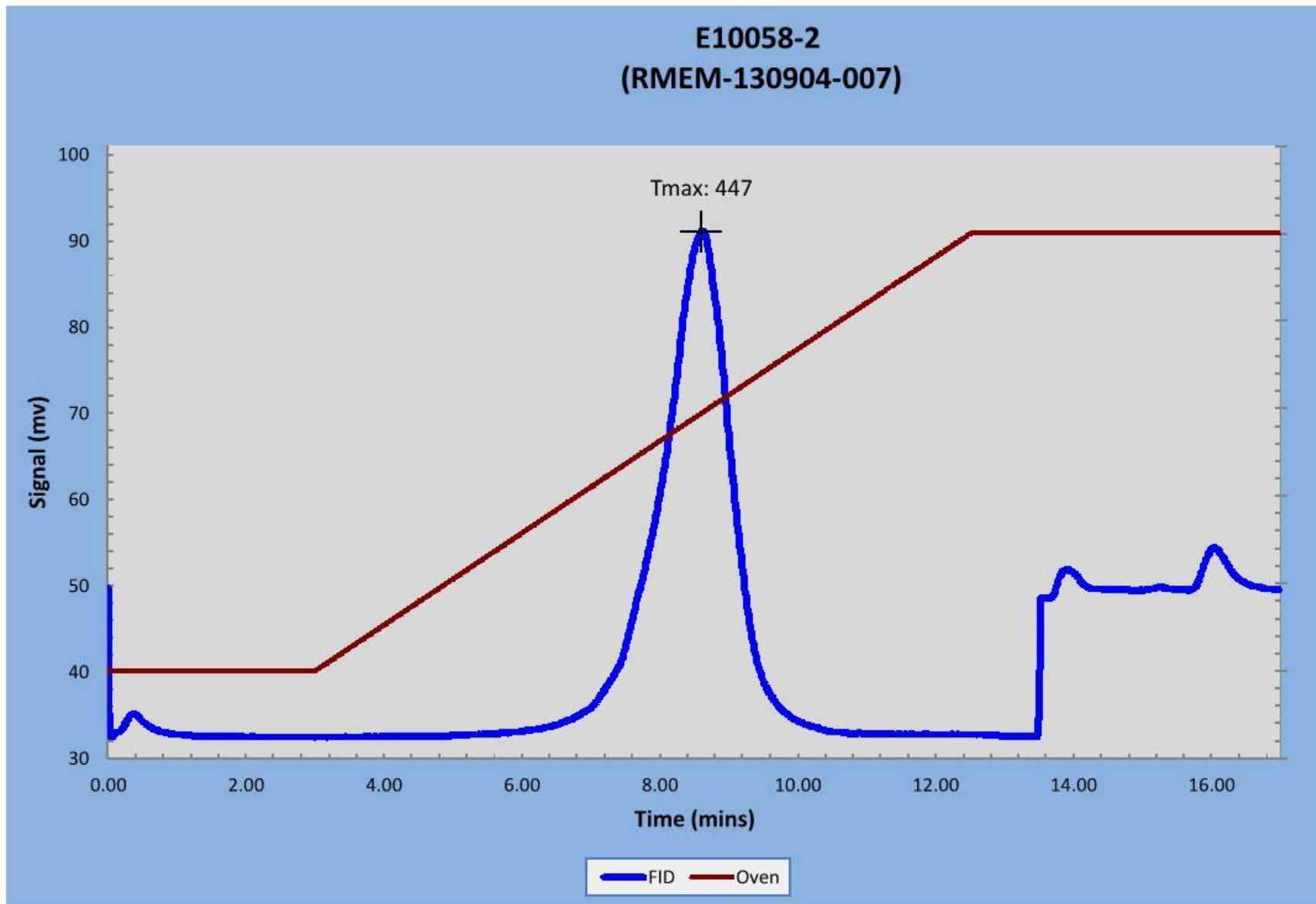


Ln12108-C  
(RMEM-130904-005)

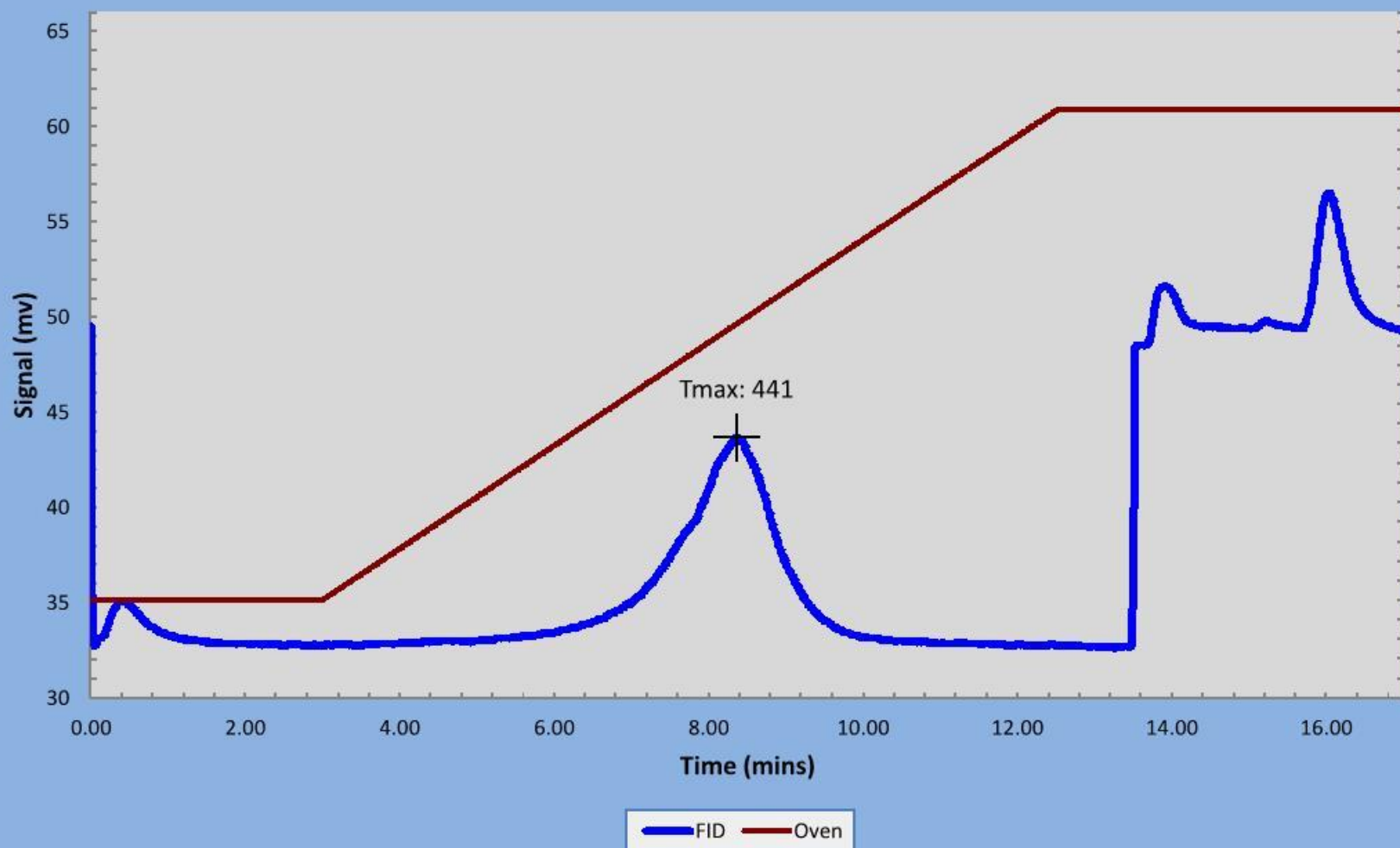


E10058-1  
(RMEM-130904-006)

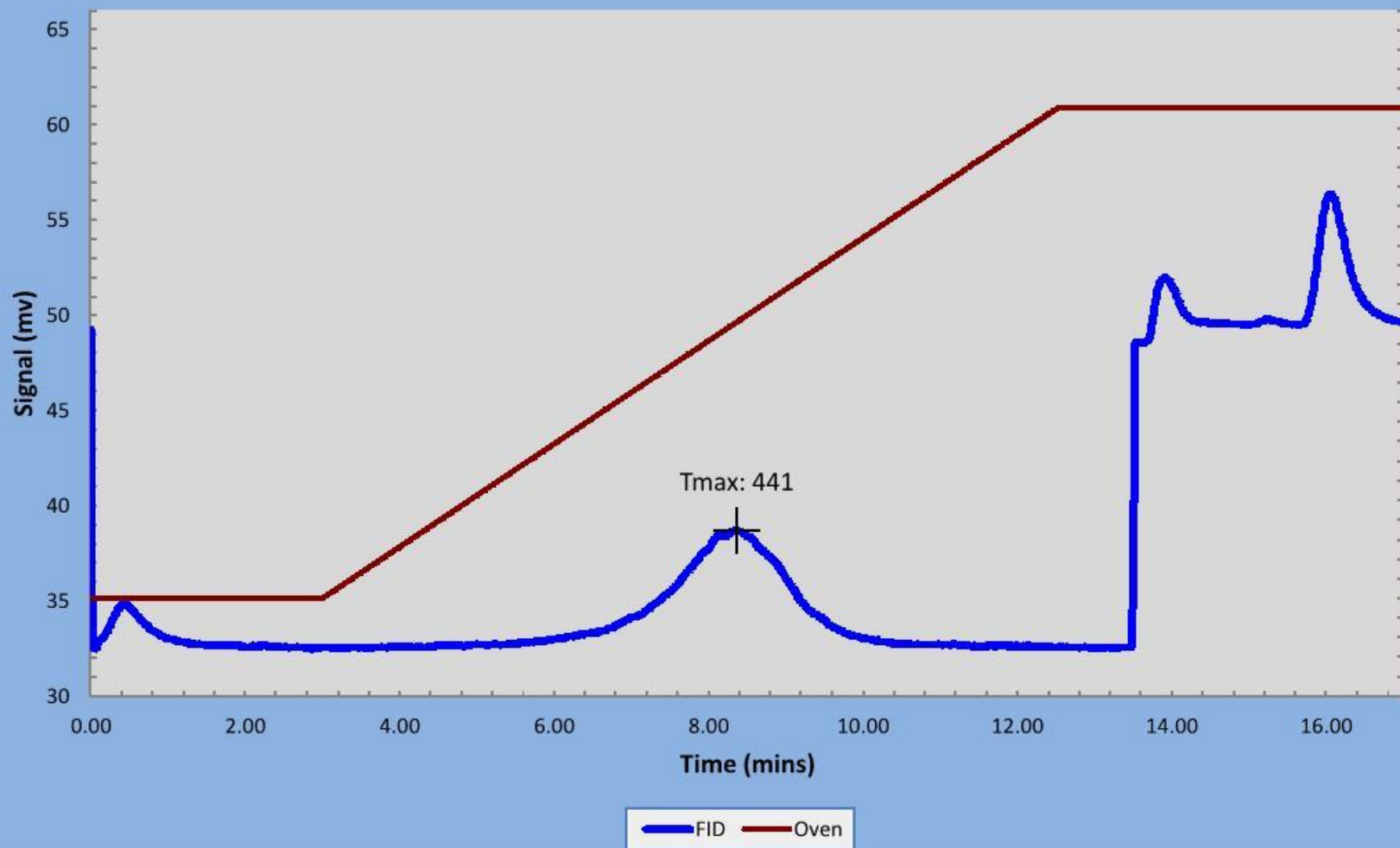




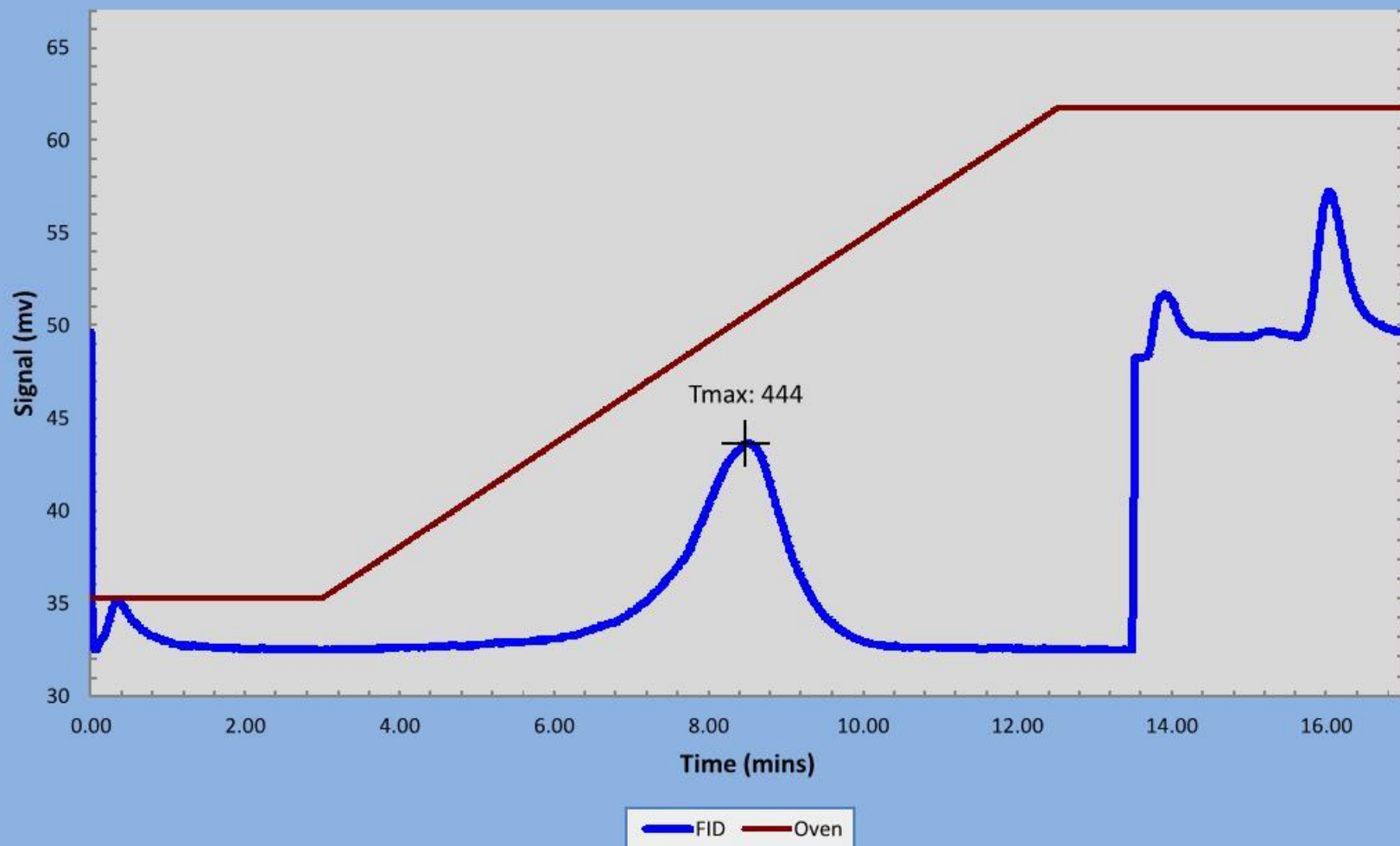
E10058-3  
(RMEM-130904-008)



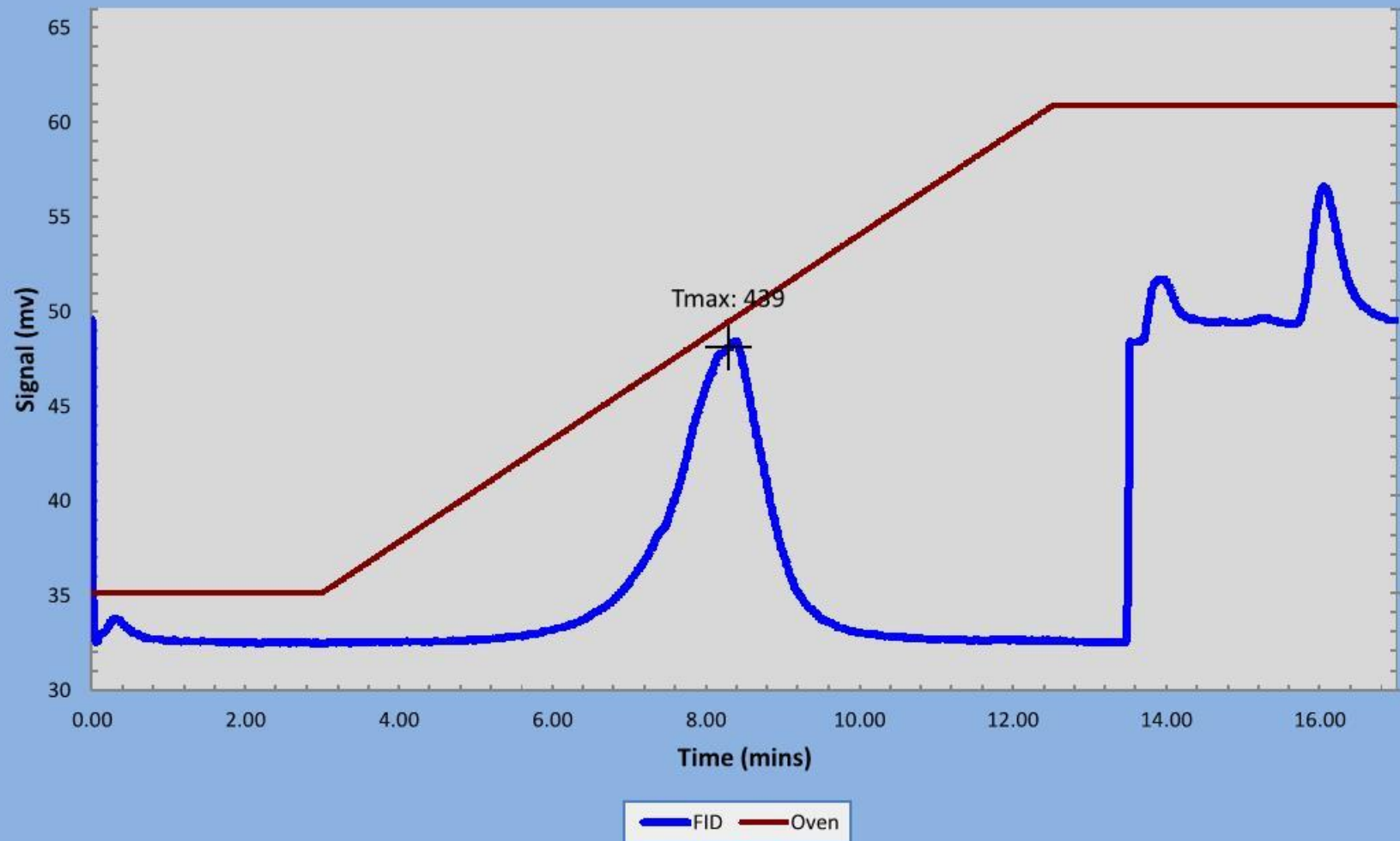
E10058-4  
(RMEM-130904-009)



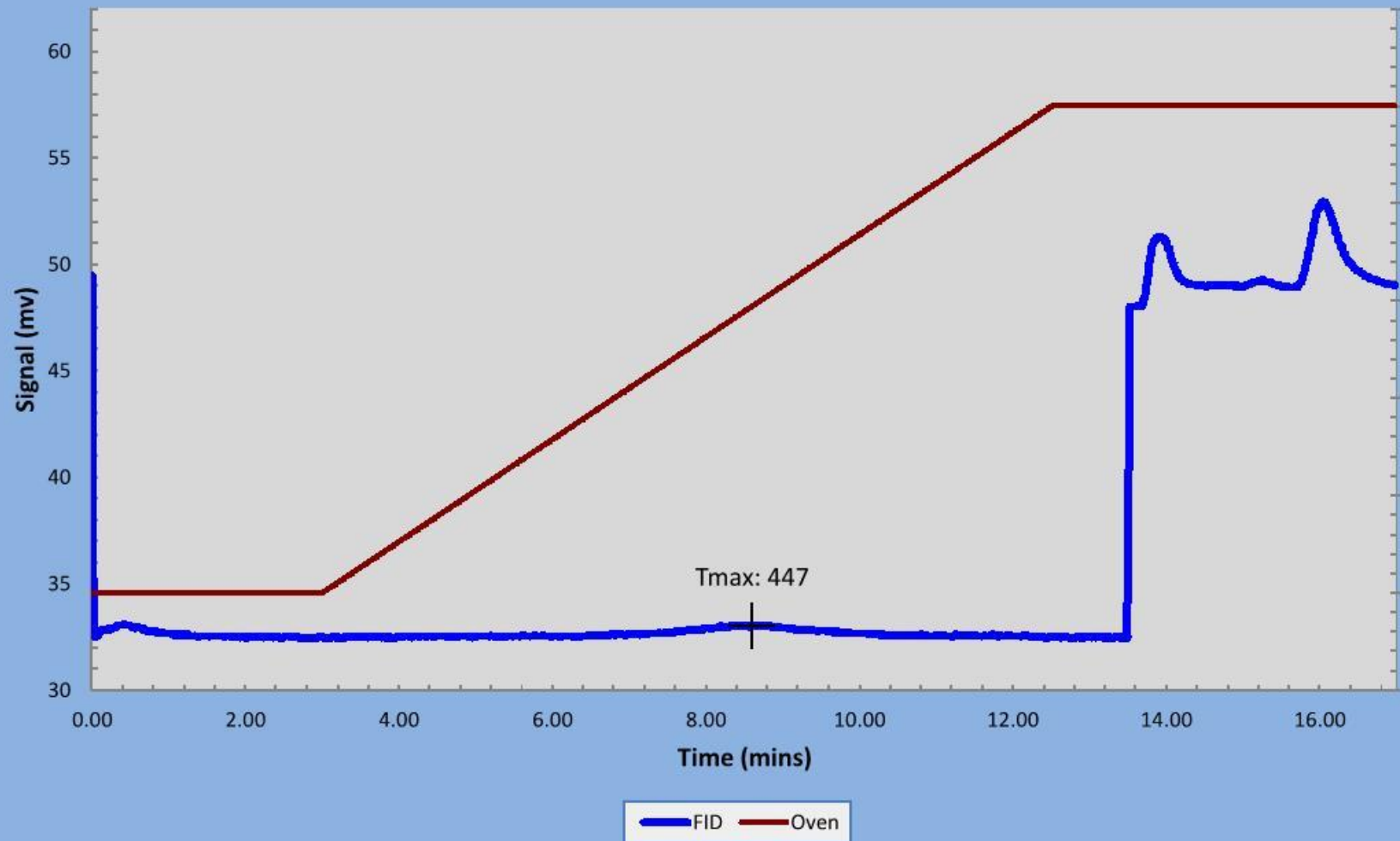
E10058-6  
(RMEM-130904-010)



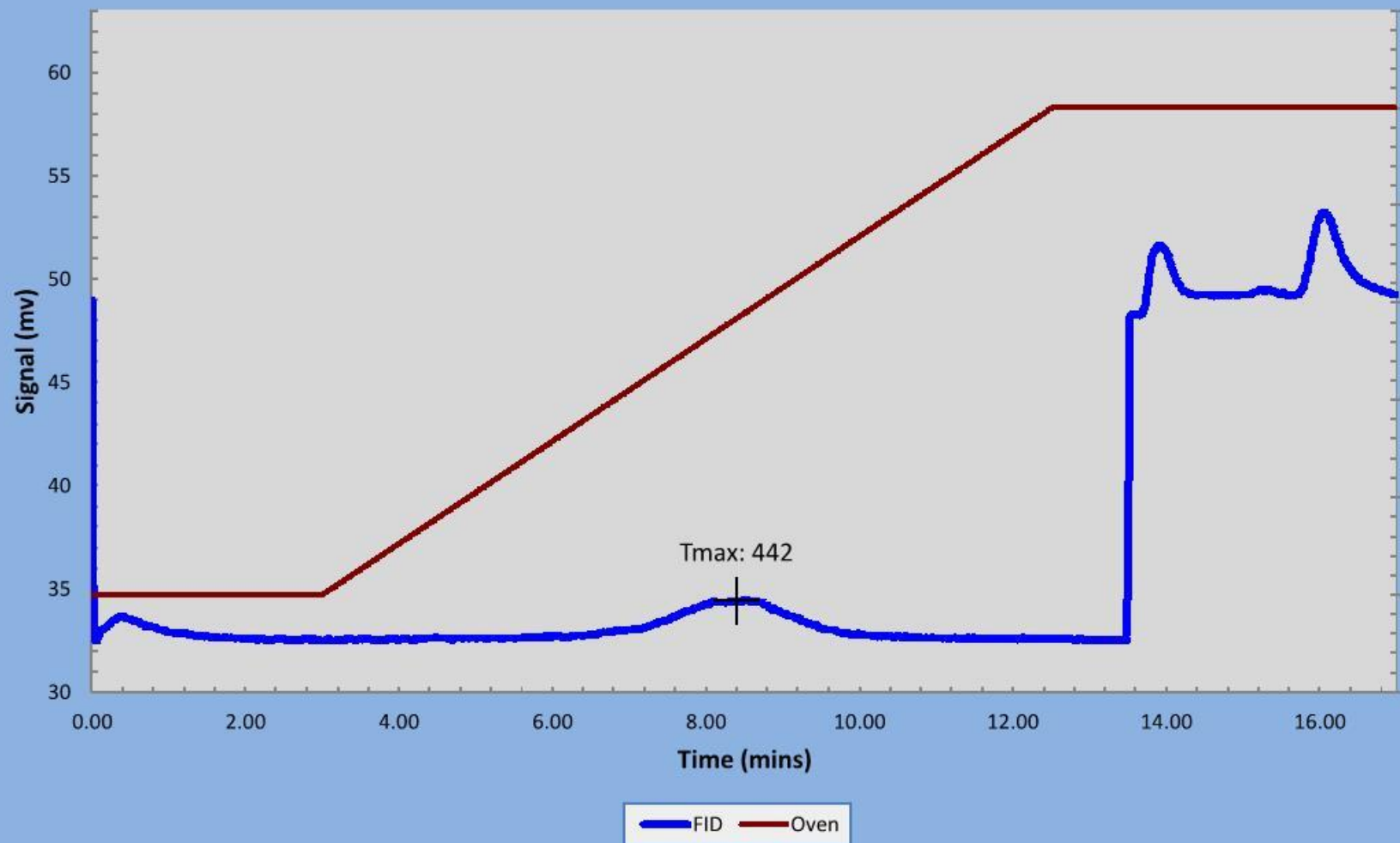
E10069-5  
(RMEM-130905-001)



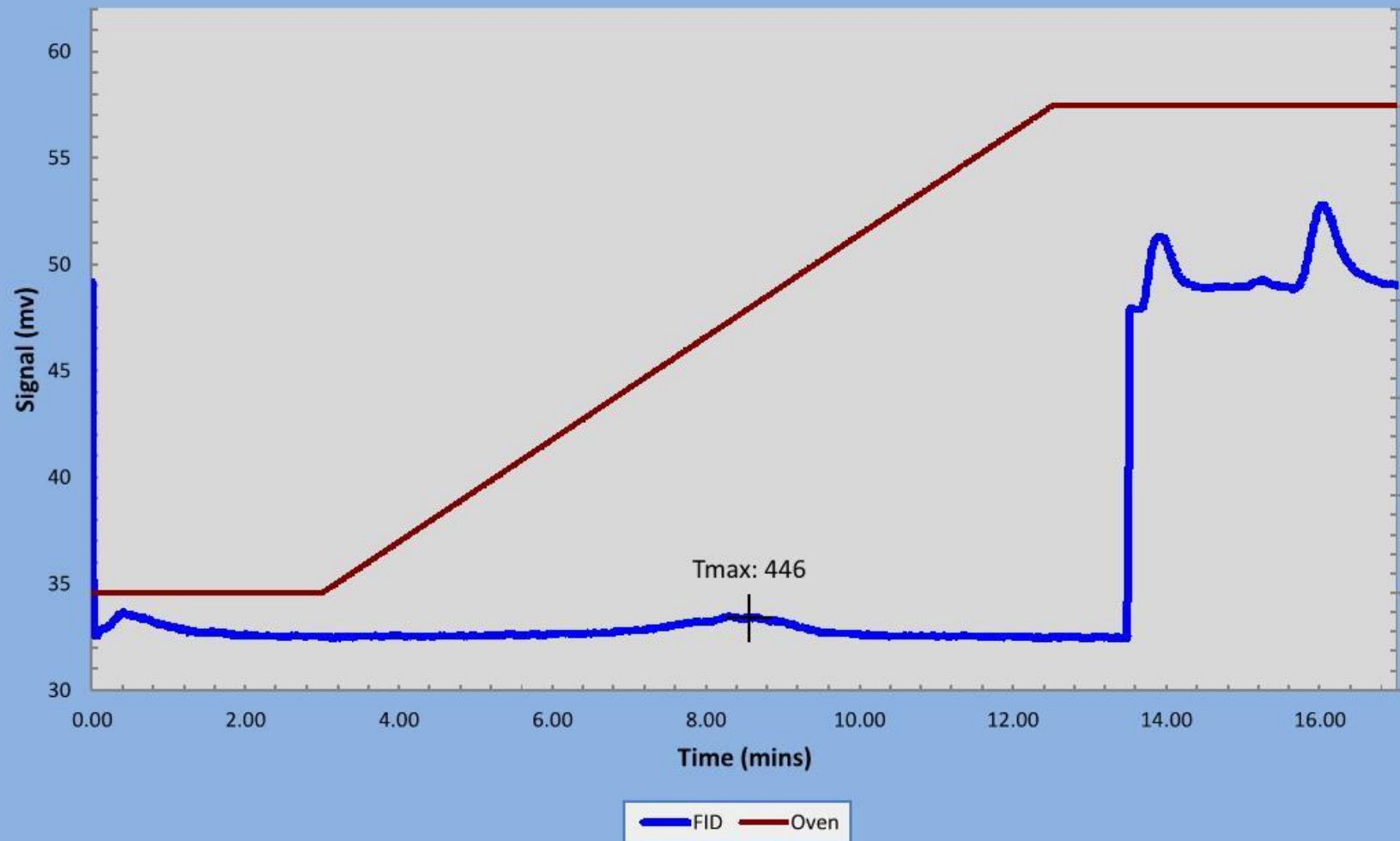
E10068-7  
(RMEM-130905-002)



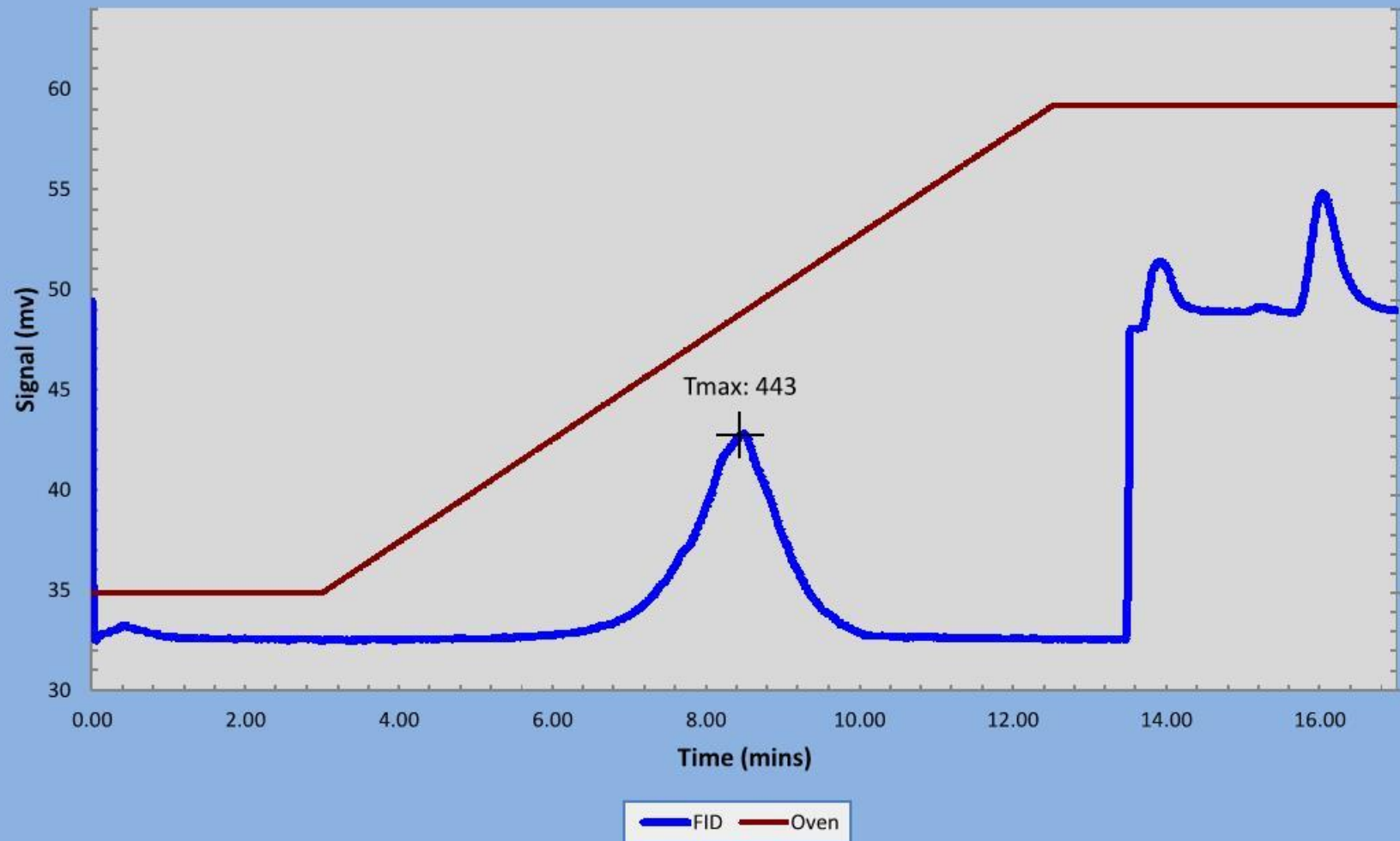
E10068-8  
(RMEM-130905-003)



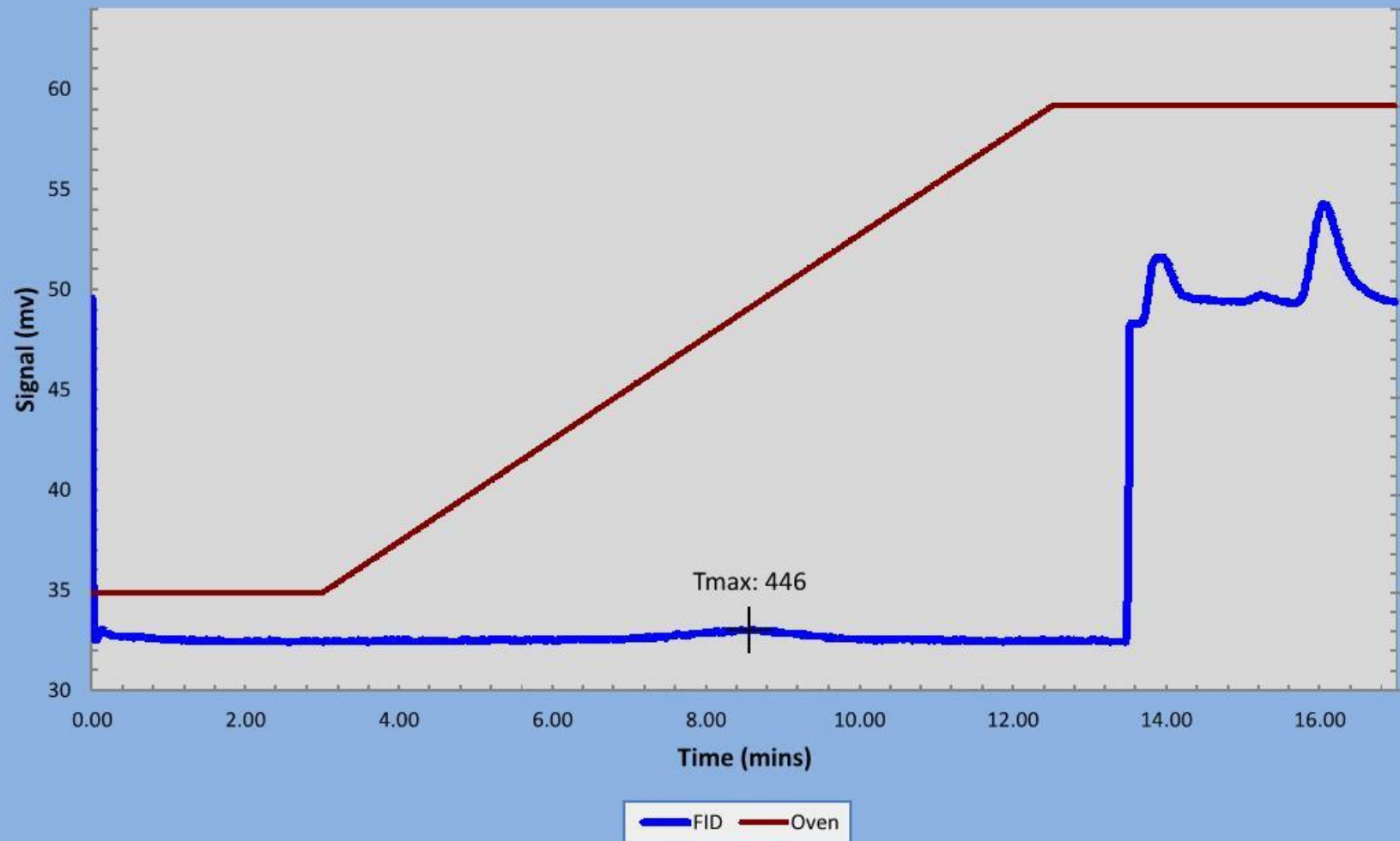
E10070-4  
(RMEM-130905-004)



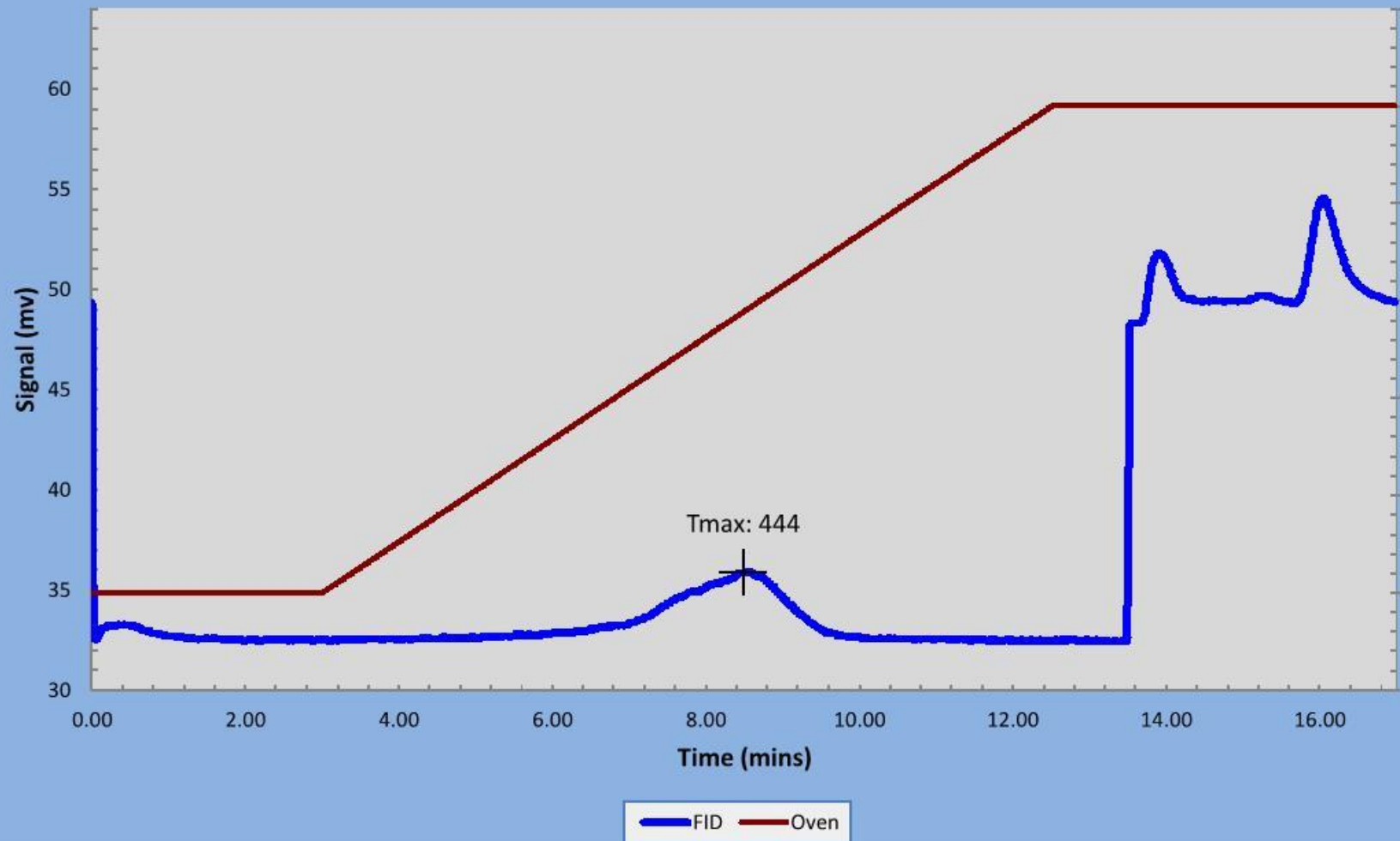
E10070-1  
(RMEM-130905-005)

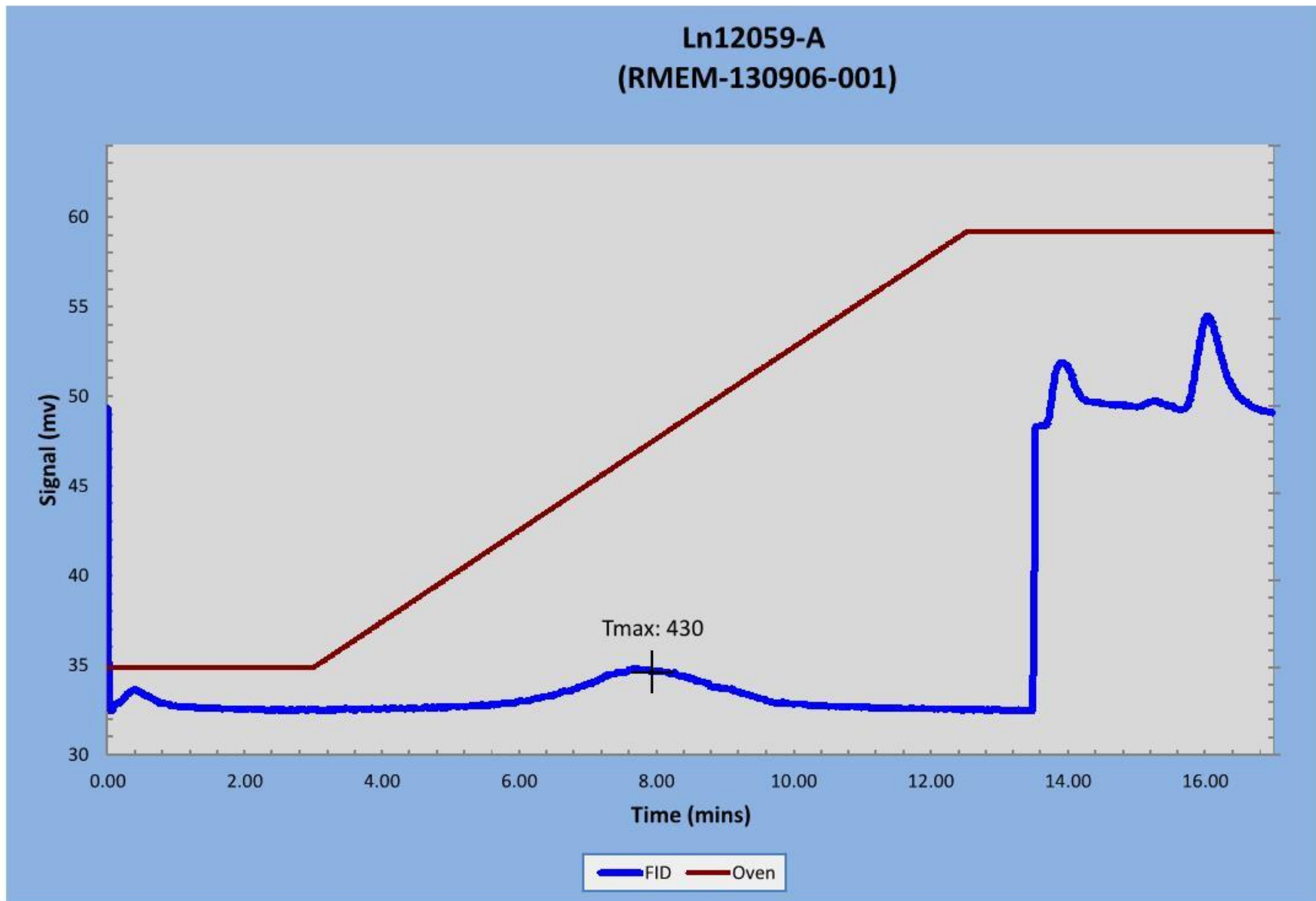


E10070-5  
(RMEM-130905-006)

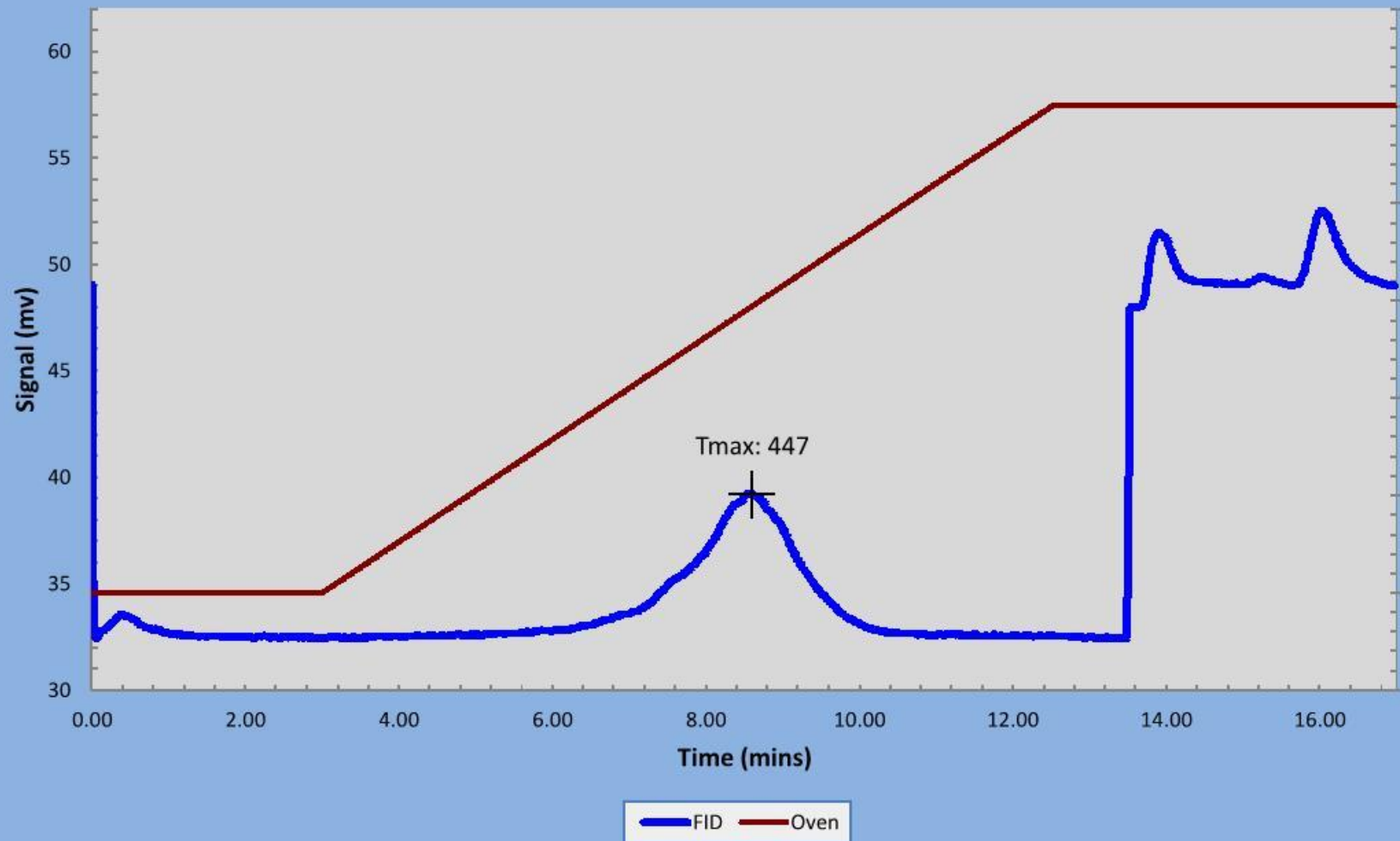


E10065-3  
(RMEM-130905-008)

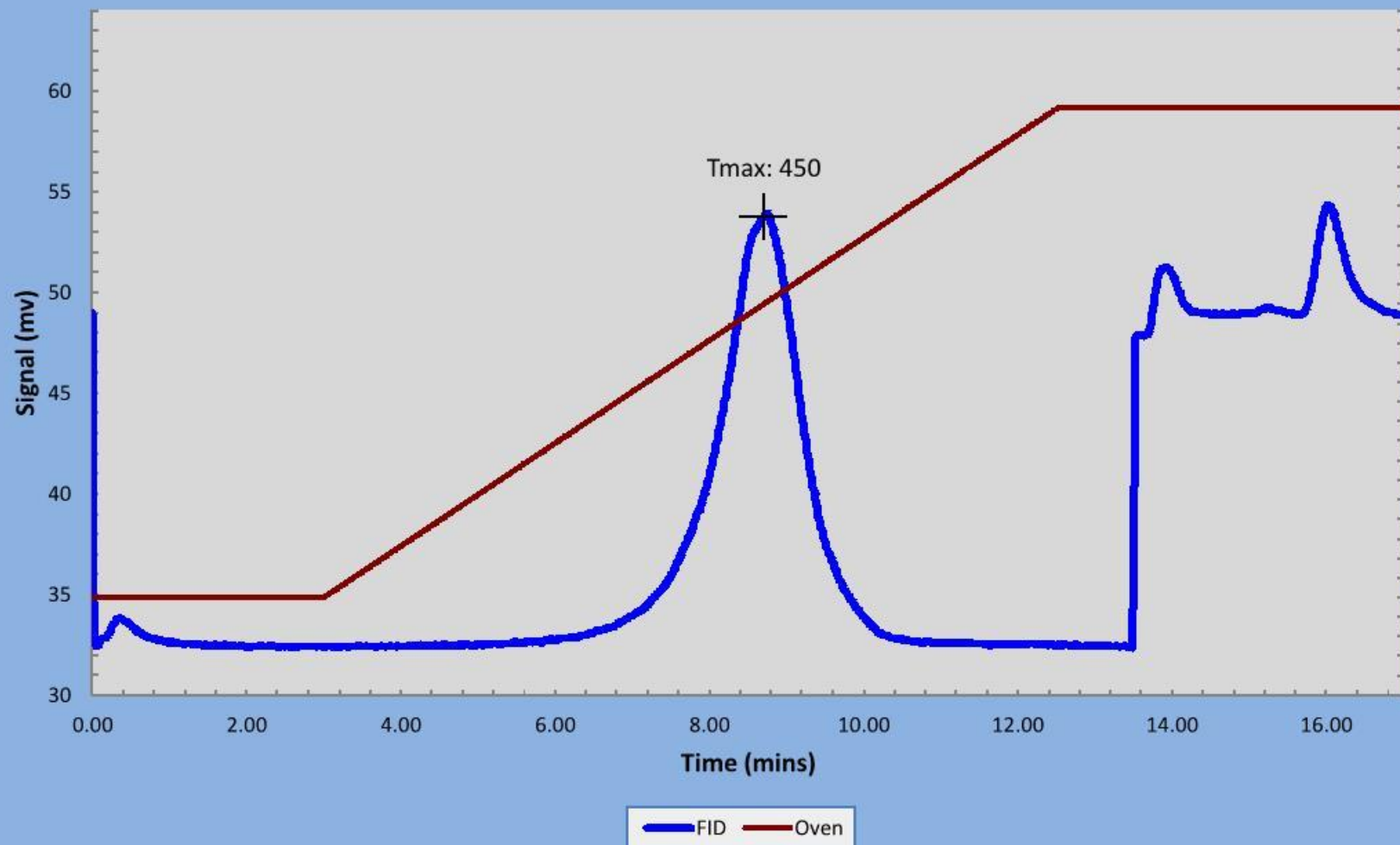




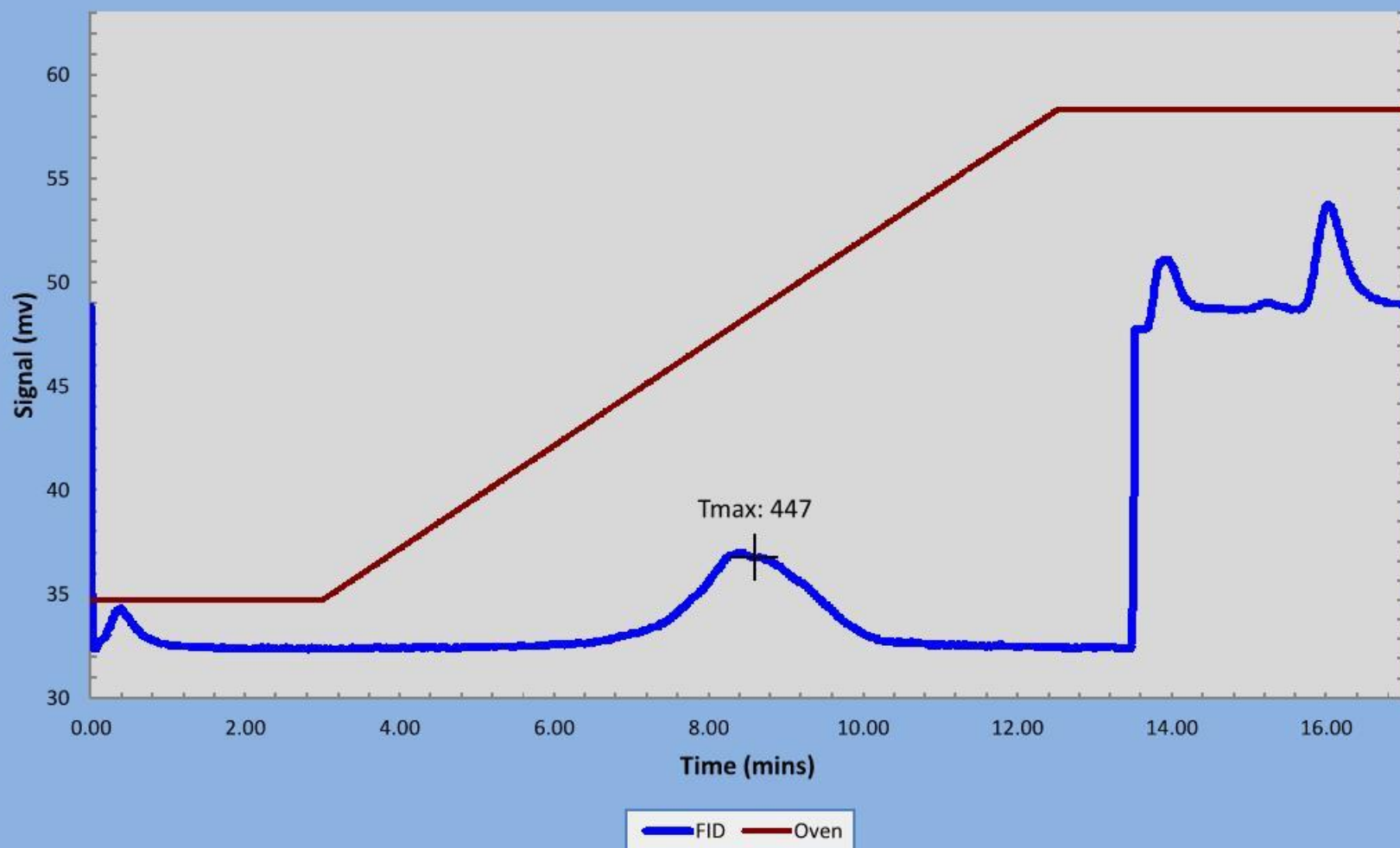
Ln12059-B  
(RMEM-130906-002)



Ln12054-A  
(RMEM-130906-003)



Ln12054-B  
(RMEM-130906-004)



Ln12054-C  
(RMEM-130906-005)

